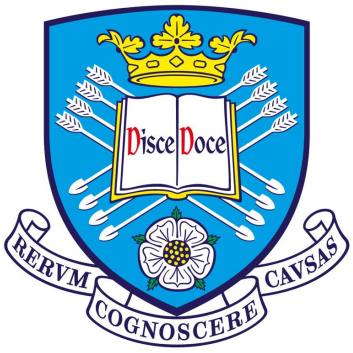

The University Of Sheffield.

One-pot synthesis of dimethyl carbonate over Zn-promoted metal alkali catalyst under mild conditions

By:

Ming Liu

A thesis submitted for the degree of

Doctor of Philosophy

The University of Sheffield

Department of Chemical and Biological Engineering

February 2020

ACKNOWLEDGE

Constant dripping wears away a stone. A four-year PhD demands a certain austerity and intensity, and I am really grateful for those who have offered their help and wisdom as I go through with my research project. I would like to express my greatest gratitude to my supervisor, Dr. James McGregor. Since our first meeting, James has been as exceedingly supportive of both my emotional and mental wellbeing. My supervisor has been incredibly busy in teaching and research, but he still invests a great deal of time in balancing my education, enculturation, development and progress, which makes him an excellent supervisor.

Additionally, I sincerely appreciate the technicians and support staffs in Department of Chemical and Biological Engineering. Thanks to Cynthia Kartey, Nur Atiqah Nasir, Ali Al – Shathr, Gareth Davies and all members in Catalysis Group, who have contributed their emotional labour and wonderful advices when it's needed. Also, thanks to my best friend in Sheffield (Mingzhe Yu), I can't forget the five years we spend together and you are my warmest big brother in Sheffield. Last but not least, I sincerely appreciate the encouragement and support from my parents. While feeling lonely and isolated as a foreign student, the concern and care for me from my parents becomes what accelerates my path to peak motivation. I want to convey my sincere gratitude and love to my parents, who always teach me to be a kind and motivated person.

EPSRC is acknowledged for support *via* grant EP/R026815/1 and, for SEM data, *via* EP/K001329/1, for SEM data. The authors also with to thank Dr. Benjamin M. Partridge, University of Sheffield, Department of Chemistry for discussions and advice on the proposed mechanisms.

Best wishes,

Ming Liu

Sheffield

27-02-2020

ABSTRACT

Carbon dioxide (CO_2) is most commonly discussed in negative terms as a greenhouse gas and major contributor to anthropogenic climate change. Recently, the use of CO_2 as an abundant carbon resource has received increased attention, with this field referred to as carbon dioxide utilisation. Direct conversion of CO_2 to green chemicals is an attractive application, as it incorporates a waste resource in the production of value-added, sustainable substances. Carbon dioxide utilisation in the synthesis of dimethyl carbonate (DMC) is attractive due to the extensive application of DMC in a variety of processes. In particular, DMC has lower toxicity and is a more environmentally friendly chemical compared to traditional alternatives, many of which have unfavourable properties such as high toxicity, *e.g*. phosgene. Previously, high selectivity to DMC has been correlate with high pressure operating environments employing supercritical CO_2. Applying high-operating pressure (8 Mpa~16.5 MPa, see Table 4-1) in chemical plants is, however, cost and energy intensive and introduces significant safety concerns. Optimisation of reaction conditions with the aim of minimizing the operating pressure while increasing reaction rate, selectivity and catalyst lifetime should be a key goal of process development. Herein, one-pot synthesis of DMC from propylene oxide, methanol and CO_2 using alkali halide catalysts under low-operating pressure (2 MPa at room temperature) was studied. This study has evaluated the catalytic activity of alkali halide-based catalysts *via* the one-pot route of DMC synthesis and the results showed that a DMC selectivity of 15.9% can be obtained when K_2CO_3-NaBr-ZnO is used as the catalyst. However, selectivity to DMC is limited by the relatively high yield of PG through the hydrolysis of PO. Therefore, both a physical drying agent (3Å molecular sieve) and a chemical dehydrating agent (acetonitrile) are applied in DMC synthesis. The production of PC increases significantly (from 1.04 mmol/ml to 1.48 mmol/ml and 1.59 mmol/ml for 3Å molecular sieve and acetonitrile, respectively, see Figure 6-5 and Figure 6-10) owing to the inhabitation of the PO hydrolysis, however, the influence of adding dehydrating agents on improving the yield of DMC is not obvious (from 0.53 mmol/ml to 0.51 mmol/ml and 0.49 mmol/ml for 3Å molecular sieve and acetonitrile, respectively). The catalyst applied in the DMC synthesis reactions are characterised using TGA, XRD, SEM, SEM/EDS, AAS and ICP-OES.

Additionally, Zn powder shows great possibility of achievement to remove water through the reaction with steam water under reaction condition. Results indicate that the addition of Zn powder to the K_2CO_3-NaBr-ZnO catalyst system increases the DMC selectivity from 15.9%

to 36.1% at 2 MPa and 160 °C for 5 h. Catalyst characterisation showed that Zn powder increases the stability of the catalyst by preventing the active ingredients on the catalyst surface from leaching. The results also show an increase in propylene oxide conversion to DMC attributed to the increase of Zn^{2+} ions in the reaction solution. Zn both promotes DMC formation through the new reaction route (Route 1) and transesterification of propylene carbonate and methanol (Route 2). More specifically, crucial intermediate products, zinc methoxide and carbonate zinc methoxide, are formed during reaction and promote the migration of carbonate species on the catalyst surface yielding more DMC *via* Route 1. Route 2 reaction pathway involves the formation of additional methoxy groups, which can attack the carbon atom of C=O in the transesterification reaction.

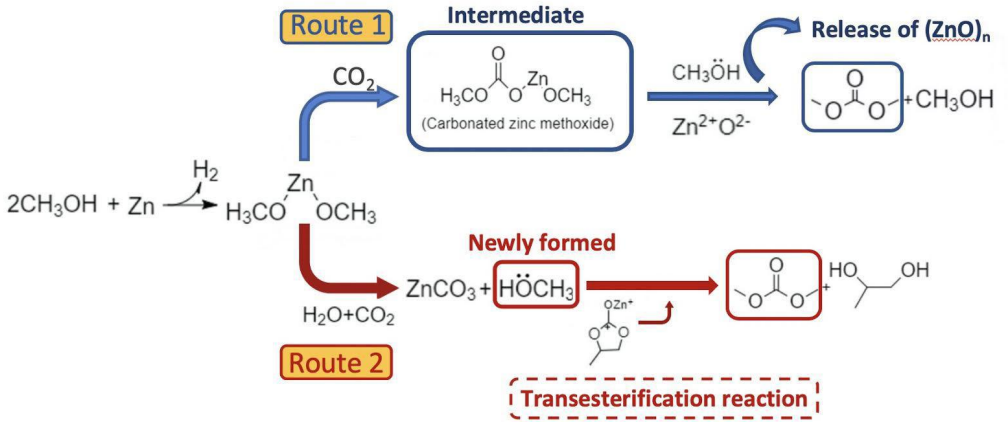

Proposed new mechanism for DMC synthesis with the addition of Zn powder

Furthermore, high pressure is not a prerequisite for the transesterification reaction and CO_2 is found to inhibit the reverse cycloaddition reaction to form PO (see Figure 7-8). This study shows that increased selectivity to DMC can be achieved at low pressure with the addition of Zn powder.

Table of Contents

ACKNOWLEDGE..... II

ABSTRACT.....III

List of Figures..... X

List of Tables..... XVI

List of Schemes.....XVIII

List of Abbreviations.....XX

CHAPTER 1 *INTRODUCTION*..... 1

1.1 Motivation.....2

1.1.1 Source of carbon dioxide emissions..... 3

1.1.2 The hardest emissions to cut.....4

1.1.3 Managing carbon dioxide emissions.....5

1.2 Carbon dioxide conversion and utilisation..... 5

1.2.1 The present and future usage of CO_2..... 5

1.2.2 Potential applications of CO_2.....6

1.2.3 The challenges for CO_2 application..... 6

1.3 Aims of the research..... 7

1.4 Structure of the thesis.....8

CHAPTER 2 *LITERATURE REVIEW*.....1112

2.1 Introduction.....12

2.2 Heterogeneous catalysts.....12

2.2.1 Reaction theories of heterogeneous catalysts..... 12

2.2.2 Un-supported (bulk) catalysts.....15

2.2.3 Supported catalysts..... 17

2.3 Catalytic transformation of CO_2..... 19

2.3.1 Hydrogenation of CO_2..... 19

2.3.2 Conversion of CO_2 to carboxylic acids.....22

2.3.3 Conversion of CO_2 to organic carbonates.....24

2.4 Introduction to dimethyl carbonate (DMC)..... 28
2.4.1 Properties of DMC..... 28
2.4.2 Applications of DMC..... 29
2.5 Synthesis of DMC..... 31
2.5.1 Oxidative carbonylation..... 32
2.5.2 Transesterification of cyclic carbonate..... 32
2.5.3 Direct transformation of CO_2..... 33
2.6 Catalysts and dehydrating agents used for DMC synthesis..... 36
2.6.1 Heterogeneous catalysts used for the one-pot synthesis of DMC..... 36
2.6.2 Dehydrating agents..... 38
2.7 Conclusions..... 38
CHAPTER 3 *EXPERMENTAL WORK AND ANALYTICAL TECHNIQUES*..... 40
3.1 Introduction..... 41
3.2 Apparatus and procedure..... 41
3.2.1 Catalyst preparation method..... 41
3.2.2 The stainless-steel reactor..... 43
3.2.3 The procedure of reaction..... 43
3.3 Analysis of liquid product..... 44
3.3.1 Gas chromatography/mass spectrometry (GC-MS)..... 45
3.3.2 Fourier transform-infrared spectroscopy (FT-IR)..... 47
3.4 Catalyst characterisation..... 48
3.4.1 Thermogravimetric Analysis (TGA)..... 48
3.4.2 X-ray diffraction (XRD)..... 49
3.4.3 Scanning electron microscopy/ Energy Dispersive X-Ray Spectroscopy (SEM/EDS) 50
3.4.4 Atomic absorption spectroscopy (AAS)..... 51
3.4.5 CO_2-Temperature-programmed desorption (CO_2-TPD)..... 51
3.4.6 N_2 adsorption isotherms..... 51

3.4.7 Inductively coupled plasma-optical emission spectroscopy (ICP-OES)..... 52
3.4.8 Fourier transform-infrared spectroscopy (FT-IR).....52
3.5 Overall experiment plan.....54
3.6 Experimental errors and error analysis..... 55
3.6.1 Systematic errors.....55
3.6.2 Random errors.....55
3.6.3 Calculating experimental error..... 55
CHAPTER 4 *ONE-POT SYNTHESIS OF DMC USING ALKALI HALIDE-ZnO CATALYST*598
4.1 Introduction.....59
4.2 Experimental methods..... 61
4.2.1 Materials..... 61
4.2.2 Methods.....61
4.3 Results and discussion..... 63
4.3.1 Influence of alkali halide species.....63
4.3.2 Influence of reaction time..... 65
4.3.3 Catalyst characterisation..... 67
4.3.4 Proposed reaction mechanism.....70
4.4 Conclusions.....75
CHAPTER 5 *CATALYST MODIFICATION: INFLUENCE OF ALKALI METALS*.....76
5.1 Introduction.....77
5.2 Experimental methods..... 78
5.2.1 Materials..... 78
5.2.2 Experimental methods..... 78
5.2.3 Catalyst characterisation..... 80
5.3 Results and discussion..... 82
5.3.1 Influence of three kinds of alkali..... 82
5.3.2 Influence of K_2CO_3 loadings.....84
5.3.3 Effect of alkali halide species..... 85

5.4 Conclusions....94
CHAPTER 6 *INFLUENCE OF DEHYDRATING AGENTS ON DMC SELECTIVITY*.... 95
6.1 Introduction....96
6.1.1 3Å molecular sieve as a physical water trap....96
6.1.2 Acetonitrile as a dehydrating agent....97
6.2 Experimental methods.... 97
6.2.1 Materials.... 97
6.2.2 Methods....99
6.3 Results and discussion.... 105
6.3.1 Influence of 3Å molecular sieve quantity....105
6.3.2 Influence of acetonitrile quantity....112
6.3.3 Comparison of dehydration efficiency of two agents....117
6.4 Conclusions....121
CHAPTER 7 *ONE-POT SYNTHESIS OF DMC USING A Zn-PROMOTED METAL ALKALI CATALYST*....122
7.1 Introduction....123
7.2 Experimental methods.... 125
7.2.1 Materials.... 125
7.2.2 Methods....125
7.3 Results and discussion.... 130
7.3.1 Influence of Zn powder adding amount on DMC selectivity.... 130
7.3.2 The role of Zn powder in cycloaddition.... 133
7.3.3 The role of Zn powder and CO_2 in the transesterification.... 135
7.3.4 $MgO(CH_3)_2$ promoted reactions....137
7.3.5 Characterisation of solid-phase catalyst....140
7.3.6 Reaction mechanism.... 148
7.4 Conclusions....149
CHAPTER 8 *CONCLUSIONS AND RECOMMENDATIONS FOR FUTURE WORK*..... 1521

8.1 Conclusions.....152
8.1.1 Preparation of the catalyst.....152
8.1.2 Modification of reaction condition.....153
8.2 Recommendations for future work.....156
8.2.1 Characterisation of the catalysts.....156
8.2.2 Directions for future study.....157
REFERENCES.....159
APPENDICES.....174
Appendix A: Calibration curves of the products obtained from DMC synthesis reactions (Chapter 3).....174
Appendix B: Photograph of the products obtained from DMC synthesis reactions in the presence of 3Å molecular sieves and acetonitrile (Chapter 6).....177

List of Figures

Figure 1-1. The sources of global CO_2 emissions in 2016 (yearly total emission: 32.5 $GtCO_2$) (Iea.org, 2019).....3

Figure 1-2. (A) shows the different sources of CO_2 emissions with the highlighted (by longer pie pieces) hard-to-cut emissions sources in 2014. Figure 1-2 (B) illustrates the level of emissions related to these hardest decarbonized energy services in 2014. (Source: Davis *et al.*, *Science)*.....4

Figure 1-3. The physical and chemical routes for CO_2 utilisation (Source: The potential and limitations of using carbon dioxide, 2017).....6

Figure 2-1. The definition of electron shells of metal atoms and the electron distribution of each shell.....14

Figure 2-2. Theoretical amount of carbon consumed by CDU for production of chemicals and fuels in 2015 (Dowson and Styring, 2017).....19

Figure 2-3. Effect of different catalysts on conversion of propylene oxide and the selectivity, and yield of propylene carbonate. Experimental conditions: 10 *wt.*% catalyst loading; 170 ℃; CO_2 pressure, 7.0 MPa; reaction time, 20 h. (Source: Adeleye, Adegboyega Isaac *et al.,* 2014). 25

Figure 2-4. The molecular structure of DMC (1, 2 represent chemically different C and O atoms).....29

Figure 3-1. The reflux apparatus used for catalyst preparation.....42

Figure 3-2. The stainless-steel batch reactor applied for the one-pot synthesis of DMC.....43

Figure 3-3. The main components of GC-MS: The GC and the inlets of GC, required detectors, the ion source, the ions' mass-to-charge (m/z) analyser, the ion detector and the computer.....45

Figure 4-1. Effect of alkali halide species on the conversion of PO and the selectivity of DMC, PC, PG and by-products in DMC synthesis. Reaction condition: 160 °C, 5 h, CO_2 (2 MPa), catalyst (17.5 *wt*% alkali halide-ZnO, 0.3 g), PO (33.33 mmol), methanol (100 mmol).....63

Figure 4-2 (a). Effect of reaction time on the selectivity of DMC, PC, PG and by-products in DMC synthesis. Reaction condition: 160 °C, CO_2 (2 MPa), catalyst (17.5 *wt*% alkali halide-ZnO, 0.3g), PO (33.33 mmol), methanol (100 mmol).....65

Figure 4-2 (b). Effect of reaction time on the conversion of PO in DMC synthesis. Reaction condition: 160 °C, CO_2 (2 MPa), catalyst (17.5 *wt.*% alkali halide-ZnO, 0.3 g), PO (33.33 mmol), methanol (100 mmol)..... 66

Figure 4-3. DTG and TG curves of (a) calcined NaBr-ZnO catalyst (b) non-calcined NaBr-ZnO catalyst..... 68

Figure 4-4. The XRD patterns of catalysts: (a) non-calcined NaBr-ZnO; (b) calcined NaBr-ZnO..... 69

Figure 5-1. Effect of alkali on the conversion of PO and the selectivity of DMC, PC, PG and by-products in DMC synthesis. Reaction condition: 160 °C, 5 h, CO_2 (2 MPa), catalyst (12 *wt.*% alkali-17.5 *wt.*% NaBr-ZnO, 0.3 g), PO (33.33 mmol), methanol (100 mmol)..... 82

Figure 5-2. Effect of alkali loadings on the conversion of PO and the selectivity of DMC, PC, PG and by-products in DMC synthesis. Reaction condition: 160 °C, 5 h, CO_2 (2 MPa), catalyst (K_2CO_3-17.5 *wt.*% NaBr-ZnO, 0.3 g), PO (33.33 mmol), methanol (100 mmol)..... 84

Figure 5-3. Effect of alkali halide species on the conversion of PO and the selectivity of DMC, PC, PG and by-products in DMC synthesis. Reaction condition: 160 °C, 5 h, CO_2 (2 MPa), catalyst (12 *wt.*% K_2CO_3-17.5 *wt.*% alkali halide-ZnO, 0.3 g), PO (33.33 mmol), methanol (100 mmol)..... 85

Figure 5-4. DTG and TG curves of (a) non-calcined K_2CO_3-NaBr-ZnO (b) mixture of K_2CO_3, NaBr and ZnO..... 87

Figure 5-5. Surface morphology of the catalyst and mixtures of catalyst and Zn powder. (a) Fresh catalyst, (b) Spent catalyst..... 88

Figure 5-6. The distribution of zinc (red), oxygen (green) and sodium (blue) on catalyst surface before and after calcination by EDX mapping: (a) catalyst before calcination; and (b) catalyst calcined at 700 °C..... 89

Figure 5-7. The XRD patterns of catalysts with various alkali: (a) 12 *wt.*% K_2CO_3-NaBr-ZnO; (b) 12 *wt.*% Na_2CO_3-NaBr-ZnO; (c) 12 *wt.*% NaOH-NaBr-ZnO..... 90

Figure 5-8. The XRD patterns of fresh and spent catalysts: (a) fresh K_2CO_3-NaBr-ZnO; (b) K_2CO_3-NaBr-ZnO after the reaction..... 91

Figure 6-1. Photograph of fresh 3 Å molecular sieves used in this work..... 97

Figure 6-2. The temperature profile for 3Å molecular sieves thermal activation..... 98

Figure 6-3. The structure (research aims and methods) of Chapter 6..... 99

Figure 6-4. The effect of the quantity of acetonitrile added in the one-pot synthesis of DMC.101

Figure 6-5. Effect of the amount of 3Å molecular sieves on the yield of each product. Reaction conditions: methanol (100 mmol), propylene oxide (33.3 mmol), catalyst (0.3 g), CO_2 (2 MPa), 160 °C, 5h..... 105

Figure 6-6. Influence of acid-base properties of zeolite on the initial transesterification rate for CLECs in *sc* fluids (Fontes *et al.*, 2001). The left and right dashed lines show reaction rate values without zeolite, at a_w = 0.75 and a_w = 0.25, respectively. pH-pNa represents the activity ratio of the two ions (H^+ and Na^+) which used to indicate the protonation state of acidic side chains *via* the exchange of Na^+ for H^+..... 107

Figure 6-7. Influence of amount of zeolite on the initial transesterification rate for CLECs in *sc* fluids (Fontes *et al.*, 2001). The zeolite 9.5 is used in the experiments..... 108

Figure 6-8. SEM images of the mixtures of catalyst and 3Å molecular sieves: (a) fresh K_2CO_3-NaBr-ZnO and 3Å molecular sieves mixture (b) spent K_2CO_3-NaBr-ZnO and 3Å molecular sieves mixture (c) higher magnification (6000x) image of fresh 3Å molecular sieves..... 110

Figure 6-9. The XRD patterns of fresh and spent catalysts: fresh K_2CO_3-NaBr-ZnO and 3Å molecular sieves mixture and K_2CO_3-NaBr-ZnO and 3Å molecular sieves mixture after reaction..... 111

Figure 6-10. The yield of each product and PO conversion of DMC synthesis reaction with the addition of different amounts of acetonitrile. Reaction conditions: methanol (100 mmol), propylene oxide (33.3 mmol), catalyst (0.3 g), CO_2 (2 MPa), 160 °C, 5 h..... 112

Figure 6-11. The chromatogram from GC-MS for the components exist in the conversion of PG reaction mixture. Reaction condition: Propylene glycol (60 mmol), acetonitrile (60 mmol), catalyst (0.3 g), CO_2 (2.0 MPa), 160 °C, 5h..... 114

Figure 6-12. The reaction mechanism of DMC synthesis reaction with the addition of acetonitrile..... 114

Figure 6-13. Photographic images of the products of reaction 1 and 2. Reaction 1 was carried out in presence of acetonitrile (66.66 mmol) and H_2O (33.33 mmol); Reaction 2 was carried out in presence of acetonitrile (66.66 mmol), methanol (100 mmol) and H_2O (33.33 mmol); Reaction conditions: catalyst (0.3 g), CO_2 (2 MPa), 160 °C, 5 h..... 116

Figure 6-14. The XRD patterns of fresh and spent catalysts: fresh K_2CO_3-NaBr-ZnO and K_2CO_3-NaBr-ZnO after reaction..... 117

Figure 6-15. (a) The effect of reaction time on PC and PG yield with the addition of acetonitrile and 3Å molecular sieves. (b) The effect of dehydrating agents on the catalytic efficiency. Reaction conditions: PO (60 mmol), acetonitrile (60 mmol), 3Å molecular sieves (0.7 g), catalyst (0.3 g), CO_2 (2 MPa), 160 °C, reaction time: 3 h,4 h or 5 h..... 118

Figure 6-16. (a) The effect of different PO adding amounts on the yield of each product in the DMC synthesis reaction with the addition 3Å molecular sieves. (b) The TOF calculation results of catalytic system with various PO adding amounts and 0.1g 3Å molecular sieves. Reaction conditions: methanol (100 mmol), 3Å molecular sieves (0.1g), catalyst (0.3g), CO_2 (2 MPa), 160 °C, 5h..... 119

Figure 6-17. (a) The effect of different PO adding amounts on the yield of each product in the DMC synthesis reaction with the addition of acetonitrile. (b) The TOF calculation results of catalytic system with various PO adding amounts and 0.57ml acetonitrile. Reaction conditions: methanol (100 mmol), acetonitrile (0.57 ml), catalyst (0.3 g), CO_2 (2 MPa), 160 °C, 5h.....120

Figure 7-1. Photographic images of fresh zinc powder used in the work.....124

Figure 7-2. Selectivity of each product and PO conversion of DMC synthesis reaction with the addition of different amounts of zinc powder. Reaction conditions: methanol (100 mmol), propylene oxide (33.3 mmol), catalyst (0.3 g), CO_2 (2 MPa), 160 °C, 5h.....130

Figure 7-3. (a) The effect of adding dehydrating agents and zinc powder on the selectivity of each product of DMC synthesis; (b) The effect of adding dehydrating agents on the catalytic efficiency. Reaction conditions: Methanol (100 mmol), PO (33.33 mmol), acetonitrile (0.57 ml), 3Å molecular sieves (0.1 g), catalyst (0.3 g), zinc powder (0.433 g), CO_2 (2 MPa), 160 °C, 5h..... 131

Figure 7-4. The effect of adding dehydrating agents and zinc powder at the same time on the selectivity of each product of DMC synthesis; Reaction conditions: Methanol (100 mmol), PO (33.33 mmol), acetonitrile (0.57 ml), 3Å molecular sieves (0.1 g), catalyst (0.3 g), zinc powder (0.433 g), 3Å molecular sieves (0.1 g), CO_2 (2 MPa), 160 °C, 5h..... 132

Figure 7-5. The FTIR spectrum of liquid products of reaction of: (a) $CH_3OH + CO_2 + Zn$ (b) $CH_3OH + He + Zn$..... 133

Figure 7-6. Yields of PG and PC in the cycloaddition reaction and the conversion of PO. Reaction conditions: PO (66.66 mmol), H_2O (44.44 mmol, reaction 3 and 4) or PG (11.11 mmol, reaction 5 and 6), catalyst (0.3 g), zinc powder (0.433 g), CO_2 (2 MPa), 160 °C, 5h.134

Figure 7-7. Molecular structure of 1,1-oxybis-2-propanol..... 134

Figure 7-8. (a) The yield of DMC, PG and PO and the conversion of PC in the transesterification reaction. (b) The activity of catalysts under various reaction conditions. Reaction conditions: 160 °C, 5 h, CO_2 (20 bar, reactions 7 and 8), Helium (20 bar, reaction 10 only), catalyst (K_2CO_3-NaBr-ZnO, 0.3 g), PC (33.3 mmol), methanol (100 mmol) and Zn powder (0.43 g)..... 136

Figure 7-9. The XRD patterns of solid reaction products resulting from (a) reaction with catalyst and $Mg(OCH_3)_2$, and (b) reaction with $Mg(OCH_3)_2$ only.....140

Figure 7-10. The XRD patterns of fresh and spent catalysts: (a) fresh K_2CO_3-NaBr-ZnO; (b) K_2CO_3-NaBr-ZnO after reaction; (c) fresh K_2CO_3-NaBr-ZnO and Zn powder mixture; and (d) K_2CO_3-NaBr-ZnO and Zn powder mixture after the reaction..... 143

Figure 7-11. SEM images of the solids resulting from reactions involving $Mg(OCH_3)_2$: (a) reaction with K_2CO_3-NaBr-ZnO catalyst, CO_2, propylene oxide, methanol and $Mg(OCH_3)_2$; (b) Higher magnification (6000x) image of identified region in (a); and (c) K_2CO_3-NaBr-ZnO catalyst before reaction (6000x).....145

Figure 7-12. Surface morphology of the catalyst and mixtures of catalyst and Zn powder. (a) the mixture of fresh catalyst and Zn (b) mixture of spent catalyst and Zn (c) spent zinc particles with a higher magnification (7000x) (d) new-formed particle with a higher magnification (7000x). 1-catalyst, 2-zinc powder, 3-new formed particle.....145

Figure 8-1. USAXS profile of catalysts (K_2CO_3-17.5 *wt.*%-ZnO) with various K_2CO_3 loadings. 156

Figure A-1. Calibration curve of dimethyl carbonate..... 174

Figure A-2. Calibration curve of propanol oxide.....175

Figure A-3. Calibration curve of propylene carbonate..... 175

Figure A-4. Calibration curve of propylene glycol.....176

Figure A-5. Calibration curve of by-products (1-methoxy-2-propanol and 2-methoxy-1-propanol)..... 176

Figure B-1. Photographic images of the product of DMC synthesis reactions with the addition of 3Å molecular sieves and the reaction is repeated twice. Reaction conditions: methanol (100 mmol), propylene oxide (33.3 mmol), catalyst (0.3 g), CO_2 (2 MPa), 3Å molecular sieves (0.1 g), 160 °C, 5h..... 177

Figure B-2. Photographic images of the product of DMC synthesis reactions with the addition of acetonitrile and the reaction is repeated twice. Reaction conditions: methanol (100 mmol), propylene oxide (33.3 mmol), catalyst (0.3 g), CO_2 (2 MPa), acetonitrile (1.14 ml), 160 °C, 5h. 178

List of Tables

Table 2-1. The applications of supported metal oxide catalysts in the industrial process.....17

Table 2-2. The applications of DMC as a green chemical.....29

Table 3-1. The reaction parameters applied in previous studies and this work.....44

Table 3-2. The parameters of HP-INNOWax column applied for GC-MS analysis.....45

Table 3-3. The setup parameters of GC-MS and the temperature program for analysis.....46

Table 3-4. Characteristic groups in different frequency regions.....48

Table 4-1. Catalysts previously applied in the one-pot synthesis of DMC, and CO_2 pressures employed.....60

Table 4-2. Catalysts used in the one-pot synthesis of DMC, and reaction time applied.....62

Table 4-3. The activity of catalysts under different reaction time.....66

Table 5-1. Properties of three types of alkali and NaBr.....78

Table 5-2. The techniques used for catalyst characterization and the set-up parameters for each technique.....81

Table 5-3. Elemental composition of the catalyst by EDX mapping analysis.....89

Table 5-4. Average crystalline size of particles before and after the reaction. '-' indicates that a crystalline phase is not observed in the diffractogram. '*' indicates that the corresponding peak is present but is beneath the size limit to accurately determine the crystallite size.....91

Table 5-5 (a). Composition of fresh and used catalysts, (12 *wt.*% K_2CO_3-17.5 *wt.*% NaBr-ZnO) as determined by AAS and ICP-OES.....92

Table 5-5 (b). ICP-OES analysis of Zn, K and Na in the liquid products after the reaction. Catalyst refers to 12 *wt.*% K_2CO_3-17.5 *wt.*% NaBr-ZnO.....92

Table 6-1. Typical properties of 3Å molecular sieves.....97

Table 6-2. The amount of acetonitrile added in the reaction system (PO molar amount: 33.33 mmol).....101

Table 6-3. The experiments design for studying the effect of reaction time on PC selectivity in cycloaddition.....102

Table 6-4. The amounts of propylene oxide added in the reaction system (methanol molar amount: 100 mmol).....103

Table 6-5. Techniques employed for the characterisation of solid samples..... 104

Table 6-6. Composition of the fresh and spent mixture of catalyst and 3Å molecular sieves by EDX spectroscopy..... 111

Table 6-7. The effect of methanol on the hydration of acetonitrile..... 115

Table 7-1. The molar ratio of propylene oxide and Zn powder and the corresponding amount of Zn powder added in the reaction..... 125

Table 7-2. Influence of the Zn powder on the cycloaddition reaction in the presence of PG or water.....126

Table 7-3. Influence of the Zn powder and CO_2 on the transesterification reaction..... 127

Table 7-4. Influence of the Zn powder and CO_2 on the transesterification reaction..... 128

Table 7-5. The content of four solid samples and the exact weight of each sample.....129

Table 7-6. Conversion of PO and selectivity of each product of DMC synthesis reactions...138

Table 7-7. Average crystalline size of particles before and after the reaction. '-' indicates that a crystalline phase is not observed in the diffractogram. '*' indicates that the corresponding peak is present but is beneath the size limit to accurately determine the crystallite size..... 144

Table 7-8. Elemental composition of the catalyst and the mixture of catalyst and zinc powder by EDX spectroscopy..... 146

Table 7-9a. Composition of fresh and used catalysts, (12 *wt.*% K_2CO_3 - 17.5 *wt.*% NaBr-ZnO) as determined by AAS and ICP-OES..... 147

Table 7-9b. ICP-OES analysis of Zn, K and Na in the liquid products after the reaction. Catalyst refers to 12 *wt.*% K_2CO_3 - 17.5 *wt.*% NaBr-ZnO..... 147

Table 8-1. The comparison of DMC selectivity between this work and former studies, and CO_2 pressures employed..... 155

List of Schemes

Scheme 2-1. The adsorption of metal or metal oxide on porous support (Marianna Cross, 2016)..... 15

Scheme 2-2. Two routes used for FA synthesis (Peng *et al.*, 2012)..... 22

Scheme 2-3. Reaction scheme of CO_2 conversion to propylene carbonate through Zn-based catalyst (Ramin *et al.*, 2006)..... 26

Scheme 2-4. The synthesis of PC over chitosan-supported quaternary ammonium salt catalysts (Zhao *et al*., 2007)..... 27

Scheme 2-5. Reaction routes for DMC synthesis: (I)phosgene route, (II) oxidative carbonylation route, (III) two-stage route with CO and NO, (IV) transesterification of cyclic carbonate from methanol and (V) direct synthesis from CO_2 and methanol (Honda *et al.*, 2014)..... 31

Scheme 2-6. One-step synthesis of DMC (Li *et al.*, 2015)..... 32

Scheme 2-7. The route of one-step synthesis of DMC (Li *et al.*, 2015)..... 34

Scheme 2-8. The route of DMC synthesis from acetals and CO_2 (Sakakura *et al.*, 1998)..... 36

Scheme 2-9. Reaction pathway of one-pot synthesis of DMC..... 37

Scheme 4-1. Proposed mechanism for the synthesis of propylene carbonate from propylene oxide and carbon dioxide (Álvarez *et al.*, 2017; Wang, Xie and Deng, 2014; Martínez-Ferraté *et al*., 2018)..... 70

Scheme 4-2. (a) Adsorption of methanol onto ZnO-based catalyst; (b) Adsorption of propylene carbonate onto ZnO-based catalyst (Kähler, Kevin *et al.,* 2010)..... 71

Scheme 4-3. Proposed mechanism for the synthesis of dimethyl carbonate from propylene carbonate and methanol (Murugan and Bajaj, 2010)..... 72

Scheme 4-4. Proposed reaction mechanism for the hydrolysis of propylene oxide under base-catalyzed reaction (Woods, 1990)..... 72

Scheme 4-5. Adsorption of propylene oxide onto ZnO-based catalyst (Timofeeva *et al*., 2016)..... 73

Scheme 4-6. Proposed reaction mechanism for the formation of by-products in the synthesis of DMC (Timofeeva *et al*., 2016)..... 73

Scheme 6-1. The formation of propylene carbonate from propylene glycol and CO_2 (Tomishige *et al*., 2004)..... 106

Scheme 6-2. The reaction of propylene oxide and methanol with acidic or basic catalyst (Liang *et al.,* 2010). The product of base-catalysed reaction is 1-methoxy-2-propanol (Route (a)) and the product of acid-catalysed reaction is 2-methoxy-1-propanol (Route (b))..... 109

Scheme 6-3. The reaction mechanism of the hydration of acetonitrile under acidic condition.112

Scheme 6-4. The formation of methyl carbamate and methanol by the reaction of DMC and NH_3.....113

Scheme 6-5. The formation of methyl acetate from the reaction of acetamide and methanol.114

Scheme 6-6. The formation of urea from the reaction of ammonia and CO_2..... 116

Scheme 7-1. The possible reaction mechanism for the formation of by-product (1,1-oxybis-2-propanol) of cycloaddition in the presence of zinc powder..... 134

Scheme 7-2. The proposed reaction mechanism for the formation of propylene carbonate *via* cycloaddition reaction in the presence of zinc powder..... 135

Scheme 7-3. Proposed mechanism for the synthesis of dimethyl carbonate from propylene carbonate and methanol..... 136

Scheme 7-4. The proposed reaction mechanism for the formation of by-products in the synthesis of DMC from propylene oxide, CO_2 and methanol..... 139

Scheme 7-5. Proposed mechanism for the cycloaddition reaction with $Mg(OCH_3)_2$ (adapted from the reaction mechanism for copolymerization of epoxides and CO_2 using alkoxide catalyst (Bahramian and Dehghani, 2016)..... 141

Scheme 7-6. Proposed mechanism for the reaction with $Mg(OCH_3)_2$ when using K_2CO_3-NaBr-ZnO as catalyst (adapted from the reaction mechanism of $Mg(OCH_3)_2$-promoted reactions, proposed by Eta (Eta *et al.*, 2010)..... 142

Scheme 7-7. Proposed new mechanism for DMC synthesis with the addition of Zn powder.149

List of Abbreviations

-C≡N	Cyano group
-CH_3O	Methoxy group
-HCO_3^-	Bicarbonate ion
-$OCOCH_3$	Ester group
1m2p	1-methoxy-2-propanol
2m1p	2-methoxy-1-propanol
AAS	Atomic absorption spectroscopy
Ac-Phe	Acetyl-l-phenylalanine
Al_2O_3	Aluminium oxide
$AlCl_3$	Aluminium chloride
Au	Gold
BET	Brunauer–Emmett–Teller
BJH	Barrett-Joyner-Halenda
BSE	Back-scattered electrons
$Bu_2Sn(OMe)_2$	Dibutyl(dimethoxy)stannane
Bu_4NBr	Tetrabutylammonium bromide
C=O	Carboxyl
C_2H_4	Ethylene
C_3H_6	Propylene
C_4H_8	Butylenes
C_5H_{10}	Cyclopentane
C_6H_{12}	Cyclohexane
$CH_3(CO)NH_2$	Acetamide
CH_3CN	Acetonitrile
CH_3COOCH_3	Methyl acetate
CH_3COOH	Acetic acid
$CH_3O(CO)NH_2$	Methyl carbamate
CH_3OH	Methanol
CH_4	Methane
CHFS	Continuous hydrothermal flow synthesis
CMM	Carbonated magnesium methoxide
Co	Cobalt
CO	Carbon monoxide
$CO(NH_2)_2$	Urea
CO_2	Carbon dioxide
CO_2-TPD	CO_2-Temperature programmed desorption
CO_3^{2-}	Carbonate ion
$COCl_2$	Phosgene
COFs	Covalent organic frameworks
Cr_2O_3	Chromic oxide
CS	Chitosan
CZM	Carbonated zinc methoxide
DMC	Dimethyl carbonate
DME	Dimethyl ether
DMS	Dimethyl sulfate
DTG	Derivative thermogravimetric curve
EC	Ethylene carbonate
EO	Ethylene oxide

Et_4NBr	Tetraethylammonium bromide
FA	Formic acid
Fe_3C	Cementite
Fe_3O_4	Ferroferric oxide
FT-IR	Fourier transform-Infrared spectroscopy
FTS	Fischer-Tropsch synthesis
FWHM	Full width at half maximum
Ga_2O_3	Gallium(III) oxide
GC-FID	Gas chromatography-Flame ionization detector
GC-MS	Gas chromatography-Mass spectrometry
HCl	Hydrogen chloride
$HCOOCH_3$	Methyl formate
HNO_3	Nitric acid
HSAB	Hard and soft acids and base
ICP-OES	Inductively coupled plasma-Optical emission spectroscopy
Ir	Iridium
K_2CO_3	Potassium carbonate
K_2O	Potassium oxide
KBr	Potassium bromide
KCl	Potassium chloride
$KHCO_3$	Potassium bicarbonate
KI	Potassium Iodide
KNO_3	Potassium nitrate
KOH	Potassium hydroxide
LAO	Linear alpha olefin
LIB	Lithium-ion battery
$Mg(OCH_3)_2$	Magnesium methoxide
$Mg(OH)_2$	Magnesium hydroxide
MgO	Magnesium oxide
MoO_3	Molybdenum oxide
MTBE	Methyl tert-butyl ether
N_2O	Nitrous oxide
Na_2CO_3	Sodium carbonate
Na_2O	Sodium oxide
NaBr	Sodium bromide
NaCl	Sodium chloride
NaOH	Sodium hydroxide
Nd_2O_3	Neodymium oxide
NEt_3	Triethylamine
NH_3	Ammonia
Ni	Nickel
OH^-	Hydroxyl ion
Pb	Lead
PC	Propylene carbonate
PG	Propylene glycol
PO	Propylene oxide
Pt	Platinum
Rh	Rhodium
RWGS	Reverse water gas shift
RT	Room temperature
SE	Secondary electrons

SEM	Scanning electron microscopy
SEM-EDX	Scanning electron microscopy-Energy Dispersive X-Ray Spectroscopy
SiO_2	Silicon dioxide
TCD	Thermal conductivity detector
TG	Thermogravimetric curve
TGA	Thermogravimetric Analysis
TiO_2	Titanium dioxide
TOF	Turnover frequency
TON	Turnover number
TMM	1,1,1,trimethoxymethane
TSA	Temperature swing adsorption
USAXS	Ultra-Small-Angle X-Ray Scattering
V_2O_5	Vanadium pentoxide
WD	Working distance
WO_3	Tungsten trioxide
XRD	X-ray Diffraction
$Zn(OCH_3)_2$	Zinc methoxide
$Zn(OH)_2$	Zinc hydroxide
ZnO	Zinc oxide
ZrO_2	Zirconium dioxide

CHAPTER 1

INTRODUCTION

Chapter 1: Introduction

1.1 Motivation

Carbon dioxide is one of the major greenhouse gases and is generated from coal-fired power plants, chemistry industries, transportations *etc*. The global average atmospheric CO_2 has increased from 367 parts per million (ppm) in 1992 to approximately 410 ppm in 2019 (NOAA/NCEI, 2019). Without innovative and more ambitious policies and techniques, carbon dioxide emission is projected to reach almost 685 ppm by 2050 (Marchal and Dellink, 2011). Increasing carbon dioxide concentration in the air will accelerate global warming, which is the most significant environmental challenge that society needs to face today.

CO_2 is non-toxic, tasteless, and relatively cheap. However, it is also equipped with some properties (such as high stability and low reactivity) which makes it difficult to be widely used as a chemical feedstock in industry. In recent years, many studies have indicated that the synthesis of useful chemicals from CO_2 could be a promising field for future sustainable development. CO_2 is a C1 block for the production of fundamental and one of the highly in-demand chemicals. These chemicals may include methanol, epoxides, cyclic carbonates, formats and dimethyl carbonate (DMC) *etc*. (Liu *et al.*, 2016). During synthesis processes, homogeneous and heterogeneous catalysts are essential to promote the reaction towards the objective direction. Typically, the selectivity and activity of homogeneous catalysts are higher than that of heterogeneous. However, the complicated and costly separation process of homogeneous reactions increases the production cost. Therefore, it is necessary to explore and develop the novel heterogeneous catalysts for CO_2 utilisation equipped with enhanced activity and selectivity.

In this research, dimethyl carbonate (DMC) is chosen as the target product owing to its extensive application in a variety of processes, such as replacing phosgene as a methoxycarbonylating agent (F. Aricò & P. Tundo, 2010), application as a methylating agent (Selva, Marques & Tundo, 1994), replacing methyl tert-butyl ether (MTBE) as a gasoline additive *etc.*(Pacheco & Marshall, 1997). A modified heterogeneous catalyst is applied in the synthesis of DMC under low CO_2 pressure condition.

1.1.1 Source of carbon dioxide emissions

The primary human sources for atmospheric CO_2 emissions are fossil fuel combustion, industrial processes and land-use changes *et al.* (Le Quéré *et al*., 2014).

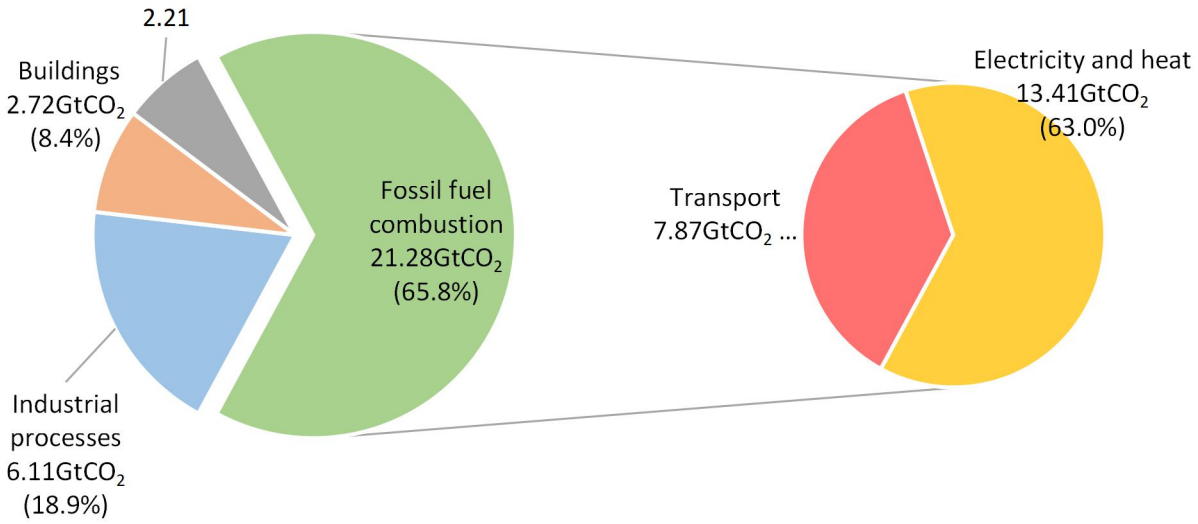

Figure 1-1. The sources of global CO_2 emissions in 2016 (yearly total emission: 32.5 $GtCO_2$) (Iea.org, 2019).

Figure 1-1 shows the primary sources of global CO_2 and their yearly emissions in 2016 (Iea.org, 2019). The combustion of fossil fuels produces a large amount of carbon dioxide emission. A more detailed description of the main sources of CO_2 emissions is shown below:

(1) Electricity and heat generation. CO_2 emissions are increasing because of the higher consumption of energy, which caused by the rapid development of the economy and the improvement of weather conditions in some areas.

(2) Transportation. A large amount of CO_2 emissions accompanies the combustion of diesel and gasoline. Transportation includes long-distance road transport, air transport, marine transportation and rail.

(3) Industry. Fossil fuels are consumed in industrial production to provide energy. There are some processes also producing carbon dioxide emissions by chemical reactions that do not burn fuel, such as cement production, iron and steel manufacturing and chemicals production.

1.1.2 The hardest emissions to cut

The current environmental degradation problem has attracted more and more attention, which leads to the increasing use of renewable and cleaner energy in industrial production and transportation. However, fossil fuel combustion is still the primary source of energy generation in rapidly developing economies. The contradiction between increasing energy demand and reducing carbon dioxide emissions has become a vital problem for society.

Davis *et al.* reported that the hard-to-eliminate sources account for around 27% (~ 9.2 $GtCO_2$) of global CO_2 emissions from fossil fuel and industrial processes in 2014 (Davis *et al.*, 2018). These sources relate to aviation, long-distance transportation and the production of cement and steel (Figure 1-2 (B).

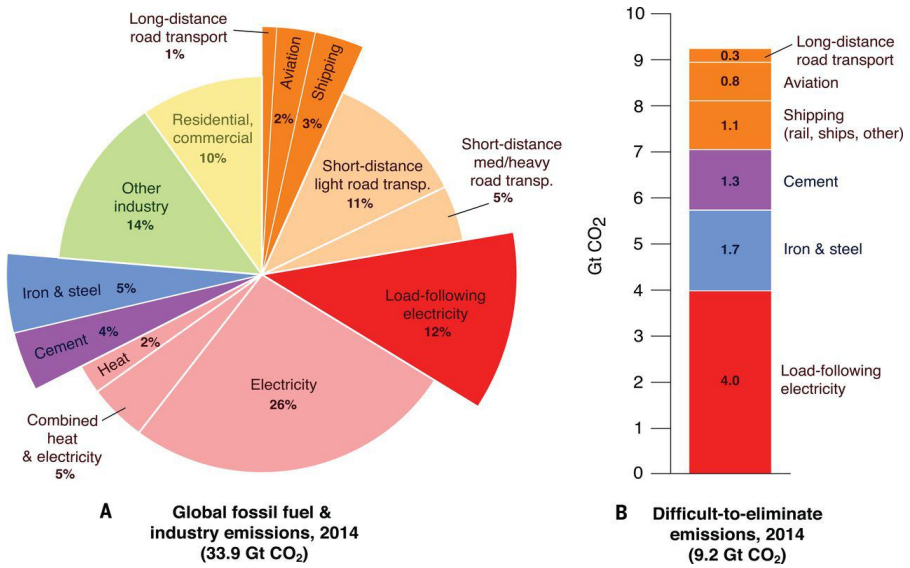

Figure 1-2. (A) shows the different sources of CO_2 emissions with the highlighted (by longer pie pieces) hard-to-cut emissions sources in 2014. Figure 1-2 (B) illustrates the level of emissions related to these hardest decarbonized energy services in 2014. (Source: Davis *et al.*, *Science)*

It is reported that 60% of the carbon dioxide emitted from the cement industry is produced by the calcination of limestone, and the remaining 40% of the carbon dioxide comes from the burning of fossil fuels (Dean, Dugwell and Fennell, 2011). Scientists have tried to reduce the carbon dioxide intensity of cement by the following methods: (1) using mineral admixtures instead of clinker (2) improving energy efficiency (3) using CO_2-neutral fuels (such as biomass). However, these approaches can only be limited to reducing, not eliminating carbon dioxide emissions because the calcination of limestone is the leading cause of carbon dioxide generation which cannot be dealt with the above approaches. The development of carbon

capture and storage technologies may be a potential solution for reducing net carbon dioxide emissions of cement.

1.1.3 Managing carbon dioxide emissions

In general, CO_2 emissions can be controlled in three ways: (1) reducing CO_2 production from the source, (2) using carbon capture and storage techniques, (3) increasing CO_2 utilisation. Decreasing the production of CO_2 can be achieved by reducing the use of fossil fuels, modifying the processes to higher efficiency and using clean and renewable energy. However, factors like population growth, higher agricultural and transportation demands, economic benefits and technical problems make it difficult to reach a reduction in CO_2 emission from the source.

Carbon capture and storage provides an alternative way to reduce CO_2 emissions. This method includes three steps: capturing CO_2 from sources (such as a power station), compressing and transporting the gas, and finally injecting the gas into the ground under high pressure for storage. This method can effectively reduce CO_2 emissions into the atmosphere, but it is associated with a high cost for construction, maintenance and operation. Moreover, there are many technical problems waiting to be overcame. For example, gas separation, compression and transportation consume a large amount of energy, advanced technology for CO_2 adsorption and desorption is needed. And there is a high risk of long-term preservation of CO_2 below ground. Therefore, the use of CO_2 becomes a much promising alternative, not only reducing the CO_2 intensity of air but also producing valuable products.

1.2 Carbon dioxide conversion and utilisation

1.2.1 The present and future usage of CO_2

The utilisation of CO_2 is a possible way to control the carbon level in the atmosphere. Currently, the actual utilisation of CO_2 as a feedstock for chemicals production is around 230 $MtCO_2$ per year. Most of CO_2 is consumed in the fertiliser industry, where 130 $MtCO_2$ is used in urea manufacturing, followed by oil and gas, with a consumption of 70 to 80 $MtCO_2$ for enhanced oil recovery (Putting CO_2 to Use: Creating Value from Emissions, 2019). CO_2 conversion to chemicals will not use a large percentage of CO_2 generated but will contribute to making capture more economically viable by producing valuable products and reduce our reliance on fossil sources for chemicals production. With the development of new techniques and processes, the proportion of CO_2 utilised will increase. There are lots of future estimates

about the potential of carbon dioxide. About 200 Mt of CO_2 per year will be used to produce chemical products and polymers, and approximately 2 $GtCO_2$ per year will be applied in the manufacture of fuels (Naims, 2016). There is a long-term estimate suggesting that nearly 15% of global CO_2 emissions will be utilized per year by 2030 (The Global CO_2 Initiative & CO_2 Sciences, 2016).

1.2.2 Potential applications of CO_2

Carbon dioxide has been used in many industrial processes such as the production of plastics, urea and cyclic carbonates. In addition to the physical or chemical transformation of CO_2, carbon dioxide can be used directly as a solvent or working fluid (Figure 1-3). Current research on carbon dioxide applications has focused on exploring new transformation processes to convert CO_2 into feedstocks for efficient manufacturing.

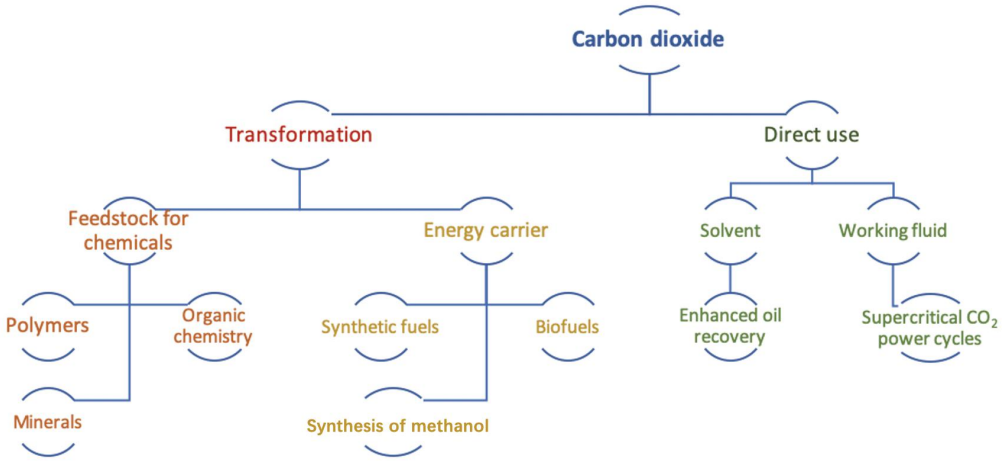

Figure 1-3. The physical and chemical routes for CO_2 utilisation (Source: The potential and limitations of using carbon dioxide, 2017).

1.2.3 The challenges for CO_2 application

Many studies have shown that CO_2 can potentially convert into value-added chemicals or fuels through physical or chemical processes, whereas many obstacles and challenges still remain in the development of CO_2 utilisation. As a result, the realisation of carbon dioxide utilisation in actual industrial production is quite complicated, and the progress is relatively slow. Specific challenges and barriers include the following three categories: technology, markets, and policies (Ahmad, 2016). The main challenges and obstacles in the market and technology fields are discussed here.

(1) Market and economic challenges: Firstly, high economic input is requested during CO_2 capture, separation, and transportation processes (Leung, Caramanna and Maroto-Valer, 2014). Secondly, the potential economic benefit of CO_2 conversion is difficult to estimate because the technology for utilisation is at an early stage of development (Cuéllar-Franca and Azapagic, 2015). The manufacturing processes of the factory have been well established, and the re-use of CO_2 requires updating existing systems. Based on the above reasons and economic benefits, the lack of economical driving force is one of the critical barriers to accelerate the development of CO_2 utilisation.

(2) Technical challenges: First, carbon dioxide is very stable, and it requires a large amount of energy to convert it into other substances through chemical or catalytic methods. The combustion of fossil fuels will generate new pollution. The development of techniques which can transfer primary non-fossil sources (like solar energy) into more usable kind of energy (like hydrogen and electricity) is needed to support the transformation of a large amount of CO_2 (Aresta, Dibenedetto and Angelini, 2013). Second, it is necessary to find more efficient and renewable catalysts. The ideal catalyst is expected to convert CO_2 to the target product in a favourable environment, such as at lower temperatures, under lower pressures, with more efficient performance (like selectivity and reaction rates) and with lower economic input.

From the above analysis, it can be concluded that the development of novel technologies cannot solve the obstacles of CO_2 utilisation fundamentally. However, innovative and efficient technology is indeed a prerequisite for addressing economic and policy barriers. Only by mastering the mature technologies can we enhance the driving force of social policies and markets for the development of CO_2 utilisation.

1.3 Aims of the research

The initial goal of this study is to improve the selectivity of dimethyl carbonate (DMC) *via* the one-pot synthesis route. The research aims of this thesis are summarised as follows:

- To evaluate the catalytic activity of alkali halide-based catalysts through the one-pot synthesis of DMC;
- To improve the selectivity of DMC by adding dehydrating agents or co-catalyst;
- To study the relationship between physical properties and the catalytic performance of the catalyst;

- To develop the proposed mechanism of the DMC synthesis reactions.

1.4 Structure of the thesis

Chapter 1 Introduction. This chapter provides the motivation for carrying out this research work. A brief introduction about the sources of CO_2 emissions, the potential application of CO_2 and the challenges in CO_2 application is presented to give the background information about this research. Additionally, it introduces the aims and objectives of this work and the structure of this thesis.

Chapter 2 Literature review. Chapter 2 focuses on the introduction of heterogeneous catalysts and catalytic transformations of CO_2. Specifically, the types of heterogeneous catalysts are discussed, and the different routes for the catalytic transformation of CO_2 to chemicals and fuels are presented. Moreover, a detailed review of dimethyl carbonate (DMC), the properties and applications of DMC in industry and the different approaches for DMC synthesis are provided. The catalysts applied in the one-pot synthesis of DMC are discussed in the subsequent section in greater detail.

Chapter 3 Experimental work and analytical techniques. In this chapter, the experimental set-up employed and the analytical techniques used for studying the composition of liquid products and the properties of catalysts are introduced. Moreover, the overall experiment plan of research work is presented and then followed by the methods used to analyse experimental errors.

Chapter 4 One-pot synthesis of DMC using alkali halide-ZnO catalysts. This chapter shows the activity of four types of alkali metal-ZnO catalysts (NaBr-ZnO, KBr-ZnO, NaCl-ZnO and KCl-ZnO) in the one-pot synthesis of DMC under mild reaction conditions (2.0 MPa CO_2, 160 °C and 5 h reaction time). This is followed by discussion of the results of catalyst characterisation. Thermogravimetric Analysis (TGA) is used to determine the thermal stability of the catalyst. X-ray diffraction (XRD) are used to study the composition of active ingredients on the catalyst surface. Furthermore, the catalytic principle of the alkali metal catalyst on cycloaddition reaction and transesterification reaction is discussed, which provides the theoretical basis for the catalyst improvement in Chapter 5.

Chapter 5 Catalyst modification: Influence of alkali metals. According to discussion of the catalyst mechanism in Chapter 4, this chapter studies the improvement of catalytic activity by loading a strong base. During catalyst preparation, NaBr and a kind of alkali metal are simultaneously supported on the catalyst support by using a wet impregnation method. The three strong bases include sodium carbonate, sodium hydroxide, and potassium carbonate. Additionally, the effect of the strong base loading on the selectivity of each product is studied and six catalysts with different base loading are prepared (8 *wt*%, 10 *wt*%, 12 *wt*%, 15 *wt*% and 18 *wt*%). The modified catalysts are characterised by using the following techniques: TGA, SEM-EDX, XRD, AAS and ICP-OES. Scanning electron microscopy (SEM) gives the detailed information on the morphology of catalyst. SEM-EDX is used to study the effect of calcination on the distribution of active ingredients. ICP-OES and AAS analysis of both solid and liquid samples is carried out to provide the information of elemental composition.

Chapter 6 Influence of dehydrating agents on DMC selectivity. The hydrolysis of PO to PG is the main reason to limit the DMC production due to equilibrium. This chapter discusses the effects of physical (3Å molecular sieve) and chemical (acetonitrile) dehydrating agents on the selectivity of DMC and PG. Moreover, the influence of the amounts of dehydrating agent on DMC yield and the dehydration efficiency of these two dehydrating agents are specifically studied. Furthermore, the advantages and disadvantages of these two dehydrating agents are presented.

Chapter 7 One-pot synthesis of DMC using a Zn-promoted metal alkali catalyst. According to the results in Chapter 6, the shortcomings of the two dehydrating agents limit their application in DMC production. There are two reasons for using zinc powder as a potential high-efficiency dehydrating agent in this chapter: (1) Zinc powder is solid, which is easy to separate from the product after the reaction; (2) Zinc powder can react with water under high temperature conditions. Therefore, zinc powder may have the advantages of both physical and chemical dehydrating agents. In order to better study the role of zinc powder in DMC synthesis, the effects of zinc powder on cycloaddition reaction and transesterification reaction are studied separately. Fresh and used catalyst and the catalyst-zinc powder mixture are characterised by using SEM, XRD, atomic absorption spectroscopy (AAS) and inductively coupled plasma-optical emission spectroscopy (ICP-OES). Furthermore, the reaction mechanism of Zn powder involved reaction is discussed.

Chapter 8 Conclusions and suggestions for future work. The general conclusions from Chapters 4 to 7 are summarized and the positive effects of zinc powder on improving DMC selectivity are highlighted. Suggestions for further research work are illustrated in this chapter.

Reference This chapter lists the references to the literatures cited in this thesis.

Appendices This chapter includes calibration curves used in GC-MS quantitative analysis and some supporting materials related to this research work.

CHAPTER 2

LITERATURE REVIEW

Chapter 2 Literature review

2.1 Introduction

The main components of greenhouse gases are methane (CH_4), nitrous oxide (N_2O) and carbon dioxide (CO_2) and ozone (Brander, 2012). Carbon dioxide (CO_2) is commonly discussed as the most important greenhouse gas and a significant contributor to global warming. The Kyoto Protocol is an international treaty controlling the release of greenhouse gases from human activities. These greenhouse gases are often referred to as "Kyoto gases". The "global warming potential" (GWP) of a greenhouse gas is an index, which represents the amount of warming caused by the gas over a given period of time (typically 100 years). The index value of CO_2 is 1, and the GWP of other GHGs is a multiple of the number of warming they cause than CO_2 (25 for CH_4 and 298 for N_2O, respectively).

Recently, the use of CO_2 as a raw material for the synthesis of valuable chemicals using active catalysts has received increased attention. Heterogeneous catalysts have been widely studied and applied in the industry because they are easy to separate and recycle in the flow reaction system. This chapter gives a comprehensive overview of the types and applications of heterogeneous catalysts, the conversion of CO_2 into value-added chemicals and different routes for DMC synthesis using various heterogeneous catalysts. The problems and challenges in each DMC synthesis route and the evaluation of catalysts applied will also be presented.

2.2 Heterogeneous catalysts

Heterogeneous catalysis describes a reaction where the catalyst and the reactants are in different phases. The catalyst is usually in the solid-state, and the reactant is a gas or liquid phase. In this section, the dynamic reaction theories of heterogeneous catalysts are discussed. Moreover, the application of heterogeneous catalysts in carbon dioxide utilisation is also discussed, especially for DMC synthesis. Generally, heterogeneous catalysts can be sorted into unsupported catalysts and supported catalysts.

2.2.1 Reaction theories of heterogeneous catalysts

Regarding the process of heterogeneously catalysed reaction, the transient adsorption of one or more reactants to the catalyst surface, the physical and chemical adsorption and desorption

of the products from the surface are of equal significance as the actual chemical process. To better understand the catalytic mechanism and to improve catalytic activity through catalyst modification, three groups of catalytic theories have been applied to describe the dynamics of the catalytic process.

(1) The geometrical theory emphasizes that it is crucial to describe the correspondence between the geometrical configuration of active atom on the catalyst surface (especially for coarser particles) and structure of the reacting molecules adsorbed on the catalyst (Strizhak *et al.*, 2011). There are two effective geometric methods. Firstly, the reaction rates on various crystal surfaces of metal are altered in line with geometry. It can be used to control the reaction rate (Boudart, 1969). Secondly, the specific catalytic activity may be significantly changed by modifying the properties of catalyst surface such as the dispersion of active sites and the degree of crystallinity. In other words, the selectivity of a catalyst is primarily influenced by its particle size, structure and other related variables (Boreskov, 1986).

(2) The electronic structure theory explains the relationship between catalytic and electronic properties of heterogeneous catalysts (especially transition metal catalyst). Correctly, the catalytic activity of transition metal-based catalysts is mostly decided by its ability to form covalent bonds with surrounding atoms (Nilsson *et al.*, 2005). Figure 2-1 shows the definition of electron shells and the electron distribution of each shell. Unpaired electrons, formed on the outer d-shells or generated by the transition of electrons from s-shell to d-shell, pair up with adsorbate to form valence bonds. Generally, more free valence electrons presented on catalyst surface facilitate the formation of reaction intermediate. In other words, the catalytic activity of the catalyst is primarily determined by the availability of charge carriers (electrons or holes) on the catalyst surface.

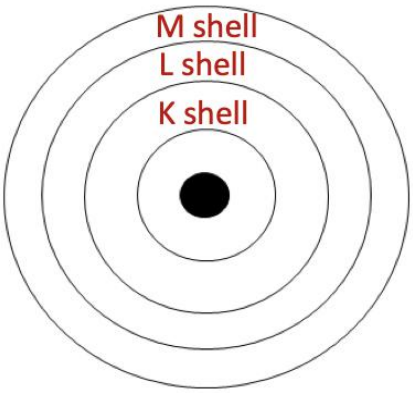

A

Shell name	Subshell name	Subshell max electrons	Shell max electrons
K	1s	2	2
L	2s	2	8
	2p	6	
M	3s	2	18
	3p	6	
	3d	10	

B

Figure 2-1. The definition of electron shells of metal atoms and the electron distribution of each shell.

(3) The chemical theories insist that catalyst can be regarded as a chemical intermediate, which generates an unstable, surface, transitory complex with reactants. The specific adsorption process is as follows (Scheme 2-1):

a. ***Diffusion***- substrates move toward the catalyst surface;
b. ***Physisorption***- reactants adhere to the surface through weak interaction (such as van der Waals force);
c. ***Chemisorption***- there are chemical bonds formed between the reactants and the surface;
d. ***Surface diffusion***- bound substrates migrate to active sites on the surface of catalyst, which is also known as ***Migration***;
e. ***Reaction***;
f. ***Desorption***-the desorption of products from catalyst surface;
g. ***Diffusion***- products released from the surface.

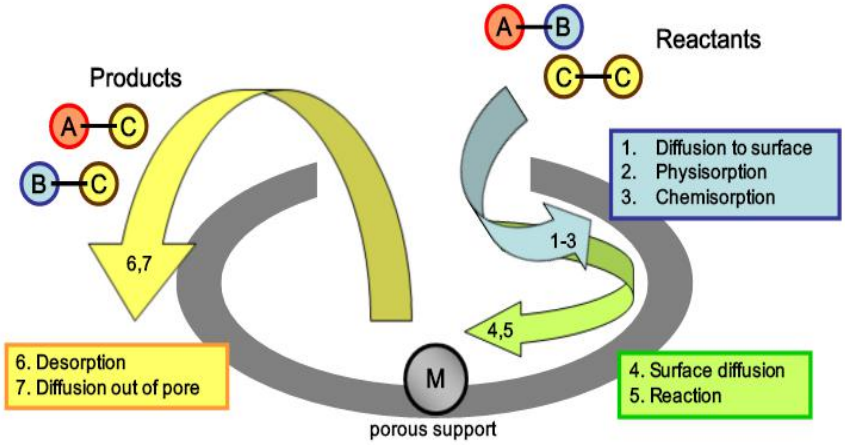

Scheme 2-1. The adsorption of metal or metal oxide on porous support (Marianna Cross, 2016).

It is difficult to use one theory to explain all dynamic changes in the catalytic activity, and all these theories should be taken into account when analysing the structure and properties of catalysts and discussing the chemisorbed species and bonding behaviours during catalytic progress. For instance, the 'reaction' step in the 3rd theory can be explained by the other theories in more detail when describing the mechanism of specific catalytic reaction. An active heterogeneous catalyst accelerates reaction close to equilibrium but does not change the equilibrium. The catalyst selectivity may be related to its capacity to direct one reaction to its equilibrium but has little or no influence on alternate its pathway so that the stable intermediate is not necessarily generated. Selectivity is mainly determined by selective chemical adsorption of the catalyst. Consideration of modifying the surface properties of the catalyst may be a promising method to find a better-performed catalyst.

2.2.2 Un-supported (bulk) catalysts

In large scale processes, most solid catalysts applied in industry are prepared by supporting active ingredients on metal oxides or porous carriers, only a few catalysts are composed of a single component, like pure metals (platinum-rhodium grids used to oxidise ammonia) (Harbord, 1974) or simple binary oxides (*e.g.* VO_x-TiO_2 used in NO_x reduction catalysis) (Kwon, Park and Hong, 2015). This section gives a brief introduction about the species and applications of bulk catalysts. The following two types of bulk catalysts are discussed.

2.2.2.1 Metal oxides

Metal oxides are one of the major and essential components of catalytic materials with high activity. The catalytic properties of metal oxide catalysts are decided mainly by the bonding character between metal and oxygen atom, the composition and structure and the coordination

of surface atoms and the hydroxyl groups (-OH) in exposed faces of terminating crystal (Deutschmann *et al.*, 2009). Some metal oxide catalysts consisting of simple composition (like binary oxide) and multicomponent materials are illustrated below.

- Simple Binary oxides

Pure binary oxides may act as solid acids or bases or amphoteric catalysts or catalyst supports. The dissolution behaviour in aqueous solution most importantly decides their catalytic properties. For example, acidic oxides (like SiO_2) form acids or anions during dissolution process. Basic oxides (*e.g.* MgO) form hydroxides or dissolve with the formation of base or cations. And amphoteric oxides (*e.g.* ZnO and Al_2O_3) generate cations and anions in acidic and basic solutions respectively (Deutschmann *et al.*, 2009).

- Complex multi-component oxides

Complex multi-component oxide is another type of major metal oxide catalytic material. Zeolite is one of the most critical metal oxide catalysts in the petrochemical industry in regard to the uniform and complex microporous structure, high stability and excellent catalytic performance. The three-dimensional framework structure of the zeolite consists of a SiO_4 and AlO_4 tetrahedron, each of which includes a silicon or aluminium atom in the centre. The empirical formula of zeolite is $M_{2/n}\cdot Al_2O_3\cdot xSiO_2\cdot yH_2O$.

Zeolites are also applied in the practical manufacturing industry, such as catalysis, gas separation and ion exchange. The main reason is that the fine pore structure allows the adsorption separation to be performed based on the molecular size and shape, so that zeolite catalysts can be regarded as molecular sieves (Kletnieks *et al*., 2007). The basic properties of zeolites can be optimized by ion exchange, such as the synthesis of adsorbents with excellent selectivity. Ion exchange performance can also improve the flexibility of catalyst synthesis. For example, the formation of highly dispersed metal catalysts (Nezamzadeh-Ejhieh and Moeinirad, 2011). In addition, zeolite performs exceptionally high activity in different acid-catalysed reactions like cracking (Anbazhagan, Kumaran and Sasidharan, 2010).

2.2.2.2 Metals and metal alloys

Un-supported metal and metal alloys catalysts are applied in only a few cases, in which hydrogen is involved in the reaction, *e.g.* hydrogenolysis, hydrogenation and catalytic

reforming. The catalysts applied in these reactions have been discussed in many studies and include iron for ammonia synthesis and Fischer-Tropsch reaction (Ma *et al.*, 2015), and nickel for steam reforming and methanation (Radfarnia and Iliuta, 2014). Metal catalysts are useful for oxidation reactions as well. For instance, platinum-rhodium wire gauze for the partial conversion of ammonia to nitric oxide or the oxidation of a mixture of methane, ammonia, and the air to hydrogen cyanide (Busby and Trimm, 1979). Mostly, the metal surface area is one of the most critical factors affecting the catalytic efficiency because the rate of the catalytic reaction is determined by the number of exposed metal atoms which is known as percentage exposed (Adamska *et al.*, 2012).

2.2.3 Supported catalysts

Supported catalysts have been applied in many industrial processes on account of their relatively higher activity and efficiency compared with bulk catalysts. In an active component-support interaction, the role of support is to give high surface area and stabilize the dispersion of the active phase. The support is sometimes actively involved in the reaction process. A typical example is bifunctional catalysts in which the support and active component interact with each other. In this section, four types of supported catalysts are discussed below.

2.2.3.1 Supported metal oxide catalysts

A typical supported metal oxide catalyst is composed of at least one active metal oxide phase immobilised on the surface of an oxide carrier. The active components could be transition metal oxides, and the carrier oxides usually include transitional Al_2O_3, SiO_2, TiO_2, ZrO_2 *etc*. Example applications of supported metal oxide catalysts are shown in Table 2-1.

Table 2-1. The applications of supported metal oxide catalysts in the industrial process.

Catalysts	Applications	References
V_2O_5-TiO_2	Selective oxidation of *o*-xylene to phthalic anhydride;	(Vedrine, 1994)
	Ammoxidation of alkyl aromatics to aromatic nitriles	(Piumetti *et al.*, 2012)
V_2O_5-Al_2O_3	Ammoxidation of alkyl aromatics to aromatic nitriles	(Piumetti *et al.*, 2012)
V_2O_5-MoO_3-TiO_2	Reduction of NO_x emissions with NH_3 (stationary	(Prins, 1997)
V_2O_5-WO_3-TiO_2	power plants)	
Cr_2O_3-Al_2O_3	Dehydrogenation of alkane; Dehydrocyclization of *n*-	(Buonomo, Sanfilippo
Cr_2O_3-ZrO_2	heptane to toluene	and Trifiro, 1997)

The advantage of using the transition metal oxides as mentioned above as carriers is that they have lower surface free energies than a typical carrier, thereby facilitating the dispersion of the active component onto the surface of the support to form a highly dispersed active oxide overlayer.

2.2.3.2 Surface-modified oxides

The dispersion of modifiers can modify the acidity or basicity of the surface of oxides. For example, the incorporation of Cl^- on or into the surface of alumina can strongly enhance its acid strength. The modification of catalyst surface is performed by impregnating with chloride-containing solutions (Che, Clause and Marcilly, 1997) or depositing $AlCl_3$. The modification of catalyst surface by deposition of chlorine has been widely applied in the catalytic reforming with Pt-Al_2O_3 catalysts (Sinfelt, 1997). The alkaline strength of oxide support (like alumina) can be strongly enhanced by immobilising alkali metal active component on its surface (Ono and Baba, 2000). Possible alkali metals modifiers include KNO_3, $KHCO_3$, K_2CO_3 and the hydroxides of the alkali metals.

2.2.3.3 Supported metal catalysts

Metal particles have a significant tendency to aggregate to reduce their surface area because metals generally have a high surface free energy (Overbury, Bertrand and Somorjai, 1975). Therefore, for the utilisation of metal catalysts, in order to stabilise nanosized particles under reaction conditions, they are generally dispersed on the oxides supports with high surface area, such as transition aluminas (Che, Clause and Marcilly, 1997). In a typical procedure, metal catalysts with uniform particle structure and size distribution can be obtained by anchoring molecular carbonyl cluster on the surface of support materials, followed by decarbonylation (Deutschmann *et al.*, 2009). Aggregation of nanoparticles should be avoided because this may result in catalyst deactivation.

Supported metal catalysts have been applied in hydrogenation and dehydrogenation reactions. These catalysts consist of metal nanoparticles (*e.g.* noble metal (Pt, Rh) and non-noble metal (Fe, Ni, Co)) and the supported porous catalysts (such as Al_2O_3, SiO_2 and active carbon). In particular, silver (Ag) on Al_2O_3 is applied in the transformation of ethylene to ethylene oxide (Yong, Kennedy and Cant, 1999). Supported Au catalysts are used for CO oxidation under low temperature (Kung and Costello, 2003).

2.3 Catalytic transformation of CO_2

Nearly 5% of global CO_2 emissions will be applied in the CO_2 utilisation by 2030 and various reasons drive the growing interest in the development of the utilisation of CO_2. One of the main concerns is its potential to contribute to alleviating the greenhouse effect. CO_2 used as a feedstock or raw material has been widely applied in many fields. The applications include direct use (non-conversion) and the transformation of CO_2 to chemicals and fuels (section 1.2.2).

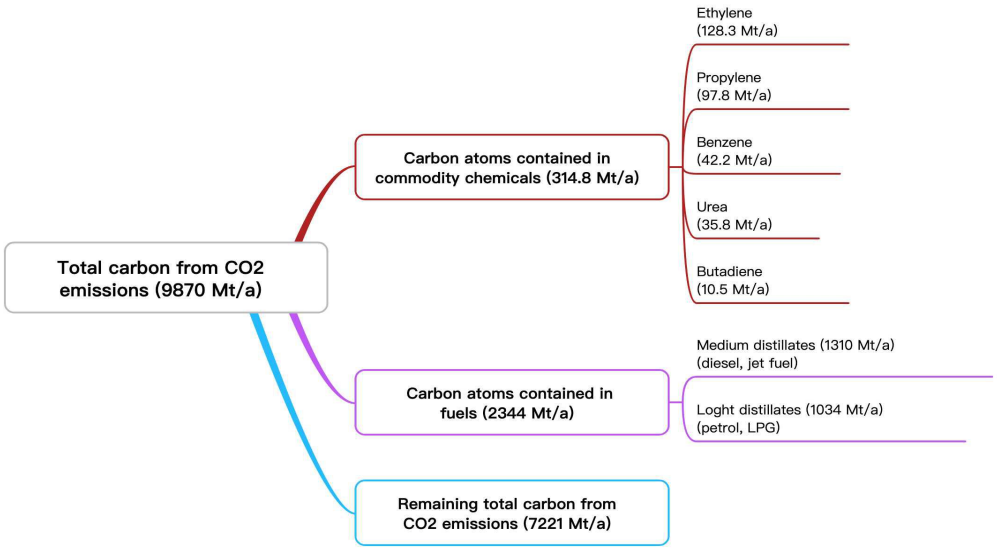

Figure 2-2. Theoretical amount of carbon consumed by CDU for production of chemicals and fuels in 2015 (Dowson and Styring, 2017).

Figure 2-2 shows that the quantity of CO_2 converted to chemicals (around 3%) is low compared to total carbon emissions. Additionally, it should be noticed that it is possible to reduce 23.7% CO_2 emissions by converting CO_2 to liquid fuels (Dowson and Styring, 2017). This section describes the application of CO_2 through catalytic transformation routes, including the hydrogenation of CO_2, the conversion of CO_2 to carboxylic acids and organic carbonates.

2.3.1 Hydrogenation of CO_2

2.3.1.1 Reaction mechanism

CO_2 hydrogenation is analogous to Fischer-Tropsch synthesis, which transfers CO and hydrogen mixtures into liquid hydrocarbons. CO_2 is more inert than CO. The first step of CO_2 hydrogenation is to convert CO_2 to CO by reverse water gas shift (RWGS) (Equation 2-1),

followed by Fischer-Tropsch synthesis to convert CO into valuable industrial feedstocks such as lower olefins and liquid hydrocarbons (Hu *et al*., 2014).

$$CO_2(g) + H_2 \leftrightarrow CO(g) + H_2O(g) \quad (2\text{-}1)$$

The catalysts used in CO_2 hydrogenation should be active for both RWGS reaction and FT reaction because these steps carry out simultaneously.

2.4.1.2 Products of CO_2 hydrogenation

- Methanol

  Methanol (MeOH) can be produced *via* hydrogenation from CO and is widely proposed as an alternative chemical energy carrier. Moreover, it is an excellent fuel and essential raw material in many industrial reactions. Methanol can be used directly or indirectly as a hydrogen source for the reforming reaction in fuel cells (Bansode and Urakawa, 2014). The two-step process which removes the water during the reaction can sharply increase the productivity of methanol (three times higher than that of the single-step process) by reason of the shift of equilibrium (Joo, Jung and Jung, 2004). Rodriguez *et al*. have shown that the catalysts of Au, Cu, and Ni deposited on TiC (001) perform high activity for the RWGS reaction and can convert CO to methanol effectively (Rodriguez *et al.*, 2013). Furthermore, Pb-ZnO on carbon nanotubes is a promising alternative because carbon nanotubes can reversibly adsorb a greater amount of hydrogen on a per mass basis (Liang *et al.*, 2009).

- Dimethyl ether (DME)

  A promising CO_2 conversion route is the formation of dimethyl ether (DME), which is a potential diesel pool additive. Nowadays, there are two methods to produce DME: one-step and two-step method. One-step method refers to synthesizing DME from the raw gases directly, and the two-step method consists of the synthesis of methanol from raw gases and the dehydration of methanol to DME. For the one-step route, dual-function catalysts are utilized in reaction processes. Usually, dual-function catalysts should keep active to both methanol synthesis reaction (which can be catalysed by Cu-ZnO-Al_2O_3) (Lei *et al.*, 2012) and methanol dehydration reaction (in which alumina, porous SiO_2-Al_2O_3 and Y-molecular sieve are applied). Many researchers focused on the modification of reaction conditions and catalyst properties to obtain higher CO_2 transformation rates.

For example, Atul Bansode *et al.* have pointed out that one-pass CO_2 transformation with remarkable selectivity (89%) is achieved under high-pressure conditions (up to 36 MPa) over co-precipitated Cu-ZnO-Al_2O_3 and H-ZSM-5 catalysts (Bansode & Urakawa, 2014b).

- Short-chain olefins

Light olefins include ethylene (C_2H_4), propylene (C_3H_6), butylenes (C_4H_8), cyclopentane (C_5H_{10}), and cyclohexane (C_6H_{12}). C_2H_4 and C_3H_6 are mainly used for the synthesis of polyethene and polypropene. C_4H_8, C_5H_{10}, and C_6H_{12} are used as monomers for the production of copolymers (Hu *et al*., 2014). Light olefins can be formed through the conversion of methanol or dimethyl ether (DME) over multifunctional catalysts (such as zeolite) (Khadzhiev *et al*., 2014). Moreover, Light olefins can be produced by CO_2 hydrogenation in the presence of manganese oxide-supported iron catalysts (Hu *et al.,* 2013). Iron, which immobilized on the manganese oxide carrier, exists in the form of Fe_3O_4, Fe_5C_2, and Fe_3C. In these catalysts, Fe_3O_4 functions as an active catalyst for the RWGS reaction, and Fe_5C_2 and Fe_3C are very active and selective Fischer-Tropsch catalysts.

- Fuels

Synthetic fuel is a kind of "green" liquid fuel produced from natural gas, coal, biomass, or oil shale, and the routes for synthetic fuels manufacture include the Fischer-Tropsch conversion, methanol to gasoline conversion or direct coal liquefaction (Hu *et al*., 2014). Fischer-Tropsch synthesis (FTS) is industrially used to produce straight-chain hydrocarbons with a wide range of carbon numbers by converting syngas. One of the major advantages of this route is that FTS products are of great environmental value because they are almost free of sulfur, nitrogen and aromatic compounds (Centi & Perathoner, 2014). The FTS method is an alternative to the production of liquid fuels from CO_2. In the FTS process, the hydrogenation of CO_2 is divided into two categories: (i) conversion of CO_2 to CO by RWGS reaction (Equation 2-2) followed by CO hydrogenation (Equations 2-3) and (ii) direct hydrogenation (DH) of CO_2 to hydrocarbons by a mechanism different from that of CO hydrogenation (Equation 2-4), as shown below:

(1) RWGS: $$CO_2 + H_2 \leftrightarrow CO + H_2O \qquad (2\text{-}2)$$

FT: $CO + 2H_2 \rightarrow (-CH_2-) + H_2O$ *(2-3)*

(2) DH: $CO_2 + 3H_2 \rightarrow (-CH_2-) + 2H_2O$ *(2-4)*

Iron-based catalysts, generally used in FTS, are regarded as the most suitable catalysts for CO_2 hydrogenation because of intrinsic WGS and reverse WGS activity (Kumaran *et al.,* 2013).

2.3.2 Conversion of CO_2 to carboxylic acids

The hydrogenation of CO_2 to formic acid (FA) or formates is also an attractive alternative for the utilisation of CO_2. Formic acid is a greener renewable fuel which can be treated as a liquid form of hydrogen. Compared with hydrogen, it is more convenient to store and transport. In addition, formic acid or formate can be used as the alkaline materials in various industries, such as controlling pH value in the leather manufacturing and dyeing industry, as a coagulant in rubber synthesis, as a preservative and antibacterial agent in livestock feed and as a de-icing agent *etc.* (Reutemann & Kieczka, 2012). Currently, there are two methods for FA synthesis: the first one is the conventional approaches which consist of two steps; the second one is the direct hydrogenation of CO_2 (Scheme 2-2).

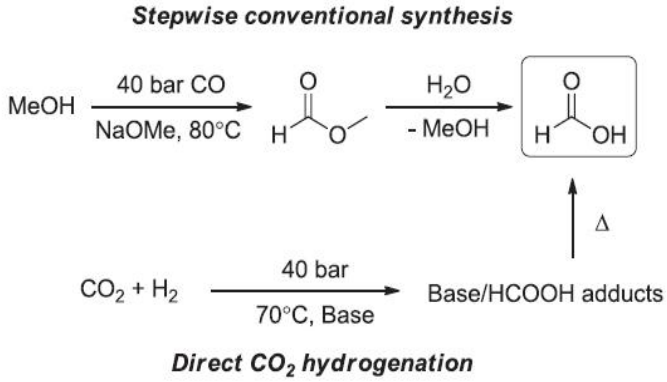

Scheme 2-2. Two routes used for FA synthesis (Peng *et al.*, 2012).

For a two-step process, methanol is carbonylated to methyl formate ($HCOOCH_3$) and then hydrolyzed to FA and methanol. Another process is the direct reduction of CO_2, which is much simpler and abides by the principles of sustainable chemistry (Peng *et al.*, 2012). However, Gibbs free energy of FA synthesis by direct CO_2 hydrogenation is positive ($\Delta G°_{298}$ = +33 kJ mol^{-1}), which means the reaction will not spontaneously take place. Therefore, the addition of base is required to shift the reaction equilibrium. Nitrogen-containing based catalysts such as triethylamine (NEt_3) have been employed in the synthesis

of formate salts from CO_2 hydrogenation. As a result, purified FA can be obtained through a high boiling base catalyst (like imidazoles) (Schaub & Paciello, 2011). Metal-based homogeneous catalysts exhibit a high catalytic activity in the synthesis process. However, the use of homogeneous catalysts has inevitable limitations in industrial applications by their properties. For example, homogeneous catalysts are soluble in the reaction medium and require complicated and costly separation steps for recycling when the operating pressures are decreased. Therefore, a heterogeneous catalyst for CO_2 hydrogenation is highly desired. Two types of heterogeneous catalysts (Au and $Ir^{(III)}$ based catalysts) are discussed.

- Au based catalysts

Fachinetti *et al.* published the first conventional supported catalyst for FA synthesis from CO_2 in 2011 (Preti *et al.*, 2011). In their study, Au-TiO_2 with a low metal loading (1 *wt*.%) is applied in the hydrogenation of supercritical CO_2 in neat NEt_3 base. The catalytic reaction formed the FA·NEt_3 adduct at 40 °C with an acid to amine ratio of 1.72, and waterless FA could be obtained by distillation. Recently, Filonenko *et al.* (Filonenko *et al*., 2015) have evaluated a series of gold-nanoparticle catalysts for the liquid phase CO_2 hydrogenation, and they pointed out that Au-Al_2O_3 is found to be the most active catalyst, even better than Au-TiO_2. According to previous research, Au-TiO_2 is one of the most active catalysts providing a turnover number (TON) of 110 at 70 °C. However, Au-Al_2O_3 catalyst shows better catalytic performance and allows reaching a two-fold higher formate yield (TON=215) than the TiO_2-supported catalyst under identical conditions (Filonenko *et al.*, 2015). Au particle sizes for the two catalysts is not the only reason for high catalytic performance and high formate yield. The properties of the support have a more significant effect on catalytic activity. Data showed that the Au dispersions of two catalysts are similar (0.43 and 0.40, respectively). In addition, the average particle sizes for Au-Al_2O_3 and Au-TiO_2 are 1.9 nm and 2.6 nm respectively, which means the sizes of support particle may lead to the marked difference on catalytic performance (Filonenko *et al.*, 2015).

- $Ir^{(III)}$ based catalysts

Some studies have reported that homogeneous Ir complexes performed an excellent catalytic activity in the hydrogenation of CO_2 to formats (Tanaka *et al.,* 2009). However, Ir-based homogeneous catalysts need to be immobilized on a suitable catalysts support to overcome high-cost separation problems. Recently, more attentions have been attracted

by covalent organic frameworks (COFs) which can be used as a catalyst carrier to immobilize homogenous catalysts *via* coordination bonds between the frameworks and the metal ions (Bavykina *et al.*, 2015). Moreover, COFs are suggested as an "ideal" catalyst support thanks to their high stabilities, pore volumes, and high surface area. Bavykina *et al*. have tested the novel catalyst ([IrCp*(HBF-2)Cl_2]), which is an iridium catalyst immobilized with a heptazine-based framework and a biphenyl linker (HBF-2) (Bavykina *et al.,* 2015). Under mild conditions (80 °C, 4 MPa, 2 h), the catalyst still has a relatively high activity with a TON value of 150. The heterogeneous catalyst can be easily separated by pump filtration. In terms of the reusability of catalyst, the slight loss of Ir content probably because of the leaching of the Ir species, possibly because of the formation of a weak complexation between Ir and heptazide nitrogen (Bavykina *et al.* 2015).

2.3.3 Conversion of CO_2 to organic carbonates

Organic carbonates are essential compounds in the chemistry industry. In this part, two kinds of synthesized products, which include propylene carbonate (PC) and dimethyl carbonate (DMC), are discussed. Specifically, the properties of applied heterogeneous catalysts, reaction mechanisms and influence factors of the reactions (like CO_2 pressure, reaction temperature, and so forth) are illustrated.

2.3.3.1 Propylene carbonate

CO_2 undergoes cycloaddition with epoxides or propylene glycol (PG) to produce cyclic carbonates, which have utility in various applications. Propylene carbonate (PC) is a commercially critical chemical material which can be used as an aprotic solvent or intermediate in fine chemistry. For example, PC as the feedstock for the synthesis of dimethyl carbonate (DMC) *via* transesterification reaction.

- Synthesis of propylene carbonate from CO_2 and propylene oxide (PO)

Currently, one of the most valuable routes for PC synthesis is to insert carbon dioxide into propylene oxide (PO) (Ramin *et al.*, 2006). The use of easy-separable, high-efficiency and high-selectivity heterogeneous catalysts are desirable. According to prior studies, there are two types of novel heterogeneous catalysts which applied in the PC formation from PO and CO_2. The following three kinds of catalyst are discussed in this part: zirconia-based catalysts, zinc-based complexes (Ramin *et al.,* 2006) and supported ionic liquid catalysts (Zhao *et al.,* 2007).

(1) Zirconia-based catalysts

Several zirconia-based catalysts have been studied for synthesis of propylene carbonate from propylene oxide and carbon dioxide without using any solvent, such as ceria and lanthana doped zirconia (Ce-La-Zr-O) catalyst, ceria doped zirconia (Ce-Zr-O), lanthana doped zirconia (La-Zr-O), lanthanum oxide (La-O) and zirconium oxide (Zr-O) (Adeleye, Adegboyega Isaac *et al*., 2014). The activity and selectivity of the solid catalysts for PC synthesis is largely decided by the structural characteristics, particle size, texture, and active sites present on the surface area of the catalyst, which are measured and discussed in Adeleye's paper. The conversion of PO and the yield and selectivity of PC are summarised in Figure 2-3.

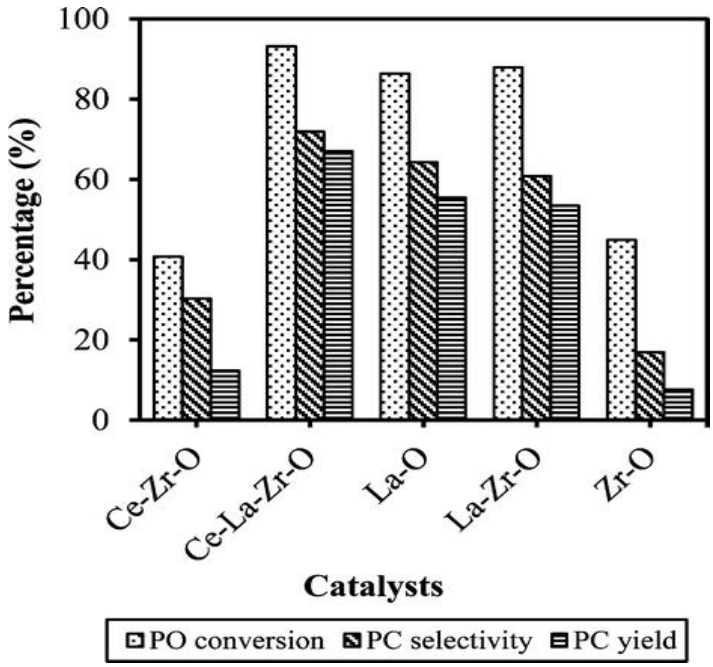

Figure 2-3. Effect of different catalysts on conversion of propylene oxide and the selectivity, and yield of propylene carbonate. Experimental conditions: 10 *wt.*% catalyst loading; 170 ℃; CO_2 pressure, 7.0 MPa; reaction time, 20 h. (Source: Adeleye, Adegboyega Isaac *et al.,* 2014).

It is shown that the reaction using Ce-La-Zr-O catalyst gives the highest PO conversion (92%) and highest PC yield (66%) and selectivity (72%). The effect of reaction time (from 0 h to 24 h), catalyst loading (from 2.5 *wt*% to 15 *wt*%), reaction temperature (from 120 ℃ to 200℃) and CO_2 pressure (from 4 MPa to 8 MPa) are discussed as well.

(2) Zinc-based catalysts

The cycloaddition reaction of epoxides and CO_2 *via* zinc-based catalysts has shown in Scheme 2-3.

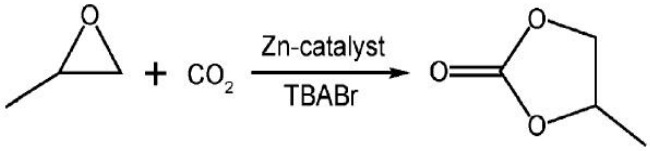

Scheme 2-3. Reaction scheme of CO_2 conversion to propylene carbonate through Zn-based catalyst (Ramin *et al.*, 2006).

In this process, CO_2 replaces toxic carbon monoxide or phosgene as a C_1 structural block participated in the reaction. A series of bifunctional catalysts (including NH_3A-Zn-SBA-15, where A^- is I^-, Br^-, Cl^- or CH_3COO^-) were prepared by immobilising Zn-based ammonium salts on SBA-15 support and were applied in the synthesis of PC from PO and CO_2 (Liu *et al.*, 2016). According to the nature of anionic species, the catalytic activity should increase in the order of $I^- > Br^- > Cl^- > CH_3COO^-$. The results show that NH_3I-Zn-SBA-15 catalyst led to the highest PC yield (99%) with a TOF number of 326 h^{-1} under mild condition (150 °C, 3 MPa, 12 hours).

(3) Supported ionic liquid catalysts

Another alternative for PC formation is quaternary ammonium salt-functionalized chitosan catalyst. Quaternary ammonium salts (such as Bu_4NBr, Et_4NBr, *etc.*) are currently used as cheap and effective homogeneous catalysts for the industrial preparation of cyclic carbonates (Baj *et al.*, 2014). However, it is difficult to separate the catalyst from the products by a purification process during reaction progress. As a result, the decomposition of the catalyst and the formation of by-products decreases the yield of PC. Immobilizing quaternary ammonium salt catalysts on the suitable supports may lead to a better product purification and facile catalyst recovery. Chitosan (CS) is a linear polysaccharide and is made by treating the chitin shell of crustaceans (like shrimp) with a basic compound (like sodium hydroxide) (Bobadilla, L. *et al.,* 2015). A chitosan-supported zinc chloride, in conjunction with 1-butyl-3-methylimidazole halides, was demonstrated to be active for the chemical fixation of CO_2 (Xiao *et al.*, 2005). Moreover, another study has shown that very high PC yield could be achieved by the cycloaddition of epoxides and CO_2 with quaternary ammonium salt-functionalized chitosan catalyst

(abbreviated as CS-$N^+R_3X^-$) (Scheme 2-4), and this catalyst showed high selectivity, recyclability and stability during reaction process (Zhao *et al.*, 2007).

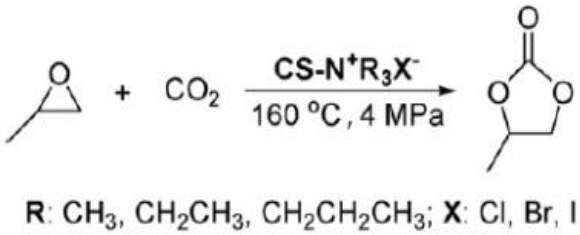

Scheme 2-4. The synthesis of PC over chitosan-supported quaternary ammonium salt catalysts (Zhao *et al*., 2007).

- Synthesis of propylene carbonate from CO_2 and propylene glycol (PG)

Propylene glycol is a by-product formed with DMC synthesis *via* transesterification reaction. Therefore, if the reaction of PG and CO_2 can generate propylene carbonate, not only PG but also CO_2 can be recycled in the reaction system, which would be a greener reaction route with higher CO_2 conversion rate and higher DMC selectivity.

CeO_2-ZrO_2 is reported as a possible catalyst by Tomishige *et al.* for the synthesis of propylene carbonate from propylene glycol and CO_2 (Tomishige *et al.*, 2000). 2% conversion of PG can be obtained without the formation of dipropylene glycol. The catalytic activity is decided by the calcination temperature and the composition of catalyst. According to the catalyst characterisation, the weak acid-base sites formed on the surface of catalyst obtained by high-temperature calcination are the active sites for PC formation. However, high calcination temperature may limit the activity of catalyst because of the very low surface area, which is one of the main reasons for low PC yield. Another possible reason for low PG conversion is water, which is concluded to limit the equilibrium but that this limitation could be overcome if water was removed. Currently, higher PG conversion and PC yield are achieved by adding dehydrating agents (such as acetonitrile) in the reaction system (Zhao *et al.*, 2008).

2.3.3.2 Dimethyl carbonate (DMC)

DMC can be widely applied as a greener organic synthetic material to replace more hazardous materials such as phosgene or dimethyl sulfate. Synthesis of DMC from methanol and CO_2 not only for the formation of value-added products but also for the reduction of CO_2 emissions. DMC is the main target product in this research, and more detailed information about the introduction of DMC, DMC synthesis methods and catalyst used will be provided in

the next sections (Section 2.4-2.6). In this section, two main challenges encountered in the direct synthesis of DMC are introduced.

- High reaction pressure (supercritical state of CO_2)

The yield and selectivity of DMC increase with the rise of CO_2 pressure and reach the maximum at the reaction pressure of 7.5 MPa, which is the supercritical CO_2 state (Cui *et al*., 2003). High operating pressure may lead to the decomposition of catalyst and, moreover, is energy-intensive and brings significant safety issues.

- Low DMC yield and selectivity due to side-product water

The side-product water is formed during DMC synthesis process, which leads to low DMC selectivity considering the deactivation of catalyst and the equilibrium limitation. Ideal dehydrating agents are required to shift the reaction equilibrium toward higher DMC yield. Generally, solid drying agents (such as 3Å molecular sieves, zeolites and $CaCl_2$) are widely used in the chemical industry because they are easy to separate. However, these solid drying agents are not suitable at high temperatures or pressures, for example, 3Å zeolite is effective for dehydration only under 100 °C as the adsorption capacity decreases with increasing temperature (Simo *et al.*, 2009). Therefore, using chemical reaction method to remove water formed during DMC synthesis process might be a more effective method. In practice, higher DMC yield (around 70%) is obtained by adding some organic dehydrating agents such as dimethyl acetal and trimethyl orthoester in the direct synthesis of DMC (Sakakura *et al.*, 1999).

2.4 Introduction to dimethyl carbonate (DMC)

DMC is an eco-friendly organic synthetic intermediate for its properties compared with traditional alternatives (*e.g.* phosgene, dimethyl sulfate (DMS) and methyl halide). This section gives a brief discussion about the physical and chemical properties of DMC and the applications of DMC based on its properties.

2.4.1 Properties of DMC

DMC is a colourless transparent and slightly sweet liquid with slight odour at room temperature, which is insoluble in water but miscible with almost all organic solvents such as alcohol, ether and ketone. The formula of DMC is $C_3H_6O_3$, and its molecular structure is

shown in Figure 2-4. DMC has a molecular structure (CH_3O-CO-OCH_3) and an extensive range of applications.

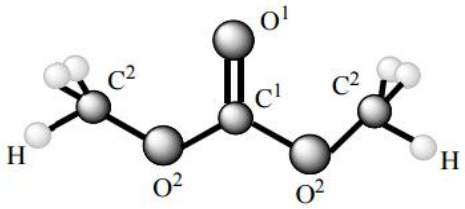

Figure 2-4. The molecular structure of DMC (1, 2 represent chemically different C and O atoms).

2.4.2 Applications of DMC

2.4.2.1 DMC as a green chemical

DMC has relatively high reactivity because the molecular structure of dimethyl carbonate consists of various active groups (Xu *et al.*, 2013), namely methoxyl, carbonyl and methyl groups. Therefore, DMC can be used to replace the highly toxic or carcinogenic substances (*e.g.* phosgene, methyl chloroformate, dimethyl sulfate and methyl chloride) in many reactions as an environmentally friendly intermediate or raw material. Table 2-2 summaries the applications of DMC as a green chemical in industry.

Table 2-2. The applications of DMC as a green chemical.

Application	Chemicals replaced by DMC	Advantage of using DMC	Reference
Methoxycarbonylating agent	Phosgene ($COCl_2$)	Selective reaction towards non-toxic products. Less hazardous reagent.	(Aricò and Tundo, 2010)
Methylating agent	Dimethyl sulfate (DMS) or methyl halide (CH_3X, X = I, Br, Cl)	Higher selectivity to mono-methylated derivatives and less harmful to environment.	(Selva, Marques and Tundo, 1994)
Synthesis of carbamates and isocyanates	Phosgene ($COCl_2$)	The most promising phosgene-free route to carbamates with high selectivity (97%).	Grego, Aricoì and Tundo, 2013)

- Polycarbonate synthesis

Currently, the synthesis of polycarbonate is one of the most promising applications of DMC as an intermediate, which accounts for more than half of DMC consumption (Coker, 2012). DMC can be used as a methoxycarbonylating agent to replace phosgene because DMC (CH_3O-CO-OCH_3) has a similar nucleophilic reaction centre with phosgene (Cl-CO-Cl). When the carbonyl of DMC is under nucleophilic attack, the acyl-oxygen bond will be broken, resulting in the formation of carbonyl compounds and the by-production of methanol. The novel catalyst (TiO_2-SiO_2-poly(vinylpyrrolidone)-based catalyst) has been applied in the polycondensation of DMC and aliphatic diols (Zhu *et al.*, 2011).

- DMC as a methylating agent

DMC can be used to replace dimethyl sulfate (DMS) as a methylating agent. DMS (CH_3O-SO-OCH_3) is a very polluting material for the environment due to the similar feature as phosgene. When DMC is used to replace DMS, the methyl carbon of DMC undergoes a nucleophilic attack, and then the alkyl-oxygen bond breaks down to produce the methylated product. Moreover, when using DMC, higher selectivity to mono-methylated compounds can be achieved, and the reaction process is simpler (Tundo *et al*., 2002). Regularly, the alkaline catalyst (such as K_2CO_3), provides nucleophile activation, is required for the methylation of amines, indoles and amides with DMC (Memoli, Selva and Tundo, 2001).

2.4.2.2 DMC as a solvent and fuel additive

DMC has extensive applications as a well-behaved solvent in organic synthesis. Specifically, DMC can be used in the upgrading of renewable unsaturated fatty esters (Fiorani, Perosa and Selva, 2018). For example, linear alpha olefins (LAO, C9 and C10) can be obtained with a yield of 21% from oleic acid using DMC as a medium. This conversion gives a possibility in oleo industry to transfer natural oils into functional intermediates. DMC has recently reported as a well-performing solvent in the electronic industry. The demand for lithium-ion battery (LIB) is expected to increase for the application in notebook PCs and mobile phones. Well-performing electrolytes of LIB should equip with the following properties: good solubility of salt, good fluidity for Li^+ ion transport and excellent stability during battery operation. With the addition of DMC, both the solubility of salt and the mobility of Li^+ are enhanced (Han, 2019).

In recent years the United States has proposed to use DMC to gradually replace methyl tert-butyl ether (MTBE) as a gasoline additive to improve the octane value and decrease the emission of particulate matters (Pacheco & Marshall 1997; Wei *et al.*, 2003). The following properties make DMC became a promising gasoline additive: high oxygen content (up to 53% oxygen in the molecule), excellent function to improve the octane number ((R + M)/2 = 105), no phase separation, low toxicity and fast biodegradability (Pacheco & Marshall, 1997). To achieve the same oxygen content of gasoline, the amount of DMC added is 4.5 times less than that of MTBE (Pacheco & Marshall, 1997), thereby reducing the total emissions of hydrocarbons, carbon monoxide and formaldehyde from the vehicle exhaust.

2.5 Synthesis of DMC

Demand for DMC in the global market is increasing, and forecasts indicate that the production for DMC is expected to reach 599 kilotons by 2023 (Samani, 2018). The mass production of DMC is developed alongside the non-phosgene synthesis of polycarbonates. The traditional production route of DMC is the phosgene method, but this method has been gradually eliminated because of the high toxicity and corrosivity of phosgene and the environmental problems caused by sodium chloride emissions. There are now five routes to the synthesis of dimethyl carbonate (Honda *et al.*, 2014): oxidative carbonylation of methanol, two-stage route with CO and NO, transesterification from cyclic carbonate and methanol, direct synthesis from CO_2 and methanol and one-pot route with epoxide, methanol and CO_2 (see Scheme 2-5 and Scheme 2-6).

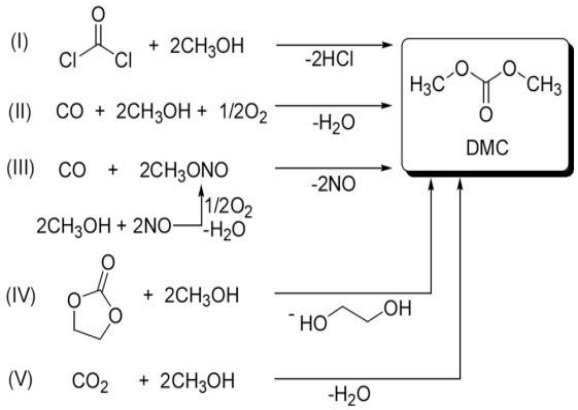

Scheme 2-5. Reaction routes for DMC synthesis: (I)phosgene route, (II) oxidative carbonylation route, (III) two-stage route with CO and NO, (IV) transesterification of cyclic carbonate from methanol and (V) direct synthesis from CO_2 and methanol (Honda *et al.*, 2014).

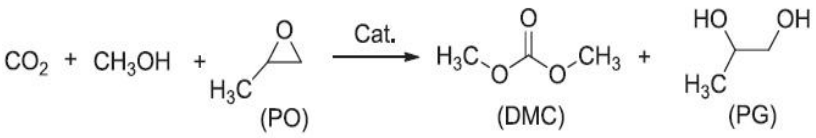

Scheme 2-6. One-step synthesis of DMC (Li *et al.*, 2015).

2.5.1 Oxidative carbonylation

DMC can be produced from the reaction of carbon monoxide, methanol and oxygen under moderate CO pressure (around 1.4 Mpa). CuCl is the best-performing catalyst for this conversion in view of the excellent selectivity and reaction rates. However, this reaction system has some problems as follows:

- The formation of DMC from methanol is highly exothermic (about 318.2 kJ mol^{-1} of DMC). In order to operate the reaction under the optimum reaction temperature (100 - 130 °C), the newly generated energy must be removed from the reactor, which may lead to high utility costs (Pacheco and Marshall, 1997).

- The formation of HCl is unavoidable, which is highly corrosive to the reactor section.

- It is challenging to separate DMC from the DMC/methanol/water mixture.

- The yield of DMC is mostly depended on the water formed during the reaction process. It is difficult and highly cost to keep an optimum water amount in the reactor by removing the excess water.

2.5.2 Transesterification of cyclic carbonate

The transesterification of cyclic carbonates (such as ethylene carbonate and propylene carbonate) is a more promising alternative route for DMC synthesis because of its high conversion of cyclic carbonate, the high selectivity of DMC and the co-generation of propylene glycol. For example, active novel heterogeneous catalysts (Tin doped zirconia (Zr–Sn–O) and tin doped zirconia/graphene nanocomposite (Zr–Sn/GO)) prepared *via* continuous hydrothermal flow synthesis (CHFS) route have been employed to the synthesis of DMC from propylene carbonate and methanol (Saada, Rim *et al.*, 2018). In Saada's study, high DMC yield (81%) and PC conversion (85.1%) is obtained at optimum conditions (173.3 °C, 12.33:1 MeOH:PC molar ratio, 4.08 h and 2.9 *wt.*% Zr–Sn/GO nanocomposite). Table 2-3

summaries the operating conditions, DMC yield and selectivity obtained by using different heterogeneous catalysts in former studies.

Table 2-3. The catalysts used for the transesterification of cyclic carbonate to form DMC.

Catalyst	Reaction conditions					Yield (%)	Selectivity (%)	References
	n_{MeOH}/n_{EC}	EC (mmol)	Catalyst (g)	Temp. (°C)	Time (h)			
MgO	8/1	25	0.50	150	4	66	100	(Bhanage *et al.*, 2003)
Si-Mg-Na-K	8/1	25	0.25	150	4	73	90	(Bhanage *et al.*, 2002)
$Na_2WO_4 \bullet H_2O$	10/1	50	1.0	20	5	80	100	(Sankar *et al.*, 2006)
Na-dawsonite	4/1	-	10 *wt.*% of EC	70	4	65	100	(Stoica, Abelló and Pérez-Ramírez, 2009)
PEL-CMC-PVA polymer	16/1	-	2.2	60	48	94	99	(Liu *et al.*, 2013)

The main problems of these routes are the equilibrium and thermodynamic limitations, high cost of cyclic carbonates and the toxic raw materials (such as ethylene oxide and propylene oxide) for producing cyclic carbonates.

2.5.3 Direct transformation of CO_2

2.5.3.1 Direct synthesis of DMC from methanol and CO_2

The direct synthesis of DMC from methanol and CO_2 is a promising alternative with many advantages such as high atom efficiency, low toxicity, cheap reactants, and simplicity of the operations (Sakakura & Kohno, 2009). A problem in the reaction is the low translation due to equilibrium limitation. Moreover, a possible side reaction is the production of ethers like dimethyl ether (DME) during DMC synthesis. The formation of ether not only expends reactant but also generates water, which can result in the hydrolysis of carbonate. Hence, the formation of ethers should be strictly inhibited.

Some studies reported that appropriate catalysts could be used to promote the reaction, such as organometallic complexes, inorganic bases and modified ZrO_2 *et al*. Specifically, these catalysts include $Co_{1.5}PW_{12}O_{40}$ (Aouissi *et al.,* 2010), K_2CO_3 (Cai *et al.* 2009), KOH (Cai *et al.*

2009), ZrO_2 (Eta & Leino, 2010) and CeO_2 (Wang*, et al.,* 2014*;* Yoshida *et al.,* 2006*;* Aresta *et al.*, 2010). Graphene-inorganic nanocomposite catalysts has studied for the direct synthesis of DMC from methanol and carbon dioxide using 1,1,1,trimethoxymethane (TMM) as a dehydrating agent in a high pressure reactor (Saada, Rim *et al*., 2015). In Rim's study, a novel ceria–zirconia oxide/graphene nanocomposite catalyst (Ce-Zr oxide/graphene, where nominal atomic ratio of Ce:Zr=1:1) with high stability and activity has been produced *via* a green, rapid and continuous hydrothermal flow synthesis (CHFS) route. The reaction is performed at optimum reaction condition (27.5 MPa, 110 °C, 16 h, 1:1(w/w) TMM:MeOH and 10wt% catalyst loading) and the highest methanol conversion of 58 % with a DMC yield of 33 %. Besides, the Ce-Zr oxide/graphene nanocomposite catalyst can be easily recycled and reused several times without any obvious reduction in the catalytic activity. As an excellent catalyst carrier equipped with the properties of both Lewis acid and base sites, cerium dioxide has been generally studied in the presence of Al_2O_3 (Aresta *et al*., 2010), ZrO_2, Ga_2O_3, Ni_2O_3, Fe_2O_3 and other lanthanides. Unfortunately, the yield from the direct synthesis of DMC illustrated in the literature is still low (up to 7.2% (Eta & Leino, 2010)) at the temperature of 80-200 °C (Cai *et al*. 2009; Aouissi *et al.,* 2010) and long reaction times which ranged from 3 h to 10 h (Cai *et al.,* 2009) because the reaction is limited by the thermodynamic stability of CO_2 and the formation of water (Aouissi *et al.*, 2010; Eta *et al.,* 2011). Although the higher yield of DMC is achieved when using orthoesters and acetals as dehydrating agents, there are several drawbacks in this route. For example, the high cost of raw materials and the difficulty in separating catalyst from product resulted from the homogeneous property of catalyst. In these cases, it is critical to find alternative ways for the formation of DMC with superior catalysts.

2.5.3.2 One-pot synthesis of DMC from epoxide, methanol and CO_2

One-pot synthesis of DMC from the epoxides, methanol and CO_2 with a bifunctional catalyst (Scheme 2-7) has gained much interest in consideration of higher DMC selectivity compared with the direct synthesis of DMC.

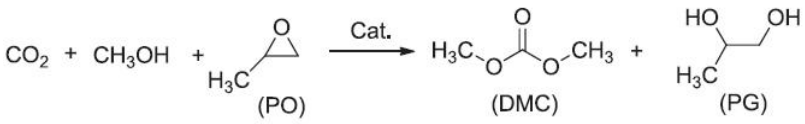

Scheme 2-7. The route of one-step synthesis of DMC (Li *et al.*, 2015).

According to the previous research, strong basic catalysts are beneficial to the transesterification of propylene carbonate to form DMC. The immobilized heterogeneous catalysts have been acknowledged to be prepared through carrying inorganic bases (*e.g.*, KOH and K_2CO_3) (Wang *et al.*, 2011), organic bases (*e.g.*, choline hydroxide) or alkali halides (*e.g.,* KI) (Jiang and Yang, 2004) on the MgO (De *et al*., 2008; Bhanage *et al*., 2001), ZnO (Chang *et al*., 2004), rare earth oxide (REO, RE = La, Ce, Y, Nd) (Jiang and Hua, 2007), smectite (Bhanage *et al*., 2002) or 4Å molecular sieve (Li, Zhao and Wang, 2005) and so on as support. Higher pressure is favourable for the formation of cyclic carbonate and DMC. For example, in Cui *et al.*'s study, ethylene oxide (EO) with supercritical CO_2 (7.5 MPa) is coupled, at the same time the reaction of ethylene carbonate (EC) with methanol is performed with high DMC selectivity (75%) under the same reaction conditions (Cui *et al.,* 2003). More detailed information about the catalysts used in the one-pot synthesis of DMC will be provided in Section 2.6.1.

During the reaction process, the formation of by-products such as 1-methoxy-2-propanol and 2-methoxy-1-propanol is unavoidable. Additionally, there are various disadvantages to these catalysts. For example, some of them are easily decomposed catalysts (Li *et al*., 2010; De *et al*., 2008; Jiang and Yang, 2004) with low efficiency (Li, Zhao and Wang, 2005), un-recycling property (Li *et al*., 2010; Tian *et al.*, 2006) and the requirements of reaction conditions is strict (*e.g.,* supercritical CO_2) (Chang *et al*., 2004; Cui *et al*., 2004; Tian *et al*., 2006). Hence, the main challenge of this route is to find a suitable catalyst which can lead to a higher yield of DMC under a mild reaction condition.

2.5.3.3 Synthesis of DMC from acetals and CO_2

Using a dehydrated MeOH derivative (like trimethyl orthoacetate or acetals) instead of methanol in the direct synthesis of DMC route can achieve enhanced catalytic efficiency, because some of the following challenges can be eliminated: the equilibrium limitation, catalyst decomposition and DMC hydrolysis due to the generation of water (Choi *et al.*, 2002). Compared with ortho ester, acetal is a more promising alternative because they are much cheaper and more easily regenerated from final by-product (carbonyl compounds) (see Scheme 2-8).

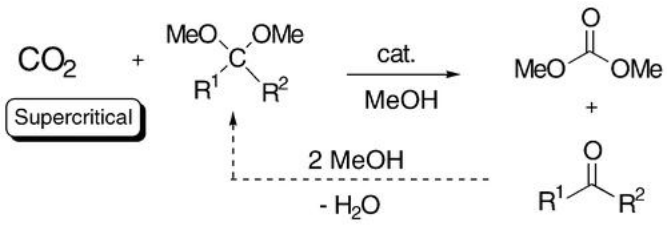

Scheme 2-8. The route of DMC synthesis from acetals and CO_2 (Sakakura *et al.*, 1998).

The yield of DMC can reach 58% in 72 h at 180 °C under 30 MPa using $Bu_2Sn(OMe)_2$ as a catalyst (Sakakura *et al.*, 1998). However, the drawbacks of this route include the requirement for high CO_2 pressure (over 30 MPa) and the separation of catalyst from the product mixture.

2.6 Catalysts and dehydrating agents used for DMC synthesis

As discussed above, conventional methods of DMC synthesis (such as methanolysis of phosgene and oxidative carbonylation of methanol) require the use of hazardous gases such as carbon monoxide (CO) or phosgene ($COCl_2$). Alternatively, the direct synthesis of DMC from methanol (CH_3OH) and CO_2 is a promising alternative with high atom efficiency, low toxicity, and the use of readily-available feedstocks (Sakakura and Kohno, 2009). However, this process is limited by low conversion due to its endothermic nature (ΔG= +26 kJ mol^{-1}) (Eta and Leino, 2010). Therefore, high conversion *via* a one-pot synthesis of DMC remains a highly desirable objective. Herein this research aims to find a suitable catalyst which can synthesize DMC *via* a one-pot route with high DMC selectivity under mild condition. This section discusses the types of heterogeneous catalysts used in published papers, as well as the corresponding DMC selectivity and reaction pressure. Moreover, the dehydrating agents used to increase DMC yield are also discussed.

2.6.1 Heterogeneous catalysts used for the one-pot synthesis of DMC

Here, only supported catalysts are discussed concerning its relatively higher activity and efficiency compared with bulk catalysts. The one-pot synthesis of DMC consists of two reversible steps (Scheme 2-9): cycloaddition and transesterification. In the cycloaddition reaction, propylene oxide reacts with CO_2 to form propylene carbonate (PC). In the transesterification step, methanol and PC are converted to DMC and propylene glycol (PG). 1-methoxy-2-propanol and 2-methoxy-1-propanol are produced as by-products through the reaction between PO and methanol.

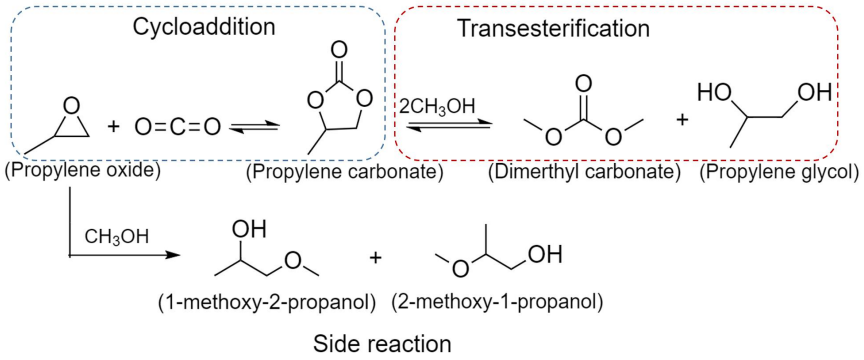

Scheme 2-9. Reaction pathway of one-pot synthesis of DMC.

It is known that high catalytic efficiency can be achieved in the cycloaddition of CO_2 and epoxide in the presence of nucleophiles (such as halide anion and quaternary ammonium salt) and basic catalyst support (Lan *et al.*, 2015). The halide anion is involved in the ring-opening of epoxide and the basic sited on catalyst surface is used for CO_2 adsorption and activation. In transesterification, the catalyst with higher basicity (higher amount of strong basic sites) is more active during the conversion of PC to form DMC (Kumar, Srivastava and Mishra, 2015).

Table 2-4. The catalysts used for the one-pot synthesis of DMC.

Catalyst	CO_2 pressure (MPa)	DMC selectivity	Reference
KOH-KI-ZnO	16.5	58.0%	(Chang *et al.*, 2004a)
Mg-KCl-ZrO_2	9.5	52.7%	(Eta *et al.*, 2010)
K_2CO_3-KI-4A	7.5	75%	(Cui *et al.*, 2008)
KOH-4A	3.0	16.8%	(Li, Zhao and Wang, 2005)
Na_2CO_3–KCl-Al_2O_3	2.5	20.1%	(Jiang and Yang, 2004)
KOH-*β*-zeolite	2.0	23.3%	(Xu *et al.*, 2013)

Table 2-4 summarises the selectivity to DMC achieved over various catalysts at differing CO_2 pressures. It is worth noting that most of these catalysts consist of a kind of alkali halide (*e.g.* KI and KCl), a strong base (such as KOH, K_2CO_3 and Na_2CO_3) and a carrier. Moreover, promoters may be added to improve the yield of DMC. For example, Mg turnings have been employed as a co-catalyst alongside KCl-promoted ZrO_2. Mg produces $Mg(OCH_3)_2$ as an intermediate product which can react with CO_2 to form carbonated magnesium methoxide (CMM) (Eta *et al.*, 2010). The exchange of oxygen atoms between methoxy groups of CMM adsorbed on the catalyst surface, and the bulk oxygen of catalyst enhances the production of DMC, increasing its yield. Higher operating pressure is more conductive to increase DMC selectivity. However, in chemical plants, this may consume more money and energy and introduce significant safety concerns. Optimisation of reaction conditions with the aim of

minimizing the operating pressure while increasing reaction rate, selectivity and catalyst lifetime should be a key goal of process development (The Royal Society, 2017).

2.6.2 Dehydrating agents

The formation of by-product PG *via* hydrolysis of PO by water limits the overall selectivity to DMC. Selectivity to DMC can therefore be increased by reducing the rate of production of PG through removing water from the system. Liquid dehydrating agents have a positive effect on increasing DMC selectivity. These agents include 2-cyanopyridine (Bansode and Urakawa, 2014), acetonitrile (Honda *et al.*, 2009) and benzonitrile (Honda *et al.*, 2011) *et al.* One of the main challenges is that the hydrolysate of a dehydrating agent may react with reactants or DMC in the reaction system. For example, acetamide ($CH_3(CO)NH_2$) is generated from the reaction of acetonitrile (CH_3CN) and water, which can react with methanol to produce ammonia (NH_3) and methyl acetate (CH_3COOCH_3). However, NH_3 may react with DMC to form methyl nitrite ($CH_3O(CO)NH_2$) (Honda *et al.*, 2009). Solid dying agents (like $CaCl_2$, MgO and molecular sieves) can be used to absorb water from the process, but most such agents, *e.g.* 3Å molecular sieve, are not active at high temperatures or pressures. 3Å molecular sieve is suitable for dehydration only under 100 °C as the adsorption capacity decreases with increasing temperature (Simo *et al.*, 2009). Therefore, it is necessary to find alternative agents to increase DMC selectivity by removing water from the system.

2.7 Conclusions

Currently, large-scale emissions of carbon dioxide and global warming phenomenon have contributed to the exploration and development of process for the conversion of CO_2 to valuable chemical products. The use of CO_2 in the production of DMC is particularly attractive as DMC that can be widely applied as a greener alternative to more hazardous materials such as phosgene or dimethyl sulfate. Various routes for DMC synthesis catalysed by heterogeneous catalysts have been extensively studied. Catalysts containing alkali halides and strong base show high catalytic efficiency under supercritical CO_2 pressure condition. However, the selectivity of DMC is relatively low and unsatisfactory when operating at the low-pressure condition. More effort is needed to develop a more effective catalytic system to enhance the selectivity of DMC under mild operating conditions. It can be realized from these two aspects: (1) the development of novel catalyst which can promote both cycloaddition and transesterification reactions; (2) the development of solid dying agent which can overcome thermodynamic limitation and lead to a higher DMC selectivity. It is also necessary to

investigate the role of catalyst and dehydrating agent in the reaction system and fully understand the reaction mechanism.

CHAPTER 3

EXPERMENTAL WORK AND ANALYTICAL TECHNIQUES

Chapter 3 Experimental work and analytical techniques

3.1 Introduction

This chapter consists of two parts: the introduction of the methodology and the set-up of the experiment. There are three phases involved in the reaction: Liquid product, solid catalyst and carbon dioxide gas. The analytical techniques for studying the composition and properties of these phases are introduced in the second part. More specifically, the qualitative and quantitative analysis of the liquid product is performed by gas chromatography-mass spectrometry (GC-MS) and is described in section 3.3. The techniques used to characterise the chemical and physical properties of catalysts are detailed in section 3.4. In the end, the overall experiment plan is discussed in section 3.5 followed by the analysis of experimental errors (section 3.6).

3.2 Apparatus and procedure

Two different experimental set-ups are employed throughout this research. One for catalyst preparation and another one for the one-pot synthesis of DMC from carbon dioxide, methanol and propylene oxide.

3.2.1 Catalyst preparation method

All catalysts are prepared by the wet impregnation method using a reflux apparatus (Figure 3-1). The essential components of a reflux system include a reaction flask, a reflux condenser, a heating source and a coolant source. The reaction flask is heated in the silicon oil and placed on a heating plate with magnetic stirrers.

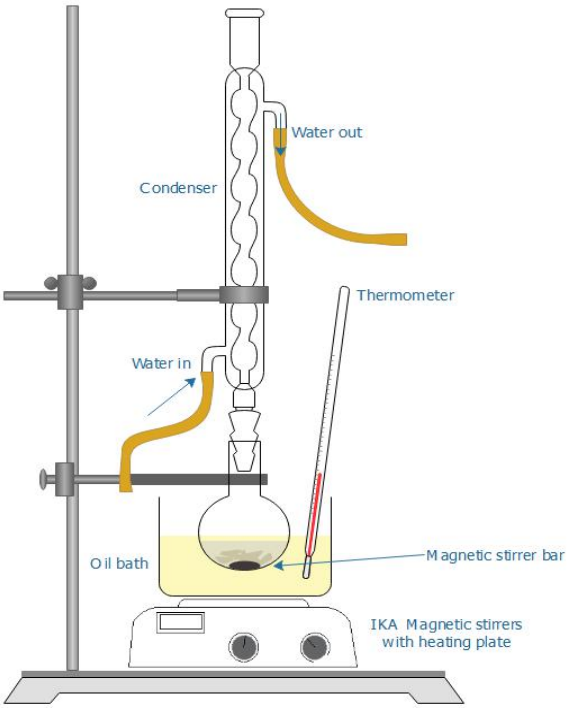

Figure 3-1. The reflux apparatus used for catalyst preparation.

Before catalysts preparation, metal oxide carrier needs to be activated through calcining at 700 ° C for 5 h. According to the modified composition of the catalyst (KF/ϒ-Al_2O_3) discussed in the previous study, higher DMC selectivity could be achieved with a KF loading of 17.5 *wt.*% (Xu *et al*., 2013). And the amount of alkali immobilised on carrier is decided by the result of experimental reactions which test a series of catalysts with various alkali loadings (range from 0 *wt.*% to 12 *wt.*%)(see Figure 5-2), the result shows that catalyst with a 12 *wt.*% K_2CO_3 loading shows better catalytic activity because both higher DMC selectivity (15.9%) and lower by-products selectivity (16.7%) is obtained when the catalyst involved in the reaction. Therefore, all the catalysts are synthesised by immobilising 17.5 *wt.*% alkali halide and 12 *wt.*% potassium carbonate on the calcined ZnO support in this study. Specifically, 3 g of each catalyst is prepared in work, thus 0.525 g NaBr and 0.36 g K_2CO_3 is dissolved into 20 ml distilled water, and 2.115 g of ZnO is added into a 50ml round-bottomed flask equipped with a stirrer bar and a condenser. The mixture is refluxing at 60 °C for 24 h, followed by vacuum filtration. Research by Chang *et al.* demonstrated that calcination could result in a higher activity of the catalyst compared with non-calcined one (Chang *et al*. 2004). Therefore, the filtered solids are dried at 100 °C for 12 h and then calcined at 700 °C for 3 h. Atomic absorption spectroscopy (AAS) was be employed to obtain the loading amount of NaBr and K_2CO_3 on support by measuring the digested catalyst and the corresponding filtrate.

3.2.2 The stainless-steel reactor

The synthesis of DMC is carried out in a stainless-steel reactor equipped with an external centigrade thermometer and a heating block (Figure 3-2). The reactor is fitted in the heating jacket and placed on an electric heater equipped with a mechanical stirrer. Both the heating temperature and stirring speed can be adjusted according to reaction requirements. Carbon dioxide is injected into the reactor through a gas line which connects with a CO_2 gas cylinder. After the air in the autoclave is removed by purging three times with pure CO_2, the reactor is pressurized to certain pressure (< 4.5 MPa) at room temperature and then heated to the reaction temperature (reaction pressure < 6.0 MPa) under stirring. The stainless-steel reactor is put into the ice-water mixture when the catalytic reaction is finished, and then the gas outlet valve is slowly opened to depressurize the reactor. For safety considerations, all operations of the reaction are carried out in a fume cupboard. The pressure of the reactor is measured by a pressure gauge, and the equipment is protected by a pressure relief valve from excessive pressure.

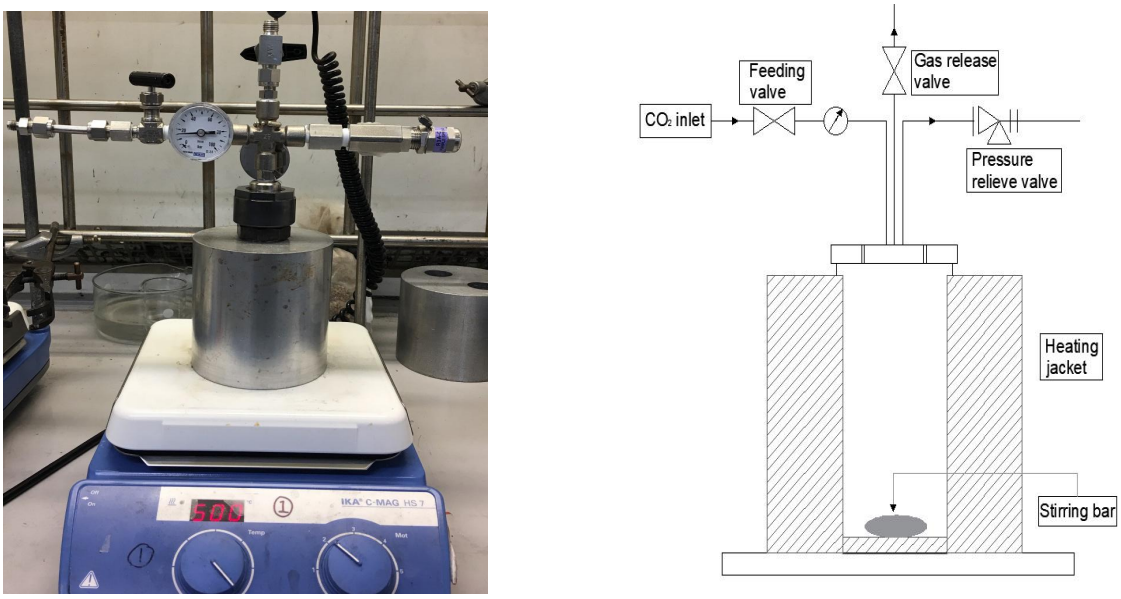

Figure 3-2. The stainless-steel batch reactor applied for the one-pot synthesis of DMC.

3.2.3 The procedure of reaction

All catalytic reactions are performed in a 45 ml stainless steel batch reactor at the desired temperature for 6 hours under stirring. Many experimental variables affect the selectivity of dimethyl carbonate, such as reaction temperature, pressure, time, methanol/PO molar ratio, the usage of catalyst, and so on. According to the modified experiment parameters given by

Chang *et al.* (Chang *et al*. 2004) and Xu *et al*. (Xu *et al.,* 2013), The parameters applied in the present work are presented in Table 3-1.

Table 3-1. The reaction parameters applied in previous studies and this work.

Parameters	Chang *et al.* (2004)	Xu *et al.* (2013)	This work
Catalysts	KI/ZnO, KI/MgO, KI/CaO	KF/ ϒ-Al_2O_3	Metal halide loaded catalyst
Temperature (°C)	**160**	180	160
CO_2 pressure (MPa)	16.5	**2.0**	2.0
Methanol/PO mole ratio	4:1	2:1	3:1
Loading amount (*wt.*%)	32.4	**17.5**	17.5
Mass of catalysts (g)	0.25g	*	0.30g
Time (h)	4h	3h	5h

The reactor is tested for gas leakage before use. In a typical reaction sequence, 0.3 g catalyst, 100mmol methanol (4.040 ml) and 33.33 mmol propylene oxide (2.330 ml) are measured and introduced into the reactor. The reactor is purged and then pressurized to 2.0 MPa with CO_2 at room temperature. The heating plate is set to a temperature of 160 °C, and the heating block is preheated to 160 °C ± 2 °C before the reactor is placed in it. When the pressure in the reactor was constant, the reaction time started to be recorded. After the reaction is carried out for 5 hours, the reactor is cooled in an ice-water mixture to quench the reaction. The pressure inside the autoclave is recorded before and after the reaction. The vacuum filtration separates the solid catalyst and liquid product, then the catalyst is dried overnight at approximately 100 °C and activated at 700 °C for the next use.

3.3 Analysis of liquid product

The liquid product is analysed by using GC-MS. The liquid sample is extracted and then filtered by using a 0.2 μm pore size Captiva syringe layered filter (Agilent). And the fine solid particles are removed by filtration. A 20 ml sample as diluted with 2000 ml of acetone (1:100) and the internal-standard substance (2-propanol) is added. GC-MS qualitatively and quantitatively analyses the diluted sample. Centrifugation is an efficient method for separating liquids and solids, but it is not suitable for this experiment because propylene oxide has a low boiling point (30 °C). Therefore, in this experiment, the sample is left to stand in ice water until the solid is settled (about 10 min), and then the supernatant is aspirated and filtered. The solid sample is washed three times with deionized water and then dried at around 100 °C. In

order to study the intermediates that may form during the reaction, ATR-FTIR is used to analyse liquid samples to obtain information about functional groups.

3.3.1 Gas chromatography/mass spectrometry (GC-MS)

Gas chromatograph-mass spectrometer is the most common analytical equipment for the separation, qualitative and quantitative analysis of vaporized organic compounds. Normally, GC is used to separate organic compounds which eluted from the column as pure gas-phase analytes. Hydrogen or helium is usually used as the carrier gas (mobile phase) which transfer the sample from the injector, through the specially prepared column, and into a detector or mass spectrometer (Sparkman, O., P *et al*., 2011). The main components of GC-MS are shown in Figure3-3.

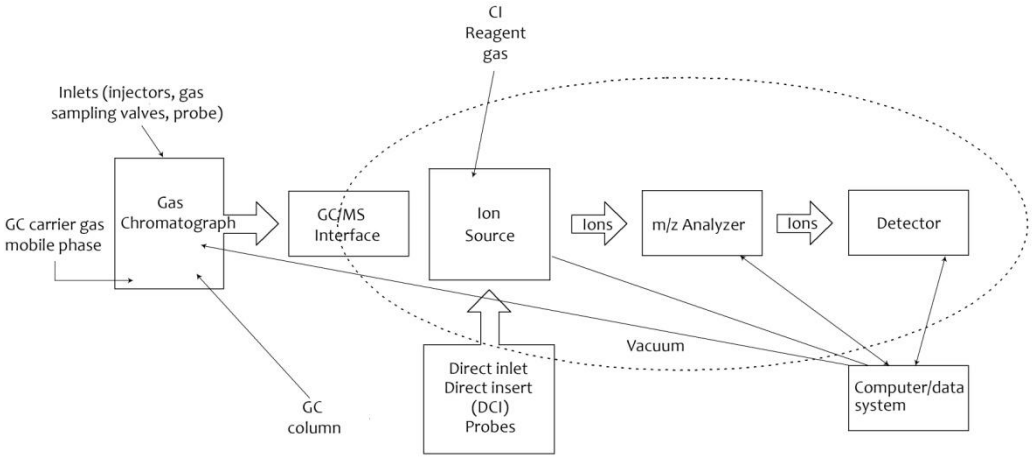

Figure 3-3. The main components of GC-MS: The GC and the inlets of GC, required detectors, the ion source, the ions' mass-to-charge (m/z) analyser, the ion detector and the computer.

The diluted liquid sample is analysed by a gas chromatograph equipped with a mass spectrometer detector (QP2010SE), which is made by Shimadzu. HP-INNOWax capillary column (Agilent) is used, and the detailed characteristics are shown in Table 3-2.

Table 3-2. The parameters of HP-INNOWax column applied for GC-MS analysis.

Column model	HP-INNOWax
Length (m)	30
Internal diameter (μm)	2.5
Film thickness (μm)	2.5
Temperature limits (°C)	260

The method developed to analyse propylene oxide (PO), 2-propanol, dimethyl carbonate (DMC), propylene glycol (PG), 1-methyl-2-propanol (1m2p), 2-methyl-1-propanol (2m1p) and propylene carbonate (PC) is shown in Table 3-3. Helium is employed as the carrier gas with a liner velocity of 64 cm sec^{-1}. The injection temperature for GC is 250 °C to make sure all the compound in the sample is completely volatilised. The injection amount of the diluted sample is 1 μl, and all the liquid products obtained from reactions are dilute 10-fold with acetone.

Table 3-3. The setup parameters of GC-MS and the temperature program for analysis.

Setup parameters for GC-MS		**Oven program for analysis**		
		Rate (°C min^{-1})	Final temp. (°C)	Hold time (min)
Split ratio	30.0	-	40	2.0
Column flow (ml min^{-1})	3.0	10.0	180.0	1.0
m/z ratios	33-500	10.0	230.0	2.0

All calculations in this work are based on the amount of PO added (Li *et al.,* 2015), since PO is a limiting reactant and 1 mol of PO could be converted to 1 mol of DMC. The calculation formulas are defined as follows:

The yield of product:

$$\text{Yield of product (i)}\ \% = \frac{\text{moles of product (i)}}{\text{moles of propylene oxide added}} \times 100\% \qquad (3\text{-}1)$$

The conversion of PO:

$$\text{Conversion of PO}\ \% = \frac{CO_{\text{propylene oxide}} - C_{\text{propylene oxide}}}{CO_{\text{propylene oxide}}} \times 100\% \qquad (3\text{-}2)$$

The selectivity of products:

$$\text{Selectivity of product (i)}\ \% = \frac{\text{moles of product (i)}}{\text{moles of propylene oxide consumed}} \times 100\% \qquad (3\text{-}3)$$

The calibration curves of dimethyl carbonate (DMC), propylene oxide (PO), propylene carbonate (PC), propylene glycol (PG) and 1-methoxy-2-propanol are shown in the Appendix A (refer Figure A-1 to A-5). Therefore, the yield and selectivity of each product, the epoxide conversion ratio can be calculated based on the amount of each product and the amount of PO added.

3.3.2 Fourier transform-infrared spectroscopy (FT-IR)

FT-IR is a widely applied technique, especially in isolating and characterising organic components or some inorganics. The application of FT-IR is based on the fact that most molecules absorb the infrared region light in the electromagnetic spectrum. This absorption will, in particular, correspond to characteristic bond vibrations within the molecule. In the measurement process, the background emission spectrum of the IR source is first determined, followed by the emission spectrum of the IR source of the sample at the appropriate location (Zhang and Cresswell, 2015). The absorption spectrum of samples directly shows the relationship between the ratio of the sample spectrum to the background spectrum and the characters of the sample. Every molecule or functional group requires different frequency for absorption. Hence the absorption spectra obtained from the natural vibration frequency of the bonds indicates that there are various chemical bonds and functional groups present in the sample (Nicolet *et al*., 2001) . Further, according to the results, the bond length and bond angle of the molecule can be measured to infer the stereo-structure of the molecule. In conclusion, FT-IR is especially suitable for the determination of organic molecular groups and compounds because of the functional groups, side chain and cross-linked involved, all of which have corresponding characteristics vibration frequencies in the infrared region. Moreover, FT-IR can be applied to determine the quality or consistency of a sample and determine the number of components in a mixture (G.R. Chatwal, S.K. Anand, 2007).

The common characteristic groups regularly appear in the frequency range of 4000~ 670 cm^{-1}. In reality, this frequency range is divided into four parts, which are summarized in Table 3-4. The bond structure represented by the absorbance (transmittance) peaks appearing on the spectrum can be found in the table.

Table 3-4. Characteristic groups in different frequency regions.

Frequency regions	Bonding types	Representative bonds
4000~2500 cm^{-1}	X-H stretching vibration region	X can be O, N, C and S atoms
2500~1900 cm^{-1}	Triple bond and cumulated double bond region	acetylenic bond (-C≡C-)，nitrile bond (-C≡N), allene bond (-C=C=C-), ketene bond(-C=C=O), isocyanate bond(-N=C=O) *et al*.
1900~1200 cm^{-1}	Double bond stretching vibration region	Mainly include the stretching vibration of C=C, C=O, C=N, -NO_2 *et al*.
<1650 cm^{-1}	X-Y stretching vibration and deformation vibration region	Mainly include the deformation vibration of C-H and N-H, the stretching vibration of C-O and C-X(halogen), and the single-bond framework vibration of C-C, *et al*.

In this work, the FT-IR spectra would be recorded on a Shimadzu FT-IR (IRAffinity-1S) equipment with an ATR accessory. Measurements are performed using a resolution of 0.5 cm^{-1} and scanning times of 256 in the region of 4000-400 cm^{-1}. When making measurements, the background spectrum can be measured with an empty sample holder. Then a drop of the liquid sample is put on the crystal, and the measurement can be processed.

3.4 Catalyst characterisation

In this part, a brief introduction to catalyst characterisation techniques is presented. Fresh and used catalysts are analysed by thermogravimetric analysis (TGA), X-ray diffraction (XRD), scanning electron microscopy (SEM), atomic absorption spectroscopy (AAS), temperature-programmed desorption (TPD), N_2 adsorption isotherms, inductively coupled plasma-optical emission spectroscopy (ICP-OES) and Fourier transform-infrared spectroscopy (FT-IR).

3.4.1 Thermogravimetric Analysis (TGA)

Thermogravimetric analysis is a technique which can characterize the sample by monitoring the change of weight of it over time and temperature (Groenewoud, 2001). The results of the analysis can reflect the properties of materials, including thermal stability, composition, oxidative stability, decomposition kinetics, *etc*. Thermogravimetric analysis can also be

applied in the field of catalysis to investigate the reaction between active component and support during calcination (Chen and Marks, 2000).

The results measured using a thermogravimetric analyser can be expressed in two curves: a thermogravimetric curve (TG) and a derivative thermogravimetric curve (DTG). The former records the changes in sample mass as a function of temperature or time, the latter being a curve obtained by the derivation of the TG curve versus temperature or time. The DTG curve accurately reflects the initial reaction temperature: the temperature at which the maximum reaction rate is reached, and the temperature at which the reaction is terminated (Abdullah, Mohammad and Maik, 2016). Therefore, the samples can be qualitatively and quantitatively analysed to some extent.

In this work, the catalysts are analysed by using a thermogravimetric analyser (PerkinElmer, TGA 4000). The sample (around 7 mg) is dried at 100 ° C overnight before placed in a ceramic pan. The sample is heated from 40 °C to 950 °C at a rate of 10 °C min^{-1} and held at this temperature for 10 min under a nitrogen purge (20.0 ml min^{-1}). Then the furnace cools down from 950 °C to 40 °C with a rate of 80 °C min^{-1}.

3.4.2 X-ray diffraction (XRD)

X-ray diffraction (XRD) is a non-destructive technique that is widely used to characterize the structure and phase composition of crystalline materials. In particular, the measurement results may reveal information about the structure, phase, crystal orientation (texture) and other structural parameters of the material, like average grain size, strain, crystal defects and crystallinity (Kohli and Mittal, 2011). When a monochromatic beam of X-rays is irradiated onto the crystal, electrons around the atom are vibrated generated by the periodic change of electric field of the X-ray, and scattered waves are generated. By measuring the angle and intensity of the diffracted X-rays, a unique diffraction pattern for each compound can be obtained, which is finally appeared in the form of X-ray diffraction peaks. Therefore, the X-ray diffraction pattern can provide fingerprint information about the atomic distribution in the crystalline materials. An online search for a standard database of X-ray powder diffraction patterns allows for rapid qualitative analysis of various crystalline samples.

In this work, solid catalysts are analysed using a Bruker D2 Phaser powder XRD instrument with Cu Kα (tube voltage: 30 keV, current: 10 mA, 2θ range from 10 ° to 80 °) radiation at a

scanning rate of 0.05 ° min^{-1}. By comparing the XRD pattern obtained with the database (PDF-4^{+} 2016), the crystalline phases are identified.

3.4.3 Scanning electron microscopy/ Energy Dispersive X-Ray Spectroscopy (SEM/EDS)

SEM analysis gives detailed information on the morphology of catalyst (like the speciation structure of the catalyst, the size and shape of particles) (Amelinckx *et al.,* 2008). A well-focused electron beam is applied to scan the surface of a sample, and various signals (like secondary electrons (SE), reflected or back-scattered electrons (BSE), *etc*.) are produced. The yield of secondary or backscattered electrons can be detected as a function of the position of the primary electron beam in a scanning electron microscope (SEM), and the contrast of the signal can determine the surface morphology. Usually, secondary electrons are mostly applied in showing morphology and topography of samples, and backscattered electrons are generally used for demonstrating contrasts in composition in multiphase catalysts (Mohale, 2017). Therefore, BSE images can determine the distribution of different elements in the sample but cannot do the identical analysis. The qualitative and semi-quantitative determination can be performed by doing an energy-dispersive analysis of the X-rays released from a specimen (EDX) (Goldstein *et al.,* 2018). The number and energy of the X-rays are recorded, and the position of peaks in the EDX spectrum can provide information about the identification and concentration of elements.

If the sample is non-conductive, it should be coated with a thin layer of electrically conductive material, typically carbon, gold or some other metal or alloy. The information you want to collect is an essential basis for determining conductive coating material: carbon is an ideal choice if the elemental analysis is prioritized, while metal coatings are most desirable for high-resolution electronic imaging applications.

In this work, JEOL JSM-6010LA Analytical Scanning Electron Microscopy is employed to analyse the samples. Before measurement, samples are pre-coated with gold for 8 seconds in an Agar Sputter Coater. The acceleration voltages are changed from 15 keV to 20 keV, and the working distance (WD) is 11 mm throughout the measurement. The morphology of the catalyst is determined using SEM and the qualitative and semi-quantitative analysis of different elements on catalyst surface are performed using SEM-EDS.

3.4.4 Atomic absorption spectroscopy (AAS)

Atomic absorption spectroscopy is an atomic spectrometric method for quantitative analysis of elements based on the absorption of characteristic radiation by the free gaseous atoms at a specific wavelength. For solid samples, it needs to be digested with concentrated acid (like HNO_3 or HCl) to make a solution analysis. In this work, the concentration of Zn both in liquid mixtures after reaction and in solid catalysts is analysed using an atomic absorption spectrometer (PerkinElmer, Analyst 400). The samples are diluted with 1 % HNO_3 to ensure that the concentration of Zn in the sample is under 10 ppm.

3.4.5 CO_2-Temperature-programmed desorption (CO_2-TPD)

Temperature-programmed desorption is used to provide information about the strength and distribution of specific sites on the catalyst surface. The most common molecule for probing the basic sites of catalyst is CO_2. The temperature of CO_2 desorption indicates the strength of basic sites and the amount of gas desorbed upon increasing temperature shows the concentration of basic sites. Before measurement, samples are pre-treated at 100 °C in flowing gas to remove H_2O molecular and then heated to high temperature (for example, the temperature for ZnO is 500 °C) to remove impurities and activate the catalyst. Then the samples are cooled to 110 °C for CO_2 adsorption. This temperature can reduce the influence of physisorption of CO_2. After saturation with CO_2, the samples are purged with helium to remove any physisorbed probes. Finally, TPD analysis is performed by increasing the heating temperature from 110 °C to 900 °C, and the thermal conductivity detector (TCD) is used to monitor the amount of desorption.

3.4.6 N_2 adsorption isotherms

Nitrogen adsorption isotherms are widely applied to the determination of the pore size distribution and specific surface area of porous materials. The analysis is supported by the Brunauer–Emmett–Teller (BET) theory, which proposes the multilayer adsorption of gas (Brunauer, Emmett and Teller, 1938). The specific surface area of the catalysts can be evaluated using the BET equation derived from the adsorption isotherm (Sing, 1985). Barrett-Joyner-Halenda (BJH) method is used to calculate the pore size distribution from experimental gas isotherms using the Kelvin model of pore filling (Barrett, Joyner and Halenda, 1951). The specific surface area and pore volume are calculated by determining the nitrogen adsorption-desorption isotherms at -196 °C. The number of gas molecules adsorbed on a solid surface is obtained according to the evolution of pressure in the system. The

adsorption isotherm can be obtained by plotting the cumulative amount of adsorbed gas relative to the pressure.

In this work, a 3 Flex Micromeritics Surface Characterization instrument is employed to analyse the fresh catalysts. Before measurements, all the samples are degassed at 150 °C for 24 h under a reduced pressure below 0.01 Pa using Vac Prep 061. Then, N_2 adsorption measurement is taken place in liquid nitrogen at -196 ° C. The measurement process is operated using the software 3 Flex version 3.02.

3.4.7 Inductively coupled plasma-optical emission spectroscopy (ICP-OES)

ICP-OES has been widely used to evaluate the element composition in aqueous and organic liquid and solid samples using plasma and a spectrometer. During the measurement, the component elements of analysis samples are excited when the plasma energy is given from outside. The emitted radiation (spectral rays) is released, and the emission rays corresponding to the wavelength of the photons are measured when the excited atoms return to the low energy position. The element type is determined according to the wavelength of the photons, and the concentration of the element is evaluated based on the total number of photons (Hou and Jones, 2000).

In this work, the instrument (Spectro Ciros Vision) with radial argon plasma is employed to analysis liquid reaction products and the solid catalysts. Liquid samples are acidified with HNO_3 to make sure that all elements remain in solution and solid samples are digested using hot acids. The software Spectro Smart Studio-Smart Analyser (V2.11) is used to monitor the instrument, calibrate and perform the measurement.

3.4.8 Fourier transform-infrared spectroscopy (FT-IR)

KBr pellet sampling method is used to measure the characteristic of synthetic catalysts. The concentration of the catalyst in KBr pellet should be around 0.2% to 1%. Too high concentrations often result in difficulties in obtaining clarified particles (Beer's law). Under this condition, the IR beam is wholly absorbed or scattered from the sample, which results in a very noisy spectrum. In the KBr pellet preparation process, some of the pure KBr powder is transferred to the mortar, and about 0.2 to 1 *wt.*% of the sample is added, mixed and milled to a fine powder, followed by placing fine powder in a pellet forming die. KBr pellet is formed under high pressure. When making measurements, the background spectrum can be measured

with an empty dish holder inserted into the sample chamber. However, if pure KBr pellet (excluding samples) put on the pellet holder are used as the background measurement, the errors caused by infrared light scattering loss in the pellet and the moisture adsorbed on the KBr can be corrected (Niu.*edu*, 2007).

3.5 Overall experiment plan

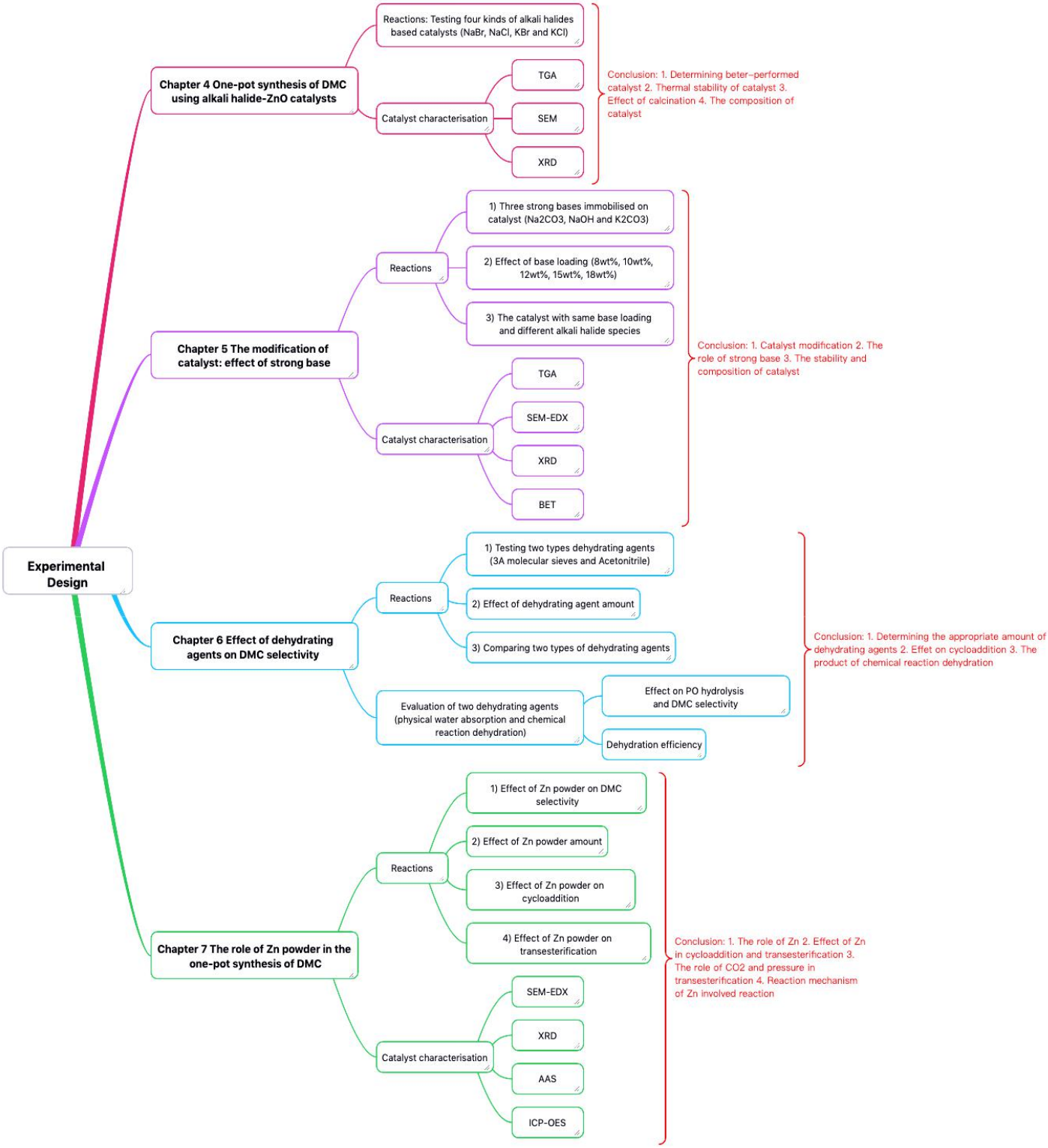

3.6 Experimental errors and error analysis

Accuracy is an indicator which can explain how close an experimental value is to the actual value, and the word "precision" is used to describe how closely two or more value agrees with others. Precision sometimes can be replaced by the word "repeatability" (Carlson, 2002).

The experimental errors can be divided into human error and experimental inherent error according to its source. The former is visible and can be avoided by trial and error. However, the latter is an inherent error in the measurement process and cannot be eliminated simply by repeated experiments. There are two types of inherent errors: systematic errors and random errors.

3.6.1 Systematic errors

Systematic errors can affect the accuracy of the experimental results. The accuracy of measurements influenced by systematic errors cannot be improved by the repeated tests (Carlson, 2002). In general, systematic errors are difficult to detect through statistical analysis. Once detected, they can be reduced by modifying measurement methods or techniques. Typical sources of systematic errors are faulty calibration of measurement equipment, poor equipment maintenance, *etc.*

3.6.2 Random errors

The random error is caused by a series of small random fluctuations in the measurement process, such as the uncertainties in environmental conditions (room temperature, relative humidity and pressure), the slight difference in the operation of the analyst and the instability of the experimental equipment. The fluctuate may above or below the true value. However, it has been found that through multiple measurements, positive and negative random errors with the same absolute value have approximately the same probability. Therefore, the random error can be reduced by increasing the parallel measurements or modifying the measurement methods.

3.6.3 Calculating experimental error

It is necessary to show the accuracy and precision of the experimental measurements in a scientific report or publication. There are three common ways to illustrate the accuracy and precision of the experiment results:

(1) Significant figures

The least significant number of digits in the measurement decided by the smallest unit that can be measured with the measuring equipment. Then the number of significant digits shown on the instrument can be applied to estimate the precision of the measurement. In general, the precision of any measurement is equal to 1/10 of the smallest graduation on the measuring instrument. For example, the minimum graduation for measurement of length is 1 mm, so the precision of the measurement is ± 0.1 mm. The smallest unit for measurement of volume using a graduated cylinder is 1ml, which means the precision of this measurement is ± 0.1 ml.

(2) Percent error

The percent error indicates the accuracy of a measurement by calculating the difference between experimental data (*E*) and true value (*A*). The calculation equation is shown below:

$$\%\ Error = \frac{|E-A|}{A} * 100\ \% \qquad (3\text{-}4)$$

(3) Mean and standard deviation

When the measurement is repeated multiple times, it can be found that the measured values are distributed around some central value. Two numbers can describe this grouping: The mean value, which represents the central value of the measurement; and the standard deviation, which describes the distribution or deviation of measured values to the mean. The standard deviation (σ_d) is calculated as follows, where *N* represents the number of experimental measurements, *[x]* represents the mean value, and x_i represents the measured value of the *i*-th measurement.

$$\sigma_x = \sqrt{\frac{1}{N-1}\sum_{i=1}^{N}(x_i - [x])^2} \qquad (3\text{-}5)$$

The standard deviation shows how far a set of experimental data distributes around the mean. The larger the standard deviation, the more data far away from the central value. When the experimental result of a measurement is reported in a paper, both mean value and variation of

measurements should be reported. The form of the measurement result should be shown as follows:

$$x = [x] \pm \sigma_x \qquad (3\text{-}6)$$

In this report, all the measurements are repeated at least five times, and all the data is shown as a form of mean ± standard deviation.

CHAPTER 4

ONE-POT SYNTHESIS OF DMC USING ALKALI HALIDE-ZnO CATSLYST

Chapter 4 One-pot synthesis of DMC using alkali halide-ZnO catalyst

4.1 Introduction

This thesis has explained one-pot synthesis of dimethyl carbonate from methanol, carbon dioxide and propylene oxide in the literature review. The one-pot synthesis of DMC consists of two reversible steps: cycloaddition and transesterification. In the cycloaddition reaction, propylene oxide reacts with CO_2 to form propylene carbonate (PC). And in the transesterification step, methanol and PC are converted to DMC and propylene glycol (PG). 1-methoxy-2-propanol and 2-methoxy-1-propanol are produced as by-products through the reaction between PO and methanol.

The choice of catalyst is a crucial parameter in achieving high yields of DMC. Alkali halide containing catalyst is conducive to promote the formation of DMC *via* the one-pot synthesis route. The main function of halide ions in the reaction system is to activate CO_2 and then to promote the formation of PC by nucleophilic attack of halide ions (Scheme 4-1). For example, KI immobilized on ZnO could be a very effective catalyst under supercritical CO_2 condition (16.5 MPa) (Chang *et al*., 2004). 36.8% of DMC selectivity and 60.7% of PC selectivity can be obtained using KI-ZnO as the catalyst. The catalytic ability of catalyst is related to their ability to donate electrons. In this study, Turnover frequency (TOF) is used to evaluate the catalytic efficiency of the reaction system. In this research, the TOF is defined as the mass of synthesised dimethyl carbonate (DMC) per gram catalyst per hour, and its calculation formula (Equation 4-1) is shown as follows:

$$\mathrm{TOF} = \frac{m_{DMC}}{W_{cat} \times t} = \frac{n_{PO} \times Yield_{DMC} \times M_{DMC}}{W_{cat} \times t} \qquad (4\text{-}1)$$

where n_{PO}, M_{DMC}, t, and W_{cat}. represent the molar amount (mmol) of PO, formula weight (g mol^{-1}) of DMC, reaction time (h), and the mass of overall catalyst (mg), respectively.

Another critical factor that affects the catalytic activity is the reaction pressure. Previously, high selectivity to DMC has been correlated with high pressure operating environments employing supercritical CO_2 (Cui *et al.*, 2003). Table 4-1 summarises the selectivity to DMC achieved over various alkali halide-containing catalysts at different CO_2 pressures. TOF

values of the catalytic systems are calculated based on the reaction conditions provided in the previous literature studies. Applying high-operating pressure in chemical plants is, however, cost and energy-intensive and introduces significant safety concerns. Optimisation of reaction conditions with the aim of minimizing the operating pressure while increasing reaction rate, selectivity and catalyst lifetime should be a key goal of process development (The Royal Society, 2017).

Table 4-1. Catalysts previously applied in the one-pot synthesis of DMC, and CO_2 pressures employed.

Catalyst	CO_2 pressure (MPa)	DMC selectivity	TOF (h^{-1})	Reference
KOH-KI-ZnO	16.5	58.0%	8.4	(Chang *et al*., 2004)
Mg-KCl-ZrO_2	9.5	52.7%	52.2	(Eta and Leino, 2010)
Na_2CO_3–KCl-Al_2O_3	2.5	20.1%	-	(Jiang and Yang, 2004)
KCl + crown ethers	2.0	23.0%	73.7	(Li *et al*., 2015)

In this section, the one-pot synthesis of DMC from propylene oxide (PO), methanol and carbon dioxide was taken place under mild condition (2.0 MPa and 160 °C) with different alkali halides catalysts. The catalysts were prepared by supporting alkali halides (like KCl, KBr, NaCl and NaBr) on the ZnO carrier, followed by the catalyst activation. The effect of reaction time on DMC selectivity has been extensively investigated by changing the reaction time from 3 hours to 7 hours.

4.2 Experimental methods

4.2.1 Materials

Reagents potassium chloride (KCl, 99.0-100.5%) and sodium bromide (NaBr, ≥99%), propylene oxide (≥99.5%) were purchased from Sigma-Aldrich. CO_2 (purity over 99.99%, water content less than 0.01%) was bought from BOC. Methanol (99.9% min), potassium bromide (KBr, ACS, 99% min) and sodium chloride (NaCl, 99+%) were purchased from Alfa-Aesar. Zinc oxide was purchased from Fisher Scientific. 2-propanol (Sigma-Aldrich, ≥ 99.8%) was used as an internal standard for GC-FID quantitative analysis. Dimethyl carbonate (DMC, 99%), propylene carbonate (PC for HPLC, 99.7%),1-methoxy-2-propanol (≥99.5%) and propylene glycol (PG, ACS reagent, ≥99.5%) were employed as reference materials for calibration curves, supplied from Sigma Aldrich. Deionized water was used in all experiments.

4.2.2 Methods

4.2.2.1 Preparation of catalyst and reaction conditions

The catalyst preparation method has been elaborated in Chapter 3.1.1. All the catalysts are synthesized by immobilizing 17.5 *wt.*% alkali halide on the calcined ZnO support. Specifically, 3 g of each catalyst is prepared in this work, thus 0.525 g alkali halide is dissolved into 20 ml distilled water. And 2.475 g of ZnO is added into a 50 ml round-bottomed flask equipped with a stirrer bar and a condenser. The mixture is refluxing at 60 °C for 24 h, followed by vacuum filtration. The filtered solids are dried at 100 °C for 12 h and then calcined at 700 °C for 4 h.

Based on the reaction parameters discussed in previous studies (see Table 3-1), the modified reaction conditions (Time: 5h, Temperature: 160 ° C,Methanol/PO mole ratio: 3/1,mass of catalyst: 0.3g) are applied in this work in order to obtain a higher selectivity of DMC.

4.2.2.2 Influence of the species of alkali halide

Alkali halide plays a critical role in the synthesis of propylene carbonate through cycloaddition. Cycloaddition is an exothermic reaction, and its standard reaction heat is about 126 kJ mol^{-1} (Korosteleva *et al.*, 2013). From the view of chemical equilibrium, lowering the reaction temperature or increasing the reaction pressure favours the shift of the chemical equilibrium toward the forward reaction. However, if the temperature is too low, it is not

conducive to the activation of the reactants, for the reaction rate is slowing down. However, increasing pressure seems to be conducive to the reaction. All the reactions in this study are carried out under 2 MPa (room temperature) pressure condition. Therefore, an appropriate catalyst is needed to activate CO_2 and then to promote the production of PC and DMC.

Based on previous literature research (Liu *et al*., 2016), the introduction of a nucleophilic group (like Cl^-, Br^- and I^-) facilitates the coupling the reaction of propylene oxide and CO_2. Moreover, the catalytic activity decreases in the order of $I^- > Br^- > Cl^-$, which is in agreement with the ability of nucleophiles to donate electrons and the leaving ability of the halide anions. Therefore, the proposed ZnO carrier with nucleophilic Br^- and Cl^- anions are applied in this research because I^- anion is expensive and toxic.

4.2.2.3 Influence of reaction time

In order to study the influence of changing the reaction time on the selectivity of each product and PO conversion, a set of reactions with various reaction time in the presence of the alkali halide-containing catalysts were carried out. The detailed parameters for the reactions are summarised in Table 4-2.

Table 4-2. Catalysts used in the one-pot synthesis of DMC, and reaction time applied.

Catalyst	Reaction time (h)	Reaction conditions
NaBr-ZnO	3, 4, 5	160 °C, CO_2 (2 MPa, room temperature), catalyst (17.5 *wt.*% alkali halide-ZnO, 0.3 g), PO (33.33 mmol), methanol (100 mmol)
NaCl-ZnO	5, 6, 7	

Two kinds of Na-based catalyst with different alkali halide species were tested in this section. It aims to study the trend of reaction products over time, so as to determine the optimal reaction time to improve the efficiency (TOF value) of the catalyst. Another objective is to compare the catalytic capabilities of two catalysts containing different alkali halides, especially the selective catalytic ability to PC.

4.3 Results and discussion

4.3.1 Influence of alkali halide species

The catalytic ability of various alkali halide catalysts was assessed for the synthesis of dimethyl carbonate from methanol, propylene oxide and CO_2 under 2 MPa and 160 °C reaction condition. The result is shown in Figure 4-1.

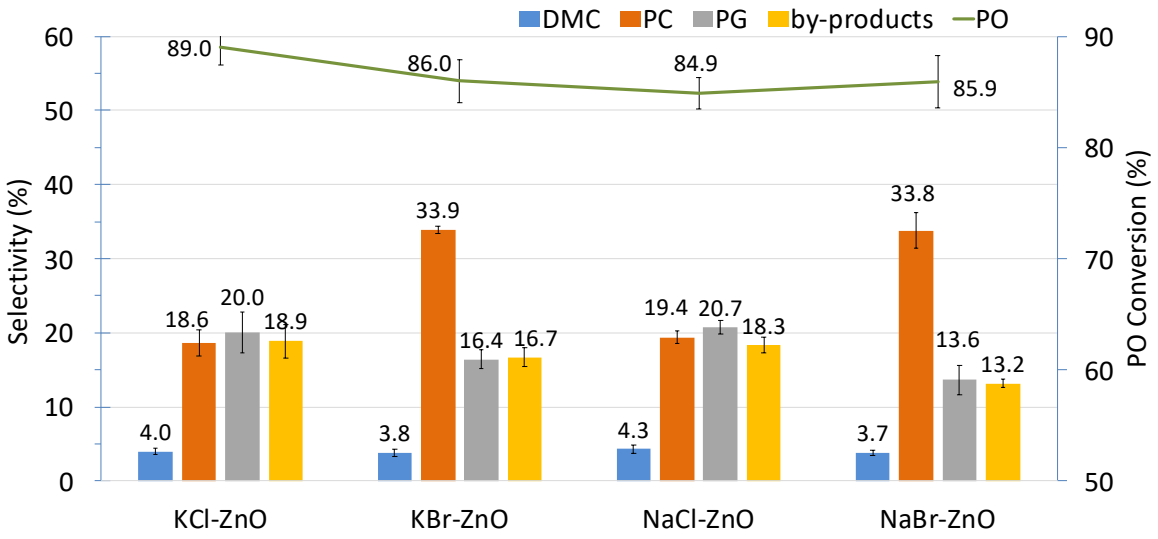

Figure 4-1. Effect of alkali halide species on the conversion of PO and the selectivity of DMC, PC, PG and by-products in DMC synthesis. Reaction condition: 160 °C, 5 h, CO_2 (2 MPa), catalyst (17.5 *wt*% alkali halide-ZnO, 0.3 g), PO (33.33 mmol), methanol (100 mmol).

The selectivity of DMC and PC and the PO conversion indicates the activity of the catalyst. As shown in Figure 4-1, the DMC selectivity of the reaction using the chlorine-containing catalyst is similar to that using the bromine-containing catalyst. Moreover, bromine-containing catalysts lead to a much higher PC selectivity. By contrast, chlorine-containing catalysts produce more PG and by-products (1-methoxy-2-propanol and 2-methoxy-1-propanol). This can be explained by the fact that the activity of catalyst decreases in the order of Br^- > Cl^- in cycloaddition reaction, which is in agreement with the ability of nucleophiles to donate electrons and the leaving ability of the halide anions. Higher PG and by-product formation is caused by the hydrolysis of PO and the reaction between PO and methanol, respectively. According to the reaction principle, one-pot synthesis of DMC includes two reaction steps: the cycloaddition of PC by CO_2 and PO (Scheme 4-1) and the transesterification of DMC by methanol and PC (Scheme 4-3). Transesterification process is often accompanied by the formation of propylene glycol. From the results, it is apparent that four kinds of catalyst have little difference in improving the selectivity of DMC, but the

catalyst containing bromine can improve the PC selectivity and reduce the PG selectivity obviously. It is crucial for transesterification reaction because higher PC concentration and lower PG content in the reactant can drive the reaction toward the direction of DMC generation.

The data in Figure 4-1 shows the conversion of PO in reactions using different catalysts. It can be seen that the reactions involving the four catalysts have similar PO conversion. There could be two explanations for the results: 1) When the reaction is carried out for 5 hours, the reaction has reached equilibrium, the PO conversion at this time is the maximum value under the corresponding reaction temperature and CO_2 pressure conditions. In other words, the further increase of the reaction time does not affect the conversion of PO; 2) The reaction has not reached the equilibrium even after 5 h and the PO conversion rate rises with the further increase of the reaction time. This conjecture could be supported by the fact that various catalysts have different catalytic rates for the reaction, and catalysts with higher PO conversion may be able to move the reaction more rapidly towards the DMC formation. In order to verify these two conjectures and to find out the trend of the selectivity of each product changes with reaction time, more reactions were performed using NaCl-ZnO and KBr-ZnO as the catalyst.

4.3.2 Influence of reaction time

In order to improve the catalytic efficiency by finding the optimised reaction time, a set of reactions were performed with increasing reaction time in a range of 3 hours to 7 hours. When NaCl-ZnO was used as the catalyst, the reaction time was extended from 5h to 6h or 7h. On the contrary, reaction time was shortened from 5 h to 3 h or 4 h with NaBr-ZnO as the catalyst. The product selectivity and PO conversion are shown in Figure 4-2 (a) and Figure 4-2 (b).

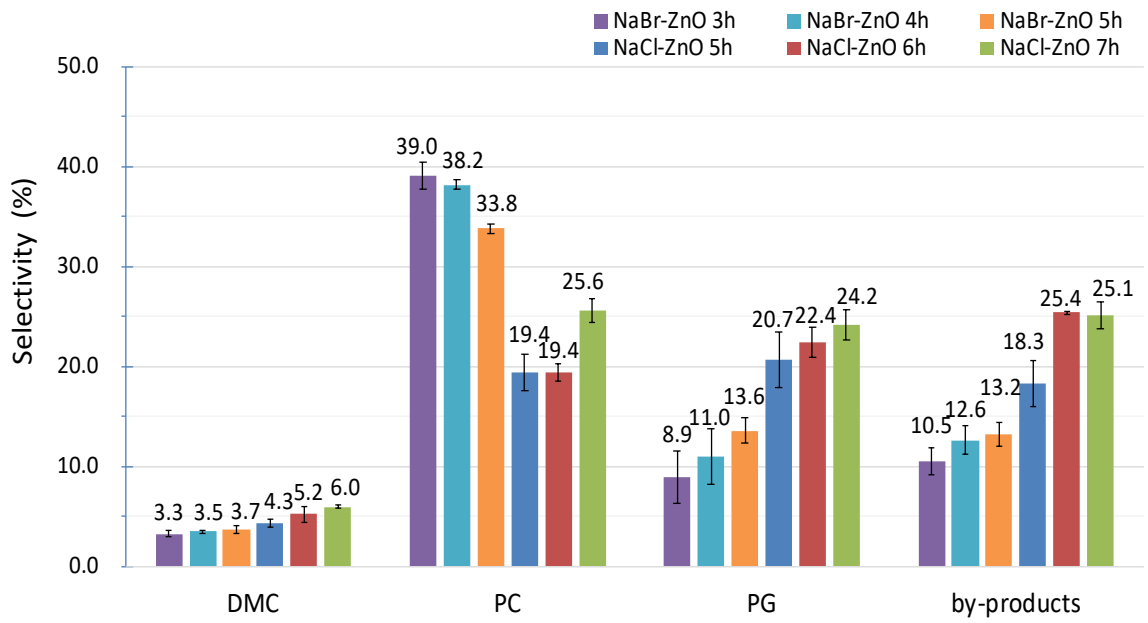

Figure 4-2 (a). Effect of reaction time on the selectivity of DMC, PC, PG and by-products in DMC synthesis. Reaction condition: 160 °C, CO_2 (2 MPa), catalyst (17.5 *wt*% alkali halide-ZnO, 0.3g), PO (33.33 mmol), methanol (100 mmol).

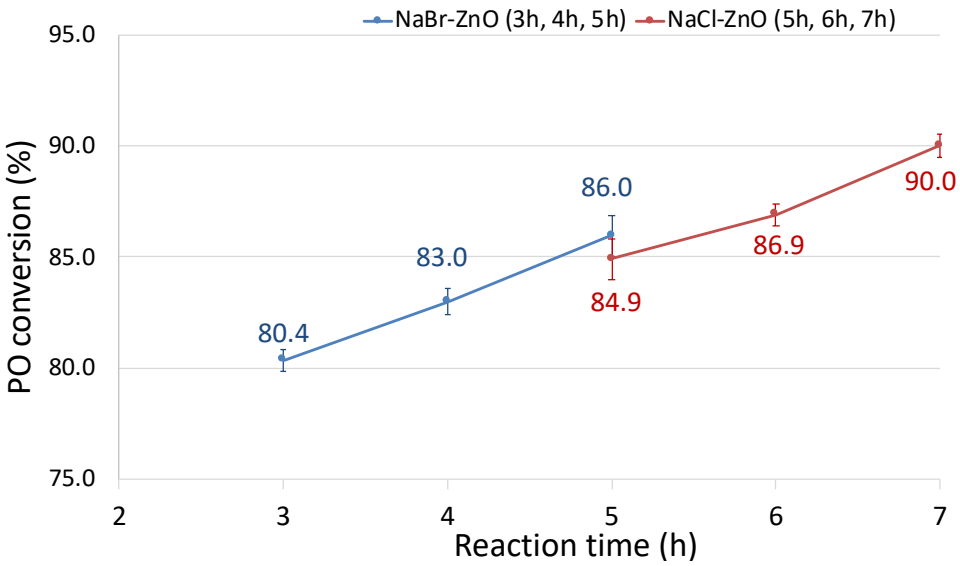

Figure 4-2 (b). Effect of reaction time on the conversion of PO in DMC synthesis. Reaction condition: 160 °C, CO_2 (2 MPa), catalyst (17.5 *wt.*% alkali halide-ZnO, 0.3 g), PO (33.33 mmol), methanol (100 mmol).

Table 4-3. The activity of catalysts under different reaction time.

Reactions	TOF (h^{-1})
NaBr-ZnO 3 h	8.8
NaBr-ZnO 4 h	7.2
NaBr-ZnO 5 h	6.3
NaCl-ZnO 5 h	7.2
NaCl-ZnO 6 h	7.6
NaCl-ZnO 7 h	7.7

As can be seen from Figure 4-2 (a) and (b), both the selectivity of PG and by-products and the PO conversion of the reactions using two kinds of catalysts goes up with the increasing reaction time. In detail, when NaBr-ZnO is used as the catalyst, the increase of DMC is not apparent, and the selectivity of PC decreases slightly with the increase of reaction time. The selectivity of PG and by-products reaches the maximum at the time point of 5 hrs. when NaCl-ZnO is used as the catalyst, the selectivity of DMC and PC increases with longer reaction time. The trend of by-products and PG is similar to that of NaBr-ZnO catalyst applied reactions. Therefore, the two catalysts are set apart by their efficiency in catalysing the reaction. With the same reaction time, the reaction rate with NaBr-ZnO as the catalyst is faster than that with NaCl-ZnO as the catalyst. For example, when NaBr-ZnO is used as a

catalyst, the TOF value can reach 8.8 h^{-1} after three hours reaction time, which is higher than that of the reactions using NaCl-ZnO catalyst.

When NaBr-ZnO is used as the catalyst, the TOF value remains basically unchanged with the increase of the reaction time (5 hours to 7 hours), which means that when the reaction proceeds to 5 hours, the reaction basically reaches an equilibrium state. Moreover, it is obvious that as the reaction time increases, the selectivity of PG and by-products increases. When NaCl-ZnO is used as the catalyst, the TOF value decreases as the reaction time increases (3 hours to 5 hours), because the formation of PC through cycloaddition is the main reaction conducted in the reaction system, and the transesterification of methanol and PC to DMC has not reached an equilibrium state. Moreover, when the reaction time reaches 5 hours, a higher PO conversion rate can be obtained. Therefore, considering PO conversion, PC and DMC selectivity, by-product selectivity and energy input, 5 hours is more appropriate reaction time.

4.3.3 Catalyst characterisation

As discussed in section 4.3.1, the bromine-based catalyst shows a higher catalytic ability to promote the formation of PC *via* cycloaddition and to limit the production of PG and by-products. In order to investigate the relationship between the active substance (NaBr) and carrier (ZnO) during the catalyst preparation process, TGA and XRD analysis is employed to obtain the information about the composition of calcined NaBr-ZnO catalyst.

4.3.3.1 Thermogravimetric analysis (TGA)

Thermogravimetric analysis was applied to study the interaction between the active ingredients NaBr and the carrier (ZnO). Figure 4-3 shows the thermogravimetric analysis of two samples, (a) calcined NaBr-ZnO and (b) non-calcined NaBr-ZnO. The original TGA data are plotted alongside the differential thermograms (DTG).

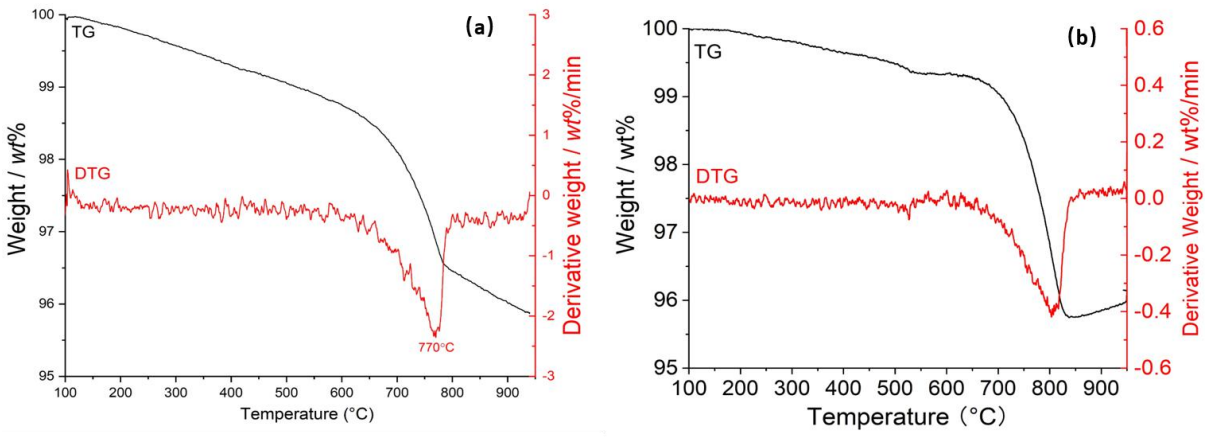

Figure 4-3. DTG and TG curves of (a) calcined NaBr-ZnO catalyst (b) non-calcined NaBr-ZnO catalyst.

The TG and DTG curves in Figure 4-3 (b) indicate that the non-calcined NaBr-ZnO catalyst shows weight loss from 700 °C and reaches the highest weight loss rate at around 800 °C. Weight loss is related to melt point of NaBr, which is around 755 °C. The TG-DTG curve in Figure 4-3 (a) shows that the weight of the calcined catalyst begins to decrease from 650 °C and the mass-loss rate reaches a maximum at ~ 770 °C due to the melt of NaBr as well. Comparing Figures 4-3 (a) and (b), it can be concluded that a new compound was probably formed during the preparation of the catalyst because the starting temperature for catalyst weight loss is reduced from 700 °C to 650 °C, or calcination makes NaBr uniformly dispersed on the surface of ZnO. During TG analysis, the dispersed NaBr starts to decompose earlier and faster than the supported NaBr on ZnO without calcination.

4.3.3.2 X-ray powder diffraction (XRD)

The crystallinity of the catalyst before and after calcination was assessed by XRD and the data is illustrated in Figure 4-4. Both samples show the characterisation peaks of ZnO crystal structure (PDF-ICDD 01-081-8838) and only non-calcined NaBr-ZnO catalyst gives the peaks assigned to NaBr (PDF-ICDD 04-007-3592) structure. The characteristic peaks of NaBr disappeared after calcination of the catalyst (Figure 4-4 (b)). A similar result is obtained by Chang (Chang *et al*., 2004), both calcined and non-calcined KI-ZnO catalyst is analysed using XRD to determine the active components on the catalyst surface. As a result, the characteristic peaks of KI disappeared on the XRD patterns after calcination. One possible explanation is that KI is uniformly dispersed on the surface of the carrier or a new amorphous phase is produced.

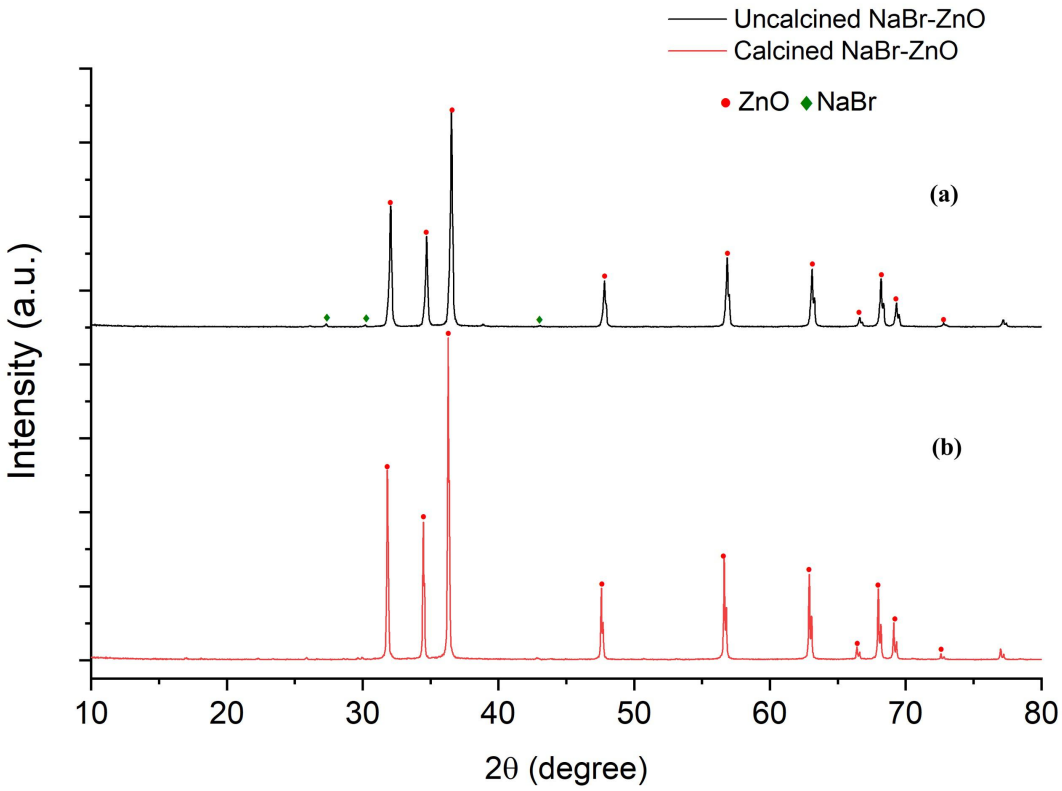

Figure 4-4. The XRD patterns of catalysts: (a) non-calcined NaBr-ZnO; (b) calcined NaBr-ZnO.

According to the analysis results of TGA, in this study, the main reason for the disappearance of the characteristic peaks of NaBr after calcination is that NaBr was uniformly dispersed on the surface of the support after calcination.

4.3.4 Proposed reaction mechanism

DMC is formed *via* cycloaddition of propylene oxide and CO_2, then followed by the transesterification of propylene carbonate and methanol with the addition of NaBr-ZnO catalyst. 1-methoxy-2-propanol and 2-methoxy-1-propanol are the side products generated by the reaction of PO and methanol. The hydrolysis of PO is another route to produce PG, which limits the transesterification to the direction of DMC formation. In this section, the proposed mechanisms for cycloaddition, transesterification, by-products formation and PO hydrolysis are discussed.

4.3.4.1 Mechanism for cycloaddition

A proposed reaction mechanism for the formation of propylene carbonate is presented in Scheme 4-1.

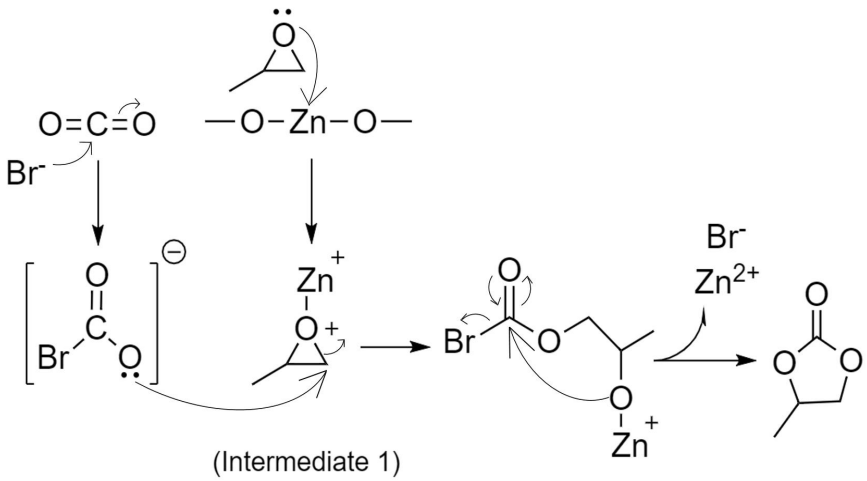

Scheme 4-1. Proposed mechanism for the synthesis of propylene carbonate from propylene oxide and carbon dioxide (Álvarez *et al.*, 2017; Wang, Xie and Deng, 2014; Martínez-Ferraté *et al*., 2018).

Carbon dioxide is a weak acidic gas which can adsorb or react at acid-base sites on solid surfaces. In previous studies where the mechanism of cycloaddition has been discussed. In this work, the reaction is proposed to be initiated by the activation of CO_2 by the Br^- nucleophile (Álvarez *et al.*, 2017) and the attack of the surface Zn^{2+} cation by propylene oxide to form intermediate 1 (Wang, Xie and Deng, 2014). Following this, the reactive CO_2^- species formed on the ZnO attacks the less substituted ring carbon atom in intermediate 1 because it is less sterically hindered than the adjacent one. The last step is the formation of propylene carbonate (Martínez-Ferraté *et al*., 2018). At the same time, Zn^{2+} and Br^- dissociate from the product and dissolve into the reaction solution. Following this mechanism, it is expected that the alkali halide ions in the reaction system would have a significant effect on

PC formation, and the PC selectivity is related to the ability of nucleophiles to donate electrons (Br^->Cl^-), in line with the experimental results presented in Figure 4-1.

4.3.4.2 Mechanism for transesterification

The active acid-base sites (unsaturated -Zn^{2+}-O^{2-}- sites) on the catalyst surface play a critical role in the transformation of propylene carbonate and methanol under mild reaction condition. In this study, NaBr-ZnO is used as the catalyst for the synthesis of DMC and a proposed reaction mechanism is shown in Scheme 4-2 and Scheme 4-3.

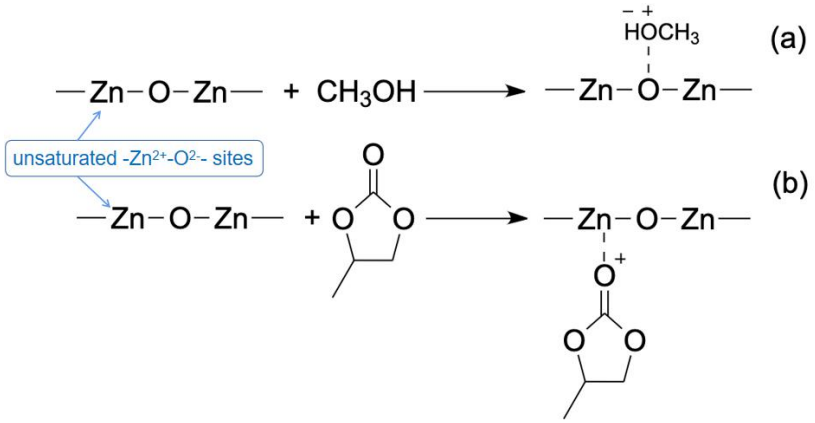

Scheme 4-2. (a) Adsorption of methanol onto ZnO-based catalyst; (b) Adsorption of propylene carbonate onto ZnO-based catalyst (Kähler, Kevin *et al.,* 2010).

Both methanol and PC is activated by the chemical adsorption onto the catalyst surface. Methanol is activated by the basic sites (oxygen atom), and methoxy species and H^+ is formed on the polar oxygen-terminated ZnO surface(Scheme 4-2 (a)) (Kähler, Kevin *et al.,* 2010). PC is activated by the chemical adsorption on the acidic (zinc atom) sites of the catalyst (Scheme 4-2 (b)).Scheme 4-3 shows the overall reaction mechanism for the formation of DMC and PG from PC and methanol. The methoxy groups of methanol attack the carbonyl C of the PC and forms an intermediate 1 (CH_3O-CO-O-$CH(CH_3)$-CH_2-OH). This intermediate further reacts with CH_3O^- to form DMC and intermediate, OH-CH_3-CH_2-CH_2-O^- which reacts with H^+ to form PG (Kumar *et al*,. 2015).

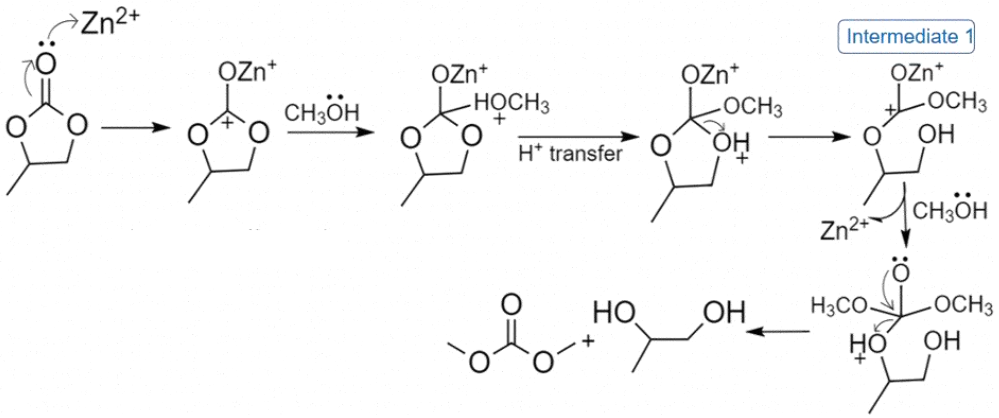

Scheme 4-3. Proposed mechanism for the synthesis of dimethyl carbonate from propylene carbonate and methanol (Murugan and Bajaj, 2010).

4.3.4.3 Mechanism for PO hydrolysis

Propylene glycol is generated by hydrolysis of propylene oxide with an excess of water, and the proposed reaction mechanism is shown in Scheme 4-4. The epoxide ring-opening reaction occurs by nucleophilic substitution to replace the epoxide oxygen atom on the epoxide carbon atom. The ring-opening orientation in propylene oxide mainly depends on the steric hindrance of the methyl group, and on the electron release effect of the methyl group (Parker and Isaacs, 1959).

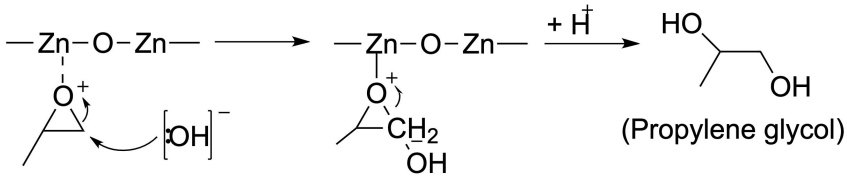

Scheme 4-4. Proposed reaction mechanism for the hydrolysis of propylene oxide under base-catalyzed reaction (Woods, 1990).

The epoxide ring of propylene oxide can be opened at any one of the two C-O bonds. In the base catalysed reaction, the bond is preferentially opened at the least spatially obstructed position, leading to the formation of PG (Woods, 1990).

4.3.4.4 Mechanism for by-products formation

The chemical adsorption of methanol (Scheme 4-2 (a)) and propylene oxide (Scheme 4-5) on the active sites of the catalyst leads to the formation of by-products. The adsorption of PO on the metallic sites of the catalyst results in the dissociative activation of PO (Timofeeva *et al*., 2016).

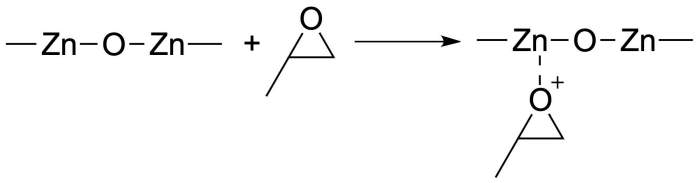

Scheme 4-5. Adsorption of propylene oxide onto ZnO-based catalyst (Timofeeva *et al*., 2016).

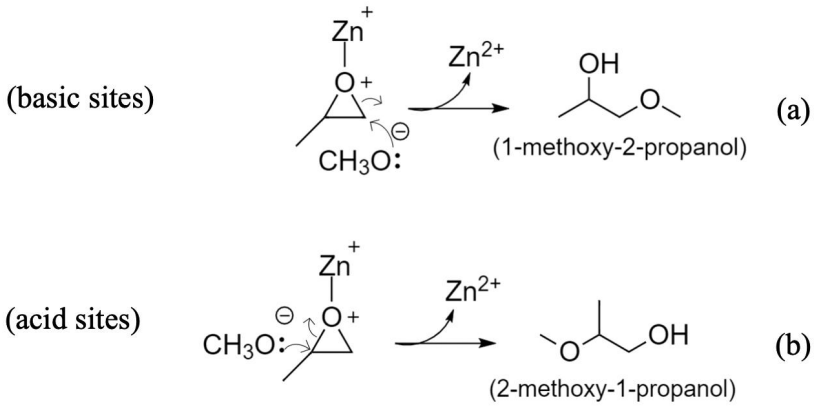

Scheme 4-6. Proposed reaction mechanism for the formation of by-products in the synthesis of DMC (Timofeeva *et al*., 2016).

The epoxide ring of PO may be opened either at the C–O bond because of the asymmetry of PO, so the reaction between PO and methanol generates a mixture of two isomers (Timofeeva *et al*., 2016): 1-methoxy-2 -Propanol (a) and 2-methoxy-1-propanol (b) (Scheme 4-6). When a basic catalyst is involved in the reaction, the C–O bond preferentially opens at the position where the steric hindrance is the smallest, resulting in the most reaction products being 1-methoxy-2-propanol (a). Besides, when the reaction is catalysed by an acid catalyst, the product is mainly 2-methoxy-1-propanol (b). Based on the mechanism study, due to the existence of a pair of "basic site-Lewis acid site" on the catalyst surface, methanol is adsorbed at the basic site (oxygen atom, Scheme 4-2 (a)) and decomposed into protons and methoxide ions. PO is activated by adsorption at acidic sites (zinc atom, Scheme 4-5). Therefore, 1-methoxy-2-propanol (a), remaining a high selectivity on a solid base catalyst, is formed.

The strength of the basic sites may affect the selectivity of DMC synthesis in two ways: (1) Increased strength of the basic site should be conducive to the formation of by-products *via* the activation of PO and methanol. However, higher alkalinity should cause the adsorption of PO and methoxy groups to the active acid-base sites on the solid surface to become energetically stable, which affects the activation of PC at acid sites, thereby reducing the rate of DMC synthesis reaction. (2) According to the reaction equilibrium of both cycloaddition and transesterification, the decrease of the concentration of PO and methanol in the reaction solution inhibit the reaction in the direction of PC and DMC formation, respectively. Therefore, it is necessary to find a suitable basic substance to increase the strength of the basic sites of the catalyst, in order to improve the selectivity of DMC through catalyst modification method.

4.4 Conclusions

The synthesis of DMC from PO, methanol and CO_2 is successfully carried out in the presence of alkali halide-ZnO catalysts under low pressure (2 MPa, room temperature) condition. It was found that the selectivity of DMC is relatively low (around 4%) using four kinds of catalyst. However, higher selectivity of PC (~33.9%) and lower by-products selectivity (~13.2%) is obtained using bromine-containing catalysts, which means Br^- is more conducive to cycloaddition reaction than Cl^-. Therefore, NaBr-ZnO is selected as the optimised catalyst for the subsequent experiment. The effect of reaction time on DMC selectivity is investigated as well, and the results indicate that 5 hours is a more suitable reaction time because the DMC synthesis reaction has reached the equilibrium.

CHAPTER 5

CATALYST MODIFICATION: INFLUENCE OF ALKALI METALS

Chapter 5 Catalyst modification: Influence of alkali metals

5.1 Introduction

Dimethyl carbonate can be synthesised through the one-pot route from methanol, propylene oxide and carbon dioxide using alkali halide-ZnO catalyst. The main challenges for improving the selectivity of DMC are the hydrolysis of propylene oxide to form propylene glycol and the low conversion rate of propylene carbonate to DMC *via* transesterification. The former problem may be improved by adding a suitable dehydrating agent in the reaction system (which is discussed in Chapters 6 and 7), and the latter problem needs to be solved by the modification of the catalyst. The modification of catalyst can be realised by adding appropriate amounts of bases (such as KOH, K_2CO_3 or Na_2CO_3) according to previous study (Chang *et al.*, 2004; Cui *et al*., 2008; Jiang and Yang, 2004) because the strong basic sites on the catalyst surface can promote the conversion of PC to DMC through transesterification. For example, 36.8% selectivity to DMC can be obtained using KI-ZnO catalyst with reaction conditions of 16.5 MPa CO_2 and 160 °C; while employing K_2CO_3 can increase DMC selectivity to 43.3% (Chang *et al.*, 2004). Therefore, a similar method for catalyst modification by supporting appropriate alkali on the carrier is applied in this study to improve the selectivity of DMC.

In this chapter, the heterogeneous catalysts (Alkali-NaBr-ZnO) with several alkalis including sodium hydroxide (NaOH), potassium carbonate (K_2CO_3) and sodium carbonate (Na_2CO_3) have been developed and assessed for the synthesis of DMC. The effect of alkali loadings has been extensively investigated. Characterisation techniques, such as TGA, SEM-EDX, XRD, ICP-OES and AAS, have been employed to better understand the effect of alkali on the stability and composition of the catalyst, and the relationship between the properties of the catalysts and their impact on the selectivity of DMC.

5.2 Experimental methods

5.2.1 Materials

Reagents sodium bromide (NaBr, ≥99%), propylene oxide (≥99.5%), sodium carbonate (BioXtra, ≥99.0%), potassium carbonate (≥99%) and sodium hydroxide (ACS reagent, ≥97.0%) were purchased from Sigma-Aldrich. CO_2 (purity over 99.99%, water content less than 0.01%) was bought from BOC. Methanol (99.9% min) was purchased from Alfa-Aesar. Zinc oxide was purchased from Fisher Scientific. 2-propanol (Sigma-Aldrich, ≥99.8%) was used as an internal standard for GC-FID quantitative analysis. Dimethyl carbonate (DMC, 99%), propylene carbonate (PC for HPLC, 99.7%),1-methoxy-2-propanol (≥99.5%) and propylene glycol (PG, ACS reagent, ≥99.5%) were employed as reference materials for calibration curves, supplied from Sigma Aldrich. Deionized water was used in all experiments.

5.2.2 Experimental methods

5.2.2.1 Effect of various alkali species

In this section, three kinds of inorganic alkalis (NaOH, Na_2CO_3 and K_2CO_3) were immobilised on the catalyst surface (NaBr-ZnO), and the activity of these catalysts was evaluated. The species of alkali supported on the catalyst surface has a significant influence on the transesterification. According to the Brønsted-Lowry acid-base theory, a base is a proton (hydrogen ion) acceptor. The base in a chemical reaction system is related to the process of deprotonation, which is determined by the pK_a value and solubility of the base in a specific solvent (Yuan, 2014). Sodium hydroxide is a strong base, and both potassium carbonate and sodium carbonate are alkaline salts due to the hydrolysis of carbonate ions (CO_3^{2-}) to form hydroxyl ions (OH^-). The solubility of three kinds of alkali in water and methanol and the pK_a value of these alkalis are presented in Table 5-1.

Table 5-1. Properties of three types of alkali and NaBr.

	NaOH	**Na_2CO_3**	**K_2CO_3**	**NaBr**
Water [a]	100.0	30.7	111.0	94.3
Methanol [a]	23.8	0.6	3.1	16.7
pK_a (strongest acidic) [b]	15.7	6.05	6.05	-

Condition: solubility (g/100 mL) measured at 25 °C and ambient pressure ("*a*" indicates the data comes from HSDB; "*b*" indicates the data comes from ChemAxon).

As discussed in Section 3.2.1, the reason for choosing alkali and NaBr as active agents immobilised on ZnO is based on the published paper. 12 *wt.*% alkali content is the optimised loading determined by the experimental data (Figure 5-2). The catalyst was prepared by the addition of 12 *wt.*% alkali and 17.5 *wt.*% NaBr to ZnO *via* wet impregnation. 3 g of each catalyst was prepared in this work; thus 0.36 g of alkali and 0.525 g NaBr was dissolved in 20 ml distilled water, then the solution and 2.115 g of ZnO were added into a 50 ml round-bottomed flask equipped with a stirrer bar and a condenser. The mixture was refluxed at 60 °C for 24 h, followed by vacuum filtration. In this process, all the alkalis are completely dissolved in water and fully contacted with the catalyst carrier. The filtered solids were dried at 100 °C for 12 h and then calcined at 700 °C for 3 h. It can be seen from Table 5-1 that the solubility of NaOH is much higher than that of two kinds of salts. The solubility of three alkalis in the reaction solvent (methanol) may affect the activity of the catalyst by changing the alkaline intensity of the reaction solution and the deprotonation ability of the alkali immobilised on the carrier. The relationship between the species of alkali and the selectivity of each product is investigated in this section.

5.2.2.2 Effect of alkali loadings

Based on the results obtained in section 5.2.2.1, K_2CO_3 was used in the further experiments to investigate the effect of alkali loadings on the formation of dimethyl carbonate. The effect of the relative quantity of K_2CO_3 in the catalyst on the yield of DMC through the one-pot synthesis route has previously been discussed in the literature. For example, K_2CO_3-KCl-Nd_2O_3 catalysts with various K_2CO_3 loadings (ranging from 6.7 *wt.*% to 26.7 *wt.*%) were tested, and the result indicated that optimal alkali loading is 17.6 *wt.*% with the highest DMC yield of 53.5% (Jiang, Cheng and Gao, 2007). When the content of K_2CO_3 is higher than 17.6 *wt.*%, the yield of DMC decreases with the increase of K_2CO_3 loading amount in the catalyst. The possible explanation for this result is that when the loading of alkaline substances was higher than a specific value, the active sites on the catalyst were partly covered after calcination, resulting in a decrease in the effective surface area of the catalyst.

As discussed in chapter 4, the amount of strong basic sites on the catalyst surface has a noticeable effect on the transesterification reaction to convert propylene carbonate to dimethyl carbonate and glycol. Wang (Wang *et al*., 2002) reported that both PC conversion and DMC yield went up with the increasing amount of catalyst added in the reaction system and reached a peak at 1.82 *wt.*%. The authors suggested that the reason for this result is that the active

basic sites on the catalyst surface are mainly used to activate methanol and to form methoxy groups (-CH_3O). When the number of active basic sites reaches a certain value, the reaction rate remains stable because the increased number of base sites has little effect on the activation of methanol. In this section, the catalysts (K_2CO_3-NaBr-ZnO) with different K_2CO_3 loadings were prepared and applied in the DMC synthesis reaction. The optimal K_2CO_3 loading was determined, and the effect of K_2CO_3 on DMC selectivity *via* transesterification was discussed.

5.2.3 Catalyst characterisation

The catalysts with different alkali species were characterised by X-ray diffraction (XRD). The optimum catalyst with a more suitable alkali species and loadings of the alkali was further analysed using inductively coupled plasma-optical emission spectrometry (ICP-OES), atomic absorption spectroscopy (AAS), thermogravimetric analysis (TGA), scanning electron microscopy-energy dispersive X-ray (SEM-EDX) spectroscopy. For example, ICP-OES was employed to obtain information about the stability of the catalyst and the mechanism of DMC synthesis reaction with the addition of alkali. The detailed discussion (principle and applications) of the above characterisation techniques has been introduced in Chapter 3. The analysis parameters of techniques used in the catalyst characterisation and the aims and the objects of each analysis technique are summarised in Table 5-2.

Table 5-2. The techniques used for catalyst characterization and the set-up parameters for each technique.

Techniques	Objects	Parameters	Aims
TGA	Uncalcined K_2CO_3-NaBr-ZnO catalyst and the mixture of K_2CO_3, NaBr and ZnO	~6 mg of a sample; increasing temperature to 950 °C at 10 °C min^{-1} under a stream of N_2 (20 ml min^{-1})	Interaction between the active components (K_2CO_3 and NaBr) and the carrier (ZnO), and the effects of the calcination step during catalyst preparation
XRD	(1) Catalysts with three different kinds of alkali; (2) K_2CO_3-NaBr-ZnO catalyst with different K_2CO_3 loadings	Bruker D2 Phaser powder XRD instrument with Cu $K\alpha$ (30 kV, 10 mA) radiation at a scanning rate of 0.05° min^{-1}	Composition of catalysts with various kinds of alkali; The effect of K_2CO_3 loadings on the average crystalline size of catalyst particles.
SEM-EDX	K_2CO_3-NaBr-ZnO catalyst	JSM-6010LA JEOL SEM instrument with an accelerating voltage of 20 keV and a working distance of 10 mm	Effect of calcination on the distribution of elements on the catalyst surface.
AAS, ICP-OES	K_2CO_3-NaBr-ZnO catalyst (fresh and spent)	The analysis is supported by the Faculty of Science Mass Spectrometry Centre of the University of Sheffield	Role of K_2CO_3 in the reaction system and the new reaction mechanism of using K_2CO_3-NaBr-ZnO catalyst.

5.3 Results and discussion

According to the experimental result discussed in Chapter 4 (Figure 4-1), the bromine-containing catalyst (NaBr-ZnO) shows improved catalytic performance as determined by higher propylene carbonate selectivity and lower PG and by-product selectivity. The main function of the halide ions in the reaction system is to activate the carbon dioxide, and then to promote the formation of propylene carbonate. In this section, NaBr-ZnO catalyst is employed, and various amounts of K_2CO_3 are added in the preparation of the catalyst.

5.3.1 Influence of three kinds of alkali

In this work, the effect of alkali species on the activity of the NaBr-ZnO based catalysts was studied to improve the catalyst performance. The results are summarised in Figure 5-1, which shows the alkali dependence of DMC synthesis. It is evident that the immobilisation of alkali on NaBr-ZnO catalyst has a significant effect on improving the selectivity of DMC. For example, when using NaBr-ZnO as the catalyst, the DMC selectivity is about 3.7%. In contrast, a DMC selectivity of 15.9 % can be obtained when the catalyst is K_2CO_3-NaBr-ZnO. Moreover, the selectivity of PC and DMC have a similar trend and the sequence of the selectivity of these two products is K_2CO_3-NaBr-ZnO > Na_2CO_3-NaBr-ZnO > NaOH-NaBr-ZnO.

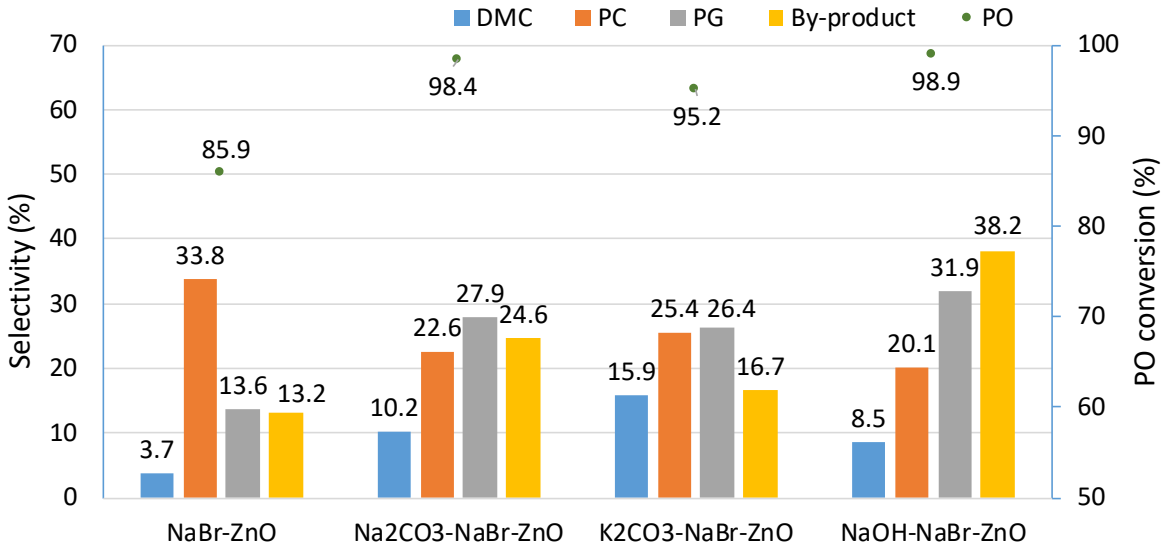

Figure 5-1. Effect of alkali on the conversion of PO and the selectivity of DMC, PC, PG and by-products in DMC synthesis. Reaction condition: 160 °C, 5 h, CO_2 (2 MPa), catalyst (12 *wt.*% alkali-17.5 *wt.*% NaBr-ZnO, 0.3 g), PO (33.33 mmol), methanol (100 mmol).

As discussed in section 5.2.2.1, the species of alkali can affect the activity of the catalyst by altering the deprotonation ability of the base immobilised on the carrier. The major function of alkali in the transesterification is to active methanol to form methoxyl groups, which attack the carbon atom of C=O in propylene carbonate to form DMC and PG. Their solubility can explain the result of the reactions using two catalysts containing various alkali carbonates (same pK_a value). Dissolution of catalytically active compound from catalyst surface into the reactants affects the reaction (Ono and Hattori, 2016). For example, K_2CO_3-loaded Al_2CO_3 catalyst shows high activity to promote the transesterification of sunflower with methanol (Xie, Yang and Chun, 2007). The reaction proceeds with the homogeneous catalyst (potassium methoxide) which is formed by the reaction of methanol and potassium ions. When the same amount of alkali carbonates loaded on the carrier, the capability to activate methanol goes up with the increase of alkali solubility. As shown in Table 5-1, the solubility of K_2CO_3 (3.1 g/100ml) in methanol at room temperature is higher than that of Na_2CO_3 (0.6 g/100ml). Therefore, the sequence of the catalytic activity is K_2CO_3-NaBr-ZnO > Na_2CO_3-NaBr-ZnO.

Compared with two kinds of alkali carbonates, NaOH shows the highest solubility (23.8 g/100ml in methanol) and higher *pKa* value (~15.7). When NaOH containing catalyst added in the reaction, a significant increase in the selectivity of the by-products (~38.2%) is shown in Figure 5-1. According to the mechanism of by-product formation in Chapter 4, the highly basic reaction condition is the main factor to promote the side reactions between PO and methanol to generate 1-methoxy-2-propanol (Scheme 4-5, route (a)). Furthermore, the hydrolysis of PO is promoted with the addition of NaOH, which leads to a slight increase in the PG selectivity. In addition to overly basic reaction condition, the increased selectivity of PG and by-products may be another reason that DMC formation is inhibited.

5.3.2 Influence of K_2CO_3 loadings

When only NaBr-ZnO employed in the reaction (*i.e.* no additional base), high PC selectivity (33.8%) was obtained, which means the catalyst is effective for the formation of PC form CO_2 and PO *via* cycloaddition. It is desirable to increase DMC selectivity and PO conversion while reducing by-product selectivity. The effect of K_2CO_3 loadings on the performance of the catalyst is studied *via* the one-pot synthesis of DMC. The results are shown in Figure 5-2.

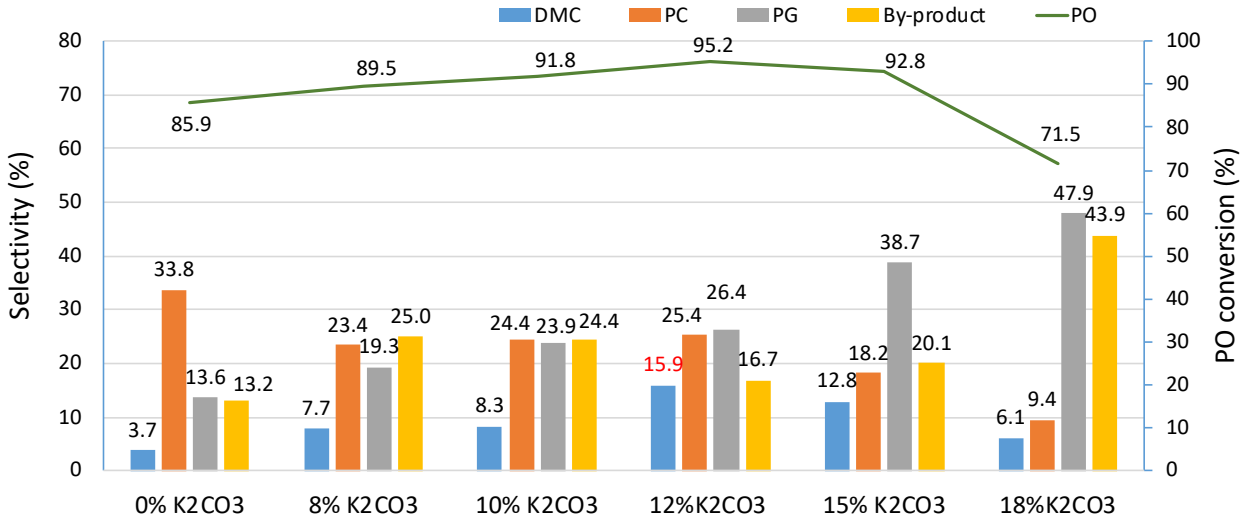

Figure 5-2. Effect of alkali loadings on the conversion of PO and the selectivity of DMC, PC, PG and by-products in DMC synthesis. Reaction condition: 160 °C, 5 h, CO_2 (2 MPa), catalyst (K_2CO_3-17.5 *wt.*% NaBr-ZnO, 0.3 g), PO (33.33 mmol), methanol (100 mmol).

It can be seen from the figure that both the PO conversion and DMC selectivity increases with increasing K_2CO_3 loadings and reaches the maximum when the loading is 12 *wt.*% (95.2% PO conversion and 15.9% DMC selectivity). The selectivity of PC decreases with the addition of K_2CO_3 and remains stable in the range of 8 *wt.*% and 12 *wt.*% (around 24%). PG is produced along with the formation of DMC through the transesterification. PG is formed by the hydration of propylene oxide. Figure 5-2 shows that higher K_2CO_3 loadings favour the hydration of PO. Two phases of active compounds exist in the reaction system: supported on the catalyst and dissolved in the reactant. ICP-OES analysis was employed to obtain the information about the elemental composition of the catalyst before and after the reaction to determine which phase of active compound promotes the DMC formation. Since PG is generated from PO and H_2O, the conversion of a large amount of PO to PG may be one of the causes of low DMC selectivity, further resulting in a low yield of DMC.

Appropriate alkaline strength is conducive to obtain higher selectivity of PC and DMC: if the system is too basic then this leads to the formation of 1-methoxy-2-propanol, which limits the formation of DMC. As can be seen from the results, when the K_2CO_3 content is higher than 12 *wt.*%, the selectivity of DMC and PC and the conversion of PO are decreased. This result can be explained by the fact that there is too much K_2CO_3 supported on the ZnO surface, which may reduce the effective surface area of catalyst or block active catalyst pore (Xu *et al.*, 2013).

5.3.3 Effect of alkali halide species

It is clear that optimising the amount of K_2CO_3 (12 *wt.*% gives the best results of the systems studied herein) has a significant influence on improving the selectivity of DMC (from 3.7% to 15.9%) through transesterification. In order to obtain a better-performing catalyst, it is necessary to determine if the selectivity of DMC can be improved by changing the metal halide species immobilised on the ZnO because the alkali halide provides active sites for the activation of carbon dioxide in cycloaddition. Therefore, four catalysts containing the same K_2CO_3 amount (12 *wt.*%) and different metal halide species were prepared and applied in the DMC synthesis reaction, and the results are shown in Figure 5-3.

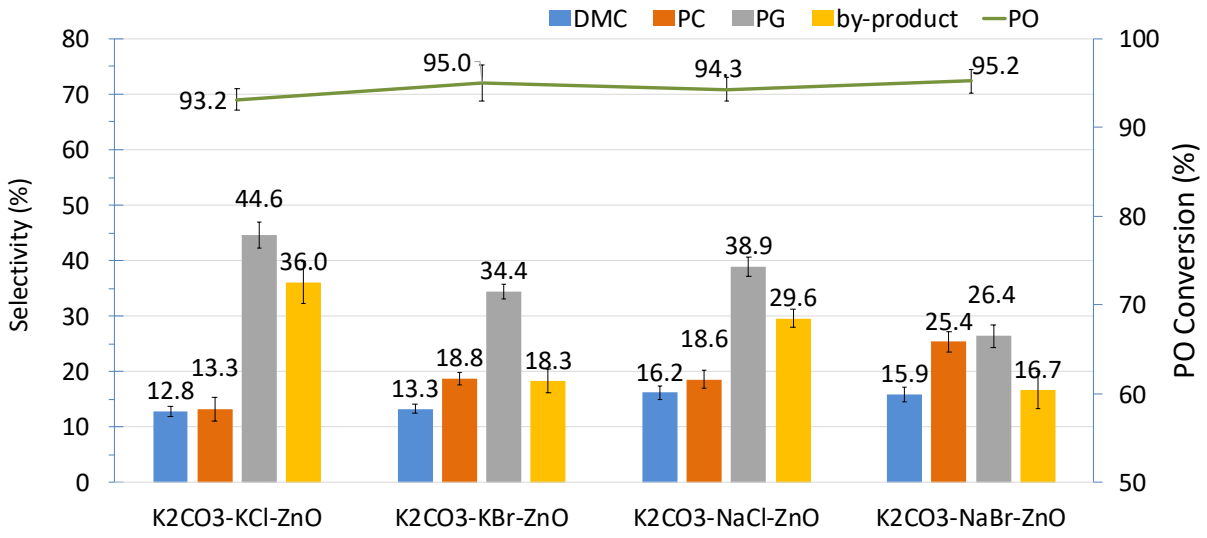

Figure 5-3. Effect of alkali halide species on the conversion of PO and the selectivity of DMC, PC, PG and by-products in DMC synthesis. Reaction condition: 160 °C, 5 h, CO_2 (2 MPa), catalyst (12 *wt.*% K_2CO_3-17.5 *wt.*% alkali halide-ZnO, 0.3 g), PO (33.33 mmol), methanol (100 mmol).

Compared with the result of only alkali halide-ZnO involved reactions (Figure 4-2), Figure 5-3 shows the similar trend of the selectivity of each product when the catalyst with the same alkali metal added in the reaction. Specifically, a higher selectivity of PG and by-products is

obtained when the catalyst containing Cl^- ions is used; in contrast, a catalyst containing Br^- ions causes a higher PC selectivity, and at the same time, PO conversion is slightly increased as well.

The highest DMC selectivity is obtained using K_2CO_3-NaCl-ZnO. However, the selectivity of both PG and by-products is much higher than that of using K_2CO_3-NaBr-ZnO. According to the mechanism of transesterification, higher PC content and lower PG concentration in the reactant is conducive to the formation of DMC during the reaction process. Therefore, K_2CO_3-NaBr-ZnO is considered to be a relatively better-performing catalyst in the one-step synthesis of DMC under mild condition because it provides the potential (higher PC production and lower PG yield) for improving the DMC selectivity by modifying the reaction conditions in subsequent studies.

5.3.3 Catalyst characterisation

Two sets of samples were analysed in this section: (1) The modified catalyst (K_2CO_3-NaBr-ZnO) with an appropriate amount of alkali (12 *wt*.% K_2CO_3) and alkali halide (17.5 *wt*.% NaBr); (2) The catalysts with various alkali species. The purpose of analysing the first set of samples is to obtain the following information, which includes the relationship between the active ingredients and the support during catalyst preparation process, the influence of calcination on the distribution of the active ingredients on the support, and changes in the structure and composition of the catalyst before and after reaction. Analysis of the second set of samples reveals the effects of different alkalis on the composition of catalyst.

5.3.3.1 Thermogravimetric analysis (TGA)

Thermogravimetric analysis was applied to study the interaction between the active ingredients - K_2CO_3 and NaBr and the carrier, and the reason for choosing 700 °C as the calcination temperature during catalyst synthesis . In Jiang and Yang's study (2004), K_2CO_3-KCl-Al_2O_3 is used as the catalyst and the relationship between calcination temperature and catalytic activity is discussed. Potassium oxide species are formed due to the decomposition of K_2CO_3 dispersed on the carrier surface, the DMC yield is increased obviously with the calcination temperature in the range of 200-700 °C and then decreases remarkably beyond 700 °C because of the sinter of catalyst at high temperature. Figure 5-4 shows the thermogravimetric analysis of two samples, (a) non-calcined K_2CO_3- NaBr- ZnO and (b) a mixture of K_2CO_3, NaBr and ZnO. The original TGA data are plotted alongside the differential thermograms (DTG).

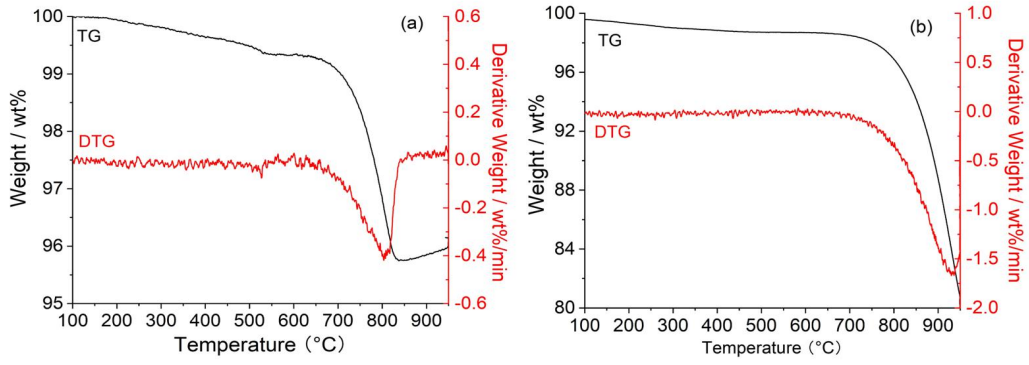

Figure 5-4. DTG and TG curves of (a) non-calcined K_2CO_3-NaBr-ZnO (b) mixture of K_2CO_3, NaBr and ZnO.

From the TG and DTG curves in Figure 5-4 (a), it can be seen that the uncalcined catalyst shows weight loss in the temperature range of 720 °C - 830 °C and reaches the maximum

weight loss rate at ~ 800 °C. During the preparation of the catalyst, active substances (K_2CO_3 and NaBr) dissolved in the solution were attached to the support surface in the form of a salt and penetrated into the inner surface of the support. After the immersion was equilibrated, the solid catalyst was filtered, and the post-treatments such as drying, calcination, and activation were performed. Weight loss is related to the decomposition of the formed carbonate groups below 800 °C (Fierro, Melián-Cabrera and López Granados, 2002). The TG-DTG curve in Figure 5-4 (b) shows that the weight of the mixture begins to decrease from ~ 750 °C, and the mass-loss rate reaches a maximum at ~ 920 °C due to the decomposition of K_2CO_3 (Sun *et al.*, 2014). Comparing Figures 5-4 (a) and (b), it can be concluded that a new compound was formed during the preparation of the catalyst. Moreover, the calcination temperature of the catalyst was selected to be 700 °C because the structure of the catalyst is unstable above 720 °C.

5.3.3.2 SEM and SEM-EDX

SEM analysis of the fresh and spend catalyst (12 *wt.*% K_2CO_3-17.5 *wt.*% NaBr-ZnO) are shown in Figure 5-5. Granular morphology is observed in the catalyst both before and after the reaction, signifying its stability.

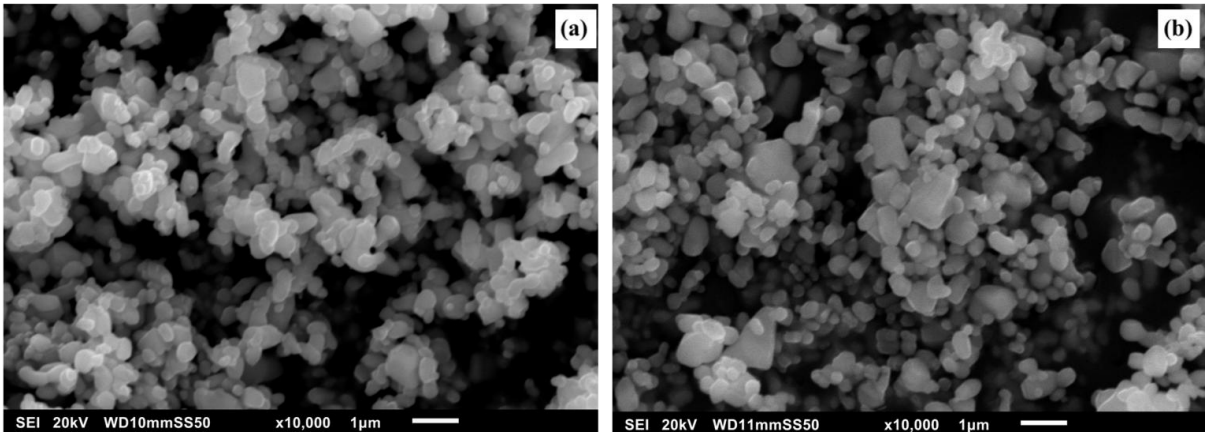

Figure 5-5. Surface morphology of the catalyst and mixtures of catalyst and Zn powder. (a) Fresh catalyst, (b) Spent catalyst.

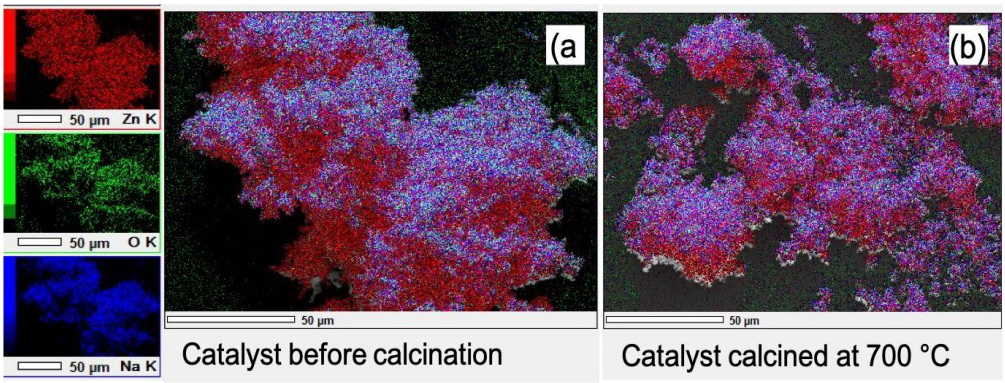

Figure 5-6. The distribution of zinc (red), oxygen (green) and sodium (blue) on catalyst surface before and after calcination by EDX mapping: (a) catalyst before calcination; and (b) catalyst calcined at 700 °C.

Table 5-3. Elemental composition of the catalyst by EDX mapping analysis.

Mass (%)	Catalyst	
	Before calcination	After calcination
Na	8.78	10.89
Zn	60.22	55.57
O	31.01	33.54

Experimental error is within ±3 %.

The effect of calcination on the distribution of elements on the catalyst surface and the elemental composition of catalyst is studied using SEM-EDX mapping analysis (Fig. 5-6 and Table 5-3). As shown in Figure 5-6, the active substance is uniformly dispersed on the surface of the carrier after calcination, which is conducive to increase the activity of the catalyst. More specifically, the formation of alkali metal oxide species after calcination enhance the alkalinity of catalyst surface, and strong basic sites promote the transesterfication reaction in improving DMC yield (Jiang and Yang, 2004). Moreover, it can be seen from Table 5-3 that the effect of calcination on the catalyst components is not apparent, and a slight increase in the mass content of oxygen ion may be due to the reaction of carbon dioxide in the air with the basic active site on the catalyst during the catalyst preparation process. More specific information about the catalyst components is discussed in the Section 5.3.3.3.

5.3.3.3 XRD

In this section, two sets of samples were tested: (1) catalysts loaded with different alkalis (K_2CO_3, Na_2CO_3 and NaOH), and (2) catalysts (K_2CO_3-NaBr-ZnO) before and after the reaction. It can be seen from Figure 5-7 that the characteristic peaks of ZnO (PDF-ICDD 01-081-8838) appear in the diffractograms of the three catalysts. The characteristic peaks of Na_2CO_3 (PDF-ICDD 04-013-9890) are also present in the diffractogram of the catalysts containing K_2CO_3 and NaOH. TG-DTG analysis (Section 5.3.3.1) suggests that Na_2CO_3 may result from the oxidation of the compound (formed in catalyst preparation) during calcination. In contrast, Na_2CO_3 is not detected in the catalyst containing sodium carbonate *via* XRD analysis. The possible reason is that the $-CO_3^{2-}$ is hydrolysed to form $-HCO_3^-$, which is completely decomposed at about 440 °C. As a result, only a small amount of Na_2CO_3 or the Na_2CO_3 with small crystal size are formed on the catalyst surface after calcination.

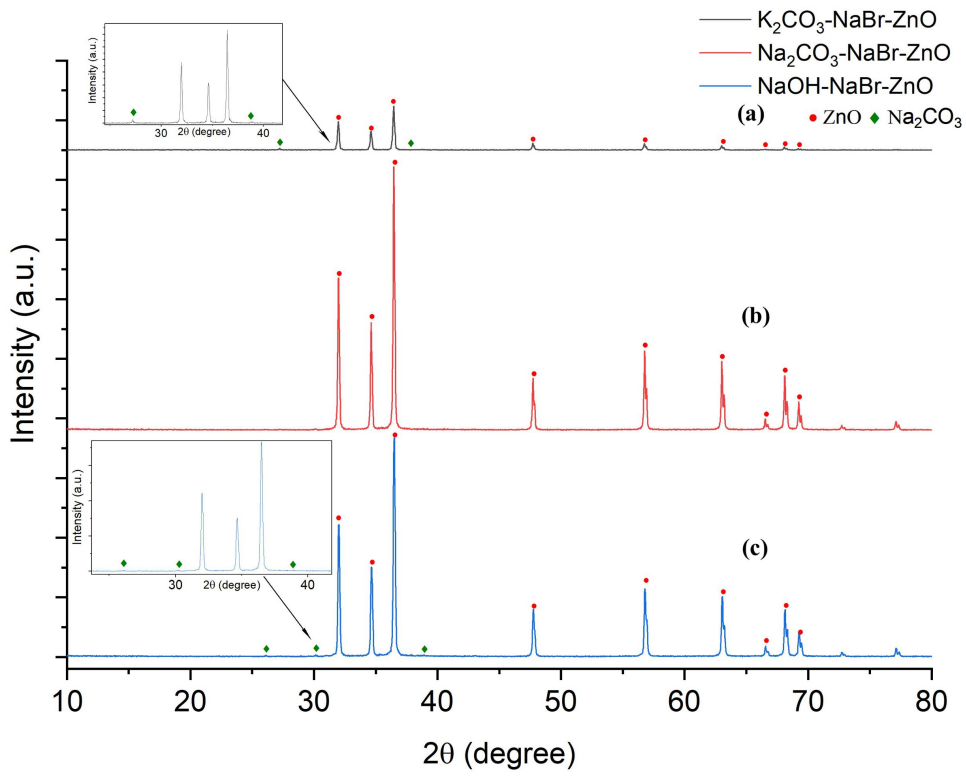

Figure 5-7. The XRD patterns of catalysts with various alkali: (a) 12 *wt.*% K_2CO_3-NaBr-ZnO; (b) 12 *wt.*% Na_2CO_3-NaBr-ZnO; (c) 12 *wt.*% NaOH-NaBr-ZnO.

The diffraction patterns of fresh and used catalysts are shown in Figure 5-8. ZnO (PDF-ICDD 01-081-8838) and Na_2CO_3 (PDF-ICDD 04-013-9890) are clearly present in the fresh catalyst (K_2CO_3-NaBr-ZnO). The diffractogram of the used catalyst (Figure 5-8 (b)) shows the characteristic peaks of $ZnCO_3$ (PDF-ICDD 04-015-6717), which indicates that the stable

carbonyl double bond is broken due to the reaction of CO_2 with the active basic sites of the catalyst. The full width at half maximum (FWHM) of the peak obtained from the XRD pattern is used to calculate the crystallite size of the particles by using the Scherrer equation (Patterson, 1939).

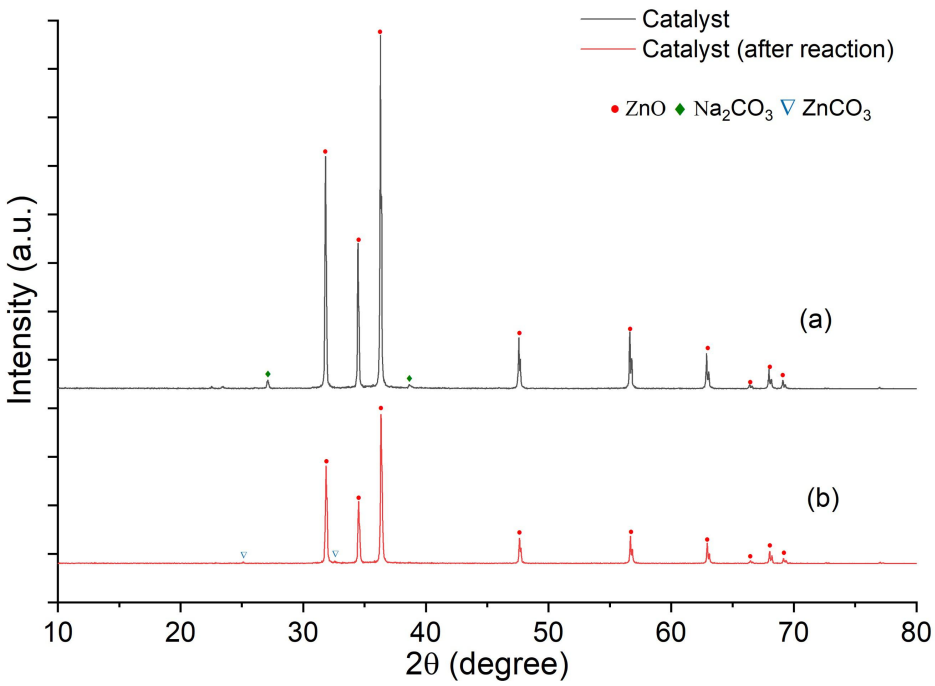

Figure 5-8. The XRD patterns of fresh and spent catalysts: (a) fresh K_2CO_3-NaBr-ZnO; (b) K_2CO_3-NaBr-ZnO after the reaction.

Table 5-4. Average crystalline size of particles before and after the reaction. '-' indicates that a crystalline phase is not observed in the diffractogram. '*' indicates that the corresponding peak is present but is beneath the size limit to accurately determine the crystallite size.

	Average crystalline size (nm)		
	ZnO	Na_2CO_3	$ZnCO_3$
Catalyst	46 ± 6	*	-
Catalyst (after reaction)	43 ± 5	-	*

The crystallite size of ZnO remained unchanged before and after the reaction (Table 5-4). This result is consistent with the result of the SEM photograph (Figure 5-5) that the structure of the support (ZnO) remains stable after the reaction.

5.3.3.4 AAS and ICP-OES

Since all of the active constituents (Na_2CO_3, K_2CO_3 and NaBr) supported on the surface of catalyst, have significant solubility in methanol (0.6 g/100 mL, 3.1 g/100 mL and 16.7 g/100 mL, respectively; Table 5-1), in order to have a better understanding of whether the catalytic activity mainly decided by these supported active ingredients or by the dissolved active ingredients, ICP-OES and AAS analysis of both solid and liquid samples was carried out. The quantity of Zn, Na and K in solid catalyst and liquid product before and after the reaction was determined and therefore to identify any leaching of potentially catalytic material and hence potential homogenous catalytic contribution to the reaction. The results of ICP and AAS analysis of catalysts and liquid product solution are shown in Tables 5-5 (a) and (b), respectively. Both of these indicate that there is little change in the total Zn^{2+} content in the K_2CO_3-NaBr-ZnO after the reaction, which indicates that the structure of ZnO remains stable under reaction condition (160 °C and 4.5 MPa). The result is consistent with the results of SEM and XRD analysis (Figure 5-5 and Table 5-4, respectively).

Table 5-5 (a). Composition of fresh and used catalysts, (12 *wt.*% K_2CO_3-17.5 *wt.*% NaBr-ZnO) as determined by AAS and ICP-OES.

Entry	Sample	AAS analysis (mg/g_{sample})		ICP-OES analysis (mg/g_{sample})		
		Total Zn^{2+}	ZnO mass	Total Zn^{2+}	K mass	Na mass
1	Fresh catalyst	786.5	984.7	731.0	4.390	2.900
2	Post-reaction catalyst	793.0	992.8	741.0	0.008	0.052

Table 5-5 (b). ICP-OES analysis of Zn, K and Na in the liquid products after the reaction. Catalyst refers to 12 *wt.*% K_2CO_3-17.5 *wt.*% NaBr-ZnO.

	Total Zn (mg/L)	K mass (mg/L)	Na mass (mg/L)
Catalyst	11.9	238.0	152.0

ICP-OES data indicate that K_2CO_3-NaBr-ZnO exhibits a loss of 99.8 *wt.*% K^+ post-reaction, while Na^+ diminishes by 98.2 *wt.*% (Table 5-5 (a)). Alkali metal ions, K^+ and Na^+, however, leach into the solution and potentially react with the feedstock (Table 5-5 (b). This result can be explained by the hard and soft acids and bases (HSAB) theory, first proposed by Pearson, Lewis acids can be classified according to the stability of the metal complexes into (i) hard Lewis acids (Na^+ and K^+); (ii) borderline Lewis acids (Zn^{2+}); and (iii) soft Lewis acids (Parr and Pearson, 1983). Generally, hard acids preferentially bind to hard bases to give ionic complexes, whereas soft acids bind to soft bases to yield covalent complexes. The oxygen

atom of the hydroxyl group in methanol displays the properties of a hard Lewis base (Laurence and Gal, 2009). The active compounds were loaded on ZnO by weak van der walls force, during the reaction process, the oxygen of OH group attacked Na^+ and K^+ and ionic complexes were formed. This process results in most of the sodium and potassium ions supported on the support were leached into the reaction solution.

As discussed in the previous session, the significant role of K_2CO_3 is to active methanol to form methoxide ion in the transesterification, which attacks the carbon atom of the carbonyl group in propylene carbonate (Scheme 4-3), then the DMC and PG are formed by the transformation of the H^+ ions (Murugan and Bajaj, 2010). According to the ICP-OES data, homogeneous catalyst formed by the dissolution of supported active compounds plays the main catalytic role in the DMC synthesis reaction.

5.4 Conclusions

The effect of the kind of alkali (NaOH, K_2CO_3 and Na_2CO_3) supported on the carrier on the modification of bromine-containing catalyst (NaBr-ZnO) is investigated in this chapter. The activity of these catalysts is examined *via* the one-pot synthesis of DMC reaction. As a result, the immobilisation of the alkali on NaBr-ZnO catalyst has a significant effect on improving the selectivity of DMC and the sequence of catalytic activity is K_2CO_3-NaBr-ZnO > Na_2CO_3-NaBr-ZnO > NaOH-NaBr-ZnO. Compard with other alkali-support catalysts (such as 16.8% DMC selectivity for KOH-4A under 3.0 MPa (Li, Zhao and Wang, 2005) and 20.1 % DMC selectivity for Na_2CO_3-KCl-Al_2O_3 under 2.5 MPa(Jiang and Yang, 2004), see Table 2-4), a DMC selectivity of 15.9% can be obtained when K_2CO_3-NaBr-ZnO is used as the catalyst under 2.0 MPa in this study. The conversion of PC to DMC in transesterification is promoted due to the rises of the number of active strong basic sites on the catalyst surface. The catalyst with a 12 *wt*.% K_2CO_3 loading shows better catalytic activity because both higher DMC selectivity (15.9%) and lower by-products selectivity (16.7%) is obtained when the catalyst involved in the reaction. The structure of the carrier remains stable after the reaction. However, the active substances supported on the catalyst surface is leached into the reactants during the reaction process. The dissolved active compounds show the main catalytic ability to promote the formation of DMC.

CHAPTER 6

INFLUENCE OF DEHYDRATING AGENTS ON DMC SELECTIVITY

Chapter 6 Influence of dehydrating agents on DMC selectivity

6.1 Introduction

Selectivity to DMC *via* the one-pot synthesis route using K_2CO_3-NaBr-ZnO as the catalyst is relatively low (around 15.9%) under 2 MPa pressure condition due to thermodynamic limitations of the reaction. Previous studies have shown a very promising way to shift the equilibrium to dimethyl carbonate by adding dehydrating agents (Eta *et al.*, 2010; Choi *et al.*, 2002). In order to both shift the equilibrium to the DMC side and to reduce PO hydrolysis, in this chapter, both a physical drying agent (3Å molecular sieve) and a chemical dehydrating agent (acetonitrile) are applied in DMC synthesis. The role of two types of agents in inhibiting PO hydrolysis and improving DMC selectivity are discussed, and the dehydration efficiency of these agents are evaluated.

6.1.1 3Å molecular sieve as a physical water trap

It has been reported that applying inorganic dehydrating agents ($CaCl_2$, $MgSO_4$ and molecular sieves, *etc*.) in the direct synthesis of DMC from methanol and CO_2 could increase DMC selectivity alongside achieving high methanol conversion (Choi *et al.*, 2002). 3Å molecular sieve is one of the most commonly used solid drying agents owing to its properties like easy recyclability. Moreover, 3Å molecular sieve is chemically inert, therefore, it does not generate co-products and can also absorb water under room temperature with high adsorption capability (adsorbed water ~ 20 % *w/w*).

3Å molecular sieve is a microporous aluminosilicate mineral and its typical formula is $0.6K_2O$: $0.40Na_2O$: Al_2O_3 : $(2.0 \pm 0.1)SiO_2$: xH_2O. This material can only adsorb the molecules whose diameter is smaller than 3Å such as water (2.6 Å) and ammonia (2.9 Å). A typical application of 3Å molecular sieves is that it is used in drying polar liquids (*e.g.* methanol/water or ethanol/water mixture) to the desired purity level. The physical properties of 3Å molecular sieves are summarised in Table 6-1.

Table 6-1. Typical properties of 3Å molecular sieves

	Pore diameter (Ångström)	Bulk density (kg/m^3)	pH value	Water absorption capacity
3Å molecular sieves	3	700 - 750 kg/m^3	8 - 11 (H_2O)	24 hrs.,80% relative humidity): ≥ 15%

6.1.2 Acetonitrile as a dehydrating agent

In response to the reaction conditions: 5.0 Mpa and 160 °C, it is difficult to dehydrate the reaction mixture with inorganic drying agents due to their low capability of dehydration (Honda *et al.*, 2009). Instead, *in-situ* dehydration with organic dehydrating agents such as acetonitrile results in higher efficiency and DMC selectivity. The dehydration product of acetonitrile is acetamide, which can react with methanol to form methyl acetate and ammonia.

The application of chemical dehydrating agents may however lead to low DMC yield due to the non-recyclability of the agents. Additionally, as a typical dehydrated derivative of methanol, it is possible that dimethyl ether (DME) limits the selectivity to DMC.

6.2 Experimental methods

6.2.1 Materials

In this chapter, the catalyst (12 *wt.*%K_2CO_3-17.5 *wt.*%NaBr-ZnO) is prepared *via* a wet impregnation method described in section 3.1.2. The present section introduces two dehydrating agents: 3Å molecular sieves (rods, 1.6mm, Figure 6-1) and acetonitrile (ACS reagent, ≥ 99.5%). Both were purchased from Sigma-Aldrich.

Figure 6-1. Photograph of fresh 3 Å molecular sieves used in this work.

As a chemical dehydrating agent, acetonitrile can be used directly in the one-pot synthesis of DMC. It should be noted that 3Å molecular sieves require thermal activation by Temperature swing adsorption (TSA) before application. The instability of potassium results on a maximum regeneration temperature of 240 °C, as its crystal structure may collapse at high temperature (Gabruś *et al.*, 2015). In this work, 3Å molecular sieves are activated in an Elite Tube Furnace and the temperature setup is controlled by the Setpoint programming controller. There are two ramps and one dwell in this programme. Segment 1 ramps slowly to 200 °C at a rate of 10 °C per minute. Segment 2 dwells at 200 °C for 180 minutes. Segment 3 cools to 30 °C at a rate of 30 °C per min. The temperature profile for this programme is shown in Figure 6-2.

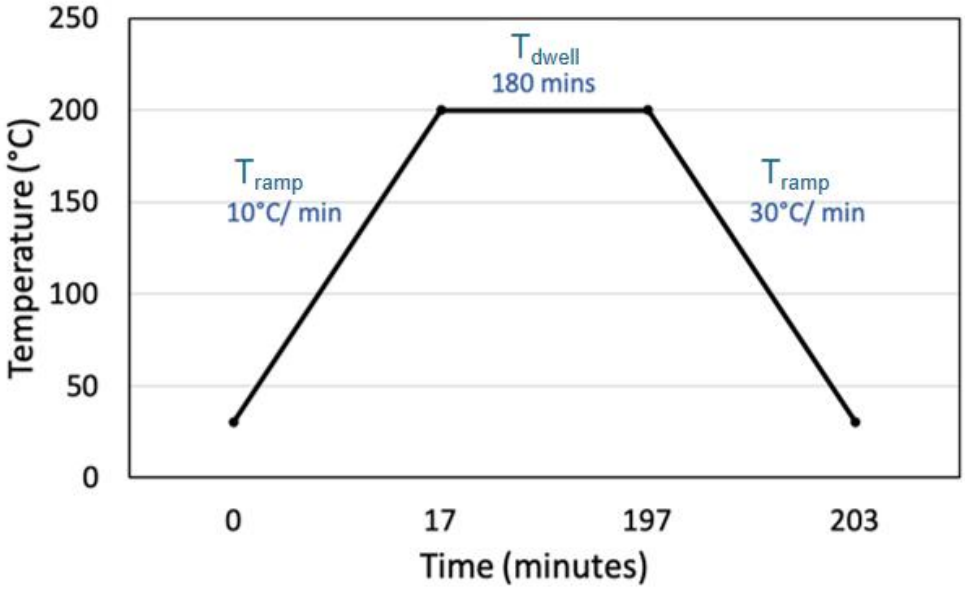

Figure 6-2. The temperature profile for 3Å molecular sieves thermal activation.

During the activation process, the tube furnace is purged with a carrier gas to make sure all the adsorbate is removed from the molecular sieves. Air is used as the carrier gas with a flow rate of 20 ml·min^{-1}. After activation, the sample was cooled to room temperature in the tube furnace while flushing with air at the same flow rate.

6.2.2 Methods

All of the reactions were carried out in a stainless-steel batch reactor (45 ml) equipped with an external centigrade thermometer and a heating jacket (Section 3.1.3). The research methodology of this chapter is summarized in Figure 6-3. In this section, turnover frequency (TOF) is defined as the mass of synthesized dimethyl carbonate (DMC) per gram catalyst per hour, and it is used to evaluate the catalytic efficiency of reaction system with the addition of dehydrating agents. Its calculation formula is shown as follows:

$$\mathrm{TOF} = \frac{m_{DMC}}{W_{cat} \times t} = \frac{n_{PO} \times Yield_{DMC} \times M_{DMC}}{W_{cat} \times t} \qquad (6\text{-}1)$$

where n_{PO}, M_{DMC}, t, and W_{cat}. represent the molar amount (mmol) of PO, formula weight (g mol^{-1}) of DMC, reaction time (h), and the mass of overall catalyst (mg), respectively.

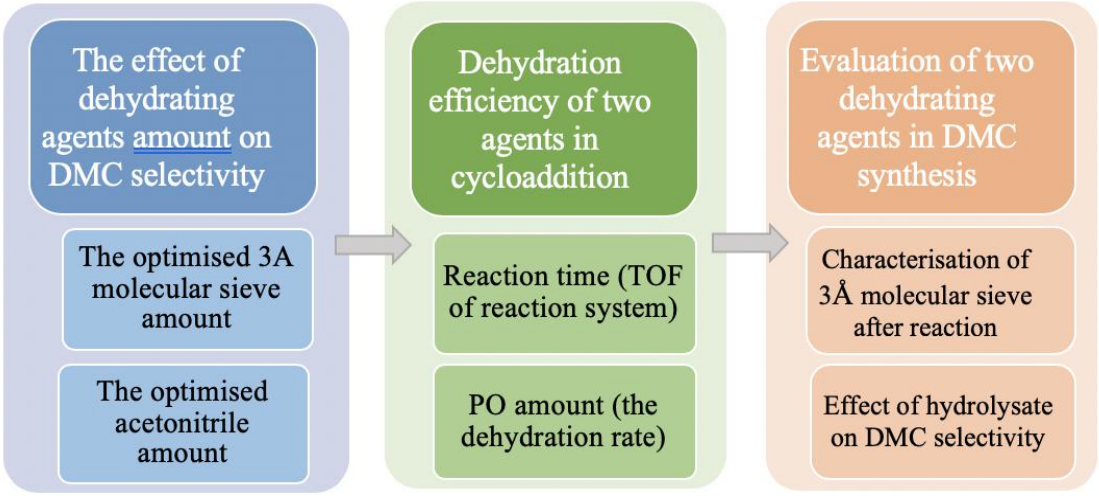

Figure 6-3. The structure (research aims and methods) of Chapter 6.

Firstly, the influence of the quantity of both 3Å molecular sieves and acetonitrile on the DMC yield is studied and a suitable quantity of each dehydrating agent is determined based on experimental results. The purpose of adding dehydrating agents in the reaction is to inhibit the hydrolysis of PO and to reduce the production of by-products formed from the reaction of methanol and PO. With a view to the reaction equilibrium, two influence factors may affect the yield of PC *via* cycloaddition reaction: 1) reaction time; and 2) the initial quantity of reactants (methanol and PO). These two factors are investigated in this chapter. Finally, the influence of two dehydrating agents on DMC synthesis are compared, and the advantages and disadvantages of the two dehydrating agents are discussed.

6.2.2.1 Influence of the quantity of 3Å molecular sieves on DMC yield

3Å molecular sieve most likely acts as a solid-state acid-base buffer in the reaction, the amount of 3Å molecular sieves added is likely to affect the selectivity of DMC through changing the alkalinity of the reaction solution. The acid-base properties of molecular sieves are altered *via* ion exchange (Fontes *et al.*, 2001). For example, 3Å molecular sieves show alkaline behaviour in aqueous solution due to the presence of ions (such as Na^+ and K^+) (Norton, 1964). In the reaction system studied herein, water is more easily to form strong bonds with the ionic Na^+ or K^+ instead of the neutral Si-OH by H^+ exchange. For this reason, if more basic reaction media is needed at the same hydration, more 3Å molecular sieves should be added during the reaction. The alkaline strength of the catalytic system affects the transesterification rate in DMC synthesis reaction. Therefore, it is necessary to adjust the basicity of reaction media by altering the amount of molecular sieve added, for the purpose of achieving higher DMC selectivity.

In this work, five sets of experiment with different 3Å molecular sieve amounts (0 g, 0.1 g, 0.2 g, 0.4 g and 0.7 g) were conducted in the small batch reactor (45 ml) at 160 °C and 2 MPa for 5 h. Typically, 100 mmol methanol and 33.3 mmol propylene oxide along with 0.3 g of the heterogeneous catalyst were added in the reactor vessel. This was followed by the injection of CO_2 to the desired pressure (2 MPa at room temperature). The reaction time is recorded from when the temperature reaches 160 ° C. From that point the reactor is continuously stirred during the reaction. After reaction, the reactor was placed in the ice-water mixture and cooled to 30 °C, followed by the depressurization of reactor, the separation of liquid product and the solid mixture of catalyst and 3Å molecular sieve.

6.2.2.2 Influence of the quantity of acetonitrile on DMC yield

It has been previously reported that using an organic dehydrating agent (acetonitrile) in the direct synthesis of DMC from methanol and CO_2 can effectively shift the equilibrium to DMC formation direction (Honda *et al*., 2009). Acetamide ($CH_3(CO)NH_2$) is formed by the reaction of acetonitrile and water in the presence of a basic catalyst. The formed acetamide can react with methanol to generate methyl acetate (CH_3COOCH_3) and ammonia (NH_3). Then, methyl carbamate ($CH_3O(CO)NH_2$) would be produced by the reaction of by-product NH_3 and DMC. The amount of acetonitrile added in the reaction may affect the DMC selectivity through the following routes (Figure 6-4):

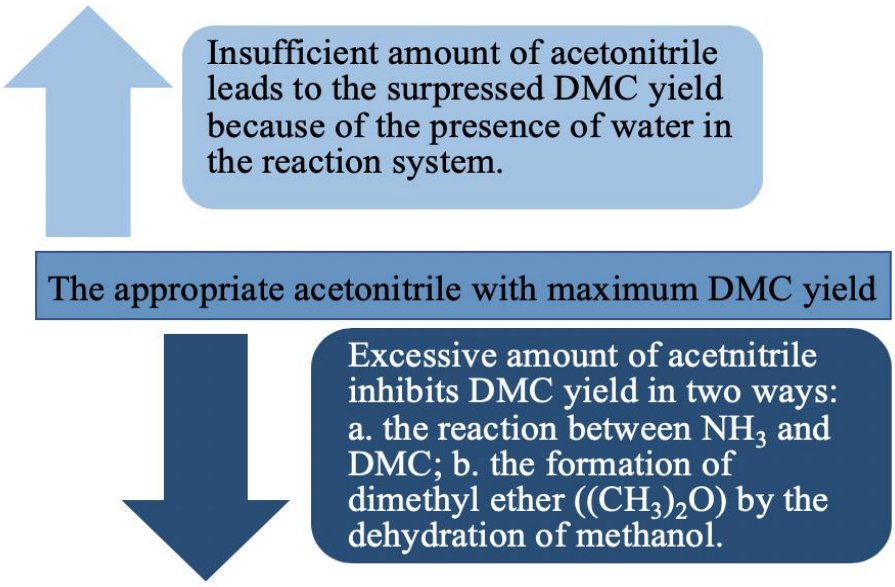

Figure 6-4. The effect of the quantity of acetonitrile added in the one-pot synthesis of DMC.

In this work, five sets of experiments were carried out in the small batch reactor (45 ml) under identical reaction conditions with various amount of acetonitrile. The quantity of acetonitrile added in terms of its molar ratio to PO is shown in Table 6-2.

Table 6-2. The amount of acetonitrile added in the reaction system (PO molar amount: 33.33 mmol).

	PO/Acetonitrile molar ratio				
	0	6/1	3/1	3/2	1/1
Acetonitrile volume (ml)	0	0.285	0.57	1.14	1.72

The experimental set-up, reaction conditions and operations are identical to those employing 3Å molecular sieve (section 6.2.2.1). Other than the addition of acetonitrile in place of 3Å molecular sieve.

6.2.2.3 Dehydration efficiency of dehydrating agents in the cycloaddition reaction

In this research, the hydrolysis of propylene oxide is the main source of propylene glycol formation which limits the reaction to DMC synthesis direction. In this section, the dehydration efficiency of two dehydrating agents (3Å molecular sieve and acetonitrile) are described with respect to: (1) reaction time; (2) quantity of PO.

(1) Reaction time

In order to analyze the cycloaddition reaction of propylene oxide to propylene carbonate either with or without dehydrating agents, the following experiments were carried out:

Table 6-3. The experiments design for studying the effect of reaction time on PC selectivity in cycloaddition.

	Reactants	Reaction conditions	Reaction time
Entry 1	PO (60 mmol)	2 MPa CO_2, 0.3 g catalyst, 160 °C	3h, 4h, 5h
Entry 2	PO (60 mmol) + Acetonitrile (60 mmol)		
Entry 3	PO (60 mmol) + 3Å molecular sieve (0.7 g)		

Both two dehydrating agents are added in excess to ensure that the reaction time is the sole variable that affects the yield of PC and PG. All of the reactions are carried out in the small batch reactor (45 ml) with stirring bars and heating jacket. Their procedures are the same as the former operations explained in section 6.2.2.1. Turnover frequency (TOF) is used to evaluate the reactivity of catalyst with the addition of dehydrating agents. In this section, the TOF is defined as the mass of synthesized propylene carbonate (PC) per gram catalyst per hour, and its calculation formula is shown as follows:

$$\mathrm{TOF} = \frac{m_{PC}}{W_{cat} \times t} = \frac{n_{PO} \times Yield_{PC} \times M_{PC}}{W_{cat} \times t} \qquad (6\text{-}2)$$

where n_{PO}, M_{PC}, t, and W_{cat}. represent the molar amount (mmol) of PO, formula weight (g mol^{-1}) of PC, reaction time (h), and the mass of overall catalyst (mg), respectively.

(2) Quantity of PO

The addition of dehydrating agents in the reaction is for two purposes: to suppress the hydrolysis of PO and thereby increase the yield of DMC, and to reduce the production of by-products formed from the reaction of methanol and PO. With a view to the reaction equilibrium, changing the initial quantity of reactants (methanol and PO) may affect the selectivity of DMC. Therefore, this section discusses the effect of reducing the quantity of PO on the DMC and by-product selectivity. The amount of PO added is shown in Table 6-4.

Table 6-4. The amounts of propylene oxide added in the reaction system (methanol molar amount: 100 mmol).

	Methanol / Propylene oxide molar ratio				
	0	10/1	8/1	5/1	3/1
PO volume (ml)	0	0.7	0.847	1.398	2.330

Reaction conditions: Methanol (100 mmol), Catalyst (0.3 g), CO_2 (2 MPa), 160 °C, 5h, Acetonitrile (0.57 ml) or 3Å molecular sieve (0.1 g).

In this section, all of the reactions were carried out in the small reactor (45 ml) with the addition of one kind of dehydrating agent and differing amounts of propylene oxide. The reaction procedure is the same as the former operations described in Section 6.2.2.1. Turnover frequency (TOF) is used to evaluate the catalytic efficiency of reaction system with various amount of reactant (propylene oxide), and the calculation method is discussed in section 6.2.2.

6.2.2.4 Analysis of liquid phase products

In this chapter, all the liquid products are analysed by using a Shimadzu gas chromatograph with a mass spectrometer and a HP-INNOWax capillary column. The detailed setup parameters of GC-MS and the temperature program for analysis has been thoroughly discussed in Section 3.2.1.

6.2.2.5 Characterisation of solid phase catalyst and 3Å molecular sieves

The catalysts used in the synthesis of DMC with the addition of dehydrating agents were characterised by means of SEM, SEM-EDX and XRD. Table 6-5 summarises the solid samples characterised in this chapter and the corresponding analytical methods.

Table 6-5. Techniques employed for the characterisation of solid samples.

	Techniques	Solid samples	Amis
Acetonitrile	XRD	Fresh catalyst and used catalyst	Testing if the hydrolysates affects the elemental composition of catalyst
3Å molecular sieve	SEM SEM-EDX XRD	**Fresh samples** (3Å molecular sieves, catalyst, mixture of 3Å molecular sieve and catalyst) **Used samples** (mixture of 3Å molecular sieve and catalyst)	1) the changes of the morphological structure of catalyst and 3Å molecular sieve before and after reaction. **(SEM)** 2) the elemental composition of samples before and after reaction. (**SEM-EDX and XRD**)

In accordance with section 3.2.3, SEM analysis can provide the detailed information about the morphology of catalyst. In this chapter, SEM was applied to find any morphological changes in catalyst and 3Å molecular sieves before and after reaction, respectively. The characterisation results may relate to the reactivity and stability of the catalyst. The role of 3Å molecular sieves in the reaction system is discussed by analysing its elemental composition before and after reaction. 3Å molecular sieves have great potential benefits in optimising the acid-base conditions of the reaction system *via* the ion exchange of H^+ (Section 6.2.2.1). For example, if the analysis results show that the proportion of alkaline cations (like Na^+ and K^+) in the 3Å molecular sieves are reduced after the reaction, then, these ions enter the reaction solution through the ion exchange during the reaction. As a result, the selectivity of DMC may be affected by the adjustment of the acid-base properties of catalytic system. Accordingly, the 3Å molecular sieve would not only act as a dehydrating agent but also as an acid-base buffer in the reaction system.

6.3 Results and discussion

6.3.1 Influence of 3Å molecular sieve quantity

6.3.1.1 Experimental results

The results of the effect of the amount of 3Å molecular sieves on DMC yield are shown in Figure 6-5.

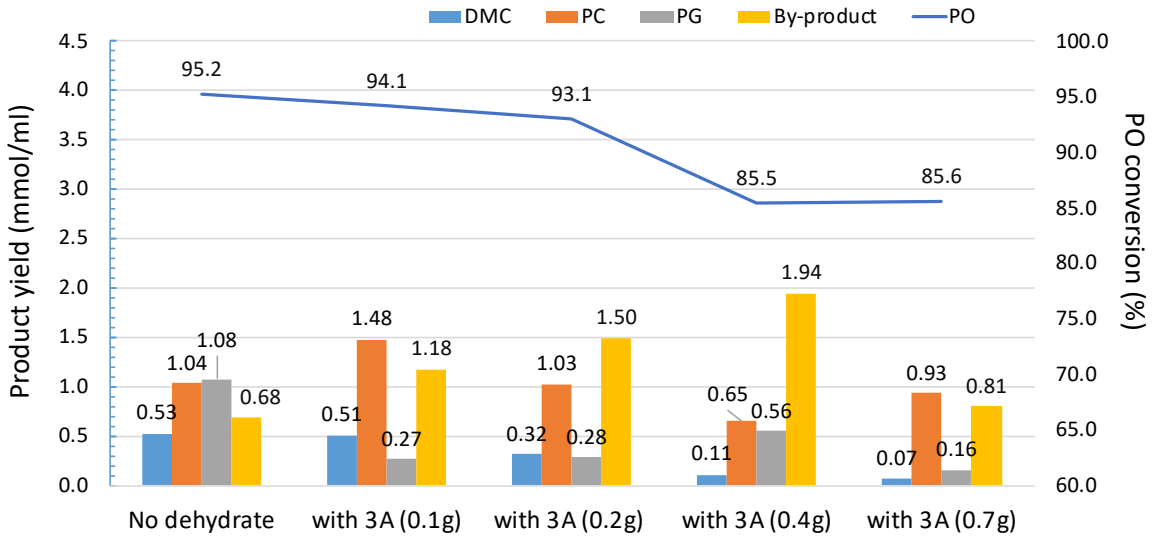

Figure 6-5. Effect of the amount of 3Å molecular sieves on the yield of each product. Reaction conditions: methanol (100 mmol), propylene oxide (33.3 mmol), catalyst (0.3 g), CO_2 (2 MPa), 160 °C, 5h.

DMC yield (blue bar) decreases, as the quantity of 3Å molecular sieves added increases. The yield of PG (gray bar) is significantly reduced in all cases when 3Å molecular sieve is present as compared to the reaction without the dehydrating agent. The obvious decline in PG production may result from the following: (1) The hydrolysis of PO is limited by the removal of H_2O; (2) The formation of PC from PG and CO_2 (scheme 6-1). In previous research, a low yield of PC was obtained with the addition of a dehydrating agent and using CeO_2-ZrO_2 as the catalyst. In this case, the conversion of PG was very low (around 2%) due to the equilibrium limitations (Tomishige et al., 2004). When the amount of 3Å is 0.1 g, the DMC yield is greater than that of PG, and the highest PC yield is obtained. This may be because the addition of a dehydrating agent promotes both the direct synthesis of the DMC and the formation of PC from PG (Scheme 6-1). Therefore, DMC formation under this condition is, in part, due to the reaction of PC with methanol. This is also derived from methanol reacting directly with CO2. When the amount of 3Å molecular sieves is higher than 0.1 g, the yield of

by-products increased with increasing 3Å, while the accompanying PC production gradually decreases. This could explain the reasons for the falling DMC yield, as more PO reacts with methanol and converts to the by-products under the reaction conditions. Higher by-products yield inhibits the direct conversion of methanol into DMC as well as limits the reaction of PO with CO2 to produce PC and further to generate DMC.

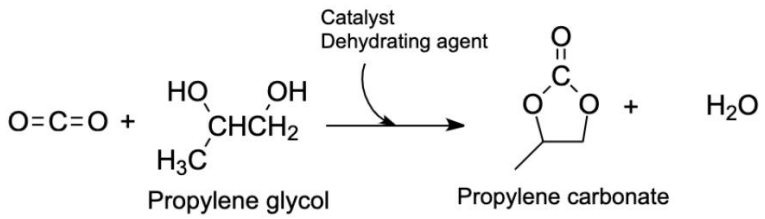

Scheme 6-1. The formation of propylene carbonate from propylene glycol and CO_2 (Tomishige *et al*., 2004).

With the addition of 3Å molecular sieves, the production of DMC is processed in two ways: (1) One-pot synthesis of DMC. The reaction of PO and CO_2 to produce PC, and the subsequent reaction of PC with methanol to form DMC and PG; (2) Direct synthesis of DMC. In the present of the dehydrating agent, methanol directly reacts with CO_2 to produce DMC and water. In light of previous studies, the addition of appropriate amount of water may promote the cycloaddition of propylene oxide and CO_2, because the presence of water may lead to a rise in silanol groups (-SiOH) on the catalyst surface (Lan *et al.*, 2014). In this work, the addition of water in suitable amount promotes the catalytic activity *via* the formation of Zn-OH group. According to the mechanism of cycloaddition, the formation of Zn-OH group is conducive to catalyse the ring-opening of propylene oxide by nucleophilic attack (Scheme 4-1). Excessive amount of 3Å molecular sieves (greater than 0.1 g) inhibits the cycloaddition reaction to form PC due to the decrease of active Zn-OH group on catalyst surface (PC production decreases from 0.1 g 3Å molecular sieves in Figure 6-5).

6.3.1.2 Influence of 3Å molecular sieve on transesterification reaction

Previous research (Fontes *et al.*, 2001) has discussed the dynamic acid-base effects of zeolites on the transesterification rate of enzyme with cross-linked subtilisin microcrystals catalyst in supercritical CO_2. There are two important conclusions from this work which elaborate the effect of adding 3Å molecular sieves on the production of DMC: (1) Effect of acid-base properties of zeolite on the transesterification rate (Figure 6-6); (2) Effect of the amount of zeolite on the transesterification rate (Figure 6-7).

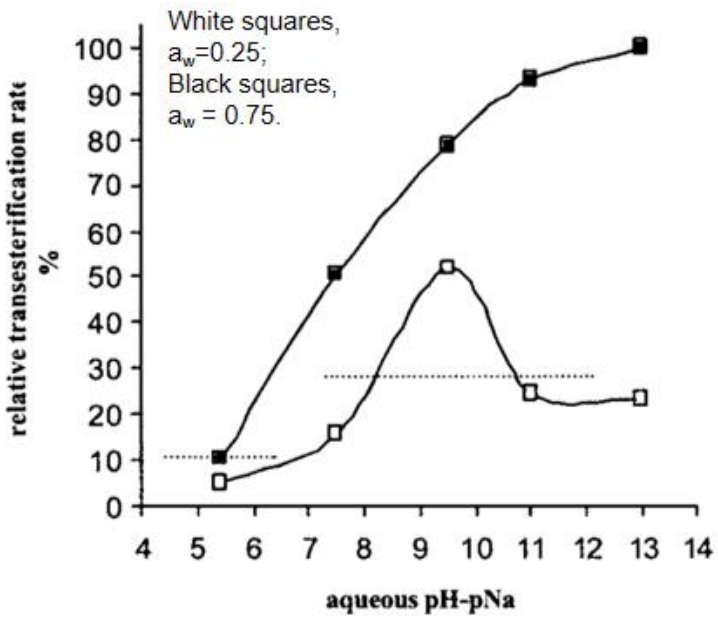

Figure 6-6. Influence of acid-base properties of zeolite on the initial transesterification rate for CLECs in *sc* fluids (Fontes *et al.*, 2001). The left and right dashed lines show reaction rate values without zeolite, at a_w = 0.75 and a_w = 0.25, respectively. pH-pNa represents the activity ratio of the two ions (H^+ and Na^+) which used to indicate the protonation state of acidic side chains *via* the exchange of Na^+ for H^+.

In Figure 6-6, a_w is a key parameter that describes the thermodynamic water activity, and higher a_w value always lead to the increasing catalytic activity because the flexibility of enzyme has been improved (Bell *et al.*, 1995). At a_w=0.25, the hydrolytic side reaction could hardly be noticed and no acid product (Ac-Phe) is formed. In the Figure 6-6, it is apparent in the fact that the reaction rate reached the maximum (around 50%) in the presence of zeolite 9.5. The initial rate is decreasing because the reaction condition is too acidic or basic. By contrast, at a_w=0.75, Ac-Phe is formed and the basic sites on the zeolite need to neutralize these acidic by-products. Therefore, zeolite 13 provides the optimal reaction condition for a_w=0.75, but it is too basic for the highest activity at a_w=0.25 (reaction rate decrease to around 25%).

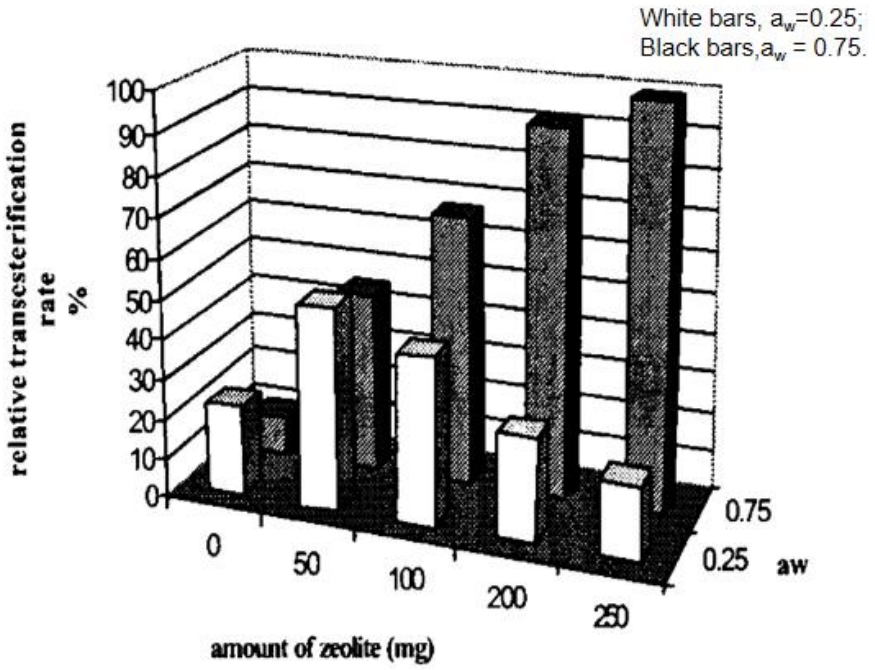

Figure 6-7. Influence of amount of zeolite on the initial transesterification rate for CLECs in *sc* fluids (Fontes *et al.*, 2001). The zeolite 9.5 is used in the experiments.

Figure 6-7 shows that the amount of zeolite affects the activity of catalyst and the trends of two sets of experiments carried out at lower and higher a_w are quite different. In the reaction system, H_2O is more likely to bind to the ionic alkaline (Na^+ and K^+) sites than to bind to the neutral sites (like Si-OH) by the ion exchange of H^+. That is to say, zeolite with a given pH-pNa value will be less basic because the alkaline sites will become more stable with a higher hydration (a_w value). At a_w=0.25, there is no need to neutralise the effects of the acidic Ac-Phe. Higher zeolites amount (more than 50 mg) may inhibit the activity of catalyst in a too basic reaction condition. At higher aw, more zeolite is required, either for the neutralization of acidic by-product, or to provide enough basic sites for the optimization of reaction conditions.

To summarise the effect of 3Å molecular sieves on transesterification, it is in effect that 3Å molecular sieves may turn into an acid-base buffer in the reaction system. The trend of DMC production curve in Figure 6-5 is similar to that of the transesterification rate curve with a_w = 0.25 in Figure 6-6 and 6-7. Therefore, the experimental results can be explained using the acid-base effects of zeolite on transformation reaction. In this study, the pH value of reaction product is around 9 when 0.1 g 3Å molecular sieves added (Appendix B-1). As shown in Figure 6-6, the highest transesterification rate (a_w=0.25) is achieved with a given pH-pNa value of 9.5, which is similar to this reaction condition. Additionally, only a small amount of water is generated during the reaction, and there are no acidic by-products formed by

hydrolysis. Adding excessive amounts of molecular sieves (> 0.1 g) causes the reaction conditions to be too basic to promote the transesterification reaction and promotes the side reactions between PO and methanol to generate 1-methoxy-2-propanol (Scheme 6-2, route (a)).

Base-catalyzed reaction

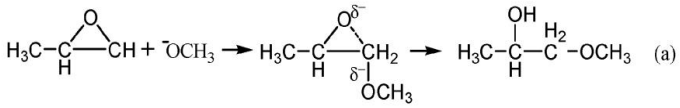

Acid-catalyzed reaction

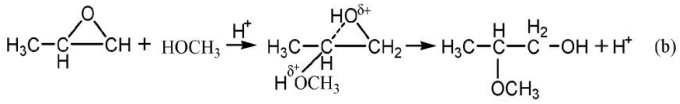

Scheme 6-2. The reaction of propylene oxide and methanol with acidic or basic catalyst (Liang *et al.,* 2010). The product of base-catalysed reaction is 1-methoxy-2-propanol (Route (a)) and the product of acid-catalysed reaction is 2-methoxy-1-propanol (Route (b)).

6.3.1.3 Catalyst characterisation

In this work, fresh and spent mixture of catalyst and 3Å molecular sieves have been assessed and characterized *via* XRD, SEM-EDX and SEM techniques. The experimental parameters for characterisation methods are discussed in Chapter 3.3. Figure 6-8 shows the surface morphology of the solid catalyst before and after reaction. The shapes of the granular catalyst and cubic 3Å molecular sieves remain constant before and after the reaction (Figures 6-8 (a) and 6-8(b), respectively). The images indicate that the physical structure of both 3Å molecular sieves and catalyst does not change after reaction under 160 ℃ reaction temperature and 4.5MPa reaction pressure.

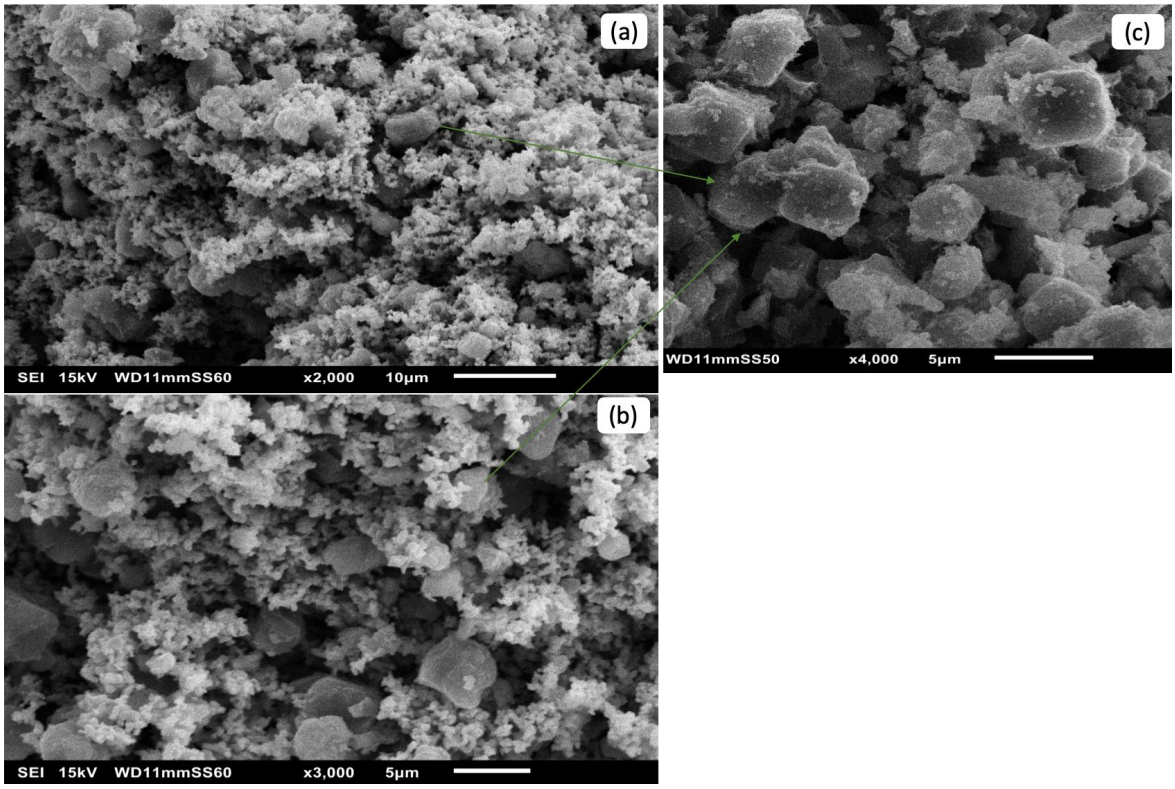

Figure 6-8. SEM images of the mixtures of catalyst and 3Å molecular sieves: (a) fresh K_2CO_3-NaBr-ZnO and 3Å molecular sieves mixture (b) spent K_2CO_3-NaBr-ZnO and 3Å molecular sieves mixture (c) higher magnification (6000x) image of fresh 3Å molecular sieves.

The XRD patterns of the solid catalyst before and after reaction are presented in Figure 6-9. The typical peaks of ZnO (PDF-ICDD 01-081-8838), SiO_2 (PDF-ICDD01-073-3411) and $Al_2(SiO_4)O$ (PDF-ICDD01-089-1483) are apparent in the solid catalysts before and after reaction conditions. The result of XRD is consistent with SEM analysis results, which indicates that the structure of catalyst and 3Å molecular sieves remain stable under high pressure and temperature condition. The typical peaks of Na_2O and K_2O are not present in

Figure 6-9, probably because the content of these two substances in the mixture is too low to be detected. Therefore, more detailed information about the composition of catalyst mixture before and after reaction is acquired by SEM-EDX (Table 6-6).

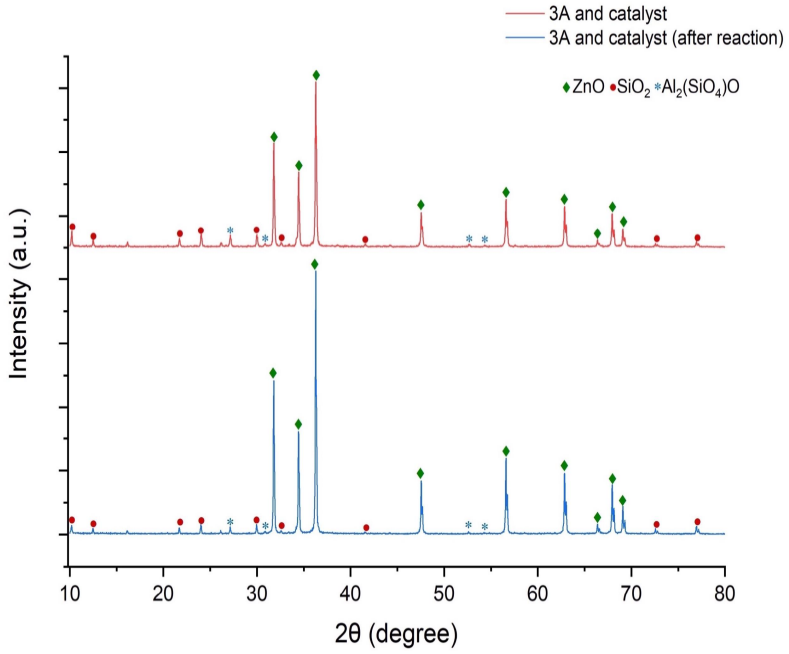

Figure 6-9. The XRD patterns of fresh and spent catalysts: fresh K_2CO_3-NaBr-ZnO and 3Å molecular sieves mixture and K_2CO_3-NaBr-ZnO and 3Å molecular sieves mixture after reaction.

Table 6-6. Composition of the fresh and spent mixture of catalyst and 3Å molecular sieves by EDX spectroscopy.

	Before reaction		**After reaction**	
	Mass %	Mol %	Mass %	Mol %
Na_2O	1.69	2.16	-	-
Al_2O_3	10.29	8.01	9.00	7.01
SiO_2	12.41	16.39	11.55	15.28
K_2O	2.05	1.72	-	-
ZnO	73.56	71.72	79.45	77.71

Experimental error is within ±3%.

Table 6-6 shows that the mole percentages of Al_2O_3, SiO_2 and ZnO remain approximately stable, and active compounds (both Na_2O and K_2O) disappear after the reaction. The composition of solid catalyst by EDX analysis is consistent with the results of SEM analysis and XRD analysis (Figure 6-8 and 6-9, respectively), which refers to that the structure of both molecular sieves and catalyst carrier is stable after reaction. The decrease of Na_2O and K_2O

content in 3Å molecular sieves is caused by the leaching of Na^+ and K^+ from the solid into the reaction solution.

6.3.2 Influence of acetonitrile quantity

Acetonitrile is a nitrile solvent which consists of a cyano group (-C≡N) and a methyl group (-CH_3). Acetamide ($CH_3(CO)NH_2$) is formed by the hydration of acetonitrile and acetamide further hydrolyse to acetic acid (CH_3COOH) under acidic reaction condition (Scheme 6-3).

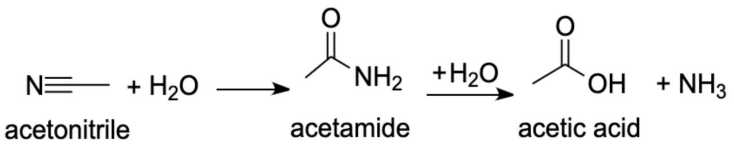

Scheme 6-3. The reaction mechanism of the hydration of acetonitrile under acidic condition.

The effect of acetonitrile (CH_3CN) amounts on the DMC synthesis reaction is explored by adding different amounts of CH_3CN as discussed in section 6.2.2.2. The reactions are carried out in the small reactor (45 ml) at 160 °C for 5 h and the test results are shown in Figure 6-10.

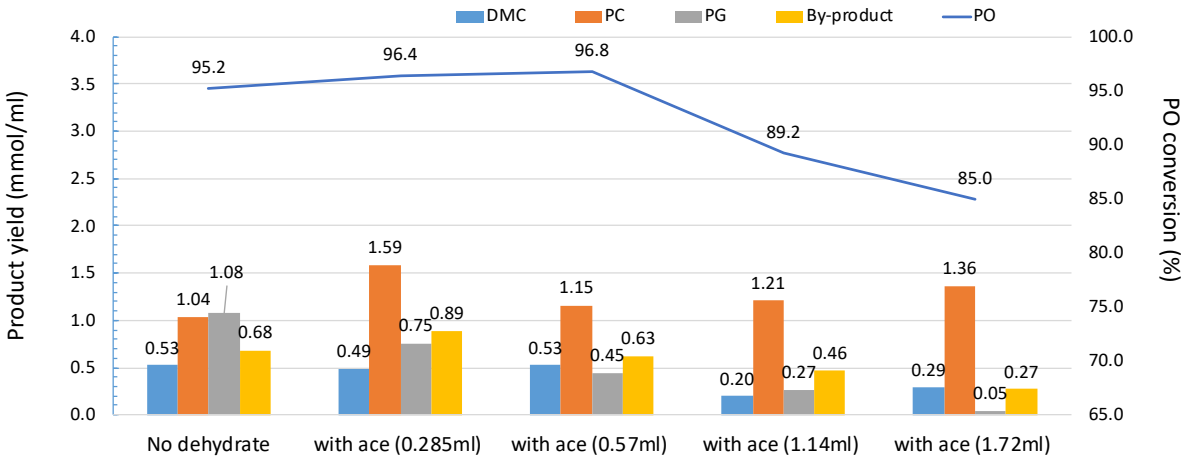

Figure 6-10. The yield of each product and PO conversion of DMC synthesis reaction with the addition of different amounts of acetonitrile. Reaction conditions: methanol (100 mmol), propylene oxide (33.3 mmol), catalyst (0.3 g), CO_2 (2 MPa), 160 °C, 5 h.

The yield of PG (grey bar) decreased with the increasing amount of CH_3CN added in the reaction system due to the inhabitation of PO hydrolysis. When $V_{(CH_3CN)} \leq 0.57$ ml, the production yield of DMC and PO conversion ratio remains stable (around 0.53 mmol ml^{-1} and 96%, respectively) and the decrease of the production of PG lead to a slight increase of PC yield (from 1.04 to 1.15 mmol ml^{-1}), the yield of by-products remains stable (from

0.68mmol/ml to 0.63 mmol/ml). When $V_{(CH_3CN)}$ >0.57 ml, the production of DMC decreases obviously from 0.53 mmol/ml to 0.29 mmol/ml, and both the yield of PG and by-products decreases with increasing acetonitrile adding amounts.

More specifically, when $V_{(CH3CN)}$ =0.285 ml, CH_3CN would end up as acetic acid going *via* acetamide (Scheme 6-3). The formation of acetic acid promotes the side reaction of PO and methanol to generate 2-methoxy-1-propanol (Scheme 6-2, route (b)), which leads to the increase of by-product yield (from 0.68 to 0.89 mmol ml^{-1}). Additionally, the formation of methyl carbamate by the reaction of DMC and ammonia (Honda *et al.*, 2009) (Scheme 6-4) results in a slight decrease of DMC yield (from 0.53 to 0.49 mmol ml^{-1}).

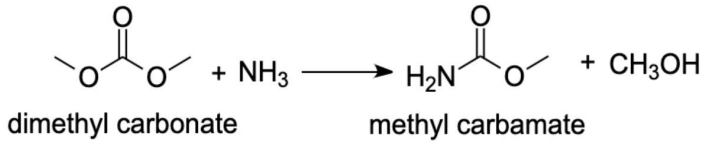

Scheme 6-4. The formation of methyl carbamate and methanol by the reaction of DMC and NH_3.

According to the mechanism of transesterification reaction (Scheme 4-3), the amount of PG and DMC formed should be in a molar ratio of 1:1. When the CH_3CN addition is 0.57 ml, the molar ratio of PG to DMC production is close to 1:1, and the reactions in the system reach the equilibrium. In line with section 6.3.1, the appropriate amount of water in the system promotes the cycloaddition reaction because water is beneficial to promote the ring-opening of epoxide as a hydrogen-bonded donor. Therefore, When the amount of CH_3CN added is greater than 0.57 ml the production of PC is suppressed. The production of PC increased with the rising amount of dehydrating agent, because the PG is converted into PC in the system (Figure 6-11). This conclusion is consistent with the new peak (Ret. Time=15.85min) observed in Figure 6-11, which shows the chromatogram from GC-MS for the components exist in the conversion of PG reaction mixture. PG and acetonitrile are added in the small reactor with the reaction condition of 2.0 MPa (room temperature) and 160 °C (reaction temperature). As a result, PC is formed *via* the reversible transesterification reaction. Additionally, excessive PC inhibit cycloaddition occurs as well (the decrease in PO conversion from 96.8% to 85.0%). The overall reaction mechanism for the one-pot synthesis of DMC when using acetonitrile as the dehydrating agent is shown in Figure 6-12.

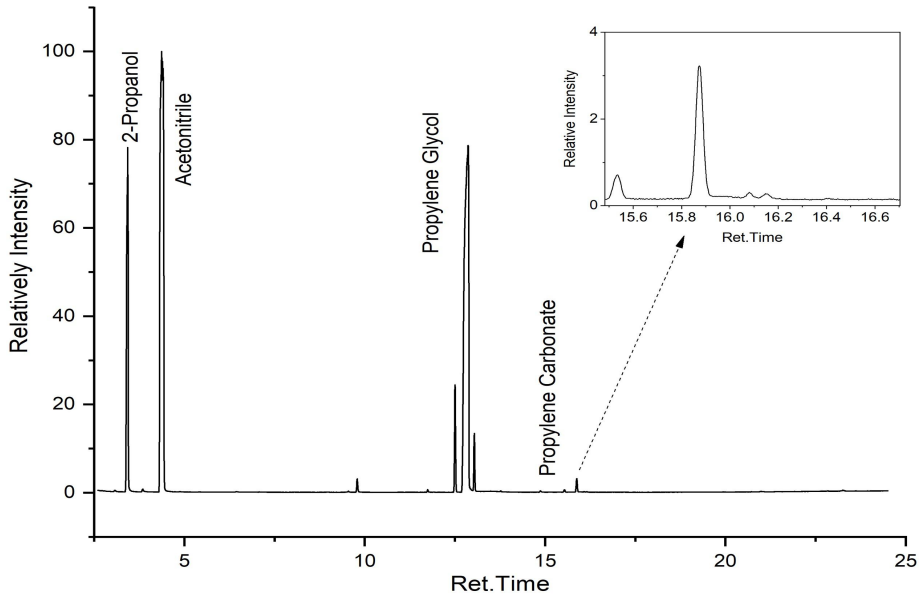

Figure 6-11. The chromatogram from GC-MS for the components exist in the conversion of PG reaction mixture. Reaction condition: Propylene glycol (60 mmol), acetonitrile (60 mmol), catalyst (0.3 g), CO_2 (2.0 MPa), 160 °C, 5h.

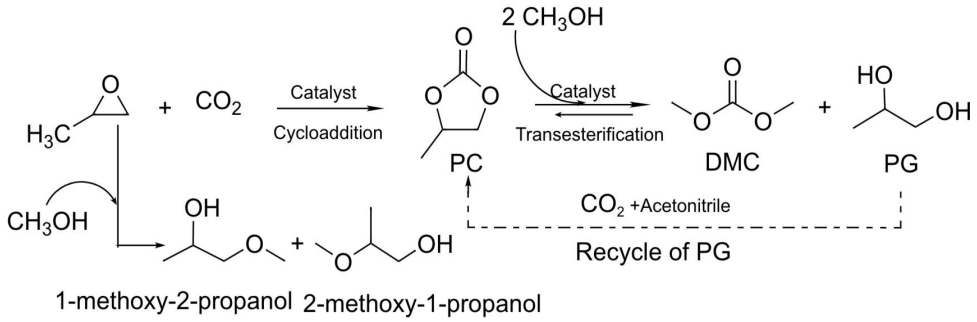

Figure 6-12. The reaction mechanism of DMC synthesis reaction with the addition of acetonitrile.

When the amount of CH_3CN added is higher than 0.57 ml, the cycloaddition is inhibited, which results in the decrease in DMC yield. There are another two possible reasons for the decrease of DMC yield: (1) The reaction between methanol and acetamide (Scheme 6-5) (Honda *et al.*, 2009); and (2) The reaction between DMC and NH_3 (Scheme 6-4).

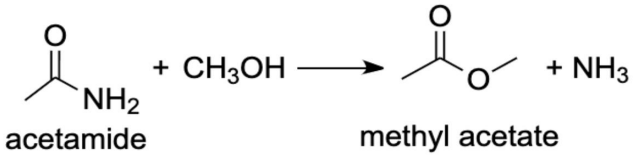

Scheme 6-5. The formation of methyl acetate from the reaction of acetamide and methanol.

In order to determine the composition of the hydrolysate and the reactions responsible for the decrease of DMC yield. The following experiments were performed (Table 6-7).

Table 6-7. The effect of methanol on the hydration of acetonitrile.

	Reactants	**Temperature (°C)**	**CO_2 Pressure**	**Catalyst**	**Reaction time (h)**
Reaction 1	Acetonitrile (66.66 mmol), H_2O (33.33 mmol)	160	2 MPa	0.3 g	5
Reaction 2	Acetonitrile (66.66 mmol), H_2O (33.33 mmol), Methanol (100 mmol)				

The qualitative analysis results obtained from GC-MS show that the hydrolysate is acetamide in the absence of methanol, and urea ($CO(NH_2)_2$) is formed in the presence of methanol. Moreover, with methanol, the colour of the reaction product changes from colourless to pale yellow (Figure 6-13), which means that methanol participates in the reaction and the composition of hydrolysate changes. In the reaction system of DMC synthesis, excessive acetonitrile promotes the reaction between acetamide and methanol to produce ammonia, which can react with both DMC and CO_2 and lead to the decrease in DMC yield.

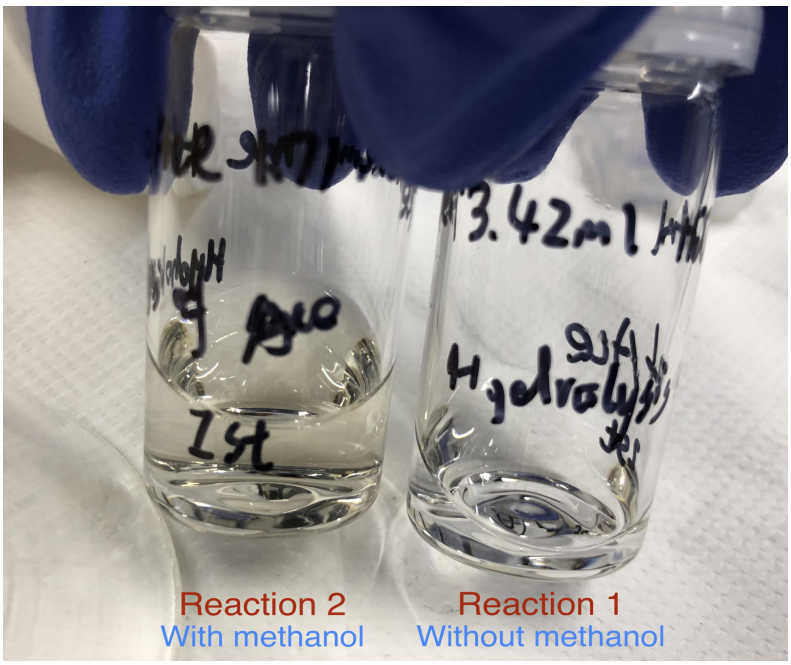

Figure 6-13. Photographic images of the products of reaction 1 and 2. Reaction 1 was carried out in presence of acetonitrile (66.66 mmol) and H_2O (33.33 mmol); Reaction 2 was carried out in presence of acetonitrile (66.66 mmol), methanol (100 mmol) and H_2O (33.33 mmol); Reaction conditions: catalyst (0.3 g), CO_2 (2 MPa), 160 °C, 5 h.

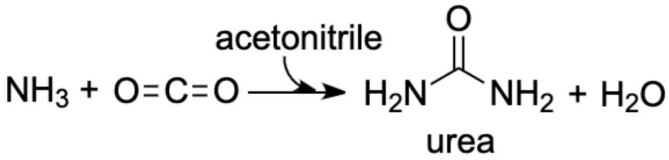

Scheme 6-6. The formation of urea from the reaction of ammonia and CO_2.

Ammonia, formed through the reaction of acetamide and methanol, can react with carbon dioxide to generate urea (Scheme 6-6) with the addition of acetonitrile. The composition analysis of the fresh and spent catalyst is performed using XRD and the diffractograms are shown in Figure 6-14. The presence of ZnO (PDF-ICDD 01-081-8838) and Na_2CO_3(PDF-ICDD 04-013-9890) are clearly present in the fresh catalyst (K_2CO_3-NaBr-ZnO). The diffractogram of the spent catalyst shows that the concentration of Na_2CO_3 decreased below the detection limit of XRD. This indicates that the changes in the colour of reaction product probably because the sodium ions supported on the catalyst are dissolved in the reaction solution.

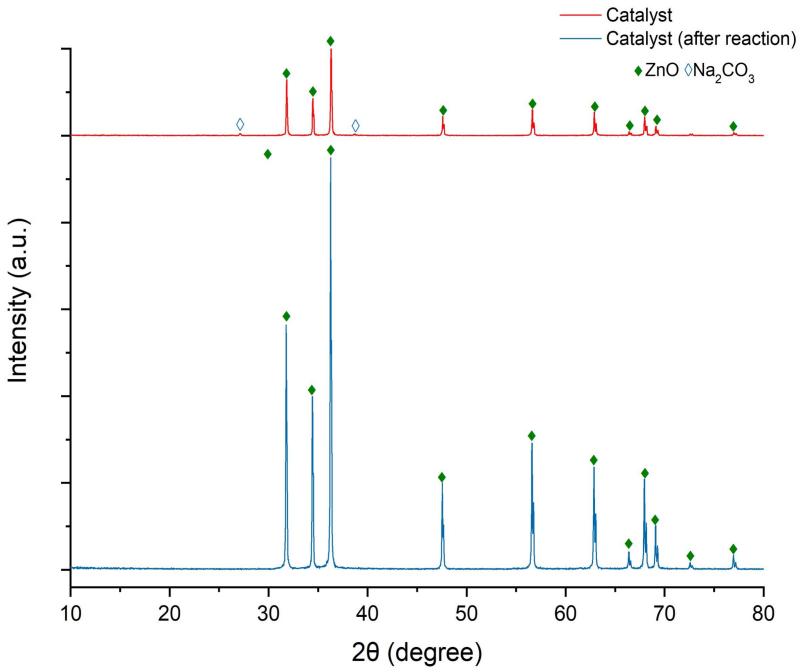

Figure 6-14. The XRD patterns of fresh and spent catalysts: fresh K_2CO_3-NaBr-ZnO and K_2CO_3-NaBr-ZnO after reaction.

The colour of the products of the DMC synthesis reactions with the excess acetonitrile (1.14 ml) is yellow and the pH value of the liquid product is around 10 (Appendix B-2). When 1.14 ml of acetonitrile added in the reaction, the new formed hydrolysate (acetamide) reacts with methanol (Scheme 6-5) or DMC (Scheme 6-4), leading to the changes in the colour of reaction product (from colourless to yellow). The pH value is between 9 and 10 after reaction as a result of the dissolution of NH_3 in methanol and the formation of urea *via* the reaction of CO_2 and NH_3 (Scheme 6-6). The above results are helpful to clarify experiment theories in the system. First, the generated acetamide reacts with methanol to produce methyl acetate and ammonia, then followed by the formation of methyl carbamate from the reaction of DMC and NH_3. With the addition of acetonitrile, urea is formed by the reaction of CO_2 and NH_3. In this process, both the reactant (methanol) for DMC synthesis and the target product (DMC) reacts with the hydrolysate, which ultimately leads to the reduction in DMC yield (from 0.53 to 0.20 mmol ml^{-1}). Additionally, the reaction between methanol and acetamide and the too basic reaction conditions inhibit the occurrence of side reaction to certain extent (by-products yield decreases from 0.63 to 0.46 mmol ml^{-1}).

6.3.3 Comparison of dehydration efficiency of two agents

The major aim of adding dehydrating agents was to inhibit the hydrolysis of propylene oxide in the reaction progress; while the amount of PO in the reaction system predominately affect

the cycloaddition reaction to form propylene carbonate. The analysis of the effect of adding dehydrating agents on cycloaddition and the influence of the quantity of PO added on DMC synthesis is given in this section.

6.3.3.1 The influence of dehydrating agents on the cycloaddition reaction

The reaction conditions are given in section 6.2.2.3 and the experiment results are shown in Figure 6-15.

(a)

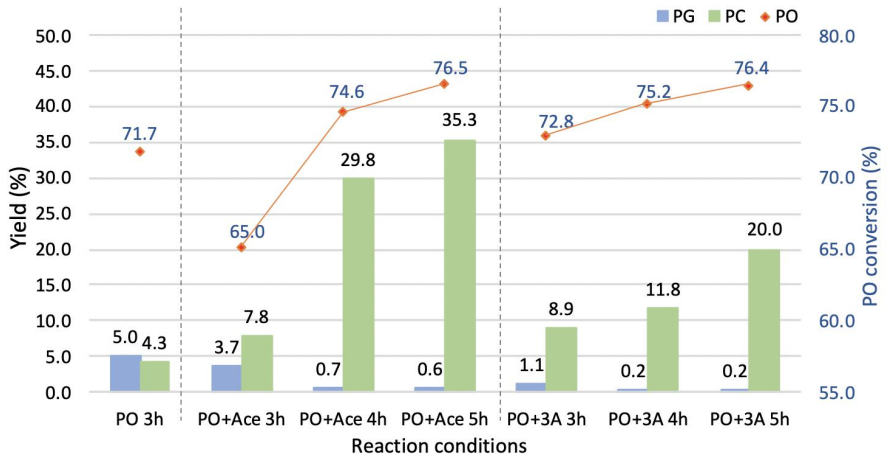

(b)

Reactions	TOF (h^{-1})
PO 3h	29.2
PO+Ace 3h	52.8
PO+Ace 4h	152.1
PO+Ace 5h	144.3
PO+3A 3h	60.7
PO+3A 4h	60.4
PO+3A 5h	81.6

Figure 6-15. (a) The effect of reaction time on PC and PG yield with the addition of acetonitrile and 3Å molecular sieves. (b) The effect of dehydrating agents on the catalytic efficiency. Reaction conditions: PO (60 mmol), acetonitrile (60 mmol), 3Å molecular sieves (0.7 g), catalyst (0.3 g), CO_2 (2 MPa), 160 °C, reaction time: 3 h,4 h or 5 h.

When acetonitrile is used as the dehydrating agent, the PO conversion and PC yield increases with longer reaction times and reaches the maximum (around 76.5% and 29.8%, respectively) with the lowest PG yield (0.6%) at 5 hours reaction time. In the formation of PC from the reaction of PO and CO_2, the molar ratio of PO to PC is 1:1. However, the increasing rate of PC yield (282.1%) is higher than that of PO conversion rate (14.7%) because of the conversion of both PO and PG to form PC with the addition of acetonitrile. The reaction of PG and CO_2 (scheme 6-1) reaches the equilibrium when the reaction time is 4 hours with the highest TOF (152.1 h^{-1}). In the presence of 3Å molecular sieves added conditions, the trend of curves is similar to the results of acetonitrile added condition. This trend explains how the conversion of PG to form PC limits the equilibrium of cycloaddition which results in the slow increase of PO conversion ratio.

Additionally, when the reaction time is short (≤ 3h), the yield of PC in the reaction using 3Å molecular sieves is higher than that using acetonitrile condition because the rate of

dehydration through physical adsorption is faster than that of dehydration through chemical reaction. However, when the reaction time is longer enough (> 3h), the effect of dehydration *via* chemical reaction on improving the catalytic efficiency is much more significant than that of dehydration *via* physical adsorption ($TOF_{(acetonitrile)}$ is almost twice the $TOF_{(3Å\ molecular\ sieves)}$). The reason for this phenomenon is that the deactivation of 3Å molecular sieves due to high temperature (160 °C) and high pressure (4.5 ~ 5 Mpa under reaction process). If dehydrating agents are used for DMC synthesis reaction, the time required for the cycloaddition to reach equilibrium should be longer than 4 to 5 hours should be more suitable, since the generated PC is continuously converted to DMC,

6.3.3.2 The influence of PO quantity on DMC synthesis

As in the section 6.2.2.3, it is necessary to find the appropriate amount of PO which results in the maximum production yield of DMC and the least amount of by-products.

(a)

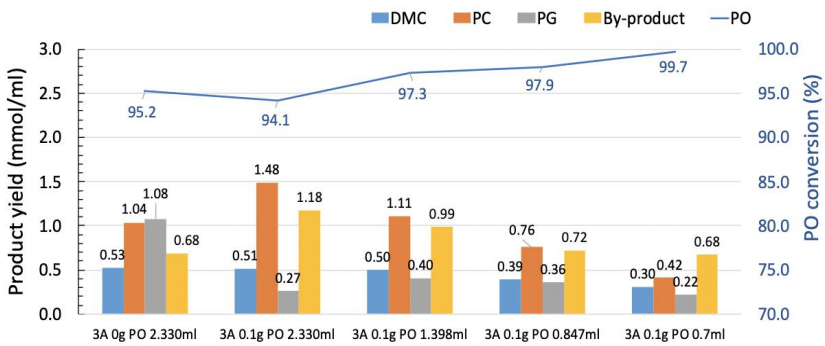

(b)

Reactions	TOF (h^{-1})
3A 0g PO 2.330ml	24.7
3A 0.1g PO 2.330ml	23.8
3A 0.1g PO 1.398ml	18.9
3A 0.1g PO 0.847ml	14.9
3A 0.1g PO 0.7ml	11.5

Figure 6-16. (a) The effect of different PO adding amounts on the yield of each product in the DMC synthesis reaction with the addition 3Å molecular sieves. (b) The TOF calculation results of catalytic system with various PO adding amounts and 0.1g 3Å molecular sieves. Reaction conditions: methanol (100 mmol), 3Å molecular sieves (0.1g), catalyst (0.3g), CO_2 (2 MPa), 160 °C, 5h.

The yield of PC and by-products reduced as the amount of PO added decreased in the presence of 3Å molecular sieve. DMC yield remained essentially stable (around 0.50 mmol ml^{-1}) when the amount of PO added is no less than 1.398 ml. With the decrease of the amount of PO added (< 2.330 ml), the molar ratio of DMC and PG production closes to 1: 1, which indicates that the main route to generate DMC under this condition is PO → PC → DMC (Scheme 2-9).The conversion of PG and CO_2 to form PC is inhibited probably because the structure of 3Å molecular sieves is damaged under the reaction conditions. Therefore, the appropriate amount of PO adding amount for DMC synthesis reaction is 1.398 ml because the reaction of DMC formation reaches equilibrium with a relative high DMC production, and the production of by-products is relatively reduced (from 1.18 to 0.99 mmol ml^{-1}).

(a)

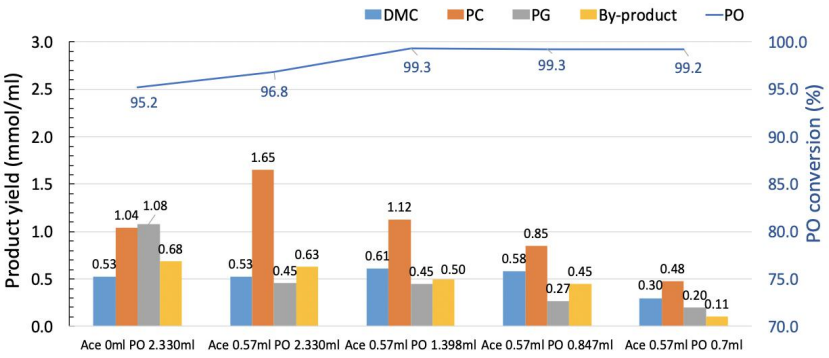

(b)

Reactions	TOF (h^{-1})
Ace 0ml PO 2.330ml	24.7
Ace 0.57ml PO 2.330ml	25.0
Ace 0.57ml PO 1.398ml	25.2
Ace 0.57ml PO 0.847ml	24.1
Ace 0.57ml PO 0.7ml	12.4

Figure 6-17. (a) The effect of different PO adding amounts on the yield of each product in the DMC synthesis reaction with the addition of acetonitrile. (b) The TOF calculation results of catalytic system with various PO adding amounts and 0.57ml acetonitrile. Reaction conditions: methanol (100 mmol), acetonitrile (0.57 ml), catalyst (0.3 g), CO_2 (2 MPa), 160 °C, 5h.

The curves (Figure 6-76 (a)) of the yield of PC, PG and by-products of the reaction in the presence of acetonitrile shows the similar trend with that of 3Å molecular sieves added reactions. The only difference is the molar ratio of the production of DMC to PG is higher than 1:1, which means the conversion of PG to PC occurs in the reaction system due to the addition of acetonitrile. More PC is generated from both cycloaddition and the reaction of PG and CO_2, which results in the increase of DMC production with a higher catalytic efficiency ($TOF_{(Acetonitrile)}$>$TOF_{(3Å\ molecular\ sieves)}$). The yield of DMC reaches the maximum (0.61 mmol ml^{-1}) when PO adding amount is 1.398 ml with the highest TOF of 25.2 h^{-1} (Figure 6-17 (b)).

Higher DMC production yield and catalytic efficiency of reaction system can be obtained *via* the reactions using acetonitrile as the dehydration agent. The dehydration efficiency of 3Å molecular sieves is higher than that of acetonitrile when reaction time is less than 3 hours. The deactivation of 3Å molecular sieves under high-temperature and high-pressure conditions is the key factor affecting its application in DMC synthesis reaction.

6.4 Conclusions

With the addition of a suitable quantity of dehydrating agents (0.1 g for 3Å molecular sieves and 0.57 ml for acetonitrile), the production of PC increases significantly owing to the inhabitation of the PO hydrolysis. The effect of adding dehydrating agents on improving the yield of DMC is not obvious probably because of the higher yield of by-products in the presence of 3Å molecular sieves added condition and the formation of hydrolysates (NH_3 and urea) with the addition of acetonitrile. Appropriate amount of water in the reaction system could facilitate the cycloaddition of propylene oxide and CO_2 *via* the formation of Zn-OH groups on the catalyst surface, which are conducive to catalyse the ring-opening of propylene oxide by nucleophilic attack. Adding dehydrating agents in the reaction can not only limit the hydrolysis of PO, but also can improve the efficiency of CO_2 utilization through the conversion of PG to PC.

Furthermore, results have shown that applying acetonitrile as the dehydrating agent in reaction system achieves higher catalytic activity than that with the 3Å molecular sieves. Although 3Å molecular sieves could offer better dehydration efficiency in the short-term reactions (reaction time $\leq$ 3 h), its unstable structure and deactivation under reaction conditions result in a lower DMC production and TOF value. Under conditions investigated (5 h reaction time and 1.398 ml PO), acetonitrile is the better-performing dehydrating agent. However, the drawbacks cannot be ignored as well, such as high cost, low boiling point, high toxicity and polarity, and the formation of nitrile and NH_3 in the reaction system. There is a need to make sure the alternative agent is equipped with the advantages of both physical water absorbent and chemical dehydrating agent for removing water from the system.

CHAPTER 7

ONE-POT SYNTHESIS OF DMC USING A Zn-PROMOTED METAL ALKALI CATALYST

Chapter 7 One-pot synthesis of DMC using a Zn-promoted metal alkali catalyst

7.1 Introduction

It has been explored that there is defect for improving DMC selectivity in one-pot synthesis of DMC *via* the cycloaddition and transesterification from methanol, propylene oxide and CO_2, which refers to the hydrolysis of propylene oxide. As described in Chapter 6, the addition of dehydrating agents can effectively inhibit the hydrolysis of PO and increase the production of PC. However, it is not apparent to recognise the positive effect of adding 3Å molecular sieves and acetonitrile on improving DMC production. These reaction systems suffer from drawbacks in terms of the high yield of by-products and the formation of inevitable hydrolysis products (acetamide, ammonia and urea) for 3Å molecular sieves and acetonitrile added conditions, respectively. The deactivation becomes the main challenge for using 3Å molecular sieves as the dehydrating agent due to the high-pressure and high-temperature reaction conditions. Compared with 3Å molecular sieves, acetonitrile would bring a higher DMC production and lower by-product yield with a TOF of 25.2 h^{-1}. However, there are few drawbacks relating to the homogeneous nature of acetonitrile, and the formation of hydrolysate intermediates limits the equilibrium of DMC synthesis reaction. The novel alternative needs to be investigated considering the advantage of both 3Å molecular sieves and acetonitrile.

It shows great possibility of achievement to remove the water *via* the reaction of active metal and steam water during the reaction process. Generally, the active metal (such as Mg, Zn) can react with water under certain conditions. For example, magnesium oxide (MgO) or magnesium hydroxide ($Mg(OH)_2$) is formed *via* the reaction of magnesium with water stream or excess steam, respectively. Zinc powder is a kind of bluish-grey coloured metal powder (Figure 7-1), and it can be used as the catalyst for organic synthesis. For example, zinc powder has been used as an active, reducing reagent for the synthesis of phenol (Sumimoto *et al.*, 2006). In this study, zinc powder has been employed as a promising dehydrating agent for the one-pot synthesis of DMC with K_2CO_3-NaBr-ZnO catalyst.

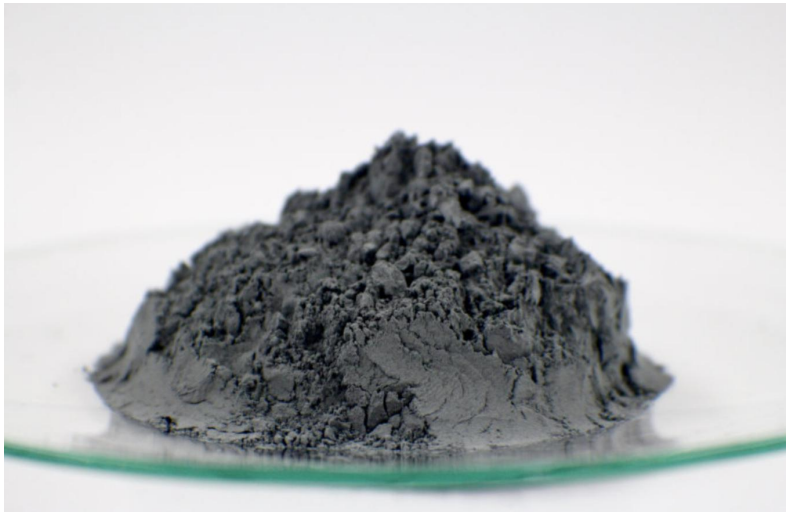

Figure 7-1. Photographic images of fresh zinc powder used in the work.

There are two reasons for choosing zinc powder as the potentially efficient dehydrating agent: (1) The heterogeneous nature of Zn powder makes it easily separate from the reaction system and be easily recyclable. (2) There is no new element being introduced into the reaction system, and the product of Zn powder hydrolysis is zinc oxide (ZnO) or zinc hydroxide ($Zn(OH)_2$); the former is a component of catalyst, and the latter can enhance the strength of strong basic sites on the catalyst surface, which is beneficial to transesterification of propylene carbonate and methanol. Scholars have extensively studied the catalytic performance of Mg-promoted KCl-ZrO_2 in order to achieve higher DMC selectivity (52.7%) at 150 °C and 9.5 MPa for 8 h (Eta *et al.*, 2010).. They also widely discussed the role of Mg turnings in both cycloaddition and transesterification with an attempt to gain much understanding on the mechanism of Mg involved reactions. Mg turnings have been used as a kind of promotor to enhance the yield of DMC by forming the intermediate magnesium methoxide ($Mg(OCH_3)_2$), which reacts with CO_2 to form carbonated magnesium methoxide (CMM). What promote the production of DMC are the oxygen of catalyst and the exchange of oxygen atoms between methoxy groups of CMM adsorbed on the catalyst surface. As magnesium methoxide has previously been reported as a reaction intermediate in the presence of Mg, zinc methoxide is expected as an intermediate in the presence of Zn. In this study, magnesium methoxide is also used to investigate the possible reaction mechanism to deconvolve the influence of the metal powder from the metal oxide support at mild conditions. In the end, the surface properties of the catalyst system are studied.

7.2 Experimental methods

7.2.1 Materials

Reagents sodium bromide (≥99%), potassium carbonate (≥99%), methanol (≥99.9%) and propylene oxide (≥99.5%) were purchased from Sigma-Aldrich. Zinc oxide (≥99%) was purchased from Fisher Scientific. Carbon dioxide gas (≥99.99%, water content <0.01%) was obtained from BOC. 2-propanol (Sigma-Aldrich, ≥99.8%) was used as an internal standard for GC–FID quantitative analysis. Dimethyl carbonate (99%), propylene carbonate (99.7%), 1-methoxy-2-propanol (≥99.5%) and propylene glycol (≥99.5%), supplied from Sigma Aldrich, were employed as reference materials for calibration curves. All materials were used as received unless otherwise stated.

7.2.2 Methods

7.2.2.1 Influence of Zn powder adding amount on DMC selectivity

The amounts of zinc powder added in the reaction system may affect the synthesis of DMC through the following two ways: (1) As discussed in the former section, the formation of $Zn(OH)_2$ *via* the hydrolysis of Zn powder may affect the transesterification reaction due to the weak alkalinity of $Zn(OH)_2$. (2) Zinc methoxide ($Zn(OCH_3)_2$) is a possible intermediate formed by the reaction of methanol and zinc powder. Metal methoxides are well-known homogeneous catalysts applied in transesterification reactions. For instance, sodium or potassium methoxide is typically generated in the reaction system during biodiesel synthesis from oils or fats (Balat, 2007). Therefore, zinc methoxide could promote the second stage of DMC synthesis, transesterification. The quantity of Zinc powder added are determined according to the molar ratio of propylene oxide and zinc powder, as shown in Table 7-1.

Table 7-1. The molar ratio of propylene oxide and Zn powder and the corresponding amount of Zn powder added in the reaction.

	Propylene oxide / Zn powder molar ratio					
	0	6/1	5/1	4/1	3/1	2/1
Zn amount	0g	0.361g	0.433g	0.542g	0.722g	1.083g

Reaction condition: Methanol (100 mmol), PO (33.33 mmol), catalyst (0.3 g), CO_2 (2 MPa), 160 °C, 5h.

In this section, all the reactions were carried out in the small reactor with the addition of 100 mmol methanol, 33.33 mmol propylene oxide, 0.3 g catalyst and various amounts of zinc powder at 2 MPa (CO_2 pressure, room temperature) and 160 ℃ for 5 h. The liquid reaction products were analysed using GC-MS, as discussed in section 3.2.1.

7.2.2.2 The role of Zn powder in the cycloaddition reaction

One-pot synthesis of DMC consists of two steps: cycloaddition and transesterification. The yield of propylene carbonate from propylene oxide and carbon dioxide *via* cycloaddition is one of the most critical factors that influences the increasing of dimethyl carbonate selectivity. However, the hydrolysis of propylene oxide to propylene glycol limits the production of propylene carbonate. To investigate the effect of zinc powder on the cycloaddition reaction, especially on the yields of propylene carbonate and propylene glycol, the following experiments in the presence of propylene oxide, CO_2, water or propylene glycol, zinc powder and catalyst were conducted (Table 7-2). Three extreme reaction conditions were considered in this section: (1) PO, CO_2 and catalyst only (Reaction 1 and 2); (2) PO, water, CO_2 and catalyst only (Reaction 3 and 4); (3) PO, PG, CO_2 and catalyst only (Reaction 5 and 6). The actual cycloaddition conditions in the DMC synthesis should be among these three reaction conditions.

Table 7-2. Influence of the Zn powder on the cycloaddition reaction in the presence of PG or water.

Conditions	Numbers	Reactants
In the absence of Zn	Reaction 1	PO + Catalyst
	Reaction 3	PO + H_2O + Catalyst
	Reaction 5	PO + PG + Catalyst
In the presence of Zn	Reaction 2	Zn+ PO + Catalyst
	Reaction 4	Zn + PO + H_2O + Catalyst
	Reaction 6	Zn +PO + PG + Catalyst

Reaction condition: 2 MPa CO_2, 160 °C, 5 h, 0.3 g catalyst, 0.433 g Zn powder, PO (66.66 mmol), PG (11.11 mmol), H_2O (44.44 mmol).

The main purpose is to study the role of zinc powder in the cycloaddition and to obtain the proposed mechanism for the synthesis of propylene carbonate from propylene oxide and CO_2.

7.2.2.3 The role of Zn powder in the transesterification reaction

According to the reaction mechanism of transesterification (Scheme 4-3), the reaction between methanol and propylene carbonate is the leading way to produce dimethyl carbonate (DMC), and CO_2 does not participate in the DMC synthesis reaction. The role of CO_2 in the transesterification reaction has not been studied in the previous literature to the best knowledge of the author. Therefore, in this study, the role of both zinc powder and CO_2 (or pressure) is discussed. Table 7-3 shows the experimental conditions for investigating the effect of both Zn powder and CO_2 on transesterification.

Table 7-3. Influence of the Zn powder and CO_2 on the transesterification reaction.

Conditions	Numbers	Reactants
CO_2 attended reactions	Reaction 7	PC + Methanol + Catalyst
	Reaction 8	PC + Methanol + Catalyst + Zn
No CO_2 attended reaction	Reaction 9	PC + Methanol + Catalyst + Zn (atm)
	Reaction 10	PC + Methanol + Catalyst + Zn (Helium, 2 MPa)

Reaction condition: 2 MPa CO_2 (reactions 7 and 8), 160 °C, 5 h, 0.3 g catalyst, 0.433 g Zn powder, PC (33.33 mmol), methanol (100 mmol).

This experiment is designed to explore the effect of Zn powder on the yield of DMC by comparing reaction 7 and reaction 8. The comparison of experiment 8, 9 and 10 helps to figure out the role of CO_2 in transesterification. The reaction mechanism for the synthesis of DMC from methanol and propylene carbonate is used for explaining the role of zinc powder in the transesterification.

7.2.2.4 Magnesium methoxide ($MgO(CH_3)_2$) promoted reactions

The formation of zinc methoxide ($Zn(OCH_3)_2$) from the reaction of methanol and zinc as an intermediate is expected in the presence of Zn powder. To study the possible new routes for the synthesis of DMC in the presence of zinc powder, a series of reactions with the participation of magnesium methoxide were carried out. Magnesium methoxide is formed by the reaction of MgO and methanol, which has previously been reported as a reaction intermediate in the presence of Mg (Eta *et al.*, 2010). Moreover, $Mg(OCH_3)_2$ contains the same methoxy group as $Zn(OCH_3)_2$ but solid products formed in the reaction, such as MgO, $Mg(OH)_2$ or $MgCO_3$, can be readily distinguished from those formed through interaction with the ZnO support.

In this study, 7~8% $Mg(OCH_3)_2$ in methanol was added in the reactions and the amount of 7~8% $Mg(OCH_3)_2$ solution was decided by the amount of methanol required for the reaction. In the previous experiment, 100 mmol methanol was applied in the reaction, and the detailed experiment design is shown in Table 7-4.

Table 7-4. Influence of the Zn powder and CO_2 on the transesterification reaction.

Conditions	Numbers	Reactants
Heterogeneous catalyst added condition	Reaction 11	Catalyst + $Mg(OCH_3)_2$ + PO
	Reaction 12	Catalyst + $Mg(OCH_3)_2$ + PO + Zn
Homogeneous catalyst added condition	Reaction 13	$Mg(OCH_3)_2$ + PO

Reaction condition: 3.3 mmol $Mg(OCH_3)_2$ and 100 mmol methanol, PO (33.3 mmol), catalyst (0.3 g, reaction 11 and 12), Zn powder (0.43 g, reaction 12); 2 MPa CO_2, 160°C, 5h.

This section aims to study the intermediates formed with the addition of zinc powder and to investigate the new possible reaction routes for the synthesis of dimethyl carbonate.

7.2.2.5 Characterisation of solid-phase catalyst

The techniques used for catalyst characterisation have discussed the in Chapter 3. In this work, these techniques are employed to analyse the fresh and spent catalysts and the mixture of catalyst and zinc powder. X-ray diffraction (XRD) was employed to analyse the morphological properties of the catalyst, and the average crystalline size of particles before and after the reaction was calculated. The full width at half maximum (FWHM) of the peak obtained from the XRD pattern is used to calculate the crystallite size of particles by using Scherrer equation (Equation 7-1) (Patterson, 1939).

$$D = \frac{K\lambda}{\beta\, COS\theta} \qquad (7\text{-}1)$$

where D is the crystallite size (nm), K is a crystal shape factor from 0.9~1, λ is the wavelength ($\mathring{A}$, 0.15406 nm), β is FWHM (radians) corrected for instrument broadening, and θ is Bragg angle (peak position). Samples were analysed using a Bruker D2 Phaser powder XRD instrument with Cu $K\alpha$ (30 kV, 10 mA) radiation at a scanning rate of 0.05° min^{-1}.

SEM and SEM-EDX analysis provided the information about the morphology and the elemental composition of the catalyst. Scanning electron micrographs and EDX were

recorded on a JSM-6010LA JEOL SEM instrument with AGAR Sputter Coater. All the samples were coated with a gold layer and analysed at 10 keV with a working distance of 10 mm.

Atomic absorption spectroscopy (AAS) was used to analyse the fresh and spent solid catalyst and the mixture of catalyst and zinc powder to obtain the concentration of zinc. In this work, the solid was digested with 69% nitric acid. The operations are as follows: Weigh about 0.3g of the sample and record the exact value (accurate to 0.0001 g) into the beaker, add 10ml of nitric acid to the beaker and place the beaker on the hot plate under stirring until the solid is completely dissolved, put it to room temperature, and then add it to a 500 ml volumetric flask. Rinse the beaker 3 times with deionised water and pour into the volumetric flask, then bring to volume by deionised water. Dilute the sample solution in the 500 ml volumetric flask by 50 times as the sample to be tested (concentration < 10 ppm). Four solid samples were analysed, and the exact weight of four samples are shown in Table 7-5.

Table 7-5. The content of four solid samples and the exact weight of each sample.

Sample content	Mass of sample (g)
S1 Catalyst + Zn powder	0.3017
S2 Catalyst	0.3005
S3 Used Catalyst + Zn powder	0.3071
S4 Used Catalyst	0.2785

Inductively coupled plasma-optical emission spectrometry (ICP-OES) was employed to analyse the spent solid catalyst and liquid reaction products. Four solid samples, as shown in Table 7-5, were analysed to obtain the information about the composition of fresh and spent catalyst (mass concentration of Zn, K and Na). Moreover, the liquid products of the reactions with or without the addition of zinc powder were analysed to acquire the mass concentration of each element leaching from the catalyst. The results indicate the catalytic stability of the catalyst. In a typical sample preparation procedure, both solid and liquid sample were digested with concentrated HNO_3, followed by dilution of digested solutions with 1% HNO_3 solution.

7.3 Results and discussion

7.3.1 Influence of Zn powder adding amount on DMC selectivity

The possible routes to influence DMC production with the addition of various amounts of zinc powder have been discussed in section 7.2.2.1. The reactions were carried out in the same reaction conditions, and the selectivity of each product and PO conversion was shown in Figure 7-2.

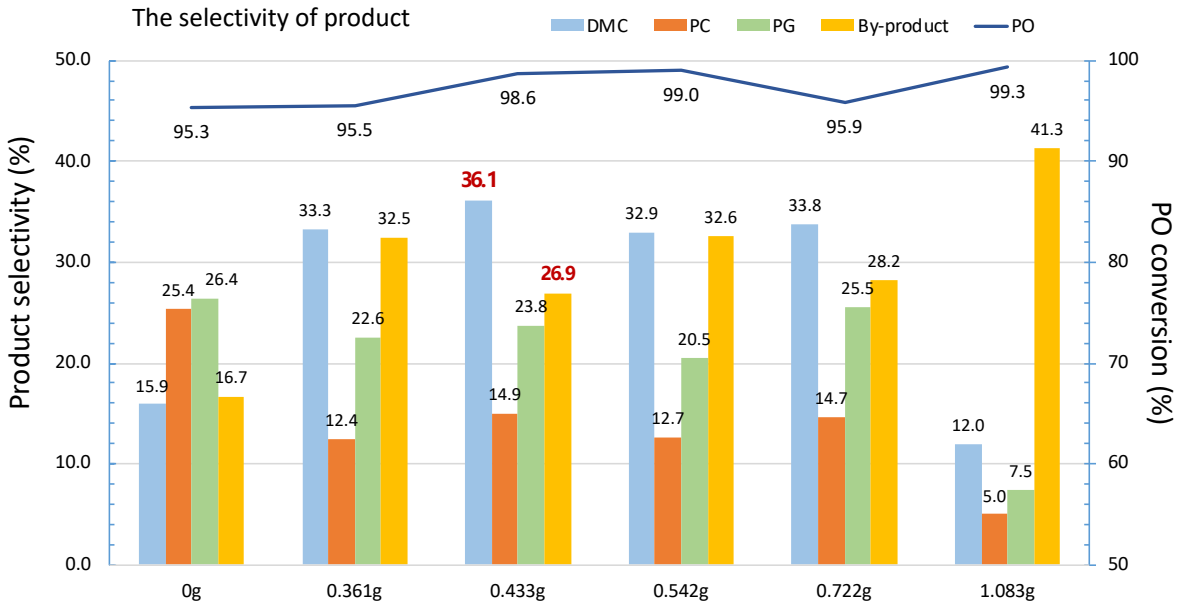

Figure 7-2. Selectivity of each product and PO conversion of DMC synthesis reaction with the addition of different amounts of zinc powder. Reaction conditions: methanol (100 mmol), propylene oxide (33.3 mmol), catalyst (0.3 g), CO_2 (2 MPa), 160 °C, 5h.

The figure shows the selectivity of various products and PO conversion when different amounts of Zn is added to the DMC formation reaction. The highest DMC selectivity (36.1%) can be achieved when 0.433 g Zn powder is added. The selectivity of PG is slightly reduced (from 26.4% to 23.8%), meanwhile the selectivity of by-products is significantly increased (from 16.7% to 26.9%) compared with that of no Zn added condition. With the increase of the amount of zinc added, the selectivity curves of DMC, PC and PG have the similar trend. That is, they all reach the maximum when the adding amount of zinc powder is 0.433 g. By contrast, the trend of the selectivity curve of by-products is completely opposite to that of the first three products. In principle, the selectivity ratio of DMC and PG should be close to 1:1 when reaching equilibrium. However, it can be seen from Figure 7-2 that with the addition of zinc powder, the amount of DMC generated is significantly higher than that of PG. This

means that in the reactions involving zinc powder, in addition to the one-pot synthesis of DMC from methanol, CO_2 and propylene oxide, there is also a new route for DMC generation, which is the focus of the following sections.

(a)

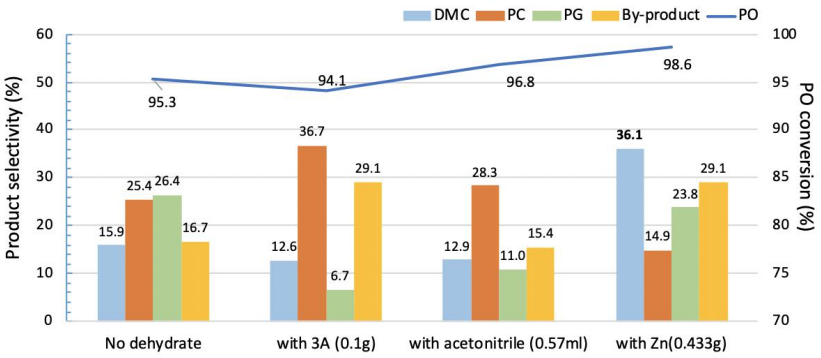

(b)

Reactions	TOF (h^{-1})
No dehydrant	24.7
With 3A (0.1g)	23.8
With acetonitrile (0.57ml)	25.0
With zinc powder (0.433g)	71.2

Figure 7-3. (a) The effect of adding dehydrating agents and zinc powder on the selectivity of each product of DMC synthesis; (b) The effect of adding dehydrating agents on the catalytic efficiency. Reaction conditions: Methanol (100 mmol), PO (33.33 mmol), acetonitrile (0.57 ml), 3Å molecular sieves (0.1 g), catalyst (0.3 g), zinc powder (0.433 g), CO_2 (2 MPa), 160 °C, 5h.

Based on the above discussion, zinc powder does not act as the dehydrating agent in the reaction system, because the PG selectivity is not significantly reduced due to the addition of zinc powder (Figure 7-3). This may be because the conversion of PG to PC does not occur in this reaction system (Scheme 6-1), which is different from the results of dehydrating agents (acetonitrile and 3Å molecular sieves) added reactions as discussed in Chapter 6. However, the catalytic efficiency is increased with a TOF value of 71.2 $h^{-1}$with the presence of zinc powder. Therefore, the role of zinc powder is more like as a promoter or co-catalyst rather than a dehydrating agent in the reaction system. The reaction in the presence of both co-catalyst (zinc powder) and dehydrating agent (3Å molecular sieves) was carried out, and the result is shown in Figure 7-4.

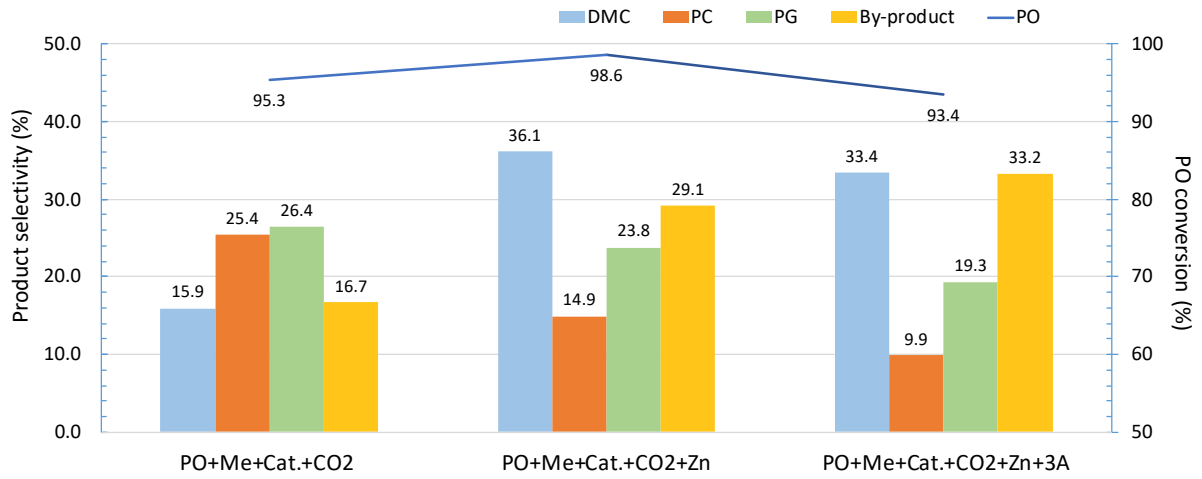

Figure 7-4. The effect of adding dehydrating agents and zinc powder at the same time on the selectivity of each product of DMC synthesis; Reaction conditions: Methanol (100 mmol), PO (33.33 mmol), acetonitrile (0.57 ml), 3Å molecular sieves (0.1 g), catalyst (0.3 g), zinc powder (0.433 g), 3Å molecular sieves (0.1 g), CO_2 (2 MPa), 160 °C, 5h.

Compared with only zinc powder added condition, the addition of both Zn powder and 3Å molecular sieves leads to the decrease of PO conversion (from 98.6% to 93.4%) and selectivity of DMC, PC and PG. As discussed in Chapter 6.3.1.1, the probable reason for this result is that cycloaddition reaction to form PC is limited by the addition of 3Å molecular sieves. Because a suitable amount of water in the reaction system can promote the catalytic activity *via* the formation of Zn-OH group, and the formation of Zn-OH group is conducive to catalyse the ring-opening of propylene oxide by the nucleophilic attack. The increase in the selectivity of by-products can be explained by the fact that the reaction condition is over basic (pH: ~9) which promotes the side reactions between PO and methanol to generate 1-methoxy-2-propanol (Scheme 6-2, route (a)).

To have a better understanding of the reaction mechanism of Zn involved reactions, FT-IR technique was employed to analyse the liquid products of the reactions to obtain information about the possible intermediates formed during the reaction process. The characteristic frequencies of CH_3 symmetric stretching and CH_3 asymmetric stretching are shown on the IR spectrum (Figure 7-5). Peaks at 2822 and 2926 cm^{-1} to CH_3O- (Wu, Chuang and Lin, 2000; Hui *et al.*, 2012). The bands of 1626, 1100 and 825 cm^{-1} are due to C=O stretching, C-O stretching and M-O stretching, respectively (Fig.7-5 (a) and 7-5 (b)) (Halmann, 1993). The FTIR spectrum indicates that zinc methoxide (CH_3O-Zn) is formed by the reaction of methanol and Zn powder. The ester group (-$OCOCH_3$) is generated as a product of the reaction of methanol, Zn powder and CO_2. The FTIR results indicate that zinc methoxide and carbonate zinc methoxide are formed during the reaction process, and the determination of important intermediates is essential for the speculation of the reaction mechanism of zinc powder involved reaction.

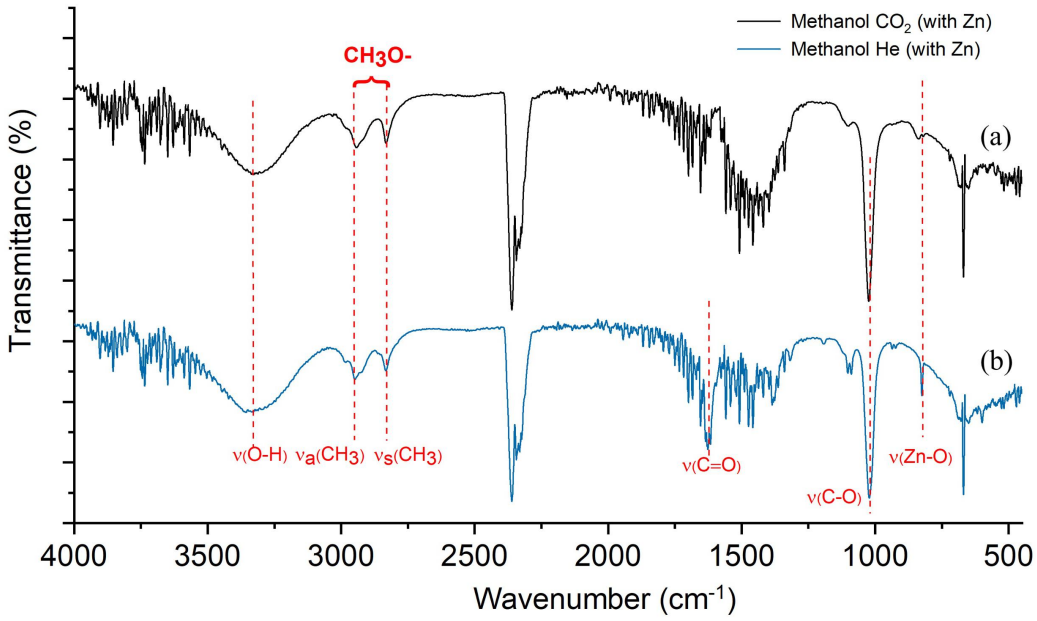

Figure 7-5. The FTIR spectrum of liquid products of reaction of: (a) $CH_3OH + CO_2 + Zn$ (b) $CH_3OH + He + Zn$.

7.3.2 The role of Zn powder in cycloaddition

Figure 7-6 shows the effect of zinc powder on the production yields of propylene carbonate and propylene glycol do not appear to be significant. Specifically, when only CO_2, PO and catalyst participate in the reaction (reaction 1 and 2), there is no change in PO conversion and PC yield, and PG yield is approximately halved to ~0.7 mmol/ml due to the addition of Zn powder. When water (reaction 3 and 4) or PG (reaction 5 and 6) is involved in the reaction,

PG production is increased by 10.1% and 17.2%, respectively, while the PC yield remain unchanged.

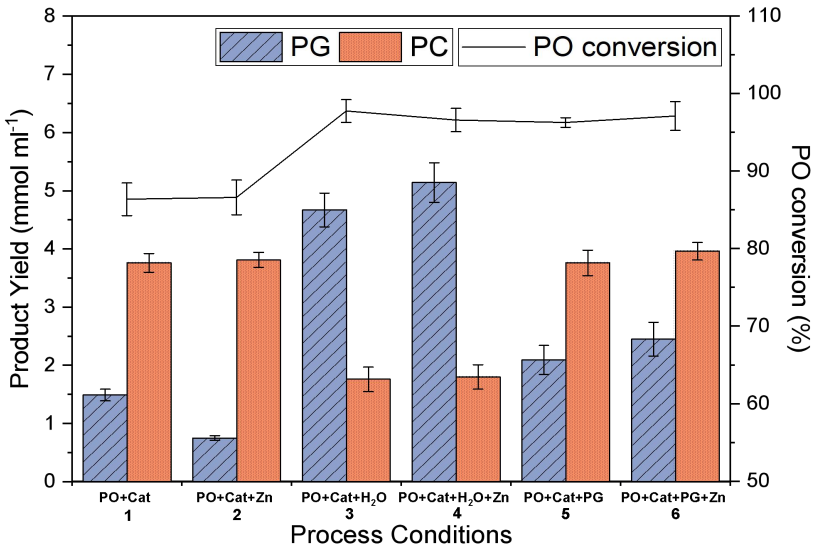

Figure 7-6. Yields of PG and PC in the cycloaddition reaction and the conversion of PO. Reaction conditions: PO (66.66 mmol), H_2O (44.44 mmol, reaction 3 and 4) or PG (11.11 mmol, reaction 5 and 6), catalyst (0.3 g), zinc powder (0.433 g), CO_2 (2 MPa), 160 °C, 5h.

The liquid reaction product was qualitatively analysed using GC-MS equipment. It is known that the by-product of cycloaddition is 1,1-oxybis-2-propanol when zinc powder participates in the reaction. The structure of the by-product is shown in Figure 7-7.

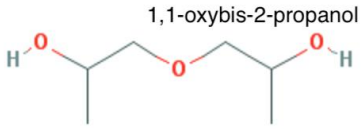

Figure 7-7. Molecular structure of 1,1-oxybis-2-propanol.

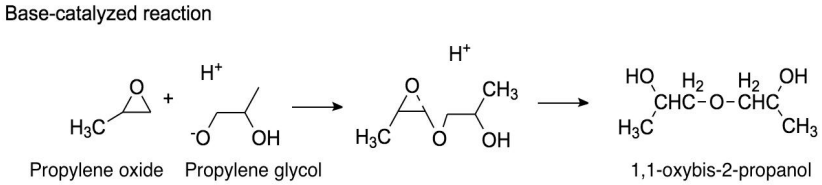

Scheme 7-1. The possible reaction mechanism for the formation of by-product (1,1-oxybis-2-propanol) of cycloaddition in the presence of zinc powder.

Based on previous literature research (Hocking, 2005), the polyol diols can be synthesised from the reaction of propylene oxide and propylene carbonate under the base-catalysed condition. The possible reaction mechanism for the formation of 1,1-oxybis-2-propanol is displayed in Scheme 7-1, which can be used to explain the decrease of PG yield with the addition of zinc powder (reaction 2 and reaction 1).

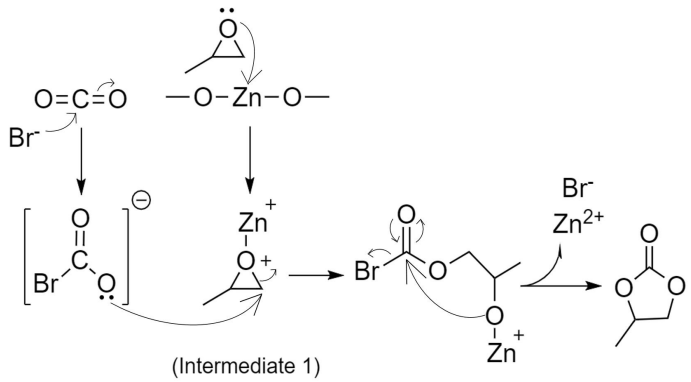

Scheme 7-2. The proposed reaction mechanism for the formation of propylene carbonate *via* cycloaddition reaction in the presence of zinc powder.

Another purpose is to explain the effect of the zinc powder on cycloaddition from the point of reaction mechanism, and the proposed reaction mechanism for the formation of propylene carbonate is presented in Scheme 7-2. Carbon dioxide is a weakly acidic gas which can adsorb or react at acid-base sites on the catalyst surfaces. In previous studies where the mechanism of cycloaddition has been discussed (Scheme 4-1). CO_2 is firstly activated by the attack of Br^- nucleophile (Álvarez *et al.*, 2017) and the attack of the surface Zn^{2+} cation by propylene oxide to form intermediate 1 (Wang, Xie and Deng, 2014). Following this, the reactive CO_2^- species formed on the catalyst surface attacks the less substituted ring carbon atom in intermediate 1 because it is less sterically hindered than the adjacent one. The last step is the formation of propylene carbonate (Martínez-Ferraté *et al.*, 2018). At the same time, Zn^{2+} and Br^- dissociate form the product and dissolve into the reaction solution. Following this mechanism, it is evident that the amount of Zn^{2+} ions from catalyst support is enough for the ring-opening of propylene oxide, and Br^- ions play a more critical role in the cycloaddition reaction. Scheme 7-2 explains that the addition of Zn powder would have little effect on PC formation, in line with the experimental results presented in Figure 7-5.

7.3.3 The role of Zn powder and CO_2 in the transesterification

In this section, the effect of zinc powder and CO_2 (or pressure) on the synthesis of dimethyl carbonate *via* transesterification has been studied, and the experimental results are shown in

Figure 7-8. Reaction 7 is carried out in the absence of zinc powder, which can be used as a baseline case to compare with other reactions.

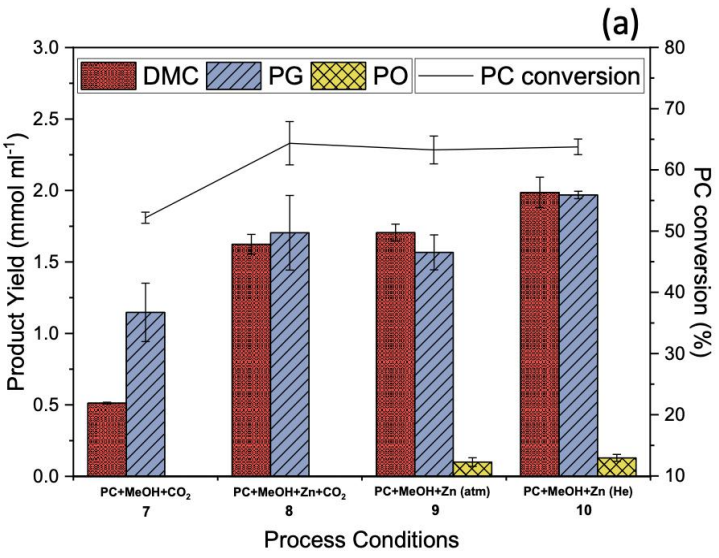

(b)

Reaction No.	TOF (h^{-1})
7	20.8
8	66.0
9	69.3
10	80.8

Figure 7-8. (a) The yield of DMC, PG and PO and the conversion of PC in the transesterification reaction. (b) The activity of catalysts under various reaction conditions. Reaction conditions: 160 °C, 5 h, CO_2 (20 bar, reactions 7 and 8), Helium (20 bar, reaction 10 only), catalyst (K_2CO_3-NaBr-ZnO, 0.3 g), PC (33.3 mmol), methanol (100 mmol) and Zn powder (0.43 g).

It is clear that zinc powder has significant influence on improving the conversion of PC (rises from 52% to 64%) and the yield of DMC (increases from 0.51 mmol ml^{-1} to 1.62 mmol ml^{-1}) in transesterification reaction, with a three-fold increase in the TOF values (from 20.8 h^{-1} to 66.0 h^{-1}). Moreover, in the absence of Zn powder, the yield of PG (1.15 mmol ml^{-1}) is much higher than that of DMC (0.51 mmol ml^{-1}). In contrast, the ratio of PG and DMC formed in the presence of Zn is approximately equal (1.70 mmol $ml^{-1}$and 1.62 mmol ml^{-1}, respectively).

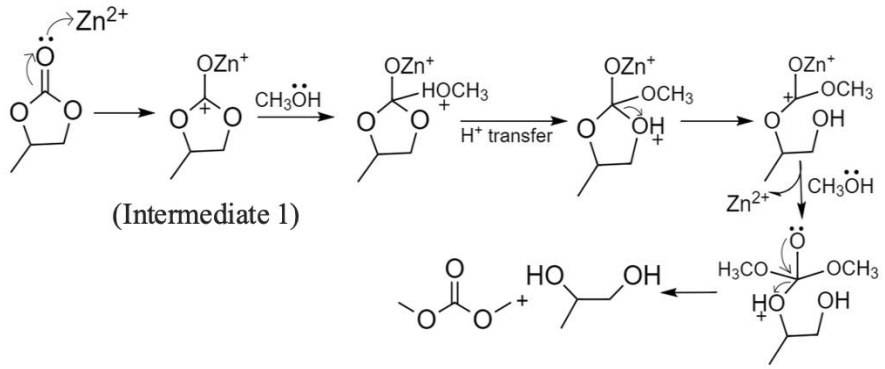

Scheme 7-3. Proposed mechanism for the synthesis of dimethyl carbonate from propylene carbonate and methanol.

Based on the possible mechanism for transesterification, as discussed in Chapter 4 (Scheme 4-3), the formation of Zn^{2+} ions could explain the increase in DMC selectivity with the addition of zinc powder, as shown in Scheme 7-3. Intermediate 1 is formed by the attack of the Zn^{2+} ions by the carbonyl of propylene carbonate, then followed by the attack of carbon atom in intermediate 1 by the methoxy groups of methanol. The transformation of H^+ leads to the formation of dimethyl carbonate and propylene glycol. Moreover, the growth rate of DMC production (217.6%) is higher than that of PG production (47.8%), indicating that there is a new reaction route generating DMC without the formation of PG.

Considering the role of CO_2 or pressure, the yields of DMC and PG and the conversion of PC generated under the helium involved condition (2 MPa, reaction 10) and at ambient pressure (reaction 9) are close to those obtained under 2 MPa CO_2 (reaction 8). However, 0.10 mmol ml $^{-1}$ of propylene oxide is generated when there is no gas injected in the reactor, which is not observed under 2 MPa CO_2 condition. Moreover, a similar result is obtained under 2 MPa He, and 0.13 mmol ml^{-1} PO is formed with the highest TOF of 80.8 h^{-1}. When zinc powder participates in the reactions, the similar yields of DMC and PG are obtained under 2 MPa CO_2, under 2 MPa He. And at atmospheric pressure demonstrates that elevated pressure is not a necessary requirement for transesterification to proceed. By contrast, CO_2 does affect the reverse cycloaddition reaction, as evidenced by the formation of PO in reactions at ambient pressure and under 2 MPa He, but not under CO_2. Therefore, it limits the reverse cycloaddition reaction to form by-product (propylene oxide). The drawback of CO_2 participating in the reaction is that the yield of DMC decreases from 1.97 mmol ml^{-1} to 1.62 mmol ml^{-1} (reaction 10 and 8, respectively), which probably because CO_2 poisons the active sites on the catalyst surface. In other words, carbon dioxide can be adsorbed on the basic active sites, which is quite important for promoting the transesterification reaction (Jiang and Yang, 2004).

7.3.4 $MgO(CH_3)_2$ promoted reactions

As described in section 7.2.2.4, $MgO(CH_3)_2$ involved reactions were conducted to study the role of $-O(CH_3)_2$ group in the DMC synthesis reaction, then further investigated the possible new routes for the synthesis of dimethyl carbonate with the addition of zinc powder. The PO conversion and selectivity of each product of reactions in the presence of zinc powder or $MgO(CH_3)_2$ is shown in Table 7-6.

Table 7-6. Conversion of PO and selectivity of each product of DMC synthesis reactions.

Entry	Catalyst	PO conversion (%)	DMC formed (mmol/ml)	Selectivity (%)				TOF (h^{-1})
				DMC	PC	PG	By-product	
1	K_2CO_3-NaBr-ZnO[a]	95.3	0.53	15.9	25.4	26.4	16.7	24.7
2	K_2CO_3-NaBr-ZnO + Zn	97.0	1.53	36.1	14.9	23.8	26.9	71.2
3	Zn powder	54.5	0.006	0.3	0.3	6.7	92.2	-
4	K_2CO_3-NaBr-ZnO + $Mg(OCH_3)_2$ [b]	99.1	1.64	43.2	33.7	29.1	30.9	85.7
5	K_2CO_3-NaBr-ZnO + $Mg(OCH_3)_2$ + Zn	96.4	1.53	37.6	27.1	26.5	36.8	72.5
6	$Mg(OCH_3)_2$	99.6	1.47	34.4	17.3	22.8	33.9	-

Reaction conditions: 2 MPa CO_2, 160° C, 5h. [a] Methanol (100 mmol), PO (33.33 mmol), catalyst (0.3 g), Zn powder (0.43 g); [b]3.3 mmol $Mg(OCH_3)_2$ and 100 mmol methanol, PO (33.3 mmol), catalyst (0.3 g), Zn powder (0.43 g); The standard deviation is within ±3.5% of the reported selectivity.

The addition of Zn powder to the reaction results in a significant increase in DMC selectivity from 15.9% to 36.1% with a TOF of 24.7 h^{-1} and 71.2 h^{-1}, respectively. This is comparable to result of reactions operated under supercritical CO_2 (Chapter 2.6.1, Table 2-4, the highest DMC selectivity is 52.7% with a TOF of 52.2 h^{-1} using Mg-KCl-ZrO_2 catalyst under 9.5 MPa CO_2) despite the reaction herein being conducted at mild conditions.

Zn powder forms zinc methoxide ($Zn(OCH_3)_2$) *via* reaction with methanol is a possible way to affect the formation of DMC in the transesterification. In order to investigate the new potential routes for the DMC synthesis in the reaction (Entry 2), the effect of adding $Mg(OCH_3)_2$ was investigated. The results show that $Mg(OCH_3)_2$ contributes to the formation of DMC regardless of the presence (selectivity of 43.2%) or absence (selectivity of 34.4%) of the solid catalyst in the reaction. $Mg(OCH_3)_2$ can successfully catalyse both steps in the one-pot reaction system. Besides, With the addition of either Zn powder or $Mg(OCH_3)_2$, the selectivity to by-product in the final liquid product increase (Table 7-6, Entries 2, 3, 4, 5 and 6). The role of $Mg(OCH_3)_2$ in the reaction system is discussed in the next section on account of the characterisation of solid catalyst and solid reaction products. As described in Chapter 4, 1-methoxy-2-propanol and 2-methoxy-1-propanol are formed through the reaction of methanol with PO (Scheme 7-4). The newly formed -OCH_3 groups (zinc powder added condition) or directly introduced -OCH_3 groups ($Mg(OCH_3)_2$ added condition) in the reaction system could be the main reason for the increased selectivity of the by-products. This result proves to a certain extent that $Zn(OCH_3)_2$ is a vital intermediate formed during the reaction process, and it can lead to an increase in the selectivity of DMC.

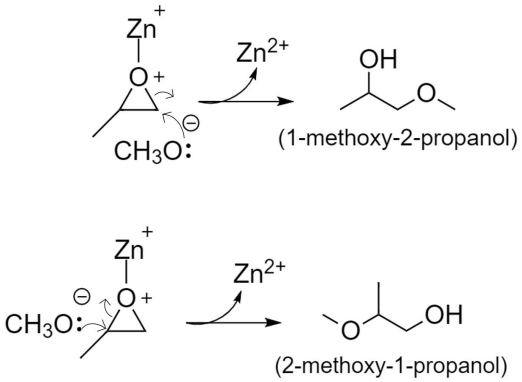

Scheme 7-4. The proposed reaction mechanism for the formation of by-products in the synthesis of DMC from propylene oxide, CO_2 and methanol.

7.3.5 Characterisation of solid-phase catalyst

7.3.5.1 X-ray diffraction (XRD)

XRD was used to investigate the composition of fresh and spent solid catalyst to obtain the mechanism of reaction with $Mg(OCH_3)_2$ (Table 7-6, Entry 4 and 6). The solid products of the reaction with the addition of the catalyst and $Mg(OCH_3)_2$ and the reaction in the presence of only $Mg(OCH_3)_2$ were analysed, and the XRD pattern results are shown in Figure 7-9. The typical peaks of $MgCO_3$ (PDF-ICDD 04-012-1188) are apparent in the solid products obtained under both reaction conditions. Moreover, the remaining peaks presented in Figure 7-9(a) are assigned to $Mg_{0.1}Zn_{0.9}O$ (PDF-ICDD04-019-9591).

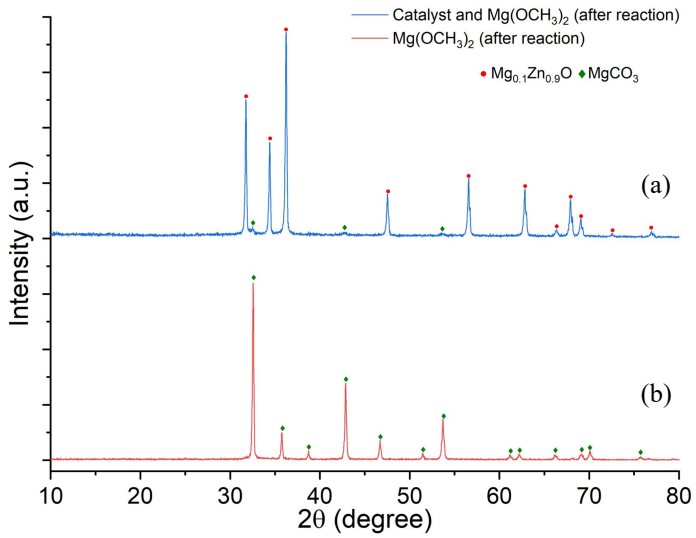

Figure 7-9. The XRD patterns of solid reaction products resulting from (a) reaction with catalyst and $Mg(OCH_3)_2$, and (b) reaction with $Mg(OCH_3)_2$ only.

When only homogeneous catalyst ($Mg(OCH_3)_2$) added in the reaction system, the main component of solid product is $MgCO_3$, which is formed by the reaction of $Mg(OCH_3)_2$, water and CO_2. As shown in Table 7-6, PC is formed in the reaction system, and DMC is generated *via* transesterification. The mechanism of -CH_3O involved transesterification has been discussed in Chapter 4. In this section, the author attempts to investigate the mechanism proposed for the formation of propylene carbonate in the presence of $Mg(OCH_3)_2$ through cycloaddition (Scheme 7-5).

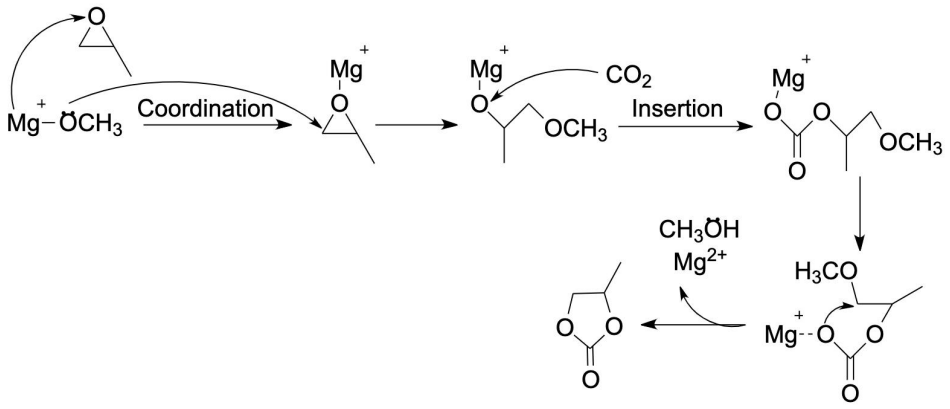

Scheme 7-5. Proposed mechanism for the cycloaddition reaction with $Mg(OCH_3)_2$ (adapted from the reaction mechanism for copolymerization of epoxides and CO_2 using alkoxide catalyst (Bahramian and Dehghani, 2016).

The reaction of propylene oxide and CO_2 is catalysed through coordination–insertion mechanism proposed by Kember *et al. via* homogeneous alkoxide catalyst with *Lewis* acid-base active sites (Kember, Buchard and Williams, 2011). During the coordination step, the propylene oxide molecule is coordinated with the metallic centre (the *Lewis* acid active site) of $Mg(OCH_3)_2$ catalyst, and then attacked by a nucleophilic site (the *Lewis* base site) and ring-opened to form a metal-bound alkoxide (Kember, Buchard and Williams, 2011). The nucleophilic attack can pass through the nucleophilic active site on the metal catalyst (bifunctional homogeneous catalyst) and lead to the activation of alkoxides (Taherimehr and Pescarmona, 2014). CO_2 molecules then insert into metal-oxygen bonds and catalyse the reaction by forming metal carbonates. Finally, propylene carbonate is formed through a ring closure reaction of the metal carbonate.

According to the description of the reaction mechanism of $Mg(OCH_3)_2$ involved reaction in the paper of Eta (Eta *et al.*, 2010), the possible reaction mechanism of $Mg(OCH_3)_2$ and K_2CO_3-NaBr-ZnO participated reaction is shown in Scheme 7-6. Bidentate carbonate is formed as an intermediate, which indicates the migration of -CO_3 species from carbonate magnesium methoxide (CMM) to the surface of the catalyst. The exchange of oxygen atom between the intermediate and catalyst finally results in the formation of DMC. The production of DMC ends up with the release of $Mg_{0.1}Zn_{0.9}O$.

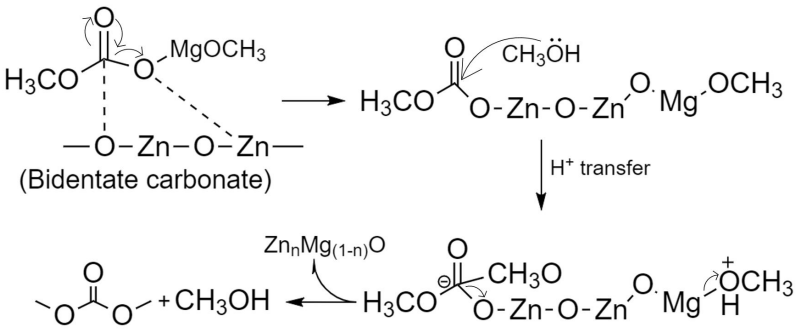

Scheme 7-6. Proposed mechanism for the reaction with $Mg(OCH_3)_2$ when using K_2CO_3-NaBr-ZnO as catalyst (adapted from the reaction mechanism of $Mg(OCH_3)_2$-promoted reactions, proposed by Eta (Eta *et al.*, 2010).

Diffractograms of the fresh and spent catalyst and the mixture of catalyst and zinc powder are shown in Figure 7-10. ZnO (PDF-ICDD 01-081-8838) and Na_2CO_3(PDF-ICDD 04-013-9890) are clearly presented in the fresh catalyst (K_2CO_3-NaBr-ZnO). TG-DTG analysis suggests that Na_2CO_3 is made from the oxidation of polymeride (formed in catalyst preparation) during calcination. The diffractogram of the spent catalyst (Figure 7-10(b)) shows the appearance of $ZnCO_3$ (PDF-ICDD 04-015-6717). This indicates that the stable carbonyl double bond is disrupted because of the reaction of CO_2 with the active site of catalyst.

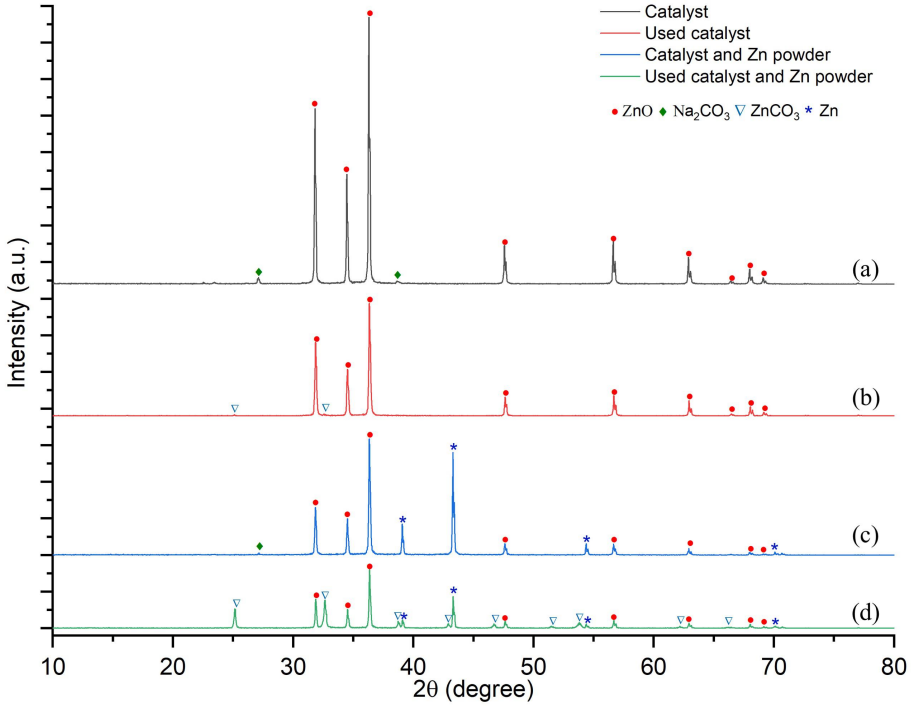

Figure 7-10. The XRD patterns of fresh and spent catalysts: (a) fresh K_2CO_3-NaBr-ZnO; (b) K_2CO_3-NaBr-ZnO after reaction; (c) fresh K_2CO_3-NaBr-ZnO and Zn powder mixture; and (d) K_2CO_3-NaBr-ZnO and Zn powder mixture after the reaction.

The mixture of K_2CO_3-NaBr-ZnO and Zn powder (Figure 7-10(c)) is found to contain Zn (PDF-ICDD 04-014-0235), ZnO (PDF-ICDD 01-083-8004), and Na_2CO_3(PDF-ICDD 04-013-9890). $ZnCO_3$ (PDF-ICDD 04-015-6717) is formed after the reaction, with higher peak intensities *cf.* Figure 7-10(d), indicating that the content or crystallinity of $ZnCO_3$ is increased compared with only catalyst added condition, and more detailed information about the crystallinity of $ZnCO_3$ is shown in Table 7-7. The full width at half maximum (FWHM) of the peak obtained from the XRD pattern is used to calculate the crystallite size of particles by using the Scherrer equation (Patterson, 1939).

Table 7-7. Average crystalline size of particles before and after the reaction. '-' indicates that a crystalline phase is not observed in the diffractogram. '*' indicates that the corresponding peak is present but is beneath the size limit to accurately determine the crystallite size.

	Average crystalline size (nm)		
	ZnO	Zn	$ZnCO_3$
Catalyst	46 ± 6	-	-
Catalyst (after reaction)	43 ± 5	-	*
Mixture of catalyst and Zn	44 ± 4	54 ± 4	-
Mixture of catalyst and Zn (after reaction)	50 ± 3	45 ± 2	42 ± 4

The crystallite size of ZnO remains the same before and after the reaction when only the catalyst is involved (Table 7-7). However, when zinc powder is added, the crystallite size of ZnO increases by approximate 6 nm after the reaction, and the average size of Zn powder decreases from 54 nm to 45 nm. This is consistent with the hypothesis that zinc powder converts to ZnO and $ZnCO_3$ during the reaction. The reaction with $Mg(OCH_3)_2$ yields analogous solid products ($Mg_{0.1}Zn_{0.9}O$ and $MgCO_3$, Figure 7-9) indicating that both Zn and Mg undergo transformation *via* similar reaction mechanisms. Based on the reaction mechanism of $Mg(OCH_3)_2$ (Scheme 7-6), it is possible to speculate on the reaction mechanism of zinc. The Zn powder is converted to $Zn(OCH_3)_2$ and subsequently reacts with CO_2 to form carbonated zinc methoxide (CZM). The carbonate group of CZM is adsorbed on the surface of the catalyst at unsaturated $Zn^{2+}O^{2-}$ *Lewis* acid-base pair sites and the intermediate bidentate carbonate is formed. The exchange of oxygen atoms in the bidentate carbonate with the oxygen atoms on the catalyst surface results in migration of the carbonate species on the catalyst surface, which facilitates the formation of DMC.

7.3.5.2 SEM and SEM-EDX analysis

SEM and EDX analysis provide information regarding the morphology and the elemental composition of the catalyst. Figure 7-11 shows the surface morphology of the solid products from reactions involving $Mg(OCH_3)_2$. Distinctly, the shape of the granular catalyst is unchanged before and after the reaction (Figures 7-11(c) and 7-11(b), respectively). Moreover, it can be seen from the figure, and the cubic product at a larger average size is formed after the reaction in the presence of $Mg(OCH_3)_2$. As $Mg(OCH_3)_2$ acts as a homogeneous catalyst in the reaction, the reaction pathway described by Scheme 7-5 and 7-6 is proposed as the major route for the formation of DMC. Based on XRD analysis (Figure 7-9), agglomerates of $MgCO_3$ are formed during the reaction. An example of this can be seen in Figure 7-11(a).

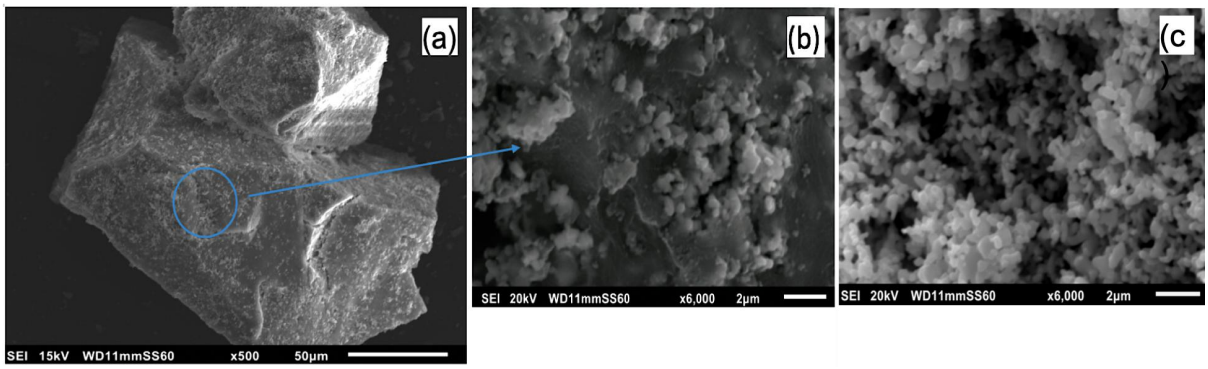

Figure 7-11. SEM images of the solids resulting from reactions involving $Mg(OCH_3)_2$: (a) reaction with K_2CO_3-NaBr-ZnO catalyst, CO_2, propylene oxide, methanol and $Mg(OCH_3)_2$; (b) Higher magnification (6000x) image of identified region in (a); and (c) K_2CO_3-NaBr-ZnO catalyst before reaction (6000x).

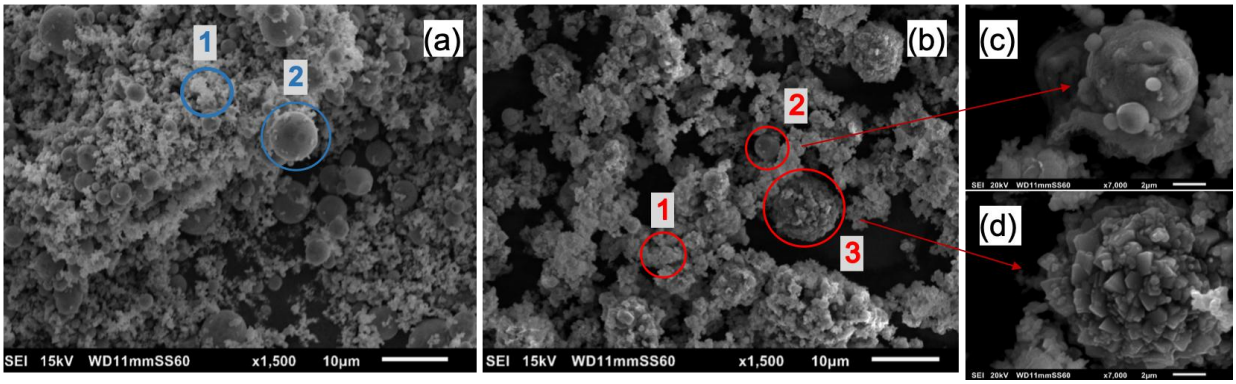

Figure 7-12. Surface morphology of the catalyst and mixtures of catalyst and Zn powder. (a) the mixture of fresh catalyst and Zn (b) mixture of spent catalyst and Zn (c) spent zinc particles with a higher magnification (7000x) (d) new-formed particle with a higher magnification (7000x). 1-catalyst, 2-zinc powder, 3-new formed particle.

SEM analysis of the mixtures of the catalyst with zinc powder is shown in Figure 7-12. Granular morphology (K_2CO_3-NaBr-ZnO catalyst) is observed in the mixture both before and after reaction (Figures 7-12(a) and 7-12(b), respectively), indicative of catalyst stability. However, it is apparent that the surface of the originally spherical particles (zinc powder) becomes rough after reaction as shown in Figure 7-12(c). The catalysts and new formed particles aggregated and formed large particles of ZnO and $ZnCO_3$ (Figure 7-12(d)), Combined with the average crystallite size of Zn determined by XRD (Table 7-7) and ICP-OES results (Tables 7-9(a), 7-9(b)), it can be hypothesised that these morphological changes to zinc powder are because Zn participates in the reaction and remains in the liquid product as Zn^{2+}. From the XRD pattern (Figure 7-10), $ZnCO_3$ is known to be made after the reaction. This agglomerates with K_2CO_3-NaBr-ZnO catalyst particles (Figure 7-12(d)). The new formed $ZnCO_3$ particles with an average crystalline size of 42 nm (Table 7-7) is obtained

through the reaction of $Zn(OH)_2$ (the hydrolysis product of $Zn(OCH_3)_2$) with CO_2 (Fujita *et al.*, 1992). This process is accompanied by the formation of methanol, promoting the transesterification reaction to generate DMC.

EDX spectroscopy was employed to obtain information on the elemental composition of the solid catalyst and to investigate the effect of Zn powder on catalyst stability. Table 7-8 shows that Na^+ can not be detected in the pure catalyst after reaction and the increase of O^{2-} mass content is partly due to the formation of a little amount of $ZnCO_3$. Moreover, the zinc content decreases by 18 mass% as a consequence of the participation of zinc (powder) in the reaction. The Na^+ and O^{2-} content should in principle increase in percentage terms as a result, however, only the O^{2-} content increases. This is ascribed to the formation of $ZnCO_3$. The decrease of Na^+ is due to the leaching of Na^+ from the catalyst surface into the reaction solution. The results of SEM-EDX indicate that the catalytic stability of K_2CO_3-NaBr-ZnO catalyst increased with the addition of zinc powder (Na^+ mass concentration remains stable after reaction). The elemental composition of the solid catalyst by EDX analysis is consistent with ICP-OES analysis results (Table 7-9(a)).

Table 7-8. Elemental composition of the catalyst and the mixture of catalyst and zinc powder by EDX spectroscopy.

Mass (%)	Catalyst		The mixture of catalyst and Zn	
	Before reaction	After reaction	Before reaction	After reaction
Na	10.89	-	8.94	6.89
Zn	55.57	57.67	60.55	42.42
O	33.54	42.33	30.50	50.68

Experimental error is within ±3%.

7.3.5.3 ICP-OES and AAS analysis

ICP-OES and AAS analysis of both solid and liquid samples were carried out in order to determine the quantity of Zn, Na and K ions in solid catalyst and liquid product before and after reaction so as to identify any leaching of potentially catalytic material. Hence, potential homogenous catalytic contribution to the reaction. The results of ICP and AAS analysis of catalysts and liquid product solution are shown in Tables 7-9(a) and 7-9(b), respectively. Both of these indicate that there is little change in the total Zn^{2+} content in the K_2CO_3-NaBr-ZnO after the reaction. It is assumed that ZnO content in the mixture of Zn powder and K_2CO_3-

NaBr-ZnO also remains stable. However, when Zn powder is also present in the reaction mixture, the mass of Zn powder is observed to decrease by ~30% using AAS analysis. This indicates that Zn powder is directly involved in the reaction and is correlated with an increase in DMC selectivity (Table 7-9a, Entry 3, 4). This is consistent with the results of SEM-EDX analysis, where zinc mass was seen to decrease by 18% post-reaction (Table 7-8). Moreover, XRD results (Table 7-7) also indicate that the average crystallite size of zinc powder decreases from 54 nm to 45nm after the reaction. It is therefore hypothesised that a fraction of Zn powder participates in the reaction, converting to solubilised Zn^{2+}.

Table 7-9a. Composition of fresh and used catalysts, (12 *wt.*% K_2CO_3 - 17.5 *wt.*% NaBr-ZnO) as determined by AAS and ICP-OES.

Entry	Sample	AAS analysis (mg/g_{sample})			ICP-OES analysis (mg/g_{sample})		
		Total Zn^{2+}	Zn mass	ZnO mass	Total Zn^{2+}	K mass	Na mass
1	Fresh catalyst	786.5	0	984.7	731.0	4.390	2.900
2	Post-reaction catalyst	793.0	0	992.8	741.0	0.008	0.052
3	Fresh catalyst and Zn mixture	905.7	608.2	372.2	842.0	2.010	1.280
4	Post-reaction catalyst and Zn mixture	725.7	428.3	372.2	675.0	0.473	1.070

Table 7-9b. ICP-OES analysis of Zn, K and Na in the liquid products after the reaction. Catalyst refers to 12 *wt.*% K_2CO_3 - 17.5 *wt.*% NaBr-ZnO.

Entry	Sample	Total Zn (mg/L)	K mass (mg/L)	Na mass (mg/L)
1	Catalyst	11.9	238.0	152.0
2	The mixture of catalyst and Zn powder	1950	197.0	13.0

While Zn powder (if added) shows a significant reduction in mass during the reaction, ICP-OES and AAS data indicate that the ZnO support is in contrast highly stable during the reaction. The active alkali metal ions, K^+ and Na^+, however, leach into the solution and potentially react with the feedstock (Table 7-9(b)). In the absence of Zn powder, K_2CO_3-NaBr-ZnO exhibits a loss of 99.8 *wt.*% K^+ post-reaction, while Na^+ diminishes by 98.2 *wt.*% (Table 7-9(a)). With the addition of Zn powder, the stability of the catalyst increases as convinced by the increased retention of alkali metals in the solid catalyst (Table 7-9(a)). Potassium content decreases 76.5 *wt.*% and Na^+ by only 16 *wt.*%. Two hypotheses are proposed to explain this phenomenon. Firstly, SEM images show that new large particles are formed due to the agglomeration of the catalyst and $ZnCO_3$ (Figure 7-12 (d). This may hinder the interaction between surface Na^+ and K^+ and the reaction solution, thereby hindering

dissolution. A second hypothesis is that Zn^{2+} content in solution increases during the reaction, thereby reducing the demand for K^+ and Na^+ in the DMC formation reaction. According to hard and soft acids and bases (HSAB) theory, first proposed by Pearson, Lewis acids can be classified according to the stability of the metal complexes into (i) hard Lewis acids (Na^+ and K^+); (ii) borderline Lewis acids (Zn^{2+}); (iii) soft Lewis acids (Parr and Pearson, 1983). Generally, hard acids preferentially bind to hard bases to give ionic complexes, whereas soft acids bind to soft bases to yield covalent complexes. The oxygen atom of the carbonyl group in propylene carbonate displays the properties of a hard Lewis base (Laurence and Gal, 2009). The reactive polar covalent complex may, therefore, form when the oxygen of the C=O group attacks the Zn^{2+} ion in transesterification reaction, contributing to the formation of DMC. Therefore, Zn^{2+} ions are more reactive to C=O of propylene carbonate than Na^+ and K^+ ions.

7.3.6 Reaction mechanism

Zn powder was originally proposed as a dehydrating agent in DMC synthesis in order to reduce the production of propylene glycol from propylene oxide hydrolysis, thereby facilitating transesterification to the final product. However, herein (Section 7.3.1), it was shown that selectivity to PG does not decrease with the addition of Zn powder. However, selectivity to DMC approximately triples from 15.9% to 36.1%. Characterisation (Section 7.3.5) reveals that Zn powder may participate in the reaction, forming zinc methoxide ($Zn(OCH_3)_2$). This species may act as a homogeneous catalyst for the conversion of propylene oxide to propylene carbonate through the coordination-insertion mechanism and for the transformation of propylene carbonate to dimethyl carbonate *via* transesterification. It can, therefore, be concluded that Zn powder acts as a promoter rather than only as a dehydrating agent in the reaction.

As shown in Table 7-6 (Entry 2), the selectivity of DMC is higher than that of PG, which means dimethyl carbonate in the presence of zinc may, therefore, be generated through two proposed reactions (Scheme 7-7). One is the synthesis of DMC *via* the reaction of intermediate (carbonated zinc methoxide) and methoxy group ($-OCH_3$) without the formation of PG. The other one is the conversion of PC to DMC and PG through transesterification with a higher catalytic efficiency ($TOF_{(catalyst)}$=20.8 h^{-1} , $TOF_{(catalyst+zinc)}$= 66.0 h^{-1}, Figure 7.7). A more detailed description of the two reaction routes is as follows:

Route 1: reaction of Zn with CO_2 and methanol to form carbonated zinc methoxide (CZM). The carbonate group of CZM then reacts with the unsaturated $Zn^{2+}O^{2-}$ Lewis acid-base pair on the catalyst surface and the intermediate bidentate carbonate is formed, the formation of which is supported by the presence of $Mg_{0.1}Zn_{0.9}O$ in XRD analysis (section 7.3.5.1, Figure 7-9). The exchange of oxygen atoms in the bidentate carbonate with the oxygen atoms on the catalyst surface results in the migration of carbonate species on the catalyst surface, thereby facilitating the formation of DMC, with the release of ZnO polymeride.

Route 2: the second proposed reaction pathway involves the formation of additional methoxy groups, which can attack the carbon atom of C=O in the transesterification reaction. As observed by XRD data (Table 7-7) and SEM images (Figure 7-12) of the spent catalyst and zinc powder, $ZnCO_3$ with an average particle size of 42 nm is formed during the reaction. This is accompanied by the release of $-CH_3O$ as a consequence of the reaction of zinc methoxide with CO_2 and H_2O. Combining these two reaction pathways, an overall mechanism is presented in Scheme 7-7.

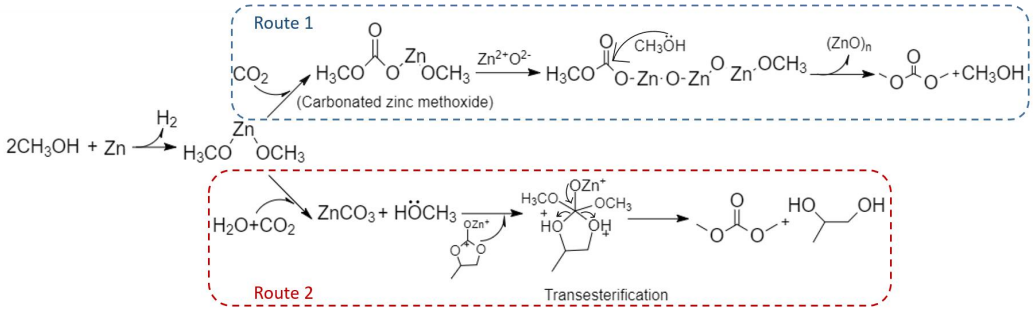

Scheme 7-7. Proposed new mechanism for DMC synthesis with the addition of Zn powder.

It is proposed that at higher pressures of carbon dioxide than those studied herein, $Zn(OCH_3)_2$ may directly catalyse carbon-carbon bond formation between methanol and CO_2, allowing the direct synthesis of DMC under mild conditions without PO. This represents a promising avenue for further study.

7.4 Conclusions

12 *wt.*%K_2CO_3-17.5 *wt.*%NaBr-ZnO has been employed as a catalyst in the synthesis of dimethyl carbonate from methanol, propylene oxide and carbon dioxide. The main limitation for increasing DMC selectivity is the high yield of propylene glycol due to the hydrolysis of propylene oxide. The role of Zn powder in this system is a promoter rather than a dehydrating

agent, which increases the selectivity to DMC. Zn not only promotes DMC formation through new reaction routes (Scheme 7-7) and but also could increase the stability of the catalyst (see ICP-OES results, Table 7-9 (a) and (b)). Crucial intermediate products, zinc methoxide and carbonate zinc methoxide, are formed during the reaction and promote the migration of carbonate species on the catalyst surface yielding more DMC. Zinc powder has negligible effect on the cycloaddition reaction but has a dramatic influence on the transesterification reaction resulting in increased DMC production through the formation of methoxide species. Furthermore, high pressure is not a prerequisite for the transesterification reaction. CO_2 has been verified to inhibit the reverse cycloaddition reaction to form PO. It is recommended to conduct future investigation into the effects of different active species on the reaction steps in DMC synthesis and the reuasbility of catalyst. Moreover, the proposed mechanism is only based on the experimental observation and detailed analysis is needed to support the proposed mechanism. For instance, in order to identify if zinc methoxide is a necessary reaction intermediate, ^{13}C labelled zinc methoxide and/or ^{13}C labelled magnesium methoxide can be employed in the experiment to evaluate the proposed reaction pathways.

CHAPTER 8

CONCLUSIONS AND RECOMMENDATIONS FOR FUTURE WORK

Chapter 8 Conclusions and recommendations for future work

In this work, active heterogeneous catalysts have been successfully applied for the one-pot synthesis of DMC under mild reaction condition. The modification of catalysts and reaction conditions has also been studied to improve the selectivity of DMC. The proposed reaction mechanisms are presented according to the results of the experiment and the characterisation of catalysts. In this chapter, the major conclusions obtained in the experimental studies and catalyst characterisation are drawn in Section 8.1. Based on the current studies, the suggestion for further research is presented in Section 8.2.

8.1 Conclusions

Alkali halide-based catalysts have been prepared and extensively studied for the one-pot synthesis of DMC. In this study, the effect of alkali halide species, reaction time, the type and loading of alkali supported on the carrier and the dehydrating agents were discussed.

8.1.1 Preparation of the catalyst

- Influence of alkali halide species

The catalysts with various alkali halide species (KCl, KBr, NaCl and NaBr) were screened in the one-pot synthesis of DMC from methanol, PO and CO_2 under 2 MPa pressure condition. The catalyst containing Br^- ions shows a higher catalytic ability to promote the formation of PC (~33.9%) by cycloaddition, at the same time, lower by-products selectivity (~13.2%) is obtained. The experiment result is in agreement with the ability of halides ions to donate electrons ($Br^- > Cl^-$). The proposed reaction mechanisms for cycloaddition, transesterification, by-products formation and PO hydrolysis using NaBr-ZnO as the catalyst are discussed. Additionally, the effect of reaction time was studied as well. 5 hours is a more appropriate reaction time because both the cycloaddition and transesterification have reached the equilibrium.

- Influence of alkali species

The selectivity of DMC was improved by supporting different kinds of alkali (NaOH, K_2CO_3 and Na_2CO_3) on the NaBr-ZnO catalyst. DMC selectivity is used as an indicator to evaluate the catalytic performance of the catalyst, and the sequence of the catalytic ability of the modified catalysts is K_2CO_3-NaBr-ZnO (15.9%) > Na_2CO_3-NaBr-ZnO (10.2%) > NaOH-

NaBr-ZnO (8.5%). The supported alkali leads to the rises of the number of strong basic sites on the catalyst surface, which promote the formation of DMC *via* transesterification. Finally, the catalytic stability of the K_2CO_3-NaBr-ZnO is determined, the morphological structure of the catalyst remains stable after reaction; however, the ICP-OES analysis results show that 99.8 *wt.*% of K^+ and 98.2 *wt.*% of Na^+ is leached into the reaction solution during the reaction process. According to the SEM images of catalyst before and after reaction, the physical structure of catalyst supporter remain stable. In the following research, it is necessary to find a novel method to optimise the chemical stability of the catalyst to reduce the percolation of active components on the catalyst surface into the reaction solution during the reaction process, so as to improve the reusability of the catalyst.

- Influence of alkali loadings

The catalysts with various K_2CO_3 loadings (8 *wt.*%, 10 *wt.*%, 12 *wt.*%, 15 *wt.*% and 18 *wt.*%) were prepared and screened in the DMC synthesis reactions. The highest DMC selectivity (15.9%) is obtained when using 12 *wt.*% K_2CO_3-NaBr-ZnO as the catalyst. The selectivity to DMC is limited by the formation of PG (26.4%) as a by-product *via* hydrolysis of PO by water in the reaction. Excessive K_2CO_3 loadings (>18 *wt*%) on the carrier results in a significant increase in the selectivity of PG (47.9%) and by-products (43.9%).

8.1.2 Modification of reaction condition

Selectivity to DMC can be increased by reducing the rate of production of PG through removing water from the system. Both solid and liquid dehydrating agents can be used to remove water from the process.

- Influence of 3Å molecular sieves and acetonitrile

Both the effect of physical drying agents (3Å molecular sieve) and chemical dehydrating agent (acetonitrile) on inhibiting PO hydrolysis and improving DMC selectivity were studied. The main conclusions drawn are illustrated as follows:

1) The selectivity of PC increases significantly because of the inhabitation of the PO hydrolysis when using both dehydrating agents. However, the effect on improving DMC selectivity is not apparent.

2) 3Å molecular sieve can give a better dehydration efficiency in the short-term reaction (reaction time ≤ 3h), its unstable structure and deactivation of molecular sieves under reaction conditions (160 °C and 4.5 MPa) result in a lower DMC production and TOF value.

3) Acetonitrile is a better-performed dehydrating agent; however, the main drawback is the formation of hydrolysates (NH_3 and urea) in the reaction system. The reaction between NH_3 and DMC leads to the low selectivity of DMC in the result.

4) With the addition of acetonitrile, the efficiency of CO_2 utilisation can be improved *via* the conversion of PG to PC in the reaction system.

5) An appropriate amount of water in the reaction system could facilitate the cycloaddition of propylene oxide and CO_2 *via* the formation of Zn-OH group on the catalyst surface, which is conducive to catalyse the ring-opening of propylene oxide by a nucleophilic attack.

- Influence of Zn powder

K_2CO_3-NaBr-ZnO has been employed as a catalyst in the synthesis of dimethyl carbonate from methanol, propylene oxide and carbon dioxide. The addition of Zn powder to this system increases the selectivity to DMC (~36.1%). Table 8-1 offers a comparison of DMC selectivity achieved in this work and under "harsher" conditions. It is clear that relatively high DMC selectivity and TOF value are obtained in this work using K_2CO_3-NaBr-ZnO as the catalyst and Zn as the promoter at 2.0 MPa (*RT*) pressure. It can be considered that this research provides the possibility of "greener chemistry", because to a certain extent low-pressure reaction condition requires lower energy input compared with high-pressure condition and reduces the safety hazards caused by high-pressure reaction.

Table 8-1. The comparison of DMC selectivity between this work and former studies, and CO_2 pressures employed.

Entry	Catalyst	DMC selectivity (%)	TOF (h^{-1})	CO_2 pressure (*RT*, MPa)	References
1	K_2CO_3-NaBr-ZnO[a]	15.9	24.7	2.0	/
2	K_2CO_3-NaBr-ZnO + Zn	36.1	71.2	2.0	/
3	KOH-KI-ZnO	58.0	8.4	16.5	(Chang *et a*l., 2004)
4	Mg-KCl-ZrO_2	52.7	52.2	9.5	(Eta *et al*., 2010)
5	KOH-4A	16.8	41.9	3.0	(Li *et al*., 2005)
6	KOH-β-zeolite	23.3	-	2.0	(Xu *et al*., 2013)

Zn powder both promotes DMC formation through new reaction routes (Scheme 7-7, Route 1) and increases the stability of the catalyst. Crucial intermediate products, zinc methoxide and carbonate zinc methoxide, are formed during the reaction and promote the migration of carbonate species on the catalyst surface yielding more DMC. Zinc powder has little effect on the cycloaddition reaction but has a dramatic influence on the transesterification reaction resulting in increased DMC production through the formation of methoxide species. Furthermore, high pressure is not a prerequisite for the transesterification reaction. CO_2 was found to inhibit the reverse cycloaddition reaction to form PO.

8.2 Recommendations for future work

The acid-base sites on the catalyst surface catalysed the synthesis of DMC. The improvement of DMC selectivity can be achieved by increasing the strength of the basic sites. In addition, further research work is needed to increase the feasibility of this study. This section mainly introduces analytical methods to supplement the description of catalyst physical properties and recommendations for future research work.

8.2.1 Characterisation of the catalysts

- Analysis of the surface area

The surface area of the catalysts with various K_2CO_3 loadings was not characterised. In order to have a better understanding about the effect of K_2CO_3 loadings on the activity of the catalyst, Ultra-Small-Angle X-Ray Scattering (USAXS) was employed to obtain the information about the size distribution of catalyst particles in this study (Figure 8-1).

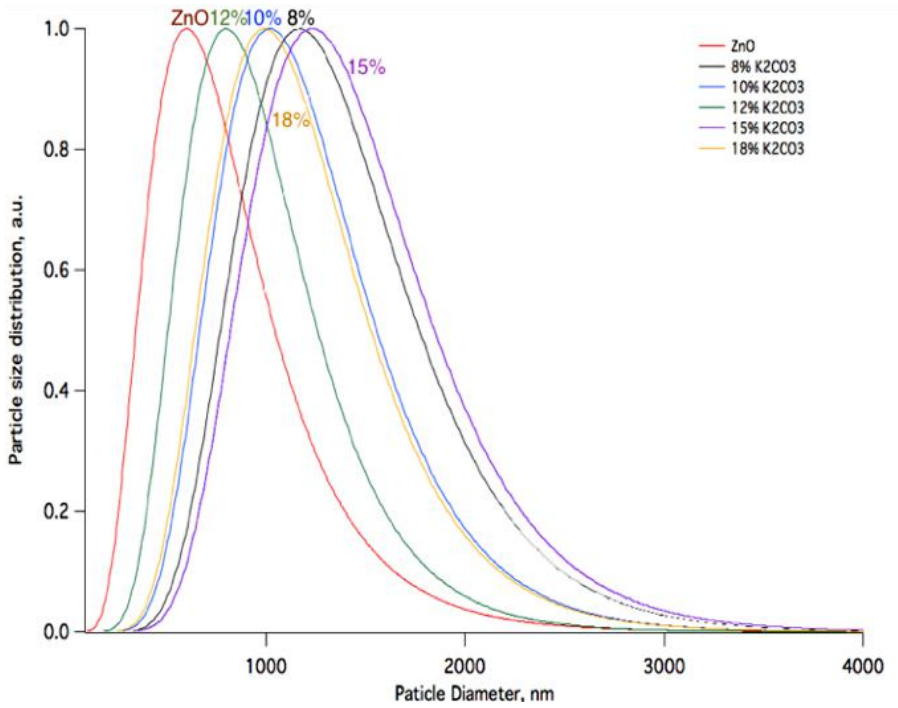

Figure 8-1. USAXS profile of catalysts (K_2CO_3-17.5 *wt.*%-ZnO) with various K_2CO_3 loadings.

The particle size distribution of catalyst is closely related to the effective surface area of the catalyst. N_2 adsorption isotherm analysis will be performed in order to explain better the trend of catalyst particle size distribution and surface area with the increase of K_2CO_3 loadings, so as to explain the relationship between the K_2CO_3 loadings and catalyst activity. The equipment used is described in section 3.2.6.

- Analysis of the basic intensity

The result of CO_2-TPD analysis indicates the strength and the concentration of basic sites on the catalyst surface. As discussed in Chapter 5, strong basic sites favour the formation of DMC *via* transesterification, and too basic condition may lead to the production of by-products (1-methoxy-2-propanol). It is necessary to obtain the intensity information of the basic sites on the catalyst surface, which can provide a basis for improving the DMC selectivity and controlling the by-products selectivity by altering the basic property of catalyst. The equipment and operating methods for CO_2-TPD analysis are described in detail in section 3.2.5.

8.2.2 Directions for future study

- Study the reusability of the catalyst and the recyclability of the Zn powder.

The catalytic stability of K_2CO_3-NaBr-ZnO is increased with the addition of Zn powder. Specifically, the content of the active components (Na^+ and K^+ ions) supported on the catalyst surface leaching into the reaction solution during the reaction is reduced. However, the main difficulty in testing the reusability of the catalyst is to separate the two solid materials after the reaction. The spent catalyst needs to be activated under high-temperature calcination (700 °C) before it can be used again, and the melting point of zinc powder is about 420 °C. From the perspective of industrial and economic applications, it is necessary to find a suitable reaction system that allows the catalyst and zinc powder to participate in the reaction at the same time but not mix.

- Direct synthesis of DMC without the addition of propylene oxide.

It is proposed that at higher pressures of carbon dioxide than those studied herein, $Zn(OCH_3)_2$ may directly catalyse carbon-carbon bond formation between methanol and CO_2, allowing the direct synthesis of DMC under mild conditions without PO. This conclusion represents a promising avenue for further study. The main problem with the direct synthesis of DMC route is the low translation rate due to the limitation of reaction equilibrium. Adding an appropriate amount of Zn powder is a possible method to improve the selectivity of DMC *via* the direct synthesis route.

- Gas analysis of the reaction using acetonitrile as the dehydrating agent.

It was introduced in Chapter 6 that the reaction between acetonitrile and water may generate ammonia gas, which reacts with the generated DMC in the reaction system. This assumption explains the result that the addition of acetonitrile does not significantly improve the DMC selectivity. In order to better verify this statement, the composition of gas-phase products generated in the reaction can be obtained by online GC-MS analysis.

- The modification of reaction conditions.

In this study, the effect of reaction time on the selectivity of various products are mainly introduced. In addition, other factors such as reaction temperature, Methanol/PO molar ratio, and catalyst addition amount need to be optimised in order to improve the selectivity of DMC.

REFERENCES

Ahmad, F. (2016) 'CO_2 Utilization: A Look Ahead', *carbon capture journal*, [online] (54), pp.11-13. Available at: http://b59d35675b007f59b1d70196d366fe21fa4c957de1aaf4b3fb16.r82.cf1.rackcdn.com/CCJ54webdge4et.pdf [Accessed 20 Oct. 2019].

Aresta, M., Dibenedetto, A. and Angelini, A. (2013) 'The changing paradigm in CO_2 utilization', *Journal of CO_2 Utilization*, 3(4), pp. 65-73. doi: 10.1016/j.jcou.2013.08.001.

Adamska, L., Lin, Y., Ross, A., Batzill, M. and Oleynik, I. (2012) 'Atomic and electronic structure of simple metal/graphene and complex metal/graphene/metal interfaces', *Physical Review B*, 85(19).

Aouissi, A., Al-Othman, Z. A., & Al-Amro, A. (2010) 'Gas-phase synthesis of dimethyl carbonate from methanol and carbon dioxide over $Co_{1.5}PW_{12}O_{40}$ keggin-type heteropolyanion', *International journal of molecular sciences*, *11*(4), pp. 1343-1351.

Aresta, M., Dibenedetto, A., Pastore, C., Angelini, A., Aresta, B., & Pápai, I. (2010) 'Influence of Al_2O_3 on the performance of CeO_2 used as catalyst in the direct carboxylation of methanol to dimethyl carbonate and the elucidation of the reaction mechanism', *Journal of Catalysis*, 269(1), pp. 44-52.

Abdullah, A., Mohammad, A. and Maik, F. (2016) *Lignin in Polymer Composites*. William Andrew, pp.153-165.

Adeleye, Adegboyega Isaac et al., (2014) 'Efficient and Greener Synthesis of Propylene Carbonate from Carbon Dioxide and Propylene Oxide', *Industrial & engineering chemistry research*, 53(49), pp.18647–18657.

Amelinckx, S., Van Dyck, D., Van Landuyt, J. and Van Tendeloo, G. (2008). *Electron Microscopy*. Weinheim: Wiley-VCH.

Álvarez, A., Borges, M., Corral-Pérez, J., Olcina, J., Hu, L., Cornu, D., Huang, R., Stoian, D. and Urakawa, A. (2017) 'CO_2 Activation over Catalytic Surfaces,' *ChemPhysChem*, 18(22), pp.3135-3141.

Anbazhagan, M., Kumaran, G. and Sasidharan, M. (2010) 'ChemInform Abstract: Selective Conversion of Nitroalcohols into Nitroolefins over Zeolite under Heterogeneous Conditions', *ChemInform*, 29(3).

Balat, M. (2007) 'Production of biodiesel from vegetable oils: A survey', *Energy Sources, Part A: Recovery, Utilization and Environmental Effects*, 29(10), pp. 895–913. doi: 10.1080/00908310500283359.

Bahramian, B. and Dehghani, F. (2016) 'New Catalytic Systems for Fixation of Carbon Dioxide into Valuable Poly(Alkylene Carbonates)', in *Advanced Catalytic Materials - Photocatalysis and Other Current Trends*. doi: 10.5772/61969

Bell, G. *et al.* (1995) 'Biocatalyst behaviour in low-water systems', *Trends in Biotechnology*, 13(11), pp. 468-473. doi: 10.1016/S0167-7799(00)89004-6.

Brander, M., & Davis, G. (2012) 'Greenhouse gases, CO_2, CO_2e, and carbon: What do all these terms mean', *Econometrica, White Papers*.

Bhanage, B. M. *et al.* (2003) 'Synthesis of dimethyl carbonate and glycols from carbon dioxide, epoxides and methanol using heterogeneous Mg containing smectite catalysts: Effect of reaction variables on activity and selectivity performance', *Green Chemistry*, 5, pp.71-75. doi: 10.1039/b207750g.

Boudart, M. (1969) 'Catalysis by Supported Metals', *Advances in Catalysis*. doi: 10.1016/S0360-0564(08)60271-0.

Boreskov, G.K. (1986) *Geterogennyi kataliz (Heterogeneous Catalysis*), Moscow: Nauka, pp. 304.

Busby, J. A., & Trimm, D. L. (1979) 'Initial Activation of Platinum-Rhodium Gauzes for the Catalytic Oxidation of Ammonia', pp. *439-449*.

Bhanage, B., Fujita, S., He, Y., Ikushima, Y., Shirai, M., Torii, K. and Arai, M. (2002). *Catalysis Letters*, 83(3/4), pp.137-141.

Brunauer, S., Emmett, P. and Teller, E. (1938) 'Adsorption of Gases in Multimolecular Layers. *Journal of the American Chemical Society*', 60(2), pp.309-319.

Barrett, E., Joyner, L. and Halenda, P. (1951) 'The Determination of Pore Volume and Area Distributions in Porous Substances. I. Computations from Nitrogen Isotherms', *Journal of the American Chemical Society*, 73(1), pp.373-380.

Bavykina, A. V., Goesten, M. G., Kapteijn, F., Makkee, M., & Gascon, J. (2015) 'Efficient production of hydrogen from formic acid using a Covalent Triazine Framework supported molecular catalyst', *ChemSusChem*, *8*(5), pp. 809–812. http://doi.org/10.1002/cssc.201403173

Baj, S., Krawczyk, T., Jasiak, K., & Siewniak, A. (2014) 'Applied Catalysis A: General Catalytic coupling of epoxides and CO_2 to cyclic carbonates by carbon nanotube-supported quaternary ammonium salts', *Applied Catalysis A, General,*488, pp. 96–102. http://doi.org/10.1016/j.apcata.2014.09.034

Bobadilla, L. F., Lima, S. and Urakawa, A. (2015) Cycloaddition of CO_2 and Epoxides over Reusable Solid Catalysts, in Advanced Catalytic Materials (eds A. Tiwari and S. Titinchi), *John Wiley & Sons, Inc., Hoboken*, NJ, USA.

Bansode, A. and Urakawa, A. (2014b) 'Towards full one-pass conversion of carbon dioxide to methanol and methanol-derived products', *Journal of Catalysis*, 309, pp.66-70.

Bhanage, B., Fujita, S., Ikushima, Y. and Arai, M. (2001) 'Synthesis of dimethyl carbonate and glycols from carbon dioxide, epoxides, and methanol using heterogeneous basic metal oxide catalysts with high activity and selectivity', *Applied Catalysis A: General*, 219(1-2), pp.259-266.

Bansode, A. and Urakawa, A. (2014) 'Continuous DMC synthesis from CO_2 and methanol over a CeO_2 catalyst in a fixed bed reactor in the presence of a dehydrating agent', *ACS Catalysis*, 4(11), pp. 3877-3880. doi: 10.1021/cs501221q.

Chen, E. and Marks, T. (2000) 'Cocatalysts for Metal-Catalyzed Olefin Polymerization: Activators, Activation Processes, and Structure−Activity Relationships', *Chemical Reviews*, 100(4), pp.1391-1434.

Carlson, G.A. (2002). Experimental Errors and Uncertainty. Splung.com physics, [online], Available at: www.ece.rochester.edu/courses/ECE111/error_uncertainty.pdf. [Accessed 20 Oct. 2019].

Choi, J. C. *et al.* (2002) 'Selective and high yield synthesis of dimethyl carbonate directly from carbon dioxide and methanol', *Green Chemistry*, 4, pp. 230-234. doi: 10.1039/b200623p.

Chang, Y., Jiang, T., Han, B., Liu, Z., Wu, W., Gao, L., Huang, J. (2004) 'One-pot synthesis of dimethyl carbonate and glycols from supercritical CO_2, ethylene oxide or propylene oxide, and methanol', *Applied Catalysis A: General*, 263(2), pp. 179–186.

Chen, L., Wang, S., Zhou, J., Shen, Y., Zhao, Y., & Ma, X. (2014) 'Dimethyl carbonate synthesis from carbon dioxide and methanol over CeO_2 versus over ZrO_2: comparison of mechanisms', *RSC Advances*, 4(59), pp. 30968-30975.

Cuéllar-Franca, R. M. and Azapagic, A. (2015) 'Carbon capture, storage and utilisation technologies: A critical analysis and comparison of their life cycle environmental impacts', *Journal of CO_2 Utilization*,9, pp.82-102. doi: 10.1016/j.jcou.2014.12.001.

Centi, G. and Perathoner, S. (2014). *Green carbon dioxide*. 1st ed. Hoboken, New Jersey: Wiley.

Cui, H., Wang, T., Wang, F., Gu, C., Wang, P., & Dai, Y. (2003) 'One-Pot Synthesis of Dimethyl Carbonate Using Ethylene Oxide, Methanol, and Carbon Dioxide under

Supercritical Conditions', *Industrial & Engineering Chemistry Research*, *42*(17), pp. 3865–3870. http://doi.org/10.1021/ie021014b

Coker, A. (2012). *Dimethyl carbonate. Chemsystems Report Abstract. PERP 2012S12*. London.

Davis, S. *et al,*. (2018) 'Net-zero emissions energy systems', *Science*, 360(6396), pp. 9793.

Dean, C., Dugwell, D. and Fennell, P. (2011) 'Investigation into potential synergy between power generation, cement manufacture and CO_2 abatement using the calcium looping cycle', *Energy & Environmental Science*, 4(6), pp. 2050.

De, Chunyan, et al. (2009) 'One-pot synthesis of dimethyl carbonate from methanol, propylene oxide and carbon dioxide over supported choline hydroxide/MgO', *Catalysis letters*, 128(3-4), pp.459-464.

Dowson, G. R. M. and Styring, P. (2017) 'Demonstration of CO_2 conversion to synthetic transport fuel at flue gas concentrations', *Frontiers in Energy Research,* 5(26). doi: 10.3389/fenrg.2017.00026.

Deutschmann, O. *et al.* (2009) 'Heterogeneous Catalysis and Solid Catalysts', in *Ullmann's Encyclopedia of Industrial Chemistry*. doi: 10.1002/14356007.a05_313.pub2.

Eta, V., Mäki-Arvela, P., Leino, A., Kordás, K., Salmi, T., Murzin, D. and Mikkola, J. (2010) 'Synthesis of Dimethyl Carbonate from Methanol and Carbon Dioxide: Circumventing Thermodynamic Limitations', *Industrial & Engineering Chemistry Research*, 49(20), pp.9609-9617.

F. Buonomo, D. Sanfilippo, F. Trifiro in G. Ertl, H. Knozinger, J. Weitkamp (eds.) (1997) *Handbook of Heterogeneous Catalysis*, Vol. 5, Wiley-VCH, pp. 2140.

Filonenko, G., Smykowski, D., Szyja, B., Li, G., Szczygieł, J., Hensen, E. and Pidko, E. (2015) 'Catalytic Hydrogenation of CO_2 to Formates by a Lutidine-Derived Ru–CNC Pincer Complex: Theoretical Insight into the Unrealized Potential', *ACS Catalysis*, 5(2), pp.1145-1154.

Fiorani, G., Perosa, A. and Selva, M. (2018) 'Dimethyl carbonate: A versatile reagent for a sustainable valorization of renewables', *Green Chemistry*, 20, pp. 288-322. doi: 10.1039/c7gc02118f.

F. Aricò and P. Tundo. (2010) 'Dimethyl carbonate: a modern green reagent and solvent', *Russian Chemical Reviews,* 79 (6), pp.479 – 489.

Fontes, N. *et al.* (2001) 'Zeolite molecular sieves have dramatic acid-base effects on enzymes in nonaqueous media', *Biotechnology and Bioengineering*, pp. 296-305. doi:

10.1002/bit.10138.

Gabruś, E. *et al.* (2015) 'Experimental studies on 3A and 4A zeolite molecular sieves regeneration in TSA process: Aliphatic alcohols dewatering-water desorption', *Chemical Engineering Journal*,259, pp. 232-242. doi: 10.1016/j.cej.2014.07.108.

Grego, S., Aricoì, F. and Tundo, P. (2013) 'Highly selective phosgene-free carbamoylation of aniline by dimethyl carbonate under continuous-flow conditions', *Organic Process Research and Development*, 17, pp. 679-683. doi: 10.1021/op4000048.

G.R. Chatwal, S.K. Anand; Instrumental Methods of Chemical Analysis, 5 Mumbai, 2007.

Groenewoud, W. (2001). *Characterisation of polymers by thermal analysis*. Amsterdam: Elsevier, pp.61-76.

Goldstein, J., Newbury, D., Michael, J., Ritchie, N., Scott, J. and Joy, D. (2018). *Scanning electron microscopy and x-ray microanalysis*. New York, NY: Springer.

Harbord, N. H. (1974) 'AMMONIA OXIDATION CATALYSTS - DEPOSITS ON SOME RHODIUM-PLATINUM GAUZES.', *Platinum Metals Review*.

Han, S. (2019) 'Structure and dynamics in the lithium solvation shell of nonaqueous electrolytes', *Scientific Reports*, 9, pp. 5555. doi: 10.1038/s41598-019-42050-y.

Honda, M., Tamura, M., Nakagawa, Y., & Tomishige, K. (2014) 'Catalysis Science & Technology Catalytic CO_2 conversion to organic carbonates with alcohols in combination with', (I), 2830–2845. http://doi.org/10.1039/c4cy00557k

Hu, B., Frueh, S., Garces, H. F., Zhang, L., Aindow, M., Brooks, C., Suib, S. L. (2013) 'Applied Catalysis B: Environmental Selective hydrogenation of CO_2 and CO to useful light olefins over octahedral molecular sieve manganese oxide supported iron catalysts', *Applied Catalysis B, Environmental,*132-133, pp. 54–61. http://doi.org/10.1016/j.apcatb.2012.11.003

Hu, B. and Suib, S. L. (2014) 'Synthesis of Useful Compounds from CO_2, in Green Carbon Dioxide: Advances in CO Utilization (eds G. Centi and S. Perathoner)', John Wiley & Sons, Inc., Hoboken, NJ, USA.

Honda, M. *et al.* (2009) 'Low pressure CO_2 to dimethyl carbonate by the reaction with methanol promoted by acetonitrile hydration', *Chemical Communications*, pp.4596. doi: 10.1039/b909610h.

Hui, S., Zhang, B., Zhang, S. and Li, W. (2012) 'In situ IR study of dimethyl oxalate hydrogenation to ethylene glycol over Cu/SiO_2 catalyst,' *Journal of Natural Gas Chemistry*, 21(6), pp.753-758.

Halmann, M. (1993) *Chemical Fixation of Carbon Dioxide: Methods for Recycling CO_2 into Useful Products*. 1st ed. CRC Press.

Hocking, M.B., 2005. *Handbook of chemical technology and pollution control [electronic resource]* 3rd ed., San Diego: Academic.

Honda, M. *et al.* (2011) 'Tandem carboxylation-hydration reaction system from methanol, CO_2 and benzonitrile to dimethyl carbonate and benzamide catalyzed by CeO_2', *ChemCatChem*, 3, pp. 365. doi: 10.1002/cctc.201000339.

Hou, X. and Jones, B. (2000) 'Inductively Coupled Plasma/Optical Emission Spectrometry', *Encyclopedia of Analytical Chemistry*, pp. 9468–9485.

H. Cui, T. Wang, F. Wang, C. Gu, P. Wang, Y. Dai,. (2003) 'One-pot synthesis of dimethyl carbonate using ethylene oxide, methanol, and carbon dioxide under supercritical conditions', Ind. Eng. Chem. Res. doi:10.1021/ie021014b.

Haynes, W.M. (2015). *CRC Handbook of Chemistry and Physics. 95th Edition.* CRC Press L LC, Boca Raton, pp. 4-89.

IEA.org. (2019). *CO_2 Emissions*. [online] Available at: https://www.iea.org/statistics/co2emissions/ [Accessed 24 Sep. 2019].

IEA.org. 2019. *Putting CO_2 To Use: Creating Value From Emissions*. [online] Available at: <https://www.maritimecyprus.com/2019/12/16/putting-co2-to-use-creating-value-from-emissions/> [Accessed 15 November 2020].

Ilavsky, J., Jemian, P., Allen, A., Zhang, F., Levine, L. and Long, G. (2009). Ultra-small-angle X-ray scattering at the Advanced Photon Source. *Journal of Applied Crystallography*, 42(3), pp.469-479.

Jiang, Q., Cheng, J. and Gao, Z. (2007) 'Direct synthesis of dimethyl carbonate over rare earth oxide supported catalyst', *Frontiers of Chemical Engineering in China*, 1(3), pp.300-303.

J. H. Sinfelt in G. Ertl, H. Knozinger, J. Weitkamp (eds.) (1997), *Handbook of Heterogeneous Catalysis*, Vol. 4, Wiley-VCH, pp. 1939.

Joo, O. S., Jung, K. D. and Jung, Y. (2004) 'CAMERE process for methanol synthesis from CO2hydrogenation', in *Studies in Surface Science and Catalysis*, 153, pp. 67-72 doi: 10.1016/s0167-2991(04)80221-0.

Jiang, S., Cai, J., Pan, L., Zhang, F., & Zhang, Y. (2009) 'Preparation technology of biodiesel using K2CO3 loaded hydrotalcite catalyst', *Nongye Jixie Xuebao:Transactions of the Chinese Society for Agricultural Machinery*, 40(4), pp.102-106.

Jiang, Q. and Yang, Y. (2004) 'The Double Component Catalyst for the Direct Synthesis of Dimethyl Carbonate from Carbon Dioxide, Propylene Oxide and Methanol', *Catalysis Letters*, 95(3/4), pp.127-133.

Kähler, K., Holz, M. C., Rohe, M., Strunk, J., & Muhler, M. (2010). Probing the reactivity of ZnO and Au/ZnO nanoparticles by methanol adsorption: a TPD and DRIFTS study. *Chemphyschem : a European journal of chemical physics and physical chemistry*, 11(12), pp. 2521–2529. https://doi.org/10.1002/cphc.201000282

Kumar, Praveen, Srivastava, Vimal Chandra & Mishra, Indra Mani, (2015). Dimethyl carbonate synthesis via transesterification of propylene carbonate with methanol by ceria-zinc catalysts: Role of catalyst support and reaction parameters. *The Korean journal of chemical engineering,* 32(9), pp.1774–1783.

Kohli, R., & Mittal, K. L. (2011). *Developments in Surface Contamination and Cleaning, Volume 4: Detection, Characterization, and Analysis of Contaminants*. William Andrew.

Kung, H. H., Kung, M. C. and Costello, C. K. (2003) 'Supported Au catalysts for low temperature CO oxidation', *Journal of Catalysis*, 216(1-2), pp. 425-432. doi: 10.1016/S0021-9517(02)00111-2.

Kember, M.R., Buchard, A. and Williams, C.K., (2011) 'Catalysts for CO_2/epoxide copolymerisation', *Chemical Communications*, 47(1), pp.141-163.

Khadzhiev, S. N., Magomedova, M. V, & Peresypkina, E. G. (2014) 'Mechanism of Olefin Synthesis from Methanol and Dimethyl Ether over Zeolite Catalysts: A Review', 54(4), pp. 245–269. http://doi.org/10.1134/S0965544114040057

Kumar, P., Srivastava, V. C. and Mishra, I. M. (2015) 'Dimethyl carbonate synthesis from propylene carbonate with methanol using Cu-Zn-Al catalyst', *Energy and Fuels*, 29, pp. 2664−2675. doi: 10.1021/ef502856z.

Korosteleva, I., Markova, N., Kolesnichenko, N., Ezhova, N., Khadzhiev, S. and Trukhmanova, N. (2013) 'Catalytic synthesis of propylene carbonate from propylene oxide and carbon dioxide in the presence of rhodium complexes modified with organophosphorus ligands and chitosan', *Petroleum Chemistry*, 53(6), pp.412-417.

Kwon, D., Park, K. and Hong, S. (2015) 'Influence of VO_x surface density and vanadyl species on the selective catalytic reduction of NO by NH_3 over VO_x /TiO_2 for superior catalytic activity', *Applied Catalysis A: General*, 499, pp.1-12.

Kletnieks, P., Liang, A., Craciun, R., Ehresmann, J., Marcus, D., Bhirud, V., Klaric, M., Hayman, M., Guenther, D., Bagatchenko, O., Dixon, D., Gates, B. and Haw, J. (2007)

'Molecular Heterogeneous Catalysis: A Single-Site Zeolite-Supported Rhodium Complex for Acetylene Cyclotrimerization', *Chemistry - A European Journal*, 13(26), pp.7294-7304.

Kumaran, M., Jacobs, G., Hamdeh, H. H., Shafer, W. D., & Davis, B. H. (2013) 'Fischer – Tropsch synthesis: Mössbauer investigation of iron containing catalysts for hydrogenation of carbon dioxide', *Catalysis Today*, 207, pp.50–56. http://doi.org/10.1016/j.cattod.2012.02.059

Liu, Q., Wu, L., Jackstell, R. and Beller, M. (2016) 'Using Carbon Dioxide as a Building Block in Organic Synthesis', *Nature Communications*, 6(5933).

Liu, J., Guo, H., Zhou, Q., Wang, J., Lin, B., Zhang, H., Gao, Z., Xia, C. and Zhou, X. (2013) 'Highly efficient enzymatic preparation for dimethyl carbonate catalyzed by lipase from Penicillium expansum immobilized on CMC–PVA film', *Journal of Molecular Catalysis B: Enzymatic*, 96, pp.96-102.

Le Quéré, *et al*,. (2014). 'Global carbon budget 2013,' *Earth System Science Data*, 6(1), pp.235-263.

Leung, D. Y. C., Caramanna, G. and Maroto-Valer, M. M. (2014) 'An overview of current status of carbon dioxide capture and storage technologies', *Renewable and Sustainable Energy Reviews*, 39, pp.426-443. doi: 10.1016/j.rser.2014.07.093.

Li, L., Shi, S., Song, L., Guo, L., Wang, Y., Ma, H., … Wang, H. (2015) 'One-step synthesis of dimethyl carbonate from carbon dioxide, propylene oxide and methanol over alkali halides promoted by crown ethers', *Journal of Organometallic Chemistry*, 794, pp.231–236. http://doi.org/10.1016/j.jorganchem.2015.07.010

Li, Y., Zhao, X. Q. and Wang, Y. J. (2005) 'Synthesis of dimethyl carbonate from methanol, propylene oxide and carbon dioxide over KOH/4A molecular sieve catalyst,' *Applied Catalysis A: General*, 279(1–2), pp. 205–208.

Liu, M. *et al.* (2016) 'Design of bifunctional NH3I-Zn/SBA-15 single-component heterogeneous catalyst for chemical fixation of carbon dioxide to cyclic carbonates', *Journal of Molecular Catalysis A: Chemical*, 418–419, pp. 78–85. doi: 10.1016/j.molcata.2016.03.037.

Liang, X. L. *et al.* (2009) 'Carbon nanotube-supported Pd-ZnO catalyst for hydrogenation of CO2 to methanol', *Applied Catalysis B: Environmental*, 88(3-4), pp. 315-322. doi: 10.1016/j.apcatb.2008.11.018.

Lei, H., Nie, R., Fei, J. and Hou, Z. (2012) 'Preparation of Cu/ZnO/Al_2O_3 catalysts in a solvent-free routine for CO hydrogenation', *Journal of Zhejiang University SCIENCE A*, 13(5), pp.395-406.

Lan, Dong-Hui, *et al.* (2015) 'One-pot synthesized multi-functional graphene oxide as a water-tolerant and efficient metal-free heterogeneous catalyst for cycloaddition reaction', *Carbon*, 93, pp.22-31.

Laurence, C. and Gal, J. (2010). *Lewis basicity and affinity scales*. Chichester, West Sussex, U.K: John Wiley, pp.44.

Lan, D. H. *et al.* (2014) 'Water-tolerant graphene oxide as a high-efficiency catalyst for the synthesis of propylene carbonate from propylene oxide and carbon dioxide', *Carbon*,73, pp. 351-360. doi: 10.1016/j.carbon.2014.02.075.

Liang, S. *et al.* (2010) 'The tetramethylguanidine-based ionic liquid-catalyzed synthesis of propylene glycol methyl ether', *New Journal of Chemistry*, 34, pp.2534-2536. doi: 10.1039/c0nj00502a.

Mohale, G. (2017) 'SEM image processing as an alternative method to determine chromite pre-reduction', *Journal of the Southern African Institute of Mining and Metallurgy*, 117(11), pp.1045-1052.

Martínez-Ferraté, O., Chacón, G., Bernardi, F., Grehl, T., Brüner, P. and Dupont, J. (2018) 'Cycloaddition of carbon dioxide to epoxides catalysed by supported ionic liquids', *Catalysis Science & Technology*, 8(12), pp.3081-3089.

Murugan, C. and Bajaj, H. C. (2010) 'Transesterification of propylene carbonate with methanol using Mg-Al-CO_3 hydrotalcite as solid base catalyst', *Indian Journal of Chemistry*, 49A, pp. 1182–1188.

Marianna Cross. (2016). *Imperial College London Answers to the question from lecture 3 Maleic anhydride may be prepared using two routes: Oxidation of benzene: Oxidation of but-1-ene: - ppt download*. [online] Available at: http://slideplayer.com/slide/4724681/ [Accessed 25 Feb. 2020].

Ma, W., Jacobs, G., Sparks, D. E., Ramana, V., Pendyala, R., Hopps, S. G., Davis, B. H. (2015) 'Fischer – Tropsch synthesis: Effect of ammonia in syngas on the Fischer – Tropsch synthesis performance of a precipitated iron catalyst', *Journal of Catalysis*, 326(x), 149–160. http://doi.org/10.1016/j.jcat.2015.04.004

M. Che, O. Clause, Ch. Marcilly in G. Ertl, H. Knozinger, J.Weitkamp (eds.) (1997), *Handbook of Heterogeneous Catalysis*, Vol. 1, Wiley-VCH, pp. 191.

Marchal, V. and Dellink, R. (2011). THE OECD ENVIRONMENTAL OUTLOOK TO 2050. *OECD*, pp.6.

Memoli, S., Selva, M. and Tundo, P. (2001) 'Dimethylcarbonate for eco-friendly methylation reactions', *Chemosphere*, 43, pp. 115-121. doi: 10.1016/S0045-6535(00)00331-3.

Meylan, F., Moreau, V. and Erkman, S. (2015) 'CO_2 utilization in the perspective of industrial ecology, an overview', *Journal of CO_2 Utilization*, 12, pp.101-108.

NOAA National Centers for Environmental Information, State of the Climate: Global Climate Report for August 2019, published online September 2019 Available at: https://www.ncdc.noaa.gov/sotc/global/201908. [Accessed 23 Sep. 2019].

Naims, H. (2016) 'Economics of carbon dioxide capture and utilization—a supply and demand perspective', *Environmental Science and Pollution Research*, 23(22), pp.22226-22241.

Nezamzadeh-Ejhieh, A. and Moeinirad, S. (2011) 'Heterogeneous photocatalytic degradation of furfural using NiS-clinoptilolite zeolite', *Desalination*, 273(2-3), pp.248-257.

Nicolet, Y., de Lacey, A. L., Vernède, X., Fernandez, V. M., Hatchikian, E. C., & Fontecilla-Camps, J. C. (2001) 'Crystallographic and FTIR Spectroscopic Evidence of Changes in Fe Coordination Upon Reduction of the Active Site of the Fe-Only Hydrogenase from Desulfovibrio desulfuricans', *Journal of the American Chemical Society*, *123*(8), pp.1596-1601.

Norton, C. J. (1964) 'Olefin polymerization over synthetic molecular sieves', *Industrial and Engineering Chemistry Process Design and Development*, pp. 230-236. doi: 10.1021/i260011a009.

Nilsson, A. *et al.* (2005) 'The electronic structure effect in heterogeneous catalysis', *Catalysis Letters*, 100(3-4), pp.111-114. doi: 10.1007/s10562-004-3434-9.

Oliver, J., Janssens-Maenhout, G., Muntean, M. and peters, J. (2013). *Trends in global CO_2 emissions: 2013 Report*. Netherlands.

Ono, Y., & Baba, T. (2000) 'Strong solid bases for organic reactions', *CATALYSIS-LONDON*, *15*, pp. 1-39.

Overbury, S. H., Bertrand, P. A. and Somorjai, G. A. (1975) 'The Surface Composition of Binary Systems. Prediction of Surface Phase Diagrams of Solid Solutions', *Chemical Reviews*, 75(5), pp. 547-560. doi: 10.1021/cr60297a001.

Ono, Y. and Hattori, H. (2016). *Solid Base Catalysis*. SPRINGER, pp.346.

Piumetti, M. *et al.* (2012) 'Vanadium-containing catalysts for oxidation reactions', *Chimica Oggi/Chemistry Today*, 30(3 SUPPL.), pp. 29–32.

Peng, G., Sibener, S. J., Schatz, G. C., Ceyer, S. T., & Mavrikakis, M. (2012) 'CO_2 Hydrogenation to Formic Acid on Ni(111),' *JOURNAL OF PHYSICAL CHEMISTRY C*, *116*, pp.3001–3006. http://doi.org/10.1021/jp210408x

Preti, D., Resta, C., Squarcialupi, S., & Fachinetti, G. (2011) 'Carbon dioxide hydrogenation to formic acid by using a heterogeneous gold catalyst', *Angewandte Chemie - International Edition*, *50*(52), pp.12551–12554. http://doi.org/10.1002/anie.201105481

Pacheco, M. A. and Marshall, C. L. (1997) 'Review of dimethyl carbonate (DMC) manufacture and its characteristics as a fuel additive', *Energy and Fuels*, 11(1), pp. 2-29. doi: 10.1021/ef9600974.

Patterson, A. (1939) 'The Scherrer Formula for X-Ray Particle Size Determination', *Physical Review*, 56(10), pp.978-982.

Parker, R. and Isaacs, N. (1959) 'Mechanisms of epoxide reactions', *Chemical Reviews*, 59(4), pp.737-799.

Radfarnia, H. R., & Iliuta, M. C. (2014) 'Development of Al-stabilized CaO – nickel hybrid sorbent – catalyst for sorption-enhanced steam methane reforming,' *Chemical Engineering Science*, *109*, pp.212–219. http://doi.org/10.1016/j.ces.2014.01.03

Rim Saada, Suela Kellici, Tobias Heil, David Morgan, Basudeb Saha. (2015) 'Greener synthesis of dimethyl carbonate using a novel ceria–zirconia oxide/graphene nanocomposite catalyst', *Applied Catalysis B: Environmental*, 168(169), pp. 353-362.

Ramin, M., Vegten, N. Van, Grunwaldt, J., & Baiker, A. (2006) 'Simple preparation routes towards novel Zn-based catalysts for the solventless synthesis of propylene carbonate using dense carbon dioxide', *258*, pp.165–171. http://doi.org/10.1016/j.molcata.2006.05.041

Royalsociety.org. 2017. The Potential And Limitations Of Using Carbon Dioxide. [online] Available at: https://royalsociety.org/topics-policy/projects/low-carbon-energy-programme/potential-limitations-carbon-dioxide/ [Accessed 15 November 2020].

Rodriguez, J. A., Evans, J., Feria, L., Vidal, A. B., Liu, P., & Nakamura, K. (2013) 'CO_2 hydrogenation on Au / TiC , Cu / TiC , and Ni / TiC catalysts : Production of CO , methanol , and methane', *307*, pp.162–169. http://doi.org/10.1016/j.jcat.2013.07.023

R. Prins in G. Ertl, H. Knozinger, J. Weitkamp (eds.) (1997), *Handbook of Heterogeneous Catalysis*, Vol. 4, Wiley-VCH, pp. 1908.

Reutemann, W., & Kieczka, H. (2012). Formic acid. *Ullmann's Encyclopedia of Industrial Chemistry*, pp. 285–313. http://doi.org/10.1002/14356007.a12

Schaub, T., & Paciello, R. A. (2011) 'A process for the synthesis of formic acid by CO_2 hydrogenation: Thermodynamic aspects and the role of CO_2', *Angewandte Chemie - International Edition*. http://doi.org/10.1002/anie.201101292

State of the Climate: Global Climate Report for August 2019. (2019). [online] NOAA National Centers for Environmental Information. Available at: https://www.ncdc.noaa.gov/sotc/global/201908. [Accessed 23 Sep. 2019].

Simo, M., Sivashanmugam, S., Brown, C. and Hlavacek, V. (2009) 'Adsorption/Desorption of Water and Ethanol on 3A Zeolite in Near-Adiabatic Fixed Bed', *Industrial & Engineering Chemistry Research*, 48(20), pp.9247-9260.

Saada, Rim *et al.*, (2018) 'Greener synthesis of dimethyl carbonate using a novel tin-zirconia/graphene nanocomposite catalyst', *Applied catalysis. B, Environmental*, 226, pp.451–462.

Sakakura, T. *et al.* (1999) 'Metal-catalyzed dimethyl carbonate synthesis from carbon dioxide and acetals', *Journal of Organic Chemistry*, 64(12), pp. 4506-4508. doi: 10.1021/jo990155t.

Selva, M., Marques, C. and Tundo, P. (1994) 'Selective mono-methylation of arylacetonitriles and methyl arylacetates by dimethyl carbonate', *Journal of the Chemical Society*, Perkin Transactions 1, (10), pp.1323.

Sankar, M., Nair, C., Murty, K. and Manikandan, P. (2006) 'Transesterification of cyclic carbonates with methanol at ambient conditions over tungstate-based solid catalysts', *Applied Catalysis A: General*, 312, pp.108-114.

Stoica, G., Abelló, S. and Pérez-Ramírez, J. (2009) 'Na-dawsonite derived aluminates for DMC production by transesterification of ethylene carbonate', *Applied Catalysis A: General*, 365(2), pp.252-260.

Strizhak, P. E. *et al.* (2011) 'Geometric and electronic approaches to size effects in heterogeneous catalysis', *Kinetics and Catalysis*. doi: 10.1134/S0023158411010186.

Sakakura, T. *et al.* (1998) 'Selective conversion of carbon dioxide to dimethyl carbonate by molecular catalysis', *Journal of Organic Chemistry*, *63*(20), pp.7095-7096. doi: 10.1021/jo980460z.

Sakakura, T., & Kohno, K. (2009) 'The synthesis of organic carbonates from carbon dioxide', *Chemical Communications*, (11), pp.1312-1330.

Sparkman, O., Penton, Zelda, & Kitson, Fulton G. (2011), *Gas chromatography and mass spectrometry [electronic resource]: A practical guide* (2nd ed.). Burlington, MA: Academic.

Sing, K. (1985) 'Reporting physisorption data for gas/solid systems with special reference to the determination of surface area and porosity (Recommendations 1984)', *Pure and Applied Chemistry*, 57(4), pp.603-619.

Samani, H. (2018), Dimethyl Carbonate Market Dynamics, Forecast, Analysis and Supply Demand -2023 - CMFE News. [online] CMFE News. Available at: https://cmfenews.com/dimethyl-carbonate-market-dynamics-forecast-analysis-and-supply-demand-2023/

Sumimoto, S. *et al.* (2006) 'Zinc powder as an effective reducing reagent during liquid-phase oxidation of benzene to phenol using molecular oxygen over V-substituted heteropoly acid catalysts', *Industrial and Engineering Chemistry Research*. 45(22). pp. 7444-7450. doi: 10.1021/ie060743e.

Taherimehr, M. and Pescarmona, P. P. (2014) 'Green polycarbonates prepared by the copolymerization of CO2 with epoxides', *Journal of Applied Polymer Science*, 131, pp. 1–17doi: 10.1002/app.41141.

Tanaka, R., Yamashita, M., & Nozaki, K. (2009) 'Catalytic hydrogenation of carbon dioxide using Ir(III)-pincer complexes,' *Journal of the American Chemical Society*, *131*(40), pp.14168–14169. http://doi.org/10.1021/ja903574e

TOMISHIGE, K., IKEDA, Y., SAKAIHORI, T. and FUJIMOTO, K. (2000) 'Catalytic properties and structure of zirconia catalysts for direct synthesis of dimethyl carbonate from methanol and carbon dioxide', *Journal of Catalysis*, 192(2), pp. 355-362.

Timofeeva, M., Kapustin, A., Panchenko, V., Butenko, E., Krupskaya, V., Gil, A. and Vicente, M. (2016) 'Synthetic and natural materials with the brucite-like layers as high active catalyst for synthesis of 1-methoxy-2-propanol from methanol and propylene oxide', *Journal of Molecular Catalysis A: Chemical*, 423, pp.22-30.

Tian, J. S., Wang, J. Q., Chen, J. Y., Fan, J. G., Cai, F., & He, L. N. (2006) 'One-pot synthesis of dimethyl carbonate catalyzed by n-Bu_4NBr/n-Bu_3N from methanol, epoxides, and supercritical CO_2', *Applied Catalysis A: General*, *301*(2), pp.215-221.

The Global CO_2 Initiative & CO_2 Sciences (2016). *2016 A Roadmap for the Global Implementation of Carbon Utilization Technologies*. [online] The Global CO_2 Initiative & CO_2 Sciences. Available at: https://assets.ctfassets.net/xg0gv1arhdr3/27vQZEvrxaQiQEAsGyoSQu/44ee0b72ceb9231ec53ed180cb759614/CO2U_ICEF_Roadmap_FINAL_2016_12_07.pdf [Accessed 26 Sep. 2019].

Tundo, P., Selva, M., Perosa, A. and Memoli, S. (2002) 'Selective Mono-C-methylations of Arylacetonitriles and Arylacetates with Dimethyl carbonate: A Mechanistic Investigation', *The Journal of Organic Chemistry*, 67(4), pp.1071-1077.

Vedrine, J. C. (1994) 'Eurocat oxide V_2O_5/TiO_2', *Catal Today*, *20*, pp. 1-178.

Woods, G. (1990). *The ICI polyurethanes book*. 2nd ed. New York: ICI Polyurethanes, pp.36.

Wang, T. T., Xie, Y. and Deng, W. Q. (2014) 'Reaction mechanism of epoxide cycloaddition to CO_2 catalyzed by salen-M (M = Co, Al, Zn)', *Journal of Physical Chemistry A*, 118(39), pp.9239-9243. doi: 10.1021/jp506124h.

Wu, W., Chuang, C. and Lin, J. (2000) 'Bonding Geometry and Reactivity of Methoxy and Ethoxy Groups Adsorbed on Powdered TiO_2', *The Journal of Physical Chemistry B*, 104(36), pp.8719-8724.

Wang, M., Wei, T., Sun, Y., Wei, W. and Zhong, B. (2002) 'Synthesis of Dimethyl Carbonate from Propylene Carbonate and Methanol over Mesoporous Solid Base Catalyst', *Catalysis of Organic Reactions*.

Xie, W., Yang, Z. and Chun, H. (2007) 'Catalytic Properties of Lithium-Doped ZnO Catalysts Used for Biodiesel Preparations', *Industrial & Engineering Chemistry Research*, 46(24), pp.7942-7949.

Xu, W., Ji, S., Quan, W., & Yu, J. (2013) 'One-Pot Synthesis of Dimethyl Carbonate over Basic Zeolite Catalysts', *2013*(June), pp.22–27.

Xiao, L., Li, F., & Xia, C. (2005) 'An easily recoverable and efficient natural biopolymer-supported zinc chloride catalyst system for the chemical fixation of carbon dioxide to cyclic carbonate', *279*, pp.125–129. http://doi.org/10.1016/j.apcata.2004.10.022

Yong, Y., Kennedy, E. M. and Cant, N. W. (1999) 'Oxide catalysed reactions of ethylene oxide under conditions relevant to ethylene epoxidation over supported silver', 76(1991), pp. 31–48.

Yuan, Z. (2014) 'Applications of Bases in Transition Metal Catalyzed Reactions', *Postdoc journal*, 2(3), pp.17-28.

Yoshida, Y., Arai, Y., Kado, S., Kunimori, K. and Tomishige, K. (2006) 'Direct synthesis of organic carbonates from the reaction of CO_2 with methanol and ethanol over CeO_2 catalysts', *Catalysis Today*, 115(1-4), pp.95-101.

Zhang, X. and Cresswell, M. (2015). *Inorganic Controlled Release Technology: Materials and Concepts for Advanced Drug Formulation*. 1st ed. Butterworth-Heinemann, pp.63-64.

Zhu, W.; Huang, X.; Li, C.; Xiao, Y.; Zhang, D.; Guan, G. (2011) 'High-molecular-weight aliphatic polycarbonates by melt polycondensation of dimethyl carbonate and aliphatic diols: Synthesis and characterization', *Polym. Int*, 60, pp.1060–1067.

Zhao, Y., Tian, J., Qi, X., & Han, Z. (2007) 'Quaternary ammonium salt-functionalized chitosan: An easily recyclable catalyst for efficient synthesis of cyclic carbonates from epoxides and carbon dioxide', 271, pp. 284–289. http://doi.org/10.1016/j.molcata.2007.03.047

APPENDICES

Appendix A: Calibration curves of the products obtained from DMC synthesis reactions (Chapter 3).

The calibration curves were made by the internal standard method using GC-FID. 6 different concentrations of standard samples with same amount of internal standard (2-propanol) were prepared. The peak area ratios and the corresponding concentrations are shown in the figure and calibration equation is obtained as well. In the figure, y is the peak area ratio of the analyte and 2-propanol, x is the concentration of analyte in g/ml.

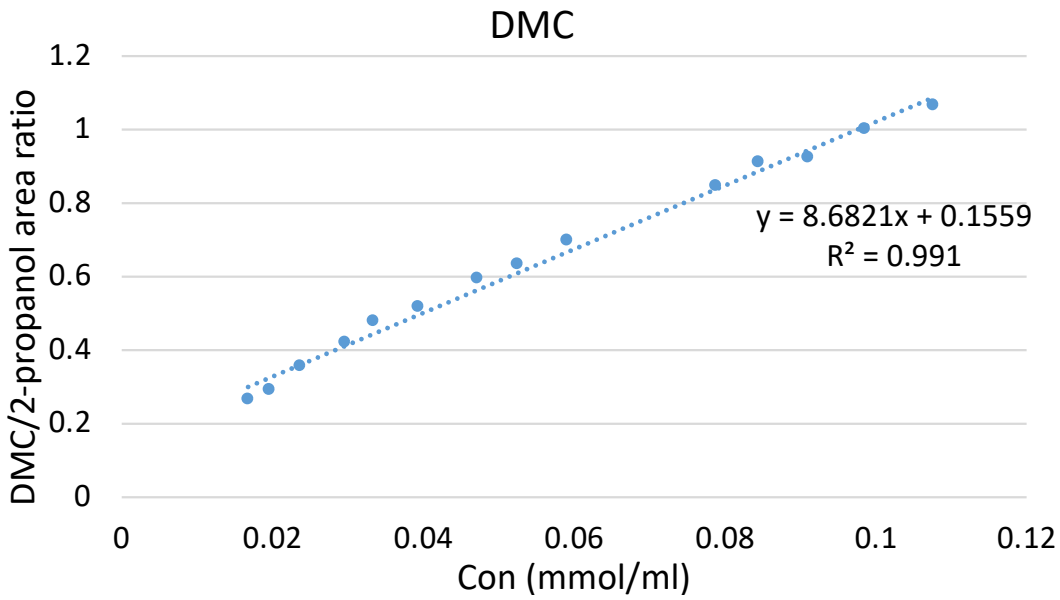

Figure A-1. Calibration curve of dimethyl carbonate.

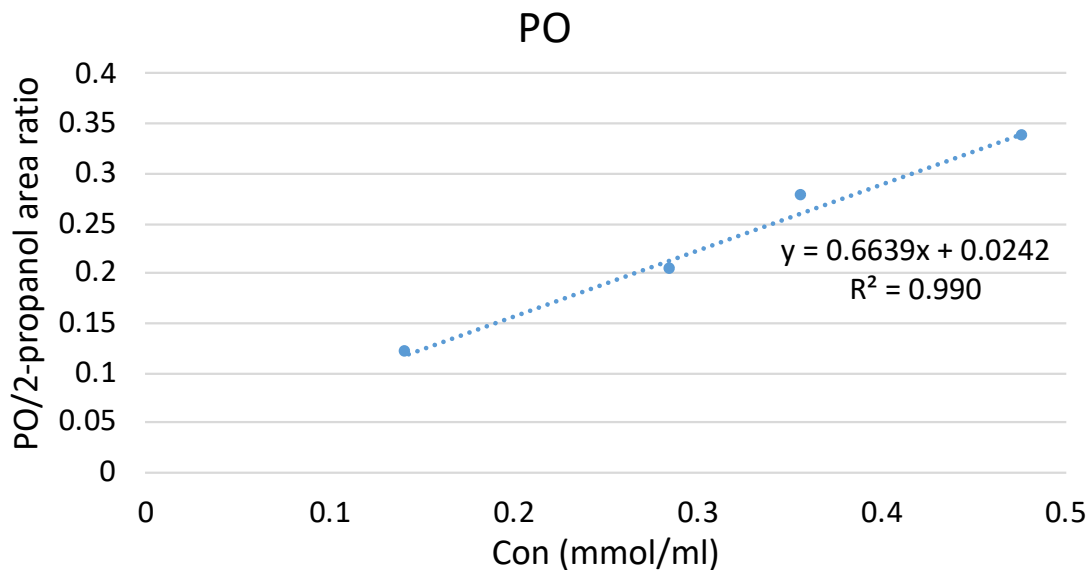

Figure A-2. Calibration curve of propanol oxide.

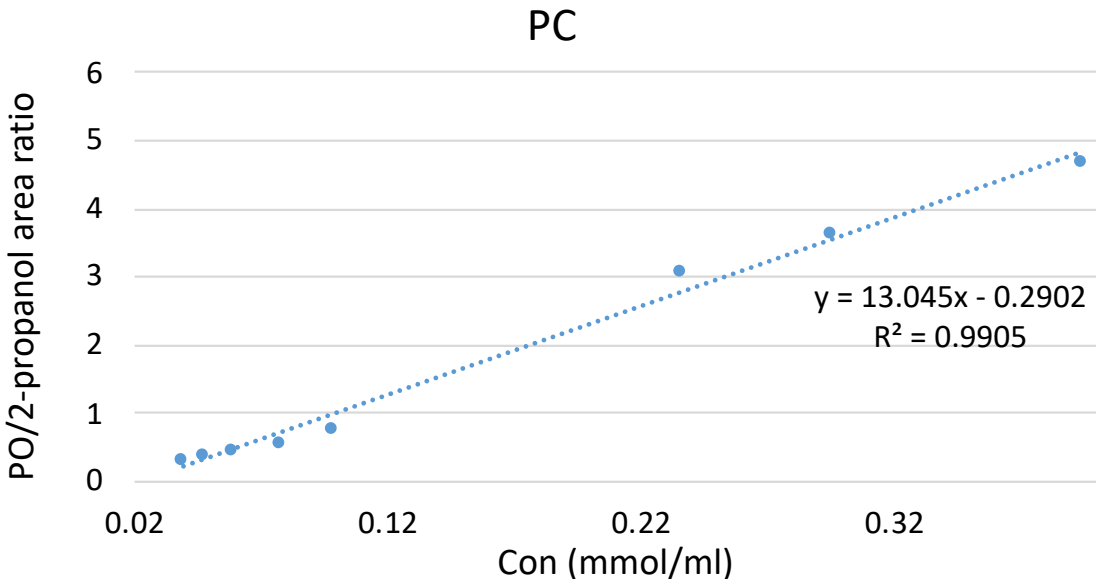

Figure A-3. Calibration curve of propylene carbonate.

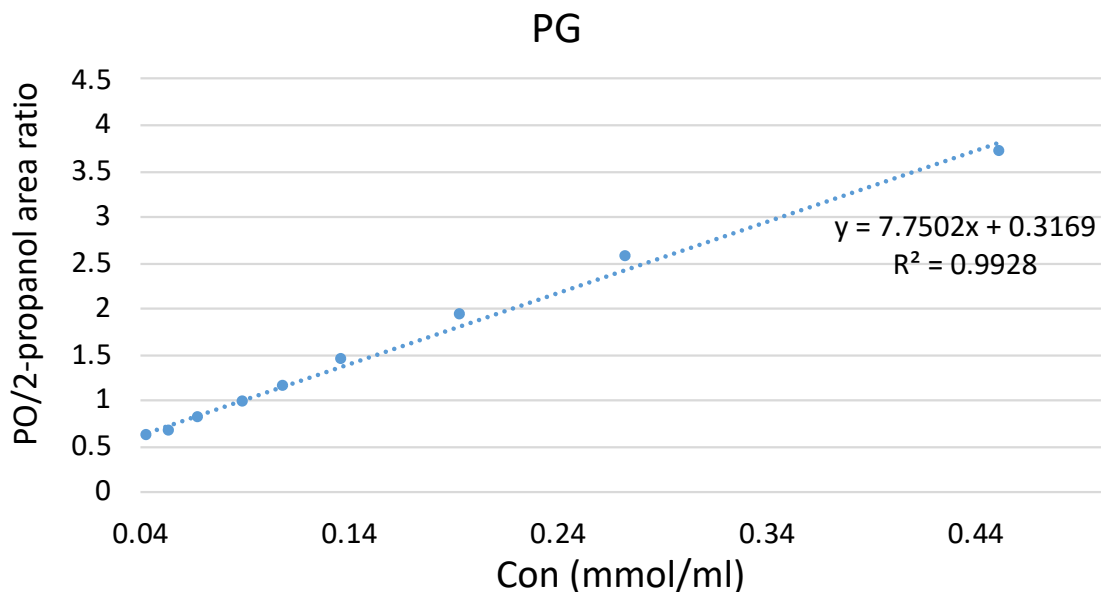

Figure A-4. Calibration curve of propylene glycol.

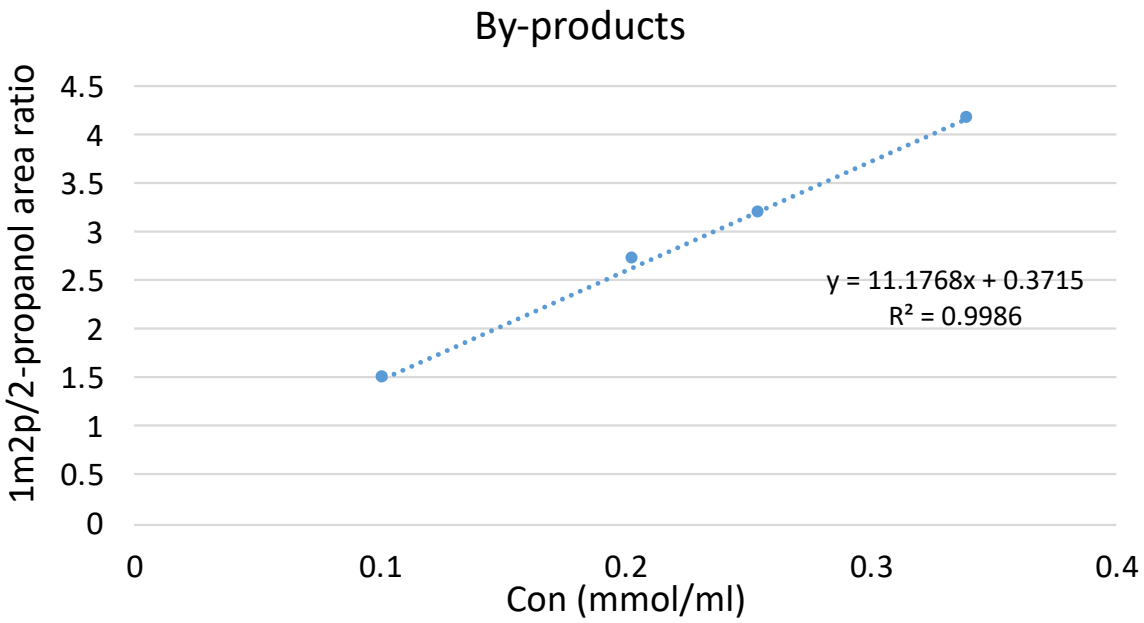

Figure A-5. Calibration curve of by-products (1-methoxy-2-propanol and 2-methoxy-1-propanol)

Appendix B: Photograph of the products obtained from DMC synthesis reactions in the presence of 3Å molecular sieves and acetonitrile (Chapter 6).

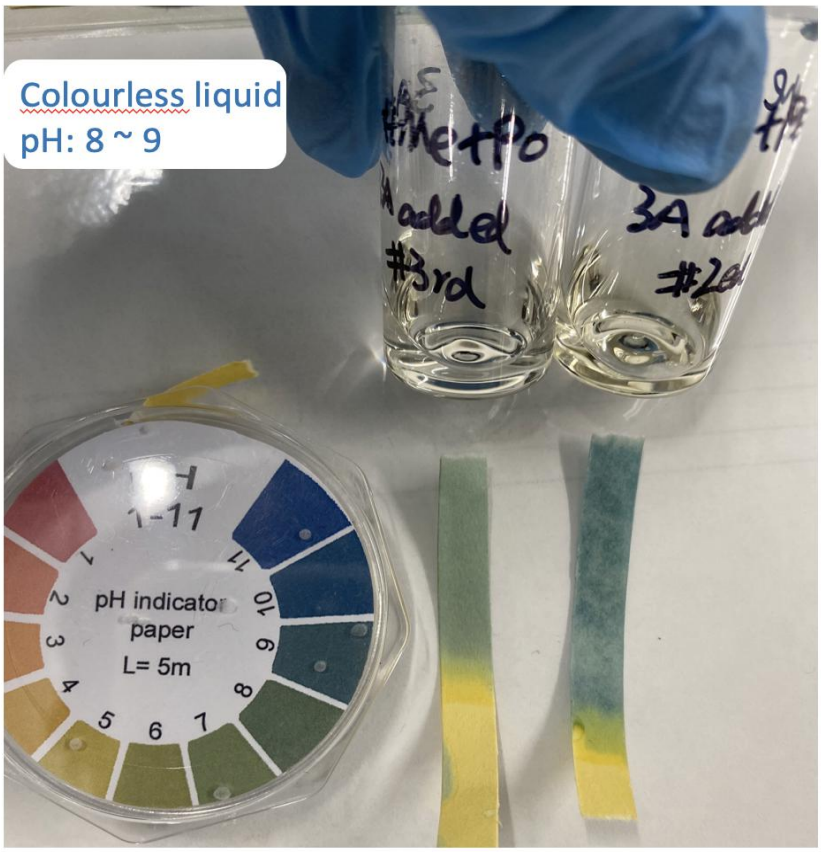

Figure B-1. Photographic images of the product of DMC synthesis reactions with the addition of 3Å molecular sieves and the reaction is repeated twice. Reaction conditions: methanol (100 mmol), propylene oxide (33.3 mmol), catalyst (0.3 g), CO_2 (2 MPa), 3Å molecular sieves (0.1 g), 160 °C, 5h.

The pH value of reaction product is around 9 and the colour of the liquid solution change from colourless to pale yellow after the reaction in the presence of 0.1g 3Å molecular sieves.

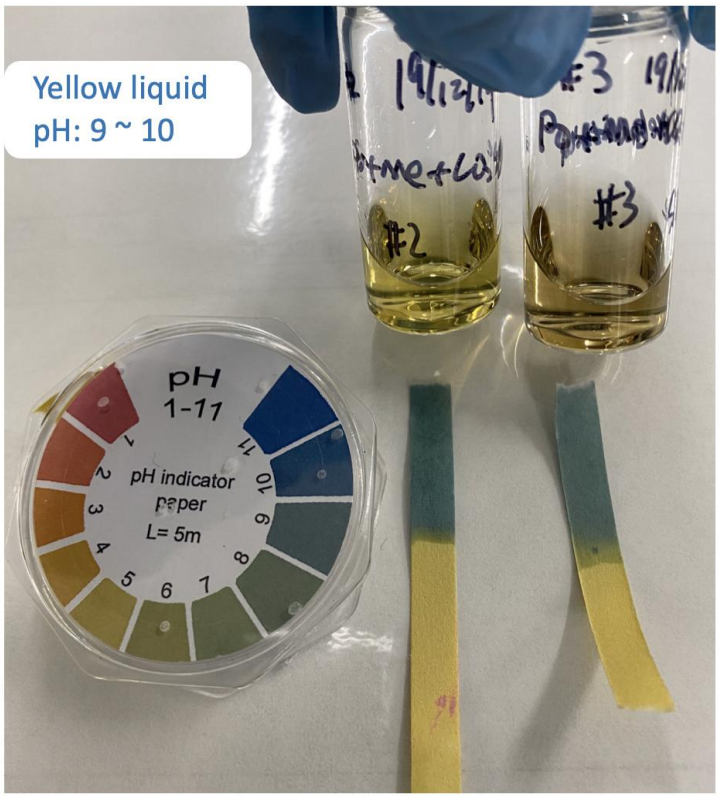

Figure B-2. Photographic images of the product of DMC synthesis reactions with the addition of acetonitrile and the reaction is repeated twice. Reaction conditions: methanol (100 mmol), propylene oxide (33.3 mmol), catalyst (0.3 g), CO_2 (2 MPa), acetonitrile (1.14 ml), 160 °C, 5h.

The colour of the products of the DMC synthesis reactions with the excess acetonitrile (1.14 ml) is yellow and the pH value of the liquid product is around 10.